2023

Volume : 12
Issue : 1
Page : 1 - 103

e-ISSN : 2147-4249

Eurasian Journal of Soil Science

http://ejss.fesss.org

Published by Federation of Eurasian Soil Science Societies

EURASIAN JOURNAL OF SOIL SCIENCE

(Peer Reviewed Open Access Journal)

Published by Federation of Eurasian Soil Science Societies

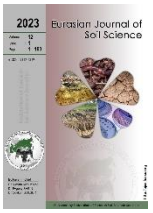

ABOUT THIS JOURNAL: Eurasian Journal of Soil Science is the official English language journal of the Federation of Eurasian Soil Science Societies. Eurasian Journal of Soil Science peer-reviewed open access journal that publishes research articles, critical reviews of basic and applied soil science in all related to soil and plant studies and general environmental soil science.

ABSTRACTING AND INDEXING: SCOPUS, CABI, FAO-Agris, EBSCOhost, ProQuest, DOAJ, OAJI, TR Dizin, TURKISH Journalpark, CrossRef, CiteFactor, CAS, etc.

Year: 2023, Volume: 12, Issue: 1, Page: 1 - 103 **e-ISSN 2147-4249**

EURASIAN JOURNAL OF SOIL SCIENCE

(Peer Reviewed Open Access Journal)

Published by Federation of Eurasian Soil Science Societies

YEAR: 2023 **VOLUME : 12** **ISSUE : 1** **PAGE : 1 – 103**

CONTENTS

Role of sorbents in early growth of barley under copper and benzo(a)pyrene contaminated soils **1**

Anatoly Barakhov, Natalia Chernikova, Tamara Dudnikova, Andrey Barbashev, Svetlana Sushkova, Saglara Mandzhieva, Vishnu Rajput, Rıdvan Kızılkaya, Elizaveta Konstantinova, Dmitry Bren, Tatiana Minkina, Alexander Konstantinov

Components and their assessment in different biogas slurries for enhanced waste management **10**

Ayten Namlı, Hanife Akça, Muhittin Onur Akça

Seasonal fluctuations in phthalates' contamination in pond water: A case study **19**

Sneh Rajput, Arpna Kumari, Ritika Sharma, Vishnu D. Rajput, Tatiana Minkina, Saroj Arora, Rajinder Kaur

Pores distribution influences the soil microorganism's response to changes in temperature and moisture **28**

Efraín Francisco Visconti-Moreno, Ibonne Geaneth Valenzuela-Balcázar

Identification of species of the genus Quercus L. with different responses to soil and climatic conditions according to hyperspectral survey data **37**

Pavel Dmitriev, Boris Kozlovsky, Anastasiya Dmitrieva, Vladimir Lysenko, Vasily Chokheli, Tatiana Minkina, Saglara Mandzhieva, Svetlana Sushkova, Tatyana Varduni

Salt accumulation in soils under furrow and drip irrigation using modified waters in Central Iran **63**

Leila Jahanbazi , Ahmad Heidari, Mohammad Hossein Mohammadi, Maria Kuniushkova

Evaluating the potential for multicropping in SE Kazakhstan : Double-cropping corn after winter triticale and winter oilseed rape **79**

Tastanbek Atakulov, Sagynbai Kaldybayev, Kenzhe Yerzhanova, Kuanysh Zholamanov, Ashirali Smanov, Ainash Seytzhan

Reducing soluble lead and cadmium in contaminated soils using dairy cattle waste based vermicompost **85**

Zainal Muktamar, Bandi Hermawan, Wulandari, Priyono Prawito, Fahrurrozi Fahrurrozi, Nanik Setyowati, Sigit Sudjatmiko, Mohammad Chozin

Modelling of soil temperature by using Phase Change Material (PCM) to regulate the plant growing media temperature **92**

Tuğba Gürmen

Effect of humic substances on yield and nutrient contents of Eggplant Santana (Solanum melongena) plants in gray-brown soil **98**

Ulviyya Mammadova

Eurasian Journal of Soil Science 2023, 12(1), 1 - 9

Eurasian Journal of Soil Science

Journal homepage : http://ejss.fesss.org

Role of sorbents in early growth of barley under copper and benzo(a)pyrene contaminated soils

Anatoly Barakhov [a,*], Natalia Chernikova [a], Tamara Dudnikova [a], Andrey Barbashev [a], Svetlana Sushkova [a], Saglara Mandzhieva [a], Vishnu Rajput [a], Rıdvan Kızılkaya [b], Elizaveta Konstantinova [a], Dmitry Bren [a], Tatiana Minkina [a], Alexander Konstantinov [c]

[a] Southern Federal University, Rostov-on-Don, Russia
[b] Ondokuz Mayıs University, Faculty of Agriculture, Department of Soil Science and Plant Nutrition, Samsun, Turkey
[c] University of Tyumen, Tyumen, Russia

Article Info

Received : 17.05.2022
Accepted : 09.09.2022
Available online : 20.09.2022

Author(s)

A.Barakhov *
N.Chernikova
T.Dudnikova
A.Barbashev
S.Sushkova
S.Mandzhieva
V.Rajput
R.Kızılkaya
E.Konstantinova
D.Bren
T.Minkina
A.Konstantinov

* Corresponding author

Abstract

In modern economic and industrial realities, agricultural lands are often located next to industrial areas, which leads to soil contamination and, as a result, agricultural products with pollutants. Pollution of soils and plants by several pollutants of various nature has acquired huge proportions. There is a threat of migration of dangerous ecotoxicants, including heavy metals and benz[a]pyrene, one of the main persistent compounds, a marker of PAH soil contamination, along trophic chains that may be dangerous to public health. This study examines the use of various types of mineral sorbents (Tripoli, Brown coal, Diatomite) and mineral sorbents (Biochar, Granular activated coal) to reduce the toxic effects of pollutants on the sources of anthropogenic emissions of heavy metals and polycyclic aromatic hydrocarbons adjacent to the sources. Using scanning electron microscopy, it was found that the sorbents have a high specific surface area. With the help of phytotesting in combined contaminated soils, the optimal dose of sorbent administration was determined at the level of 1% and 2% for various pollution variants. In addition, the analyzed sorbents are ordered by the effect of reducing the phytotoxicity of combined soil pollution. It was found that the introduction of sorbents into contaminated soil contributed to an increase in the morphometric parameters of the test culture - barley (Hordeum sativum distichum), which confirms the effectiveness of the sorption remediation of jointly contaminated soils with heavy metals and benz(a)pyrene.

Keywords: Heavy metals, polycyclic aromatic hydrocarbons, remediation, sorbents, biochar, germination energy.

Introduction

Heavy metals (HMs) and polycyclic aromatic hydrocarbons (PAHs) are among the most hazardous soil pollutants. The combined pollution of soils by HMs and PAHs constitutes a significant threat to the environment and human health. In the last decades, among HMs, copper (Cu) got a great deal of environmental and toxicological concern (Ben-Ali et al., 2017; Sushkova et al., 2017; Li et al., 2020). Copper compounds are among the most widely distributed contaminants; nonetheless, copper is a trace element that is required by plants to function properly. Now coming to PAHs, benzo(a)pyrene (BaP) is one of the most harmful members of this class of chemicals. BaP is subject to statutory control around the world and is a critical indication of contamination of soil with organic pollutants (Skłodowski et al., 2006; Abdel-Shafy and Mansour, 2016; Eeshwarasinghe et al., 2019). There is no universal method for restoring soils contaminated with heavy metals and polycyclic aromatic hydrocarbons. The effectiveness of the methods used depends on the soil properties,

: https://doi.org/10.18393/ejss.1177672
: http://ejss.fesss.org/10.18393/ejss.1177672
Publisher : Federation of Eurasian Soil Science Societies
e-ISSN : 2147-4249

the degree of adaptation, and the stability of the plants growing on it. The main approach for the restoration of combined contaminated soils lies mainly in either reducing the content of pollutants to a safe level or stabilizing and immobilizing pollutants to reduce their bioavailability.

Hence, the introduction of natural and artificial sorbents can be used as an independent method of soil remediation. While this soil reclamation method is economic and straightforward in its application, it is exceptionally effective in both the selective removal of contaminants and the restoration of the soil's natural condition. For soil remediation, the common sorbents based on natural resources and mineral raw materials (diatomites, tripoli), or obtained because of pyrolysis of biomass (activated carbon, biochar) (Ding and Luo, 2005; Gutiérrez-Ginés et al., 2014; Smirnov and Konstantinov, 2016; Smirnov et al., 2017; Singh et al., 2017; Xu et al., 2021). The current work is designed, and the scientific novelty of this work is in the choice of sorbents and the doses of their introduction into soils under the combined contamination of Cu and BaP has been substantiated. This work aims to study the transformation of Cu and BaP in the soil, as well as the effect of combined pollution on the growth and development of barley *(Hordeum sativum* distichum*).*

Material and Methods

The experiment was carried out in a climate chamber at the Academy of Biology and Biotechnology of the Southern Federal University. The soil (0-20 cm) of the specially protected natural area "Persianovsky reserved steppe", which is represented by Haplic chernozem, was used. Vegetative vessels with a closed drainage system with a volume of 3 l were loaded with soil sifted through a 2 mm sieve. The mass of soil in the vessels was 3 kg. Added an aqueous solution $Cu(CH_3COO)_3$ (275 and 550 mg/kg, which corresponds to 5 and 10 maximum permissible concentration (MPC) of the metal, and BaP solution in acetonitrile (200 and 400 mg/kg BaP), which corresponds to 10 and 20 MPC of polyarene. The selection of pollutant doses is carried out based on the degree of soil destruction in the Rostov region (Minkina et al., 2009; Sushkova et al., 2016; Bauer et al., 2020).

After 30 days from the moment the pollutants were introduced into the soil, sorbents were introduced according to the experimental scheme: 1) Control; 2) Control + 0.5% sorbent; 3) Control + 1% sorbent; 4) Control + 1% sorbent; 5) Control + 2% sorbent; 6) Control + 2.5% sorbent; 7) 10 MPC BaP + 5 MPC Cu (Background 1); 8) Background 1 + 0.5% sorbent; 9) Background 1 + 1% sorbent; 10) Background 1 + 1.5% sorbent; 11) Background 1 + 2% sorbent; 12) Background 1 + 2.5% sorbent; 13) 20 MPC BaP + 10 MPC Cu (Background 2); 14) Background 2 + 0.5% sorbent; 15) Background 2 + 1% sorbent; 16) Background 2 + 1.5% sorbent; 17) Background 2 + 2% sorbent; 18) Background 2 + 2.5% sorbent (Figure 1).

Figure 1. Growing experiment with spring barley (*Hordeum sativum distichum*)

The sorbents used were granular activated carbon (GAC), biochar produced at the Academy of Biology and Biotechnology of the Southern Federal University, diatomite from the Kamyshlov deposit, brown coal, and tripolite from Razrer Brusyan. The doses of sorbents were selected based on previous studies (Bolan et al., 2014; Minkina et al., 2016; Pinskii et al., 2018; Gholizadeh and Hu, 2021). In total, there were 53 variants in the experiment in 3-fold repetition. Soil incubation with sorbents lasted 30 days, after which a test culture was sown - two-row barley of the Ratnik variety (Hordeum sativum distichum) in the amount of 20 pieces per 3-liter pot. Plants were grown for 45 days - until the booting phase. Based on the previously obtained results of photo-testing, the choice of sorbents and their application rates were substantiated

Scanning electron microscopy (Carl Zeiss EVO-40 XVP microscope) was used to analyze the topography and morphology (microgeometry) of carbon sorbent fragments (Figure 2) (Bain et al., 2010; Rajput et al., 2021a,b). GAU consists of cylindrical granules 0.5-3 mm in size. Microscopic examination showed that it is heterogeneous in its dispersed and morphological composition and contains both rhombohedral fragments

up to 20-25 microns in length and particles several hundred microns in size (Figure 2). Large particles are sieve-like structures with through cylindrical holes with a diameter of approximately 10-20 microns and 1-2 microns. These formations in their shape and structure repeat the capillary structure of the wood from which they were obtained as a result of incomplete combustion of the feedstock. The biochar sample is a coarse-grained, highly porous material with a large surface area. The size and structure of the particles is determined by the characteristics of the feedstock.

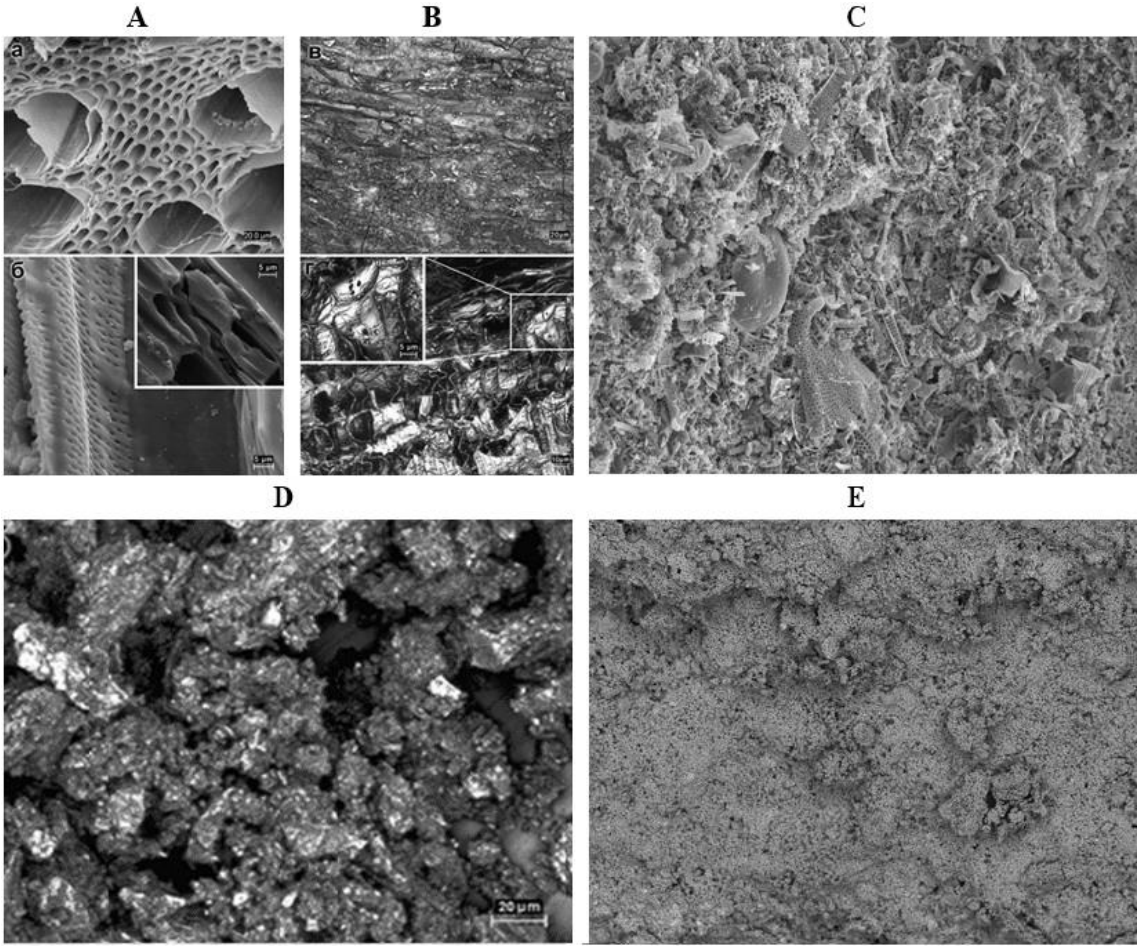

Figure 2. Images of the surface of the sorbents were made using scanning electron microscopy, microphotograph of A-granulated activated carbon, B – biochar from sunflower husk, C - surface of diatomite from the Kamyshlovskoye deposit, D - brown coal, E - surface of Brusyan-Logacharsky tripolite

Microscopic examination showed that, as in the GAC sample, biochar particles have an anisotropic structure of pores, which are long cylindrical cavities located along the longitudinal axis of sunflower husk particles (Minkina et al., 2013; Chen et al., 2020; Wang et al., 2020; Cheng et al., 2021). On the sagittal view (Figure 3), a developed surface is visible with many cracks and slit-like pores 1-2 microns wide. A segmental cleavage contains many rounded pores 10–30 µm in size, as well as pores 0.5–1 µm in size (Table 1). A brown coal sample consists of particles 0.1-1 mm in size. Microscopic examination showed the homogeneity of the sample. Most of the material has a loose texture and granular structure, irregularly shaped pores (Figure 2). The particles predominantly have an isomorphic, close to rounded shape. The total mass of the samples can be divided into the skeletal part and the finely dispersed component. Dust consists of both aggregates and individual particles (Figure 2). Aggregates are formed not only from small particles (<5 µm), they include large mineral grains, on the surface of which smaller particles adhere. The aggregates have sizes from tens of micrometers to 1 mm. Microaggregates of size from 20 to 70 µm prevail.

Table 1. Physical characteristics of the private surface and porosity of sorbents

Sorbent brand	Feedstock	Sorbent form	Granule size (mm)	Specific surface area (m2/g)	Pore volume (cm3/g)			
					General	Macro >500 нм	Mezo2-500 нм	Micro >2 нм
GAU	Wood	Granules	0,5-3	950	0,98	0,4	0,19	0,39
Biochar	Husk	Records	1-5	640	0,81	0,14	0,04	0,63
Brown coal	Brown coal	Powder	0,1-1	451	0,17	0,03	0,05	0,09

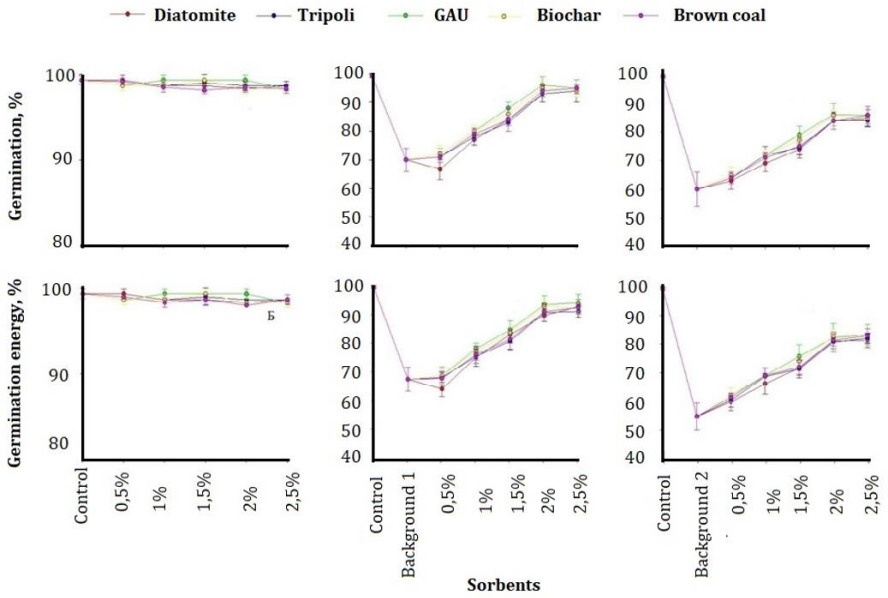

Figure 3. Germination and germination energy of the test culture of *Hordeum sativum distichum* in a model laboratory experiment

The Kamyshlovskoye deposit of diatomites is located on the northeastern outskirts of the city of Kamyshlov, Sverdlovsk region, 2 km from the Kamyshlov railway station, and is a large sheet-like deposit of diatomites. The thickness of diatomites within the deposit does not change significantly, except for the eastern part of the deposit, where the thickness of the deposit increases significantly. Within the boundaries of the explored area, the deposit is composed of diatomites of the Irbit Formation and opoks of the Serov Formation. Diatomites over the entire area are overlain by Pliocene-Quaternary sediments with a maximum thickness of 6 m or more. The diatom complex in the rocks of the productive strata of the Kamyshlovskoye deposit is represented by Coscinodiscus payeri (lower part of the Lower Eocene) - large isometric diatoms with dense and thick valve walls predominate (Figure 2).

Diatomites (mainly from Eastern Europe) with a relatively low SiO2 content of about 50% are effective as soil additives, including pollutant immobilization. At the same time, in the diatomites of the Trans-Urals, the average content of SiO_2, as a rule, ranges from 75 to 80%. In addition, there are numerous, relatively simple and cheap methods for their mechanical, thermal and chemical treatment, which make it possible to reduce the content of the clay component and bring the content of SiO_2 to 95% or more, as well as increase the specific surface area. Chemical properties, granulometric and mineral composition of the used sorbents are presented in Table 1 (Figure 2) (Fedorenko et al., 2021).

Methods

The toxic effect of pollutants is evaluated by such indicators as germination energy, germination, shoot length, root length. Germination energy was observed on the third day. Then, on the seventh day, germination was determined. At the end of the experiment, the experimental plants were collected and their morphometric characteristics were determined: the length of the shoots and the length of the roots. Next, the toxicity index was calculated for each factor in order to determine the toxicity of the studied soil before and after pollution. The toxicity index of the evaluated factor for each biological test object was determined by the formula (Kotyak, 2019; Kotyak et al., 2019): TF = TF0 /TFk, where is TF0 – the value of the measured indicator in the studied variant, TFk – on control. To assess the toxicity of the factor, the following scale was used: VI toxicity class (stimulation) –ITF >1.10; V (norm) - 0.91 – 1.10; IV (low toxicity) - 0.71 – 0.90; III (medium toxicity) - 0.50 – 0.70; II (high toxicity) - <0.50; I (ultrahigh toxicity) - the environment is not suitable for the life of the test object.Statistical data processing was carried out using the software package Microsoft Excel 2016, STATISTICA 2010. The average value of the indicator was determined, the standard deviation and validation of the samples were performed using a comparative Student's test.

Results

Germination and germination energy in uncontaminated soil amounted to 99%, which indicates high sowing qualities of the test crop. The average length of the roots varied in the range of 104-110 mm, and the stems - 106-112 mm (Figure 3, 4). The combined contamination of the soil with Cu and BaP has a toxic effect on the growth and development of the test culture. So, in the variant with the introduction of 275 mg/kg of Cu into

the soil (corresponds to 5 MPC) together with 200 mcg / kg of BaP (corresponds to 10 MPC), root length and stem height are suppressed by 79% compared to the control sample, in addition, germination and seed germination energy are reduced by 29% and 33% (Figure 4).

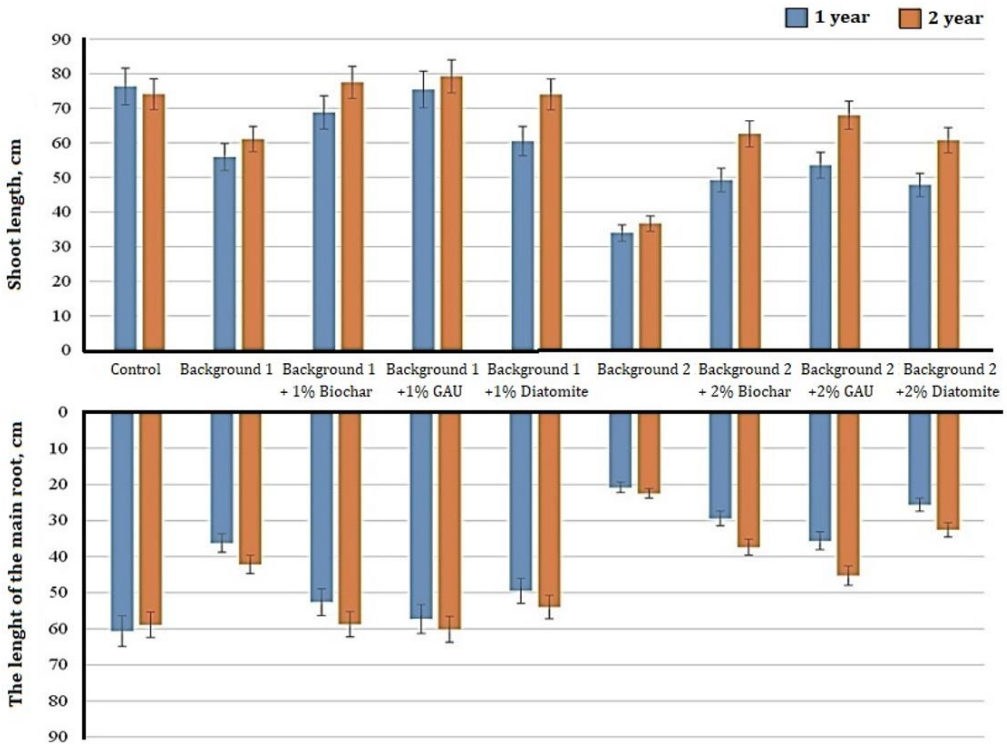

Figure 4. The effect of sorbents on the morphometric parameters of double row spring barley (*Hordeum sativum distichum*) in the tubulation phase (45 days), expressed in the variant with 5 MPC Cu and 10 MPC BaP (Background 1) and with 10 MPC Cu and 20 MPC BaP (Background 2)

Accordingly, with an increase in the content of introduced pollutants to 550 mg/kg Cu (10 MPC) and 400 mcg/kg BaP (20 MPC), the negative effect on the growth of roots and stems increases by 90%, as well as on germination and germination energy by 39% and 46% compared to plants (Figure 3), growing on unpolluted soil. Effective dose also remained 2.5%, but its effect is noticeably lower than that of the two previous sorbents: the length of the roots reached 79 mm, and the shoots – 73.

In the study results, the germination energy of spring barley seeds in uncontaminated soil was length of the roots varied between 104-110 mm, and for the stems between 106-112 mm. The combined soil contamination with Cu and BaP had toxic effect on the growth and development of the test culture. So, in the variant with 275 mg/kg Cu in soil (corresponds to 5 MPC) together with 200 μg / kg BaP (corresponds to 10 MPC), the root length and stem height were inhibited by 79% in comparison to the control. Additionally, the germination rate and seed germination energy decreased by 29% and 33%, respectively. As the pollutants' concentration increased to 550 mg/kg Cu (10 MPC) and 400 μg / kg BaP (20 MPC), the rate of stem and root growth decreased by up to 90%, as well as the germination energy by 39% and 46 % compared to plants growing in uncontaminated soil. It is noted that the joint soil contamination with organic and inorganic pollutants has a maximal toxic effect on plants as compared to the effects of individual pollution. Plant morpho-biometric parameters were not significantly affected by the introduction of mineral and carbonaceous sorbents into uncontaminated soil for shorter duration; however, in several studies involving a longer vegetation experiment, a positive effect on plant growth and productivity was observed. The use of mineral sorbents in contaminated soil had a positive effect on the morpho-biometric parameters of plants (Dietz et al., 1999; Kabata-Pendias, 2011; Mousavi et al., 2018).

Discussion

Germination and germination energy in variants with the introduction of different doses of diatomite was 70-94% and 66-90%, and in variants with tripoli - 71-94% and 67-91%, respectively (Figure 3). The introduction of diatomite into the soil with artificial pollution of 10 MPC BaP + 5 MPC Cu in doses of 0.5-2.5% increased the length of roots and stems in comparison with the contaminated soil. The best morpho-biom etric indicators of plants grown on contaminated soil were established with the introduction of 1.5% diatomite and 2% tripoli. With an increase in the content of pollutants in the soil to 20 MPC BaP + 10 MPC Cu, the efficiency of the

introduced doses of mineral sorbents slightly decreases. Germination and germination energy with different doses of diatomite in the soil observed to be 63-85% and 59-81%, and for tripoli - 64-84% and 60-83%. A dose of 0.5% diatomite and tripoli improved the parameters of the root length only by 1.5, 1.4 times, and the stem height by 1.4 times. With an increase in the doses of sorbents introduced into the soil, their effectiveness increases (Bauer et al., 2018; Rajput et al., 2021a,b; Kumar et al., 2021). The amendments efficiency was visible at 2.5% diatomite and tripoli. Similar phytotoxic effects were shown by diatomite and tripoli on the in regard to their physicochemical properties. The addition of carbon sorbents to the contaminated soil (10 MPC BaP + 5 MPC Cu) led to an improvement in the morpho-biometric parameters of plants. High germination (≤95%) of the test culture was recorded when 2–2.5% carbon sorbents were used, the germination energy varied within 90–94%. On variants of contamination of 10 MPC BaP + 5 MPC Cu at application rates> 1% GAU and biochar, the morpho-biometric parameters of plants reach the control sample. The lowest efficiency was found when using brown coal: 2.5% of brown coal, which contributed to an increase in root length, stem height by 3.7, and 4.0 times compared to the contaminated version (soil), however, the growth and development of plants do not reach control. The content of carbon sorbents in the contaminated soil 20 MPC BaP + 10 MPC had a positive effect on the growth and development of plants, whereas the sorbent concentration increased their efficiency become more evident. The use of GAU in doses 0.5-2.5% increases the length of the roots and the height of plants up to1.6-9.2 times, and biochar – up to 1.7-8.9 times.

The optimal dose of GAU and biochar application was 2% since with the introduction of 2.5% mathematically (statistically) reliable changes in morpho-biometric parameters were not observed GAU and biochar, in comparison with brown coal, were the most effective, which is associated with their characteristics especially specific surface area and pore volume. Thereby, in 2% brown coal concentration in soil, the root length increased by 7.1 times and the stem height by 6.1 times, while in the case of GAU and biochar, the increase was approximately 9 times (Chikhi et al., 2011).

With combined contamination, the morphometric parameters of spring barley deteriorated compared to the control (Figure 4). One of the most sensitive characteristics is the length of barley roots, which showed a significant impact on the formation of yield. It was found that the length of the roots decreased with combined contamination by 40% in the variant with 10 MPC BaP and 5 MPC Cu (Background 1) and by 66% with a doubling of the dose of pollutants compared with the control. This may be caused by the high carcinogenicity and mutagenicity of BaP, as well as other metabolites, which are the representatives of PAHs, and their carcinogenic metabolites formed during the degradation of BaP. It is generally recognized that the negative influence of heavy metals on growth processes, the development of stem meristems and roots increases with an increase in the concentration of metal in the soil.

The height of cereal plants reflects the general condition of plants when the main biomass is growing and forming, and reveals their reaction to nutritional conditions and soil toxicity. Based on current research outcomes, it was found that the length of the stems decreased by 27% and 56%. The inhibition in the growth and development of plants was not only reported in cultivated, but also in wild conditions under combined pollution by many researchers (Matsumoto et al., 1979; Zhou et al., 2021). Such processes may be related with a disruption of the antioxidant enzyme functions of plants as a result of the harmful effect of BaP's influence on these enzymes' activities. In the work of Bernard (Bernard et al., 2015), it was shown by the example of broccoli (*Brassica oleracea*) and white clover (*Trifolium repens*) that the level of resistance to oxidative stress (reactive oxygen species) at the biochemical level is directly associated with disturbed morphological characteristics of the plants.

There is an increase in the length of the barley root by 37% compared to the contaminated version of 20 MPC BaP and 10 MPC Cu (Background 2) with the introduction of 1% diatomite, and the length of the stem - by 8% and 7%, respectively. In the variants with higher pollution, a similar increase in the growth of spring barley is observed. The reduction of the toxic effect of pollutants during the introduction of diatomite occurs due to the fixation of bioavailable Cu compounds and the strengthening of the transformation of BaP. The maximum decrease in the morphobiometric parameters of plants on polluted soil (Background 1) was recorded when 1% of GAU is applied: the length of the barley root increased by 58%, and the root by 35% (Figure 4). The decrease in phytotoxicity might be due to a decrease in Cu mobility and BaP transformation (clause 1.3). GAU also has a stimulating effect on the development of agricultural crops (Feng et al., 2016; Bauer et al., 2020a,b).

In the second year of research, the effect of sorbents increases, which leads to better growth and development of test cultures, but the trends observed in the first year of research persist (Figure 4, 5, 6). Thus, the combined introduction of Cu and BaP into the soil has a negative impact on the morphometric parameters of barley. The most sensitive indicators of combined contamination are the length of the roots and stem. Further, the inhibition of the growth and development of test crops depends on the degree of contamination. When mineral

and carbon sorbents are applied, morphometric parameters of spring barley are improved by reducing the content of BaP and mobile Cu compounds. The best effect is observed when applying GAU. In the second year of research, there is a tendency to reduce the toxic effect of pollutants on the growth of test cultures. An increase in the effect of mineral and carbon sorbents was found as a result of greater fixation of Cu compounds and transformation of BaP.

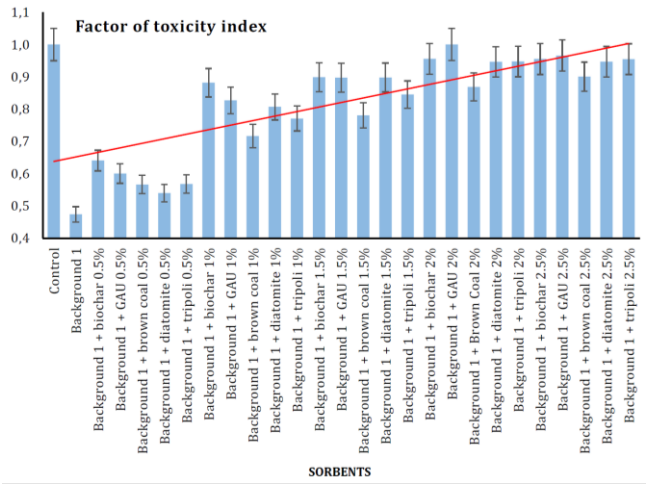

Figure 5. The effect of sorbents on on factor of toxicity index of double row spring barley (*Hordeum sativum distichum*), expressed in the variant with 5 MPC Cu and 10 MPC BaP (Background 1)

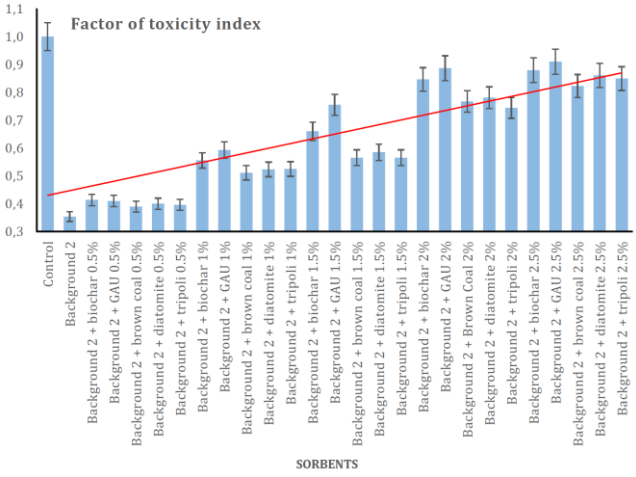

Figure 6. The effect of sorbents on factor of toxicity index of double row spring barley (*Hordeum sativum distichum*), expressed in the variant with 10 MPC Cu and 20 MPC BaP (Background 2)

Conclusion

It was shown that the introduction of mineral and carbonaceous sorbents into uncontaminated soil did not significantly affect the morpho-biometric parameters of plants. Germination energy was almost the same between different types of carbon sorbents. By reducing the phytotoxicity of the combined contamination of soil, the analyzed sorbents can be sequenced (sequenced) as follows: GAU> biochar> diatomite> tripoli> brown coal. In Haplic chernozem, combined contamination with Cu and BaP, the introduction of GAU, biochar, and diatomite to reduce the phytotoxicity of the soil showed the most noticeable changes when adding sorbents at a dose of 1% in the variant 10 MPC BaP + 5 MPC Cu and 2% in the variant 20 MPC BaP + 10 MPC Cu. Thus, these research outcomes will be helpful for remediation of combined polluted soils by heavy metals and benzo(a)pyrene and leveling the negative impact of pollutants on plant growth and development.

Acknowledgements

The study was carried out with the financial support of the Russian Science Foundation, project No. 19-74-10046.

References

Abdel-Shafy, H.I., Mansour, M.S.M., 2016. A review on polycyclic aromatic hydrocarbons: Source, environmental impact, effect on human health and remediation. *Egyptian Journal of Petroleum* 25(1): 107–123.

Bain, E.J., Calo, J.M., Spitz-Steinberg, R., Kirchner, J., Axén J., 2010. Electrosorption Electrodesorption of arsenic on a granular activated carbon in the presence of other heavy metals. *Energy and Fuels* 24(6): 3415-3421.

Bauer, T., Linnik, V., Minkina, T., Mandzhieva, S., Nevidomskaya, D., 2018. Ecological–geochemical studies of technogenic soils in the flood plain landscapes of the Seversky Donets, Lower Don Basin. *Geochemistry International* 10: 992–1002.

Bauer, T., Minkina, T., Mandzhieva, S., Burachevskaya, M., Zharkova, M., 2020. Biochar application to detoxification of the heavy metal-contaminated fluvisols. E3S Web of Conferences XIII International Scientific and Practical Conference "State and Prospects for the Development of Agribusiness – INTERAGROMASH 2020" 175: 09009.

Bauer, T., Minkina, T., Sushkova, S., Rajput, V., Tereshenko, A., Nazarenko, A., Mandzhieva, S., Sushkov, A., 2020. Mechanisms of copper immobilization in fluvisol after the carbon sorbent applying. *Eurasian Journal of Soil Science* 9(4): 356-361.

Ben-Ali, S., Jaouali, I., Souissi-Najar, S., Ouederni, A., 2017. Characterization and adsorption capacity of raw pomegranate peel biosorbent for copper removal. *Journal of Cleaner Production* 142(4): 3809-3821.

Bernard, L., Sawallisch, A., Heinze, S., Joergensen, R., Vohland, M., 2015. Usefulness of middle infrared spectroscopy for an estimation of chemical and biological soil properties – Underlying principles and comparison of different software packages. *Soil Biology and Biochemistry* 86: 116-125.

Bolan, N., Kunhikrishnan, A., Thangarajan, R., Kumpiene, J., Park, J., Makino, T., Kirkham, M.B., Scheckel, K., 2014. Remediation of heavy metal(loid)s contaminated soils – To mobilize or to immobilize?. *Journal of Hazardous Materials* 266: 141-166.

Chen, H., Yuan, X., Xiong, T., Jiang, L., Wang, H., Wu, Z., 2020. Biochar facilitated hydroxyapatite/calcium silicate hydrate for remediation of heavy metals contaminated soils. *Water, Air, and Soil Pollution* 231: 66.

Cheng, P., Zhang, S., Wang, Q., Feng, X., Zhang, S., Sun, Y., Wang, F., 2021. Contribution of nano-zero-valent iron and arbuscular mycorrhizal fungi to phytoremediation of heavy metal-contaminated soil. *Nanomaterials* 11(5): 1264.

Chikhi, M., Balask, F., Benchaabi, R., Ayat, A., Maameche, K., Meniai, A.H., 2011. Experimental study of coupling complexation-adsorption of Cu(II) on activated carbon. *Energy Procedia* 6: 284–291.

Dietz K.J., Baier, M., Krämer, U., 1999. Free radicals and reactive oxygen species as mediators of heavy metal toxicity in plants. In: Heavy metal stress in plants. Dietz, K.J., (Ed.). Springer-Verlag Berlin, Heidelberg, pp. 73-97.

Ding, K., Luo, Y., 2005. Bioremediation of copper and benzo[a]pyrene–contaminated soil by alfalfa J. *Journal of Agro-Environment Science* 24(4): 766–770.

Eeshwarasinghe, D., Loganathan, P., Vigneswaran, S., 2019. Simultaneous removal of polycyclic aromatic hydrocarbons and heavy metals from water using granular activated carbon. *Chemosphere* 223: 616-627.

Fedorenko, A.G., Minkina, T.M., Chernikova, N.P., Fedorenko, G.M., Mandzhieva, S.S., Rajput, V.D., Burachevskaya, M.V., Chaplygin, V.A., Bauer, T.V., Sushkova, S.N., Soldatov, A.V., 2021. The toxic effect of CuO of different dispersion degrees on the structure and ultrastructure of spring barley cells (Hordeum sativum distichum). *Environmental Geochemistry and Health* 43: 1673–1687.

Feng, N., Ghoveisi, H., Bitton, G., Bonzongo, J.C.J., 2016. Removal of phyto-accessible copper from contaminated soils using zero valent iron amendment and magnetic separation methods: Assessment of residual toxicity using plant and MetPLATE™ studies. *Environmental Pollution* 219: 9–18.

Gholizadeh, M., Hu, X., 2021. Removal of heavy metals from soil with biochar composite: A critical review of the mechanism. *Journal of Environmental Chemical Engineering* 9(5): 105830.

Gutiérrez-Ginés, M., Hernández, A., Pérez-Leblic, M., Pastor, J., Vangronsveld, J., 2014. Phytoremediation of soils co-contaminated by organic compounds and heavy metals: Bioassays with Lupinus luteus L. and associated endophytic bacteria. *Journal of Environmental Management* 143: 197–207.

Kabata-Pendias, A., 2011. Trace Elements in Soils and Plants. 4th Edition. CRC Press Boca Raton, USA. 548p.

Kotyak, P.A., 2019. Assessment of the toxic condition of sod-podzolic soil at different food levels. In: Fertility management and agroecological improvement. Kotyak, P.A. (Ed.). 25 April 2019, Yaroslavl, Russia. pp. 49-54. [in Russian].

Kotyak, P.A., Chebykina, E.V., Voronin, A.N., 2019. Estimation of toxicity of sod-podzolyy soil depending on applicable agricultures. In: Actual problems of environmental management, water use, agrochemistry, soil science and ecology. Kotyak, P.A., Chebykina, E.V., Voronin, A.N. (Eds.). 18 April 2019. Omsk, Russia. pp.696–702. [in Russian].

Kumar, V., Pandita, S., Sidhu, G.P.S., Sharma, A., Khanna, K., Kaur, P., Bali, A.S., Setia, R., 2021. Copper bioavailability, uptake, toxicity and tolerance in plants: A comprehensive review. *Chemosphere* 262: 127810.

Li, S., Song, K., Zhao, D., Rugarabamu, J., Diao, R., Gu, Y., 2020. Molecular simulation of benzene adsorption on different activated carbon under different temperatures. *Microporous and Mesoporous Materials* 302: 110220.

Matsumoto, H.K., Okada, E., Takahashi, E., 1979. Excretion products of maize roots from seedling to seed development stage. *Plant and Soil* 53: 17–26.

Minkina, T.M., Nazarenko, O.G., Motuzova, G.V, Mandzhieva, S.S., 2009. Group composition of heavy metal compounds in the soils contaminated by emissions from the Novocherkassk power station. *Eurasian Soil Science* 42(13): 1533–1542.

Minkina, T.M., Soldatov, A.V., Motuzova, G.V., Podkovyrina, Y.S., Nevidomskaya, D.G., 2013. Molecular-structural analysis of the Cu (II) ion in ordinary chernozem: Evidence from XANES spectroscopy and methods of molecular dynamics. *Doklady Earth Sciences* 449: 418–421.

Minkina, T., Fedorov, A., Nevidomskaya, D., Mandzhieva, S,. Kozlova M., 2016. Specific features of content and mobility of heavy metals in soils of floodplain of the Don River. *Arid Ecosystems* 6: 70–79.

Mousavi, S.J., Parvini, M., Ghorbani, M., 2018. Adsorption of heavy metals (Cu^{2+} and Zn^{2+}) on novel bifunctional ordered mesoporous silica: Optimization by response surface methodology. *Journal of the Taiwan Institute of Chemical Engineers* 84: 123-141.

Pinskii, D.L., Minkina, T.M., Bauer, T.V., Nevidomskaya, D.G., Mandzhieva, S.S., Burachevskaya, M.V., 2018. Copper adsorption by chernozem soils and parent rocks in Southern Russia. *Geochemistry International* 56(3): 266–275.

Rajput, V.D., Minkina, T., Morteza, F., Kumari, A., Khan, M., Mandzhieva, S., Sushkova, S., El-Ramady, H., Verma, K.K., Singh, A., Eric, D. van Hullebusch., Kumar, R., 2021a. Singh effects of silicon and silicon-based nanoparticles on rhizosphere microbiome. *Biology* 10: 791.

Rajput, V., Chaplygin, V., Gorovtsov, A., Fedorenko, A., Azarov, A., Chernikova, N., Barakhov, A., Minkina, T., Maksimov, A., Mandzhieva, S., Sushkova, S., 2021b. Assessing the toxicity and accumulation of bulk- and nanoCuO in Hordeum sativum L. *Environmental Geochemistry and Health* 43: 2443–2454.

Smirnov, P.V., Konstantinov, A.O., Gursky, H.J., 2017. Petrology and industrial application of main diatomite deposits in the Transuralian region (Russian Federation). *Environmental Earth Sciences* 76(20): 1-19.

Smirnov, P., Konstantinov, A.O., 2016. Comparative studies of Eocene and Paleocene diatomite from Trans-Urals (on the example of Kamyshlov deposit and section Brusyana). *Bulletin of the Tomsk Polytechnic University - Geo Assets Engineering* 327(11): 96-104.

Singh, H., Verma, A., Kumar, M., Sharma, R., Gupta, R., Kaur, M., Negi, M., Sharma, S.K., 2017. Phytoremediation: A green technology to clean up the sites with low and moderate level of heavy metals. *Austin Biochemistry* 2(2): 1012.

Skłodowski, P., Maciejewska, A., Kwiatkowska, J., 2006. The effect of organic matter from brown coal on bioavailability of heavy metals in contaminated soils, In: Soil and Water Pollution Monitoring, Protection and Remediation. Skłodowski, P., (Ed.). Springer-Dordrecht. Vol.69. pp. 299-307.

Sushkova, S., Minkina, T., Turina, I., Mandzhieva, S., Batuer, T., Zamulina, I., Kızılkaya, R., 2016. Benzo[a]pyrene contamination in Rostov Region of Russian Federation: A 10-year retrospective of soil monitoring under the effect of long-term technogenic pollution. *Eurasian Journal of Soil Science* 5(2): 155-165.

Sushkova, S., Minkina, T., Turina, I., Mandzhieva, S.S., Bauer, T., Kızılkaya, R., Zamuline, I., 2017. Monitoring of benzo[a]pyrene content in soils under the effect of long-term technogenic polution. *Journal of Geochemical Exploration* 174: 100-106

Wang, T., Xue, Y., Zhou, M., Liang, A., Liu, J., Mei, M., Li, J., 2020. Effect of addition of rice husk on the fate and speciation of heavy metals in the bottom ash during dyeing sludge incineration. *Journal of Cleaner Production* 244: 118851.

Xu, D.M., Fu, R.B., Wang, J.X., Shi, Y.X., Guo, X.P., 2021. Chemical stabilization remediation for heavy metals in contaminated soils on the latest decade: Available stabilizing materials and associated evaluation methods—A critical review. *Journal of Cleaner Production* 321: 128730.

Zhou, P., Adeel, M., Shakoor, N., Guo, M., Hao, Y., Azeem, I., Rui, Y., 2021. Application of nanoparticles alleviates heavy metals stress and promotes plant growth an overview. *Nanomaterials* 11(1): 26.

Eurasian Journal of Soil Science 2023, 12(1), 10 - 18

Eurasian Journal of Soil Science

Journal homepage : http://ejss.fesss.org

Components and their assessment in different biogas slurries for enhanced waste management

Ayten Namlı, Hanife Akça, Muhittin Onur Akça *

Ankara University, Faculty of Agriculture, Department of Soil Science and Plant Nutrition, Ankara, Türkiye

Article Info

Received : 25.01.2022
Accepted : 07.09.2022
Available online : 20.09.2022

Author(s)

A.Namlı
H.Akça
M.O.Akça *

* Corresponding author

Abstract

In this study, liquid fermented wastes from 15 licensed biogas plants located within different regions of Türkiye were determined and the parameters that are important to waste management evaluations were revealed. Accordingly, some physical, chemical, and biological analyses include moisture, dry matter (DM), organic matter (OM), pH, EC, total N, P, K, *Salmonella, Escherichia coli, E.coli* O157:H7, and *Enterobacteria* were conducted. Spearman's correlation analysis was conducted to determine the relationship among the results, and a regression analysis was conducted to reveal the effect of the results on each other. In the wastes, DM values were between 0.53-9.71%, OM values were between 0.53-7.76%, N contents were between 0.10-0.74%, P contents were between 0.04-0.22%, K contents were between 0.15-0.56%, EC values were between 1.50-6.51 dSm^{-1}, B contents were between 16.96-34.63 mg kg^{-1}, and Na contents were between 0.11-0.40%. A correlation analysis was conducted to reveal the relationship of OM and DM to other parameters. OM content had a significant correlation with N (73.9%), P (80.4%9, Fe (71.4%), Mn (75.7%), EC (53.2%), K (60.7%), and Mg at 72.1%. The DM contents had a significant correlation with N (68.2%), P (95.4%), Cu (60.0%), Fe (88.2%), Mn (94.3%), Zn (67.5%), EC (76.1%), K (81.4%), and Mg at 83.9%. A significant regression model and the variances of DM and OM variables were 37.8 and 24.8% for N (%), 61.7 and 31.5% for P (%), 53.9 and 22.4% for K (%), 46.6 and 23.8% for Ca (%), and 70.0 and 45.7% for Mg (%), respectively. Finally, these observations should be used to demonstrate the usability of liquid fermented wastes for agricultural purposes.

Keywords: Biogas, slurry, dry matter, organic matter, correlation, regression.

Introduction

Interest in the anaerobic digestion of organic wastes is gaining more and more attention for helping to reduce greenhouse gas emissions and facilitating the sustainable development of biogas production and energy supplies. It has been observed that as a result of the daily increases in agricultural activities based on the increase in the population and the investments made in agriculture, large amounts of agricultural biomass wastes are being released.

Biogas power plants are one of the most suitable alternatives for eliminating the negative effects of these wastes on soil and surface waters by processing manure and other organic wastes from livestock and creating a waste management plan. Nearly 19,000 biogas plants operating in Europe and investments in these plants have increased in recent years. The biogas industry has the potential to reduce greenhouse gas emissions worldwide by 10-13% and create jobs for thousands of people by 2050 by increasing the volume of renewable energy sources (Anonymous, 2021).

Biogas power plants produce clean energy from waste and are indispensable disposal facilities for modern, sustainable, environmental policies that not only generate electricity from natural resources, such as renewable energy facilities but are also taken under record. Biogas facilities are important in terms of finding

: https://doi.org/10.18393/ejss.1177712
: http://ejss.fesss.org/10.18393/ejss.1177712
Publisher : Federation of Eurasian Soil Science Societies
e-ISSN : 2147-4249

solutions to the energy deficit of Turkey, preventing environmental pollution, and serving the liberation of the major agricultural areas of the country that are about to experience desertification; however, the industry is already facing the issue of what to do with the liquid fermented wastes. Biogas facilities for the use of liquid fermented products in agricultural areas are attempting to resolve the issues within their means and knowledge within their regions. The Ministry of Environment and Urbanization and the Ministry of Agriculture and Forestry, who are the investigators of these issues, evaluate them from their perspective and have different legislation for implementation. In addition, the high cost of pasteurization of the wastes from biogas enterprises and the lack of standard quality and the continuity of security for the raw material source are the main problems of the biogas sector in Turkey. The most important of these problems is how to evaluate the liquid fermented waste. Under current conditions, the current use and storage methods of liquid waste in agriculture cause significant environmental problems. This rich byproduct has the potential to seriously pollute the environment if not appropriately handled (Yan et al., 2019). Many environmental problems are created from the irresponsible use of these wastes (Nasir et al., 2012).

Biogas slurry/waste is defined as an easily absorbable byproduct of plants, rich in macro- and micronutrients, such as N, P, and K, also known as anaerobic digestion products (Wang et al., 2018). The nutritional content of this waste may change depending on the raw material and anaerobic process. It has been stated that the composition of these slurries from biogas power plants generally comprises 93-99% water and 1-7% dry matter (DM), most of which are organic but some of which inorganic (Stinner et al., 2008; Fouda et al., 2013; Wentzel and Joergensen, 2016).

The current system in biogas facilities is continuously fed. The products released are separated into solid and liquid phases. The solid waste is fermented biogas fertilizer, while the liquid waste is ~200 T d^{-1} for every 1 MWh. Considering the power of biogas plants operating in Turkey at 150 MWh, ~10.950.000 m^3 of waste is generated annually. With the foresight that this amount of waste will continue to increase each day, the resulting wastes must be well identified and characterized to create a sustainable management plan. If not, the damage to the environment will be considerably greater.

One example of the negative effects of fermented wastes has to do with the negative effects on the soil of applying higher than the recommended doses of fertilizer, depending on the content of the waste, the creation of diseases as a result of this application without pathogen removal, and the effect of high doses on climate change by increasing N_2O and releasing ammonia (Warnars and Oppenoorth, 2014). Some studies conducted on biogas wastes have considered such criteria as nutritional value, compliance with hygiene legislation, application time, application method, effects on climate change, and economic value when evaluating the products of fermentation from biogas plants (Al Seadi et al., 2013; Dahlin et al., 2017; Herbes et al., 2020). Without determining these properties, no wastes should be delivered directly to the soil or the environment.

The characteristics of the wastes may change at the end of the production processes based on the properties of the raw material used or the protocols of the biogas plant operations. For example, thermal pretreatment may be suitable for protein-rich waste but not for lipid-rich waste. The products released can be different depending on waste composition and quality. Certain features, such as high moisture content of the wastes, low energy density, storage requirements, and deterioration during storage, reveal the importance of determining the waste characteristics (Egieya et al., 2018). It is of great importance to determine waste quality for a sustainable evaluation.

In the present study, liquid fermented biogas wastes taken from 15 biogas plants licensed within different regions of Turkey were used. The aim of the present study was to (i) determine and characterize the liquid fermented biogas wastes, (ii) determine the waste pathogenicity, and (iii) obtain information about the nature of the waste by making certain inferences based on the data obtained.

Material and Methods

Collection and preparation of biogas wastes

Biogas liquid fermented wastes were taken from the lagoons of 15 licensed biogas plants located within different regions of Turkey and saved in clean polyethylene containers 40 cm high by 15 cm in diameter with the mouth of the container open and the container placed upside down at a distance of at least 1 m. After collecting the waste, we measured ~5 L after removing any air (e.g., it's the mouth was tightly closed and wrapped with aluminum foil). The sampled liquid fermented wastes were carefully transported to the Department of Soil Science and Plant Nutrition Laboratories, Ankara University and stored at 4 ^oC (liquid fermented wastes were kept until the analysis was completed) in the fridge.

Composition of biogas wastes

The composition of the liquid fermented wastes taken from the biogas plants comprised animal manure (13 samples) and urban wastes (2 samples). The samples were first filtered to remove the coarse particles in the

waste and then kept at 4°C before the analysis process. Some of the chemical properties of the liquid fermented wastes are shown in Table 1. In determining the wastes composition, moisture (%), dry matter (DM, %), organic matter (OM, %), pH (1:10), EC (1:10), total N (%), P (%), Ca (%), Mg (%), K (%), Na (%), Fe (mg kg^{-1}), Zn (mg kg^{-1}), Cu (mg kg^{-1}), Mn (mg kg^{-1}), B (mg kg^{-1}), Cd (mg kg^{-1}), Cr (mg kg^{-1}), Pb (mg kg^{-1}) and Ni (mg kg^{-1}) were analyzed.

Standard methods commonly used in liquid fermented wastes were used to determine the basic properties of the slurries examined in the study as follows: The moisture and dry matter (DM) content of the slurry was determined by oven drying at 70 °C. Organic matter content (OM) in the slurry was determined after ashing in an oven at 550°C and weighing (Bauer et al., 2009). pH and electrical conductivity (EC) in a 1:10 slurry/water mixture were determined as potentiometrically (Jackson, 1958); total nitrogen (N) by Kjeldahl method (Bremner, 1965); slurry samples digested with HNO_3-$HClO_4$ acid mixture (Kalra, 1997). Total P, Ca, Mg, K, Na, Fe, Zn, Cu, Mn, B, Cd, Cr, Pb, and Ni in the acid digest concentrations were determined by ICP-OES (Perkin Elmer Optima 2100 DV, Waltham, MA, USA).

Biogas liquid fermented wastes were analyzed for pathogens in their original state and after the heat treatment at 70°C for 1 h; *Salmonella*, *Escherichia coli* (*E. coli*), *E. coli* O157:H7, and *Enterobacteria* presence were analyzed.

Determination of *Salmonella*:

Salmonella was determined using a 25 g or 1 mL sample and the following methods (Mooijman et al., 2019):

i. **Pre-enrichment:** 1 mL biogas sample was added to a nonselective liquid medium (buffered peptone water; BPW) and incubated at 37 ± 1°C for 18 ± 2 h.
ii. **Growth on selective media:** After pre-enrichment, 100 µL sample taken from the culture medium was diluted with phosphate-buffered saline (PBS) up to 10^{-6}, and 100 µL each dilution was transferred to xylose lysine deoxycholate (XLD) agar and inoculated using the smear plate method in bismuth sulfite agar medium. The agar plates were incubated at 37 ± 1°C for 24 ± 3 h.
iii. **Verification:** Colonies with a black center and black precipitate zone with a metallic glow around bismuth sulfite agar and colonies with a black center on XLD agar medium were determined to be *Salmonella*.

Determination of *E. coli*:

Escherichia coli was determined according to the following methods for 25 g or 1 mL samples:

i. **Pre-enrichment:** 1 mL biogas sample was added to BPW and incubated at 37 ± 1°C for 18 ± 2 h.
ii. **Growth on selective medium:** After pre-enrichment, 100 µL sample taken from the culture medium was diluted with PBS up to 10^{-6}, and 100 µL each dilution was transferred to eosin methylene-blue lactose sucrose (EMB) agar medium and smear inoculated. The agar plates were incubated at 37 ± 1°C for 24 ± 3 h.
iii. **Verification:** After incubation, the colonies with a violet color and greenish metallic glow with reflected light on the EMB agar medium were determined to be *E. coli* (Leininger et al., 2001).

Determination of *E. coli* O157:H7:

Escherichia coli O157:H7 was determined according to the following methods for 25 g or 1 mL samples:

i. **Pre-enrichment:** 1 mL biogas sample was taken onto tryptone soy liquid medium containing novobiocin and enriched at 41.5 ± 1°C for 6 h and then for 12-18 h.
ii. **Isolation:** After pre-enrichment, cefixime telluride sorbitol was inoculated on MacConkey agar (CT-SMAC) selective medium from the culture medium. The agar plates were incubated at 37°C for 18-24 h.
iii. **Verification:** MacConkey agar with sorbitol, cefixime, and tellurite inhibit the growth of most noncytotoxigenic *E. coli* strains and other strains of *E. coli* that cannot ferment sorbitol. Other microorganisms that can be confused with *E. coli* O157:H7 on traditional MacConkey agar with sorbitol were inhibited by CT-SMAC (Zadik et al., 1993). Sorbitol-negative colorless colonies formed on the CT-SMAC agar surface were determined to be *E. coli* O157:H7.

Determination of *Enterobacteriaceae*:

Enterobacteriaceae was determined by calculating the number in a 1 g or 1 mL sample. Inoculum suspensions were prepared using 10-fold dilutions of the sample taken from the test sample (ISO 21528).

i. **Inoculation using selective media:** 100 µL each of the prepared suspensions was taken and smeared on violet red bile glucose (VRBG) agar medium. The agar plates were incubated at 37°C for 24 ± 2 h.
ii. **Verification and calculation of colony-forming units:** After incubation, the red colonies surrounded by a reddish precipitate zone of 1-2 mm in diameter were counted as members of the *Enterobacteriaceae* family. Counted colonies were calculated according to the following formula:

cfu / g (mL) = average of two parallel plates x dilution factor

Statistical analyses

SPSS ver. 24.0 (IBM Corp., Armonk, NY, USA) was used for statistical analyses. While evaluating the obtained data, in addition to the descriptive statistical results (average, standard deviation, median, frequency, ratio, minimum, maximum), a Spearman's correlation analysis was conducted to determine the relationship among the measurements. A regression analysis was conducted to analyze the effects of the measurements on each other. Significance was determined at $p < 0.01$ and $p < 0.05$ levels.

Results and Discussion

The components and pathogen content values of the liquid fermented wastes are provided in Tables 1 and 2. Some of the physical properties were cloudy, clear, scented, odorless, and dense. We determined that the physical properties of the liquid wastes were considerably different based on the analysis results.

Table 1. Some chemical properties of liquid fermented wastes

No	Waste Type	Moisture	Dry matter	Organic matter	pH (1:10)	EC ds m^{-1} (1:10)	N	P	K	Ca	Mg	Na	Fe	Zn	Cu	Mn	B	Cd	Cr	Pb	Ni
		(%)					(%)						(mg kg^{-1})								
1	Manure	94.68	5.32	4.63	8.51	1.74	0.24	0.09	0.33	0.28	0.09	0.16	404	16.29	6.21	19.31	17.59	3.19	5.43	3.45	3.62
2	Manure	98.16	1.84	1.83	8.93	2.44	0.43	0.09	0.25	0.20	0.01	0.11	134	22.59	3.29	11.96	16.96	2.34	4.11	2.59	2.72
3	Manure	99.47	0.53	0.53	8.59	1.63	0.14	0.04	0.15	0.20	0.02	0.14	73.41	6.88	2.68	5.43	21.45	2.68	4.64	2.97	2.97
4	Urban	94.25	5.75	3.31	8.88	5.10	0.74	0.22	0.36	0.54	0.09	0.27	376	48.15	10.19	32.13	34.63	3.52	6.85	6.57	4.72
5	Manure	96.50	3.50	2.87	8.52	2.27	0.29	0.09	0.38	0.67	0.07	0.24	151	11.42	4.15	14.06	25.09	3.49	6.04	4.06	3.96
6	Manure	93.21	6.79	2.38	8.86	4.00	0.36	0.19	0.47	0.60	0.19	0.40	1638	32.25	10.78	37.16	27.55	3.53	6.57	4.02	4.80
7	Urban	98.64	1.36	1.36	8.67	1.50	0.25	0.05	0.21	0.15	0.02	0.31	78.89	6.67	1.94	3.89	33.43	3.43	5.83	3.89	3.98
8	Manure	97.96	2.04	1.19	8.86	1.82	0.10	0.09	0.31	0.20	0.02	0.18	199	23.80	4.10	6.40	29.20	3.70	6.40	4.10	4.20
9	Manure	94.53	5.47	2.93	8.89	3.31	0.62	0.11	0.56	0.40	0.03	0.22	298	46.83	9.13	27.46	22.86	2.94	4.92	3.10	3.73
10	Manure	96.84	3.16	1.20	8.75	2.19	0.12	0.06	0.43	0.27	0.04	0.32	322	104	33.17	22.31	27.40	8.27	11.73	8.75	9.04
11	Manure	98.88	1.12	0.47	5.62	1.84	0.11	0.06	0.16	0.23	0.02	0.25	60.00	18.80	9.10	9.40	26.90	8.60	12.20	8.90	8.70
12	Manure	98.51	1.49	0.82	7.87	2.05	0.10	0.06	0.17	0.22	0.04	0.24	86.50	17.60	7.50	8.30	25.20	8.50	11.70	9.00	8.60
13	Manure	90.29	9.71	7.76	8.08	3.12	0.48	0.16	0.42	0.48	0.16	0.33	381	35.60	8.00	37.30	28.38	6.80	5.10	5.60	5.20
14	Manure	93.35	6.65	4.65	8.56	3.27	0.40	0.14	0.38	0.55	0.09	0.26	457	34.5	14	35.9	21.30	n.d.	8.40	4.70	4.30
15	Manure	94.54	5.46	2.81	8.73	6.51	0.48	0.10	0.40	0.53	0.07	0.26	753	26.00	26.60	27.90	25.00	n.d.	1.40	0.60	2.10

n.d.: not determined

Table 2. Pathogen values of liquid fermented wastes

No	Waste Type	Before70°C *E.coli* (cfu mL^{-1})	After 70°C *E.coli*	Before 70°C *E.coli* O157:H7	After 70°C *E.coli* O157:H7	Before 70°C *Salmonella* (cfu mL^{-1})	After 70°C *Salmonella*	Before 70°C *Enterobacteriaceae* (cfu mL^{-1})	After 70°C *Enterobacteriaceae*
1	Manure	None	None	None	None	None	None	4.4 x 10^4	None
2	Manure	Present (1.12 x 10^4)	None	None	None	Present (4.55 x 10^3)	None	1.45 x 10^5	None
3	Manure	Present (4.8 x 10^3)	None	None	None	None	None	8.4 x 10^4	None
4	Urban	Present (6.55 x 10^3)	None	None	None	Present (1.05 x 10^3)	None	5.1 x 10^4	None
5	Manure	Present (9.75 x 10^3)	None	None	None	Present (4 x 10^3)	None	2.42 x 10^4	None
6	Manure	Present (4 x 10^2)	None	None	None	Present (4 x 10^2)	None	2.11 x 10^4	None
7	Urban	Present (9 x 10^2)	None	None	None	Present (4 x 10^2)	None	5.4 x 10^4	None
8	Manure	Present (3.7 x 10^3)	None	None	None	Present (1.05 x 10^3)	None	3 x 10^4	None
9	Manure	Present (4.9 x 10^3)	None	None	None	Present (5 x 10^3)	None	7.4 x 10^4	None
10	Manure	None	None	None	None	Present (2 x 10)	None	1.46 x 10^5	None
11	Manure	Present (3.6 x 10^2)	None	None	None	None	None	4.6 x 10^4	None
12	Manure	Present (1.59 x 10^5)	None	None	None	Present (1.15 x 10^4)	None	4.7 x 10^5	None
13	Manure	Present (7 x 10^2)	None	None	None	None	None	4.75 x 10^3	None
14	Manure	Present (1.8 x 10^4)	None	None	None	Present (1.45 x 10^3)	None	4.55 x 10^5	None
15	Manure	Present (4.2 x 10^3)	None	None	None	None	None	7.3 x 10^3	None

E. coli: *Escherichia coli;* cfu: colony forming unit.

Because the substrate mixtures used in biogas production were very heterogeneous in terms of plant nutrients and OM composition, their chemical composition was also very diverse. The DM content of the liquid fermented wastes varied considerably, and the DM amounts varied between 0.53-9.71%. The OM content of the liquid wastes were between 0.53-7.76%. The pH of the liquid fermented wastes was slight to strongly alkaline. The EC values of the liquid fermented wastes were between 1.50-6.51 dS m^{-1}. The total N contents of the liquid wastes were between 0.10-0.74%, P contents were between 0.04-0.22%, and K contents were between 0.15-0.56%. The B contents of the liquid wastes were between 16.96-34.63 mg kg^{-1}, and the Na contents were between 0.11-0.40%. The Fe contents of the liquid wastes were between 60.00-1638 mg kg^{-1} and the Mn contents were between 3.89-37.30 mg kg^{-1}. The Cd, Cu, Cr, Ni, Pb, and Zn contents of the liquid fermented wastes were below the limits determined by the "Regulation on Organic, Mineral and Microbial Originated Fertilizers Used in Agriculture" (Tables 1 and 3).

Correlation analyses

OM and DM contents of the fermented liquid biogas wastes are the main characteristics taken into consideration in the evaluation of wastes. In addition, these two parameters can be determined easily and quickly; therefore, correlation analyses were conducted to reveal the OM and DM relationships with other parameters.

Table 3. Distribution of statistical parameters

Parameters	Mean	Standard deviation	Maximm	Minimum	Median	Skewness	Kurtosis
Moisture (%)	96.0	2.7	99.5	90.3	96.5	-0.515	-0.451
Dry Matter (%)	4.0	2.7	9.7	0.5	3.5	0.515	-0.451
Organic Matter (%)	2.6	2.0	7.8	0.5	2.4	1.372	2.271
pH (1:10)	8.4	0.8	8.9	5.6	8.7	-3.095	9.460
EC (1:10)	2.9	1.4	6.5	1.5	2.3	1.509	1.979
N (%)	0.3	0.2	0.7	0.1	0.3	0.618	-0.401
P (%)	0.1	0.1	0.2	0.0	0.1	0.953	0.155
K (%)	0.3	0.1	0.6	0.1	0.4	-0.076	-0.725
Ca (%)	0.4	0.2	0.7	0.1	0.3	0,452	-1.480
Mg (%)	0.1	0.1	0.2	0.0	0.0	1.162	0.677
Na (%)	0.2	0.1	0.4	0.1	0.2	0.130	0.014
Fe (mg kg^{-1})	360.9	401.1	1638.2	60.0	297.7	2.588	7.773
Zn (mg kg^{-1})	30.1	24.0	103.7	6.7	23.8	2.198	6.189
Cu (mg kg^{-1})	10.1	8.8	33.2	1.9	8.0	1.828	3.015
Mn (mg kg^{-1})	19.9	12.3	37.3	3.9	19.3	0.181	-1.603
B (mg kg^{-1})	25.5	5.0	34.6	17.0	25.2	0.030	-0.171
Cd (mg kg^{-1})	0.5	0.2	0.9	0.2	0.4	0.951	-0.989
Cr (mg kg^{-1})	6.8	3.1	12.2	1.4	6.0	0.616	0.003
Pb (mg kg^{-1})	4.8	2.5	9.0	0.6	4.1	0.562	-0.351
Ni (mg kg^{-1})	4.8	2.2	9.0	2.1	4.2	1.116	0.161

Table 4. Distribution of statistical parameters of animal manure and urban waste

Type of waste	Parameters	Mean	Standard Deviation	Maximum	Minimum	Median
Manure waste	Moisture (%)	95.9	2.7	99.5	90.3	96.5
	Dry Matter (%)	4.1	2.7	9.7	0.5	3.5
	Organic Matter (%)	2.6	2.1	7.8	0.5	2.4
	pH (1:10)	8.4	0.9	8.9	5.6	8.6
	EC (1:10)	2.8	1.3	6.5	1.6	2.3
	N (%)	0.3	0.2	0.6	0.1	0.3
	P (%)	0.1	0.0	0.2	0.0	0.1
	K (%)	0.3	0.1	0.6	0.1	0.4
	Ca (%)	0.4	0.2	0.7	0.2	0.3
	Mg (%)	0.1	0.1	0.2	0.0	0.0
	Na (%)	0.2	0.1	0.4	0.1	0.2
	Fe (mg kg^{-1})	381.4	424.9	1638.2	60.0	297.7
	Zn (mg kg^{-1})	30.5	24.5	103.7	6.9	23.8
	Cu (mg kg^{-1})	10.7	9.2	33.2	2.7	8.0
	Mn (mg kg^{-1})	20.2	12.0	37.3	5.4	19.3
	B (mg kg^{-1})	24.2	4.0	29.2	17.0	25.1
	Cd (mg kg^{-1})	0.5	0.3	0.9	0.2	0.4
	Cr (mg kg^{-1})	6.8	3.3	12.2	1.4	6.0
	Pb (mg kg^{-1})	4.8	2.6	9.0	0.6	4.1
	Ni (mg kg^{-1})	4.9	2.4	9.0	2.1	4.2
Urban waste	Moisture (%)	96.4	3.1	98.6	94.3	96.4
	Dry Matter (%)	3.6	3.1	5.7	1.4	3.6
	Organic Matter (%)	2.3	1.4	3.3	1.4	2.3
	pH (1:10)	8.8	0.2	8.9	8.7	8.8
	EC (1:10)	3.3	2.6	5	1.5	3.3
	N (%)	0.5	0.3	0.7	0.3	0.5
	P (%)	0.1	0.1	0.2	0.1	0.1
	K (%)	0.3	0.1	0.4	0.2	0.3
	Ca (%)	0.3	0.3	0.5	0.1	0.3
	Mg (%)	0.1	0.0	0.1	0.0	0.1
	Na (%)	0.3	0.0	0.3	0.3	0.3
	Fe (mg kg^{-1})	227.6	210.4	376.4	78.9	227.6
	Zn (mg kg^{-1})	27.4	29.3	48.2	6.7	27.4
	Cu (mg kg^{-1})	6.1	5.8	10.2	1.9	6.1
	Mn (mg kg^{-1})	18.0	20.0	32.1	3.9	18.0
	B (mg kg^{-1})	34.0	0.9	34.6	33.4	34.0
	Cd (mg kg^{-1})	0.3	0.0	0.4	0.3	0.3
	Cr (mg kg^{-1})	6.3	0.7	6.8	5.8	6.3
	Pb (mg kg^{-1})	5.2	1.9	6.6	3.9	5.2
	Ni (mg kg^{-1})	4.3	0.5	4.7	4.0	4.3

The OM content, in a positive direction, had a significant correlation with N at 73.9%, P at 80.4%, Fe at 71.4%, Mn at 75.7%, EC at 53.2%, K at 60.7%, and Mg at 72.1% (Figure 1). The numbers obtained show the correlation coefficient between the organic matter and the determined parameters. This order was determined as P > Mn > N > Mg > Fe > K > EC. There was no statistically significant relationship between OM and Cd, Cr, Cu, Ni, Pb, and Zn, or pH parameters ($p > 0.05$). This order given is based on the highest positive correlation coefficient between the organic matter and the determined parameters.

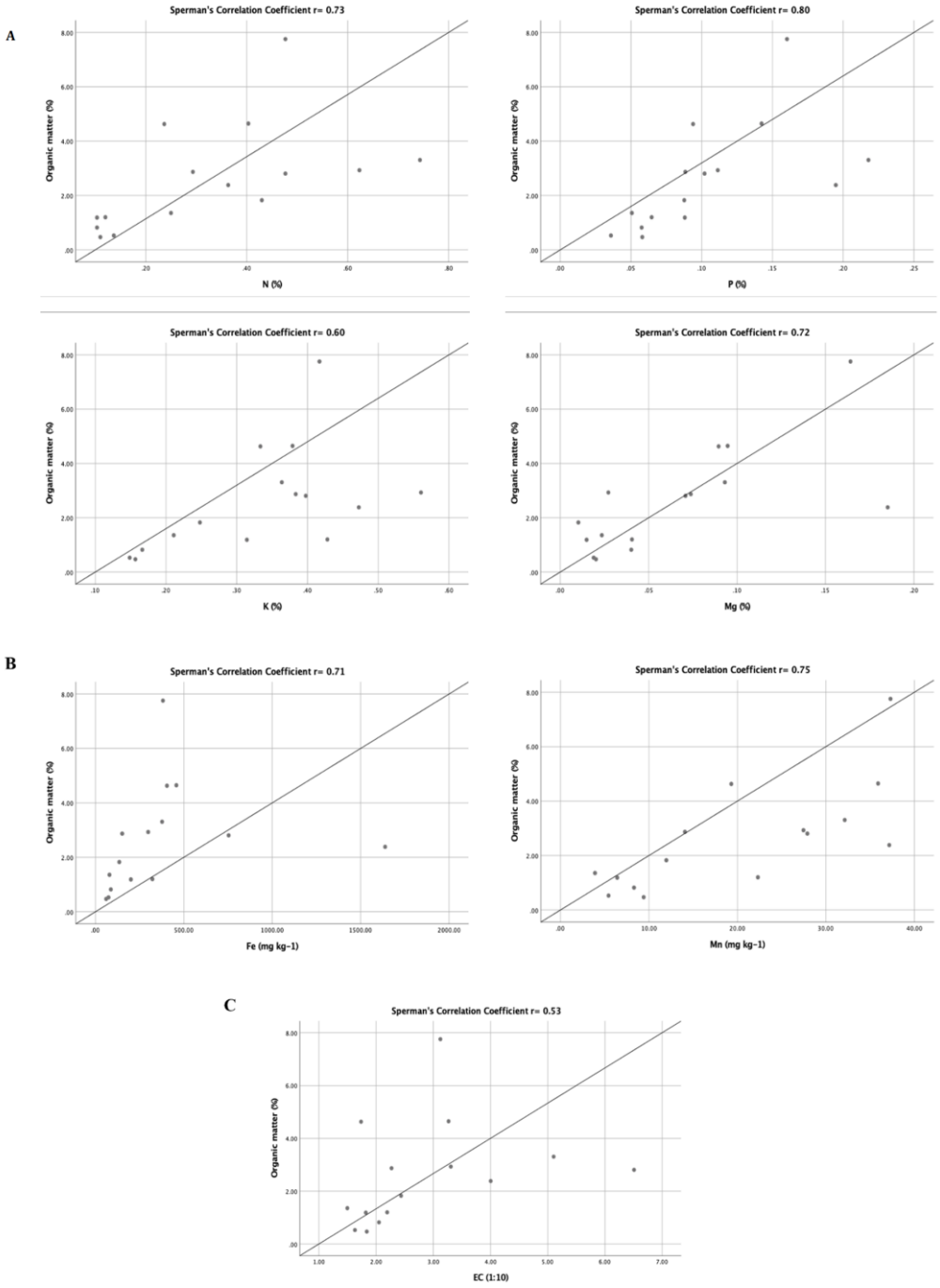

Figure 1. The relationship of organic matter with macro elements (A), micro elements (B) and EC (C)

Correlation analyses

OM and DM contents of the fermented liquid biogas wastes are the main characteristics taken into consideration in the evaluation of wastes. In addition, these two parameters can be determined easily and quickly; therefore, correlation analyses were conducted to reveal the OM and DM relationships with other parameters. The OM content, in a positive direction, had a significant correlation with N at 73.9%, P at 80.4%, Fe at 71.4%, Mn at 75.7%, EC at 53.2%, K at 60.7%, and Mg at 72.1% (Figure 1). The numbers obtained show the correlation coefficient between the organic matter and the determined parameters. This order was determined as P > Mn > N > Mg > Fe > K > EC. There was no statistically significant relationship between OM and Cd, Cr, Cu, Ni, Pb, and Zn, or pH parameters ($p > 0.05$). This order given is based on the highest positive

correlation coefficient between the organic matter and the determined parameters. The DM content, in a positive direction, had a significant correlation with N at 68.2%, P at 95.4%, Cu at 60.0%, Fe at 88.2%, Mn at 94.3%, Zn at 67.5%, EC at 76.1%, K at 81.4%, and Mg at 83.9% (Figure 2). This order was determined as P > Mn > Fe > Mg > K > EC > N > Zn > Cu. There was no statistically significant relationship between DM and Cd, Cr, Ni, Pb, and pH parameters ($p > 0.05$).

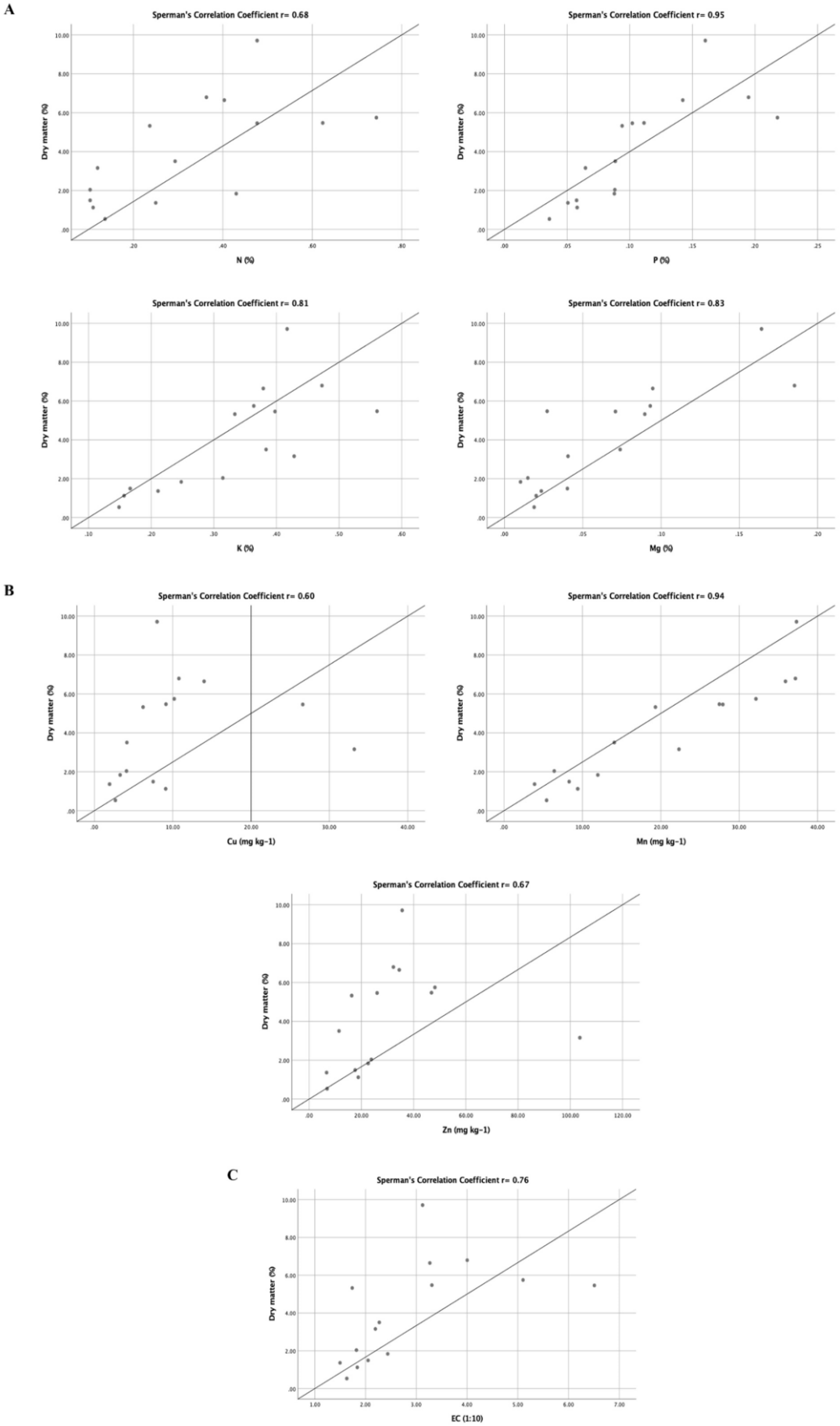

Figure 2. The relationship of dry matter with macro elements (A), micro elements (B) and EC (C)

Regression analysis

Regression analysis was conducted to predict how the independent variables affected the dependent variable in the parameters determined in the wastes. OM and DM contained in the fermented liquid biogas wastes as independent variables were examined for the reasons explained in section 3.1.

Table 5. Regression results of macro-elements in biogas waste according to dry matter and organic matter independent variables

N (%) **p < 0.01					
Independent variables	Univariate p-value	Odd's Ratio	95% C.I. for EXP(B) Lower	Upper	$R^2_{adjusted}$
Dry Matter	0.009	0.049	0.015	0.83	0.378
Organic Matter	0.034	0.056	0.005	0.108	0.248
P (%) **p < 0.01					
Independent variables	Univariate p value	Odd's Ratio	95% C.I. for EXP(B) Lower	Upper	$R^2_{adjusted}$
Dry Matter	0.001	0.016	0.009	0.023	0.617
Organic Matter	0.017	0.016	0.003	0.030	0.315
K (%) **p < 0.01					
Independent variables	Univariate p value	Odd's Ratio	95% C.I. for EXP(B) Lower	Upper	$R^2_{adjusted}$
Dry Matter	0.001	0.035	0.017	0.053	0.539
Organic Matter	0.043	0.033	0.001	0.065	0.224
Ca (%) **p < 0.01					
Independent variables	Univariate p value	Odd's Ratio	95% C.I. for EXP(B) Lower	Upper	$R^2_{adjusted}$
Dry Matter	0.003	0.047	0.019	0.075	0.466
Organic Matter	0.037	0.049	0.003	0.094	0.238
Mg (%) **p < 0.01					
Independent variables	Univariate p value	Odd's Ratio	95% C.I. for EXP(B) Lower	Upper	$R^2_{adjusted}$
Dry Matter	0.001	0.017	0.011	0.024	0.700
Organic Matter	0.003	0.019	0.008	0.031	0.457

C.I.: confidence interval; EXP:Exponentiation

A regression analysis was conducted to estimate the values of N, P, K, Ca, and Mg using the results of DM and OM parameters found in the biogas waste. A significant regression model and variances of DM and OM variables were 37.8% ($R^2_{adjusted}$ = 0.37) and 24.8% ($R^2_{adjusted}$ = 0.24) for N (%), 61.7% ($R^2_{adjusted}$ = 0.61) and 31.5% ($R^2_{adjusted}$ = 0.31) for P (%),53.9% ($R^2_{adjusted}$ = 0.53) and 22.4% ($R^2_{adjusted}$ = 0.22) for K (%), 46.6% ($R^2_{adjusted}$ = 0.46) and 23.8% ($R^2_{adjusted}$ = 0.23) for Ca (%), and 70.0% ($R^2_{adjusted}$ = 0.70) and 45.7% ($R^2_{adjusted}$ = 0.45) for Mg (%). According to these data, the DM and OM parameters and macro-elements can be predicted to be positive and significant (Table 5). Also according to these data, the DM result can be estimated to be sorted as Mg (70%) > P (61.7%) > K (53.9%) > Ca (46.6%) > N (37.8%). The OM result can be estimated to be sorted as Mg (45.7%) > P (31.5%) > N (24.8%) > Ca (23.8%) > K (22.4%). As a result of the regression analysis, the DM and OM parameters, micro element and the heavy metal analyses, no significant regression model was found for Fe, Zn, Cu, Mn, B, Cd, Cr, Pb or Ni parameters ($p > 0.05$).

Conclusion

The present study evaluated the liquid fermented wastes after production from 15 biogas plants (2 urban, 13 manure) being actively produced in Türkiye. The evaluation of the biogas liquid fermented wastes is one of the important factors in the construction of biogas plants. In the evaluation of these liquid wastes, it is possible that they can be considered as organic input and used in agricultural production; however, the properties of the liquid fermented waste is an important issue. In general, the type of waste used in the process of producing biogas the quality of that waste is based on the properties of the liquid fermented waste. The pathogen problem is important in liquid fermented wastes, especially those obtained from animals, and sound sanitation protocols are methods by which to overcome this problem. The fact that 15 plants contained important pathogens in the liquid fermented waste before sanitation and that no pathogenic microorganisms that may pose any risk were found after sanitizing at 70°C reveals the importance of sanitation. Because of some economic concerns, this process is not applied in biogas facilities; therefore, its release and application to the lands without pathogen removal should be strictly controlled. Another negative factor to using biogas liquid fermented wastes is their salt content. EC values in original liquid fermented waste samples, which give the total soluble salt content, can be high enough to limit agricultural use. The EC values of the 15 biogas liquid fermented wastes considered within the scope of the present study were within the range of 13-30 dS m^{-1} in the original samples. This factor should not be ignored over long-term and overlapping applications of liquid fermented wastes to the soils. The most important properties in the application of liquid fermented wastes

are the OM and DM amounts. Detection of these two parameters is both easy and fast; therefore, OM and DM parameters were considered independent variables, and correlation and regression analyzes were conducted to estimate the distribution of macro-and micronutrients and heavy metals, which affect crop production and productivity, based on the presence of these two parameters. According to the results, DM and OM parameters, and macro-elements can be predicted significantly. The amount of macro-elements in the liquid fermented waste varied depending on the increase and decrease in OM and DM. On the other hand, a significant correlation and a regression model were not determined between OM and DM and their heavy metal contents. It is important to determine the pathogenicity, EC values, and OM and DM contents in studies to determine the usability of liquid fermented wastes for agricultural purposes.

Acknowledgements

We thank Berfu Arıkan, Ozge Gun, and Murat Aksit for assistance in the laboratory and data analysis. We are also grateful to "Biyotar Corp." and "Renewable Energy and Environmental Technologies Cluster" for providing the necessary facilities for undertaking this research. This study was supported by the "Investıgatıon of the Agricultural Usage Potential of Liquid Fermented Products From Biogas Power Plants" project.

References

Al Seadi, T., Drosg, B., Fuchs, W., Rutz, D., Janssen, R., 2013. Biogas digestate quality and utilization. In: The biogas handbook. The Biogas Handbook : Science, Production and Applications. Wellinger, A., Murphy, J., Baxter, D. (Eds.). Woodhead Publishing, pp. 267-301.

Anonymous, 2021. European Biogas Association: Number of Biogas Plants in Europe. Available at [Acces date: 01.06.2021]. https://www.europeanbiogas.eu/the-contribution-of-the-biogas-and-biomethane-industries-to-medium-term-greenhouse-gas-reduction-targets-and-climate-neutrality-by-2050/

Bauer, A., Mayr, H., Hopfner-Sixt, K., Amon, T., 2009. Detailed monitoring of two biogas plants and mechanical solid-liquid separation of fermentation residues. *Journal of Biotechnology* 142(1): 56-63.

Bremner, J.M., 1965. Total nitrogen, In: Methods of soil analysis. Part 2. Chemical and microbiological properties. Black, C.A., Evans, D.D., White, J.L., Ensminger, L.E., Clark F.E. (Eds.), Soil Science Society of America. Madison, Wisconsin, USA. pp. 1149-1176.

Dahlin, J., Nelles, M., Herbes, C., 2017. Biogas digestate management: Evaluating the attitudes and perceptions of German gardeners towards digestate-based soil amendments. Resources, *Conservation and Recycling* 118: 27-38.

Egieya, J.M., Cucek, L., Zirngast, K., Isafiade, A.J., Pahor, B., Kravanja, Z., 2018. Biogas supply chain optimization considering different multi-period scenarios. *Chemical Engineering Transactions* 70: 985-990.

Fouda, S., von Tucher, S., Lichti, F., Schmidhalter, U., 2013. Nitrogen availability of various biogas residues applied to ryegrass. *Journal of Plant Nutrition and Soil Science* 176(4): 572-584.

Herbes, C., Roth, U., Wulf, S., Dahlin, J., 2020. Economic assessment of different biogas digestate processing technologies: A scenario-based analysis. *Journal of Cleaner Production* 255: 120282.

ISO 21528-1, Microbiology of the food chain-Horizontal method for the detection and enumeration of *Enterobacteriaceae*-Part 1: Detection of *Enterobacteriaceae.*

Jackson, M.L. 1958. Soil Chemical Analysis. Prentice Hall Inc., Englewood Chiffs, 498p.

Kalra, Y. 1997. Handbook of reference methods for plant analysis. CRC press. 300p.

Leininger, D.J., Roberson, J.R., Elvinger, F., 2001. Use of eosin methylene blue agar to differentiate *Escherichia coli* from other gram-negative mastitis pathogens. *Journal of Veterinary Diagnostic Investigation* 13(3): 273-275.

Mooijman, K.A., Pielaat, A., Kuijpers, A.F.A., 2019. Validation of EN ISO 6579-1- Microbiology of the food chain-Horizontal method for the detection, enumeration and serotyping of *Salmonella* - Part 1 detection of *Salmonella* spp. *International Journal of Food Microbiology* 288: 3-12.

Nasir, I.M., Ghazi, T.I.M., Omar, R., 2012. Production of biogas from solid organic wastes through anaerobic digestion: a review. *Applied Microbiology and Biotechnology* 95(2): 321-329.

Stinner, W., Moller, K., Leithold, G., 2008. Effects of biogas digestion of clover/grass-leys, cover crops and crop residues on nitrogen cycle and crop yield in organic stockless farming systems. *European Journal of Agronomy* 29(2-3): 125-134.

Wang, H., Xu, J., Sheng, L., Liu, X., 2018. Effect of addition of biogas slurry for anaerobic fermentation of deer manure on biogas production. *Energy* 165: 411-418.

Warnars, L., Oppenoorth, H., 2014. Bio slurry: A supreme fertilizer. A study on bio slurry results and uses. Hivos People Unlimited, FSC. Hague, Netherlands. 49p.

Wentzel, S., Joergensen, R.G., 2016. Quantitative microbial indices in biogas and raw cattle slurries. *Engineering in Life Sciences* 16(3): 231-237.

Yan, L., Liu, Q., Liu, C., Liu, Y., Zhang, M., Zhang, Y., Gu, W., 2019. Effect of swine biogas slurry application on soil dissolved organic matter (DOM) content and fluorescence characteristics. *Ecotoxicology and Environmental Safety* 184: 109616.

Zadik, P.M., Chapman, P.A., Siddons, C.A., 1993. Use of tellurite for the selection of verocytotoxigenic *Escherichia coli* O157. *Journal of Medical Microbiology* 39(2): 155-158.

Eurasian Journal of Soil Science 2023, 12(1), 19 - 27

Eurasian Journal of Soil Science

Journal homepage : http://ejss.fesss.org

Seasonal fluctuations in phthalates' contamination in pond water: A case study

Sneh Rajput [a], Arpna Kumari [a,b], Ritika Sharma [a], Vishnu D. Rajput [b], Tatiana Minkina [b], Saroj Arora [c], Rajinder Kaur [c,*]

[a] Department of Botanical and Environmental Sciences, Guru Nanak Dev University, Amritsar, Punjab, India
[b] Southern Federal University, Academy of Biology and Biotechnology, Rostov-on-Don, Russia
[c] Department of Botanical and Environmental Sciences, Guru Nanak Dev University, Amritsar, Punjab, India

Article Info

Received : 09.05.2022
Accepted : 07.09.2022
Available online : 28.09.2022

Author(s)

S.Rajput
A.Kumari
R.Sharma
V.D. Rajput
T.Minkina
S.Arora
R.Kaur *

* Corresponding author

Abstract

Phthalates are endocrine disruptors, reported to cause deformities and reproductive damages in animals. Numerous studies reported the presence of phthalates in water samples of rivers, wetlands, and estuaries, while the scenario in case of ponds is different, however they are reported as an integral part of biosphere. In this study, the level of phthalates' contamination in the water samples collected from the different ponds of Amritsar district for four consecutive seasons in two years was analysed. The maximal level of phthalate contamination was found in samples collected during the monsoon season (July 2015) of first year of sampling followed by post-monsoon (October 2015) and winter season (January 2016). S8 sampling site was found to be the most phthalate contaminated site followed by S1=S11>S2=S9=S4=S5=S7>S6=S3>S10. Benzyl butyl phthalate was most abundant (found in 32% water samples) followed by di-n-butyl and dimethyl phthalate, while diallyl phthalate and diethyl phthalate were not detected. The two main drivers for these seasonal variations were observed to be temperature and precipitation. Hence, this data will be useful to explain the temporal and spatial distributions of phthalates in aquatic ecosystem, as well as to devise cost-effective ways to reduce their ecological footprints.

Keywords: Ponds, endocrine disruptor, plasticizers, priority contaminants, HPLC analysis.

Introduction

Plastic industry is significantly expanding with 368 million tons of production since 2019 (Prevarić et al., 2021). Phthalates are a well-known class of plasticizers that are produced in vast amount alongside plastic (González-Sálamo et al., 2018). They are poorly water-soluble chemicals with low volatility and have been used in numerous industries for the production of plastic products, cosmetics, medical equipment, insect repellent, propellant, etc. They are used widely due to their strength, plasticity, cost-effectiveness, and durability (Kumari and Kaur, 2021). But indiscriminate usage of phthalates has contaminated the different environmental matrices (Tao et al., 2020; Weizhen et al., 2020; Zhang et al., 2021; Suresh and Jindal, 2022). In polyvinyl chloride plastics, rubber, cellulose, and styrene manufacturing for softness and flexibility, phthalates are documented as a primary plasticizer (Cao et al,. 2016; Gao and Wen, 2016). Phthalates have the ability to leach, migrate, and evaporate into the atmosphere during the manufacturing process, usage, and dumping of plastic waste as they are not chemically bonded which causes environmental pollution. Moreover, phthalates are not easily degraded by microorganisms leading to the widespread presence in sewage sludge, landfill, sediments, and various water bodies (Qu et al., 2015). High consumption rate, continuous release into the

: https://doi.org/10.18393/ejss.1181205
: http://ejss.fesss.org/10.18393/ejss.1181205
Publisher : Federation of Eurasian Soil Science Societies
e-ISSN : 2147-4249

environment, and resistance to microbial degradation is the main factors for their ubiquitous presence in the air, water, and food (Liu et al., 2014; Kumari and Kaur, 2020).

Humans get exposed to phthalates through different pathways like inhalation, ingestion, and direct contact through the skin which can cause developmental and reproductive toxicity. Once phthalates enter the human body, they are metabolized within hours to some days (Frederiksen et al., 2007). Exposure to these toxic substances can cause detrimental health effects including cardiovascular diseases, neuro disorders, alterations in metabolic activities, teratogenicity, etc. (Pirsaheb et al., 2022; Tran et al., 2022). Phthalates have endocrine-disrupting properties (Lyche et al., 2009) and higher concentrations can cause cancer, fetal death, injuries to the liver and kidney, deformities in the body, and reproductive damage in animals (Kay et al., 2014; Posnack, 2014; Kumari et al., 2020a). Furthermore, the United States Environmental Protection Agency (USEPA) has declared butyl benzyl phthalate (BBP), di-ethyl phthalate (DEP), dibutyl phthalate (DBP), di-(2-ethlyexyl) phthalate (DEHP), di-n-octyl phthalate and dimethyl phthalate (DMP) as priority pollutants out of 25 phthalate esters available in the market (Semenov et al., 2021; Wang et al., 2021).

Among the various aquatic ecosystems, ponds are neglected. Several reports have documented the phthalate contamination in zooplankton, wastewater, sediments, river water, wetlands, and estuaries (Li et al., 2017; Wang et al., 2017; Ramzi et al., 2018; Abtahi et al., 2019; Lee et al., 2020; Schmidt et al., 2021; Jönander et al., 2022) but few studies have been reported on phthalate contamination in ponds. Ponds are exceptional freshwater resources that exhibit self-sufficient and self-regulating ecosystems. They are a significant part of the water cycle and contribute to miscellaneous roles in the biosphere. Ponds contribute to regional biodiversity and act as steppingstones between aquatic ecosystems and landscapes (Hassal, 2014). The Ramsar convention and literature studies have defined ponds as wetlands and have also revealed the significance of ponds (Linton and Goulder, 2000). Thus, contamination of pond water by toxic chemicals is a serious ecological problem. Detailed studies on rivers and wetlands are being investigated by various researchers. However, studies on pond water bodies have been often neglected and only few studies are available in the literature mostly for physicochemical, metal, and pesticides analyses (Rehan et al., 2017; Rajput et al., 2017; Rajput et al., 2018; Kaur and Hundal, 2018; Rajput et al., 2019). Phthalates' detection in water bodies has been not reported earlier in the same geographical region but similar studies have been conducted by other researchers in the adjacent areas. For example, Ajay et al. (2021) reported the presence of phthalates in sediments samples collected from Lake Basin. Dibutyl phthalate and di(2-ethlyhexyl) phthalate were found to be ranged from 6-357 ng/g DW, which could be contributed to anthropogenic activities in the adjacent areas. Keeping in view, the research was carried out to investigate the presence of phthalic esters in pond water and its seasonal fluctuation over a period of two years using reverse-phase-ultra-high-performance liquid chromatography coupled with photodiode array detector as it has high sensitivity and selectivity for the determination of contaminants (Rajput et al., 2021).

Material and Methods

Study area

Amritsar is situated in the Majha region of Punjab which falls in the north-western part of India. It is located at 31.63° N and 74.87° E with an area of 2673 Km^2 and population density of 932. The region is characterized by semi-arid conditions. The year may be divided into four seasons: monsoon (July-September), post-monsoon (September-November), winter (December-March), and summer (April-June). Weather variations can be observed during different seasons. The heat during summer is intense with a maximum temperature of 48°C. Due to western disturbances; the region is affected by cold waves during the winter season. January is the coldest month with foggy conditions and the temperature drops down below the freezing point of water.

Sample collection

For the systematic collection of water samples, the map of the study area was prepared, and gridding was done (Figure 1). The sampling points were chosen with the help of GPS (Global positioning system). Eleven different locations were selected, and the codes were allotted to the sampling points (Table 1). Sampling was carried out from 2015-2017 in July 2015 (monsoon season), October 2015 (post-monsoon season), January 2016 (winter season), May 2016 (summer season), July 2016 (monsoon season), October 2016 (post-monsoon season), January 2017 (winter season) and May 2017 (summer season). The samples were collected in prewashed glass bottles. To prevent plastic contamination no plastic products were used during sampling and analysis. The collected samples were transferred to the laboratory immediately and stored at 4°C.

Extraction procedure

All the solvents (HPLC grade) were procured from Himedia Laboratories Private Limited (India). Dichloromethane and methanol were used as a solvent for the extraction of phthalates. An aliquot of 100 mL of each sample was taken in a separating funnel, and 10 mL of methanol and dichloromethane (1:1, v/v) was

added and shaken several times till an organic layer of 2 cm was formed. All the samples were extracted thrice, the obtained extract was reduced to 1.0 mL using a rotary evaporator and then the residue was dissolved in 2 mL acetonitrile followed by filtration using a 0.22 µm membrane filter.

Table 1. Sampling sites along with their coordinates.

Sampling site	Code	Coordinates	
		Latitude	Longitude
Baserke Gallan	S1	31°61'77" N	74°71'90" E
Ajnala	S2	31°84'00" N	74°76'00" E
Raja Sansi	S3	31°72'45" N	74°78'60" E
Manawala	S4	31°74'06" N	74°68'83" E
Majitha	S5	31°76'00" N	74°95'00" E
Lopoke	S6	31°71'70" N	74°63'27" E
Attari	S7	31°69'31" N	74°65'79" E
Jandiala	S8	31°58'93" N	75°05'68" E
Sathiala	S9	31°55'50" N	75°26'55" E
Mehta	S10	31°63'39" N	74°87'22" E
Kathunangal	S11	31°73'24" N	75°02'31" E

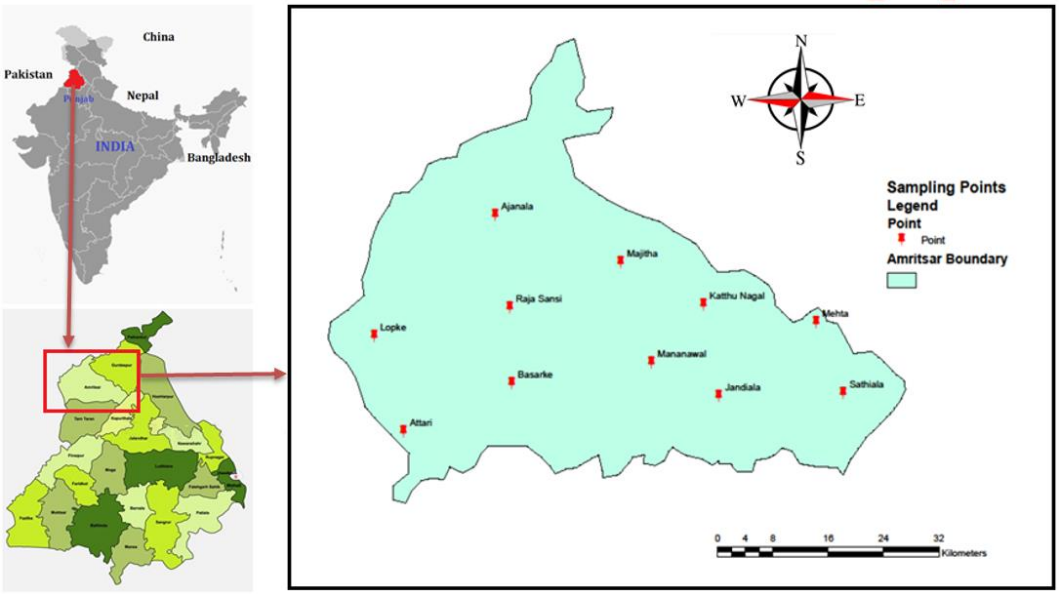

Figure 1. Map of the study area with sampling sites.

Phthalates estimation and chromatographic conditions

The quantification of phthalates (*i.e.,* dimethyl phthalate, diethyl phthalate, di-n-butyl phthalate, diallyl phthalate, benzyl butyl phthalate) in water samples was executed using a validated reverse-phase-ultra-high-performance liquid chromatography coupled with photodiode array detector (RP-UHPLC-PDA) (Kumari et al., 2020b). The stock solution (1000 mg/L) of phthalates was prepared in HPLC acetonitrile and working concentrations ranging from 2.5-1000 mg/L were prepared by serial dilution method. The operating conditions of HPLC for phthalate estimation are given in Table 2. The use of plastic or plastic products was avoided to evade the background contamination of phthalates as well as potential interference. The procedural blanks were included during the whole analytical procedure. The final concentrations of phthalates were corrected by excluding the concentrations if detected in procedural blanks (Kumari et al., 2020b). The values of limit of detection (LOD) were 0.69, 0.93, 0.68, 0.67, and 0.93 for BBP, DAP, DBP, DEP, and DMP, respectively. Correspondingly, the recorded values for limit of quantification (LOQ) were 2.08, 2.81, 2.05, 2.03, and 2.81 (Kumari et al., 2020b).

All the experiments were performed in triplicate and the results were expressed as mean ± standard error.

Table 2. Operating Conditions of HPLC for phthalate estimation (Kumari et al., 2020).

Phthalates	Dibutyl phthalate (DBP), Benzyl butyl phthalate (BBP) and Dimethyl phthalate (DMP), Diethyl phthalate (DEP), Diallyl phthalate (DAP)
Column and column temperature	C_{18} column and 40°C
Flow rate and injection volume	0.9 ml/min and 20 µL
Detection wavelength	226 nm

Results and Discussion

Urban water bodies are more prone to contaminated with different pollutants like phthalates due to the discharge of untreated effluents from industries and municipal sewage (Zeng et al., 2009). The half-life of phthalates in the aquatic environment can range from days to several weeks depending upon the environmental conditions and chemical structure of the phthalate (Staples et al., 1997). Phthalates enter surface water through non-point sources like disposal of plastic material, road runoff, aerosol deposition, industrial discharge, agricultural activities, etc. (Roslev et al., 2007). Phthalates can occur in the aquatic environment due to the lack of covalent bonding with the polymeric matrix which accelerates their presence in the environment. This release of phthalates in the environment can occur either during the industrial processes or by leakage from the final product (Gani et al., 2017). Humans get exposed to phthalate toxicity through different pathways like inhalation, ingestion, and direct contact through the skin which can cause developmental and reproductive toxicity. In this context, Wang et al. (2014) reported daily phthalate exposure ranging from 2.6 to 7.4 µg/kg/day from indoor air and dust. Phthalate exposure leads to higher concentrations of phthalate metabolites in urine, blood, and serum of human beings. These metabolites are formed in subsequent oxidation of parent phthalates to mono phthalate ester in the human body (Singh and Li, 2012). Benzyl-n-butyl is converted into monobenzyl phthalate. Net et al. (2015) found monobutyl phthalate (71.42 µg/L) in human urine.

The present study revealed the presence of different phthalates in pond water samples (Table 3). The effect of seasonal variations on phthalate concentration was also found in the study. It was observed that maximum phthalates were detected in the water samples collected during July 2015 (monsoon season) followed by October 2015 (post-monsoon season) and January 2016 (winter season). No phthalate was detected in the samples collected during January 2017 (the winter season of the second year of sampling). The summer season of both years exhibited a lower concentration of phthalates which can be due to the higher biodegradation rate of phthalates in summers (Liu et al. 2010). Moreover, lower concentrations of phthalates in the summer season can be due to dilution, which is further affected by precipitation. Loraine and Pettigrove (2006) advocated that more use of personal care products in the summer season can cause increased levels of phthalates in surface water. Seasonal variations in the presence of endocrine disrupters in the aquatic environment have been reported in preceding studies also. In a study, Zhou et al. (2016) reported higher concentrations of steroid hormones in Lake Water in November than in May. Likewise, Kim and Kannan (2007) reported peaked concentrations of perfluorinated acids in summer season than winter season in various lakes in Albany, USA. Furthermore, Wang et al. (2012) reported a lower concentration of bisphenol-A in May than in November, whereas an inverted trend was observed in the case of 4-nonylphenol. Seasonal fluctuation in the occurrence of phthalates is important as they mainly originate from several non-point sources and their existence could be inflated by precipitation and hydrological situations which contribute to significant seasonal variations in different regions (Muller et al., 2019; Luo et al., 2021).

Among the different samples of monsoon season (July 2015) benzyl butyl phthalate was detected at eight sites *viz*., S1, S2, S4, S5, S6, S7, S9, and S11. The minimum concentration of 0.16±0.02 mg/L was found at the S9 site whereas the highest concentration of 2.43±0.01 mg/L was observed at the S2 site. Di-n-butyl phthalate was found at two sampling sites *i.e.,* S2 and S4 with concentrations of 48.66±1.29 and 39.54±1.59 mg/L respectively. Di-n-butyl is extensively used in polyvinyl chloride and polyvinyl acetates to increase flexibility. It is also used in various cosmetic products. In the natural environment, the concentration usually ranges from 30-100 µg/L whereas in urban areas it can reach from 10-1472 mg/L (Hu et al., 2020). In July 2015, water samples did not show the presence of dimethyl phthalate. During October 2015 (post-monsoon season), benzyl butyl phthalate was the only detected phthalate. Its maximum concentration was detected in the water sample collected from the S1 sampling site whereas minimum concentration was detected at the S5 sampling site *i.e.,* 2.78±0.07 mg/L and 0.29±0.01 mg/L respectively. Benzyl butyl phthalate is commonly used as an adhesive in packaging material, perfumes, vinyl gloves, etc. (Li et al., 2021). Exposure of BBP has been reported to cause eczema, rhitis, decrease in ovary weight and uterine and increase in liver size (Ema and Miyawaki, 2002; Bornehag et al., 2004). Gao et al. (2019) detected the presence of BBP in sediments and water of Taihu Lake of China with concentration of 1.30 mg/Kg and 4.72 µg/L respectively. The dissemination of phthalates in water bodies is affected by seasonal variations. In monsoon season, the high surface water runoff could act as a causative agent for higher contamination of phthalates in monsoon and post-monsoon season. During the winter season (January 2016), BBP was detected at seven sampling sites viz., S1, S2, S3, S6, S8, S9, S11 whereas dimethyl phthalate was present only at S3 sampling site with the concentration of 1.6±0.03 mg/L. Di-n-butyl phthalate was not found in any water sample. In April 2016 sampling (summer season), only DBP was detected in the water sample collected from the S8 sampling site *i.e.* 11.61±0.59 mg/L.

Di-n-butyl phthalate is used in many personal care products like body lotions, perfumes etc. as a solvent (Ahuactzin-Pérez et al., 2018b). It is one of the chief phthalates that are present in various environmental matrices like water and sediments (Gao and Wen, 2016). DBP can enter the food chain by getting absorbed by plants and other living organisms (Muneer et al., 2021).

Table 3. Phthalate esters (mg/L) in water samples collected from different sites from July 2015-May 2017.

Phthalic ester	Site code	First year of sampling (July 2015-May 2016)				Second-year of sampling (July 2016-May 2017)			
		Monsoon	Post-monsoon	Winter	Summer	Monsoon	Post-monsoon	Winter	Summer
Benzyl butyl phthalate	S1	0.73±0.01	2.78±0.07	0.58±0.01	-	-	-	-	-
	S2	2.43±0.01	0.50±0.09	0.76±0.03	-	-	-	-	-
	S3	-	-	0.70±0.03	-	-	-	-	-
	S4	1.59±0.01	1.24±0.02	-	-	-	-	-	-
	S5	1.09±0.03	0.29±0.01	-	-	-	-	-	0.18±0.01
	S6	0.35±0.04	-	0.32±0.06	-	-	-	-	-
	S7	0.43±0.04	0.84±0.02	-	-	-	0.46±0.01	-	-
	S8	-	0.59±0.01	1.68±0.07	11.61±0.59	-	-	-	0.37±0.05
	S9	0.16±0.02	0.60±0.03	1.33±0.04	-	-	-	-	-
	S11	0.74±0.04	1.77±0.13	0.41±0.005	-	63±0.98	-	-	-
Di-n-butyl phthalate	S1	-	-	-	-	-	33.14±0.58	-	-
	S2	48.66±1.29	-	-	-	-	-	-	-
	S4	39.54±1.59	-	-	-	-	-	-	-
Dimethyl phthalate	S3	-	-	1.60±0.03	-	-	-	-	-

Results are presented as Mean±S.E.

In most of the sampling sites, where phthalates were detected, the stormwater and municipal sewage were released into the ponds. The untreated municipal sewage containing various anthropogenic contaminants such as phthalates found their way into the aquatic ecosystem. Rainfall provides a basic force for surface runoff and atmospheric deposition of contaminants in the water body as evident from the higher concentrations of phthalates in monsoon season. There was also a substantial difference in the phthalate concentration in water at different sites. Higher concentration was measured at sites which were surrounded by houses, and streets, thus receiving a great number of contaminants from surroundings. Whereas, no phthalate was detected at S10 sampling site which was well maintained pond. The results are suggestive that phthalates contamination is mainly dominated by local inputs. Furthermore, phthalates are also used as solvents for many pesticides besides getting leached from packaging material (Wang et al., 2013; Li et al., 2016). Therefore, application of pesticides and fertilizers in nearby agricultural fields could be the main reason of the accumulation of phthalates in water (Liu et al., 2010; Zeng et al., 2013).

In July 2016 (monsoon season of the second year of sampling), benzyl butyl phthalate was the only detected phthalate with a concentration of 63±0.98 mg/L at the S11 sampling site. In October 2016 (post-monsoon season), BBP (0.46±0.01 mg/L) and DBP (33.14±0.58 mg/L) was detected in water samples collected from S7 and S1 sampling sites respectively. Phthalates were not detected during the winter season (January 2017) whereas in summer season (May 2017) benzyl butyl phthalate was detected at S5 (0.18±0.01 mg/L) and S8 (0.37±0.05 mg/L) sampling sites. Benzyl butyl phthalate softens the resins without chemically binding with them thus also known as an external plasticizer (Kumari and Kaur, 2019). Due to this, BBP migrates slowly from the discarded plastic material and get diffused into an aquatic environment where it can last for long periods (Dominguez-Morueco et al,. 2014; Liu et al., 2015). When aquatic organisms are exposed to phthalates, mortality occurs due to sub-lethal effects of peroxisome proliferator activator receptors. Moreover, phthalates are known for their capacity to disrupt reactive oxygen species, plummeting cells' capability to combat oxidative stress and inducing apoptosis. These events may lead to mortality of aquatic organisms (Mathieu-Denoncourt et al., 2015). Benzyl butyl phthalate can also accumulate in tissues of organisms thus entering into the food chain by process of bioaccumulation. When these aquatic organisms are consumed by another organism of the higher trophic level, they get biomagnified in the food chain. Thus, the risk of phthalates exposure to humans increases because humans are at the top of the food chain (Chatterjee and Karlovsky, 2010; NTP-CERHR, 2003). Phthalate exposure during pregnancy can lead to various adverse health effects on mother as well as on child (Sol et al., 2020; Van den Dries et al., 2020; Philips et al., 2020; Deierlein et al., 2022). Phthalates are also reported to cross the placental barrier and may lead to suboptimal foetal development and adversarial genetic effects (Santos et al., 2021).

Di-n-butyl phthalate was the second most detected phthalates in the study. The frequent occurrence of DBP in the environment has gained a lot of attention due to its endocrine disrupting properties in animals and

adversarial effects on the reproductive system in humans (Xu et al., 2014; Ahuactzin-Pérez et al., 2018a). Di-n-butyl phthalate is not soluble in water and does not degrade easily, therefore, the most found phthalate in various water bodies. Di-n-butyl phthalate can enter into waterbody through direct discharge into the aquatic environment from many plastic products as they are not chemically bonded to plastic (Liu et al., 2014). Experimental studies have proved DBP as a reproductive toxicant and anti-androgenic (Motohashi et al., 2016). Studies have been reported that DBP exposure leads to dysfunction of serum reproductive hormones (Mendiola et al., 2012; Joensen et al., 2012; Meeker and Ferguson, 2014). Dimethyl phthalate was found only in one sample during the winter season of the first year of sampling. Dimethyl phthalate easily leached into the environment from plastics tubing, plates, paper, and containers (Xu et al., 2009). Due to its wide applications in various fields, DMP has contaminated soil, air, groundwater, sediments, aerosol particles and surface water (Montuori et al., 2008; Wang et al., 2008; Wu et al., 2011; Huang et al., 2015). DMP is a stable phthalate as compared to others and has the half-life of approximately 20 years (Staples et al., 1997). Among various aquatic organism, amphipods are the most sensitive species towards DMP toxicity with LC_{50} ranges from 0.0282 to 0.377 ml/L (Mathieu-Denoncourt et al., 2016). Dimethyl phthalate can cause excess accumulation of reactive oxygen species in algal cells which can lead damage in thylakoid membranes, disruption in chloroplast structure and alterations in photosynthetic functions of cells (Gao et al., 2021). Overall, it can be concluded that the seasonal variations of phthalates in water varied with the sampling site, the surrounding aquatic environment and local atmospheric deposition. The highest number of phthalates were detected at S8 sampling site followed by S1=S11>S2=S9=S4=S5=S7>S6=S3>S10. In case of phthalates, BBP was the most abundantly found phthalate followed by DBP and DMP. Diallyl phthalate and diethyl phthalate were not detected in any water sample. The outcomes of the present research strongly indicate that the phthalate contamination in pond water is significantly associated with anthropogenic activities.

Conclusion

The current study implies the first set of data on the occurrence of phthalates in the pond water of Amritsar district (Punjab, India). The outcomes uncover the presence of phthalic acid esters in the pond water. Dumping of municipal waste containing plastic product could be the main responsible cue of phthalates' contamination. Among all phthalates, BBP was the predominant one. Furthermore, the study revealed that the climate variations have played an imperative role in phthalates' distribution as their higher concentrations were reported during the monsoon and post monsoon seasons. Thus, prevalence of phthalates in the pond water can severely induce detrimental impacts on the surrounding biota.

Acknowledgements

The authors are grateful to the Emerging Life Science Block – The Central Instrumentation Facility, Guru Nanak Dev University, Amritsar for providing the necessary facilities. The authors are also deeply indebted to University Grants Commission, New Delhi (India) for providing financial assistance under scheme Basic Scientific Research fellowship (UGC-BSR). The research was financially supported by the Ministry of Science and Higher Education of the Russian Federation within the framework of the state task in the field of scientific activity (No. 0852-2020-0029).

References

Abtahi, M., Dobaradaran, S., Torabbeigi, M., Jorfi, S., Gholamnia, R., Koolivand, A., Saeedi, R., 2019. Health risk of phthalates in water environment: occurrence in water resources, bottled water, and tap water, and burden of disease from exposure through drinking water in Tehran, Iran. *Environmental Research* 173: 469-479.

Ahuactzin-Pérez, M., Tlecuitl-Beristain S., García-Dávila, J., Santacruz-Juárez, E., González-Pérez, M., Gutiérrez-Ruíz, M.C., Sánchez, C., 2018a. A novel biodegradation pathway of the endocrine-disruptor Di(2-ethyl Hexyl) phthalate by *Pleurotus ostreatus* based on quantum chemical investigation. *Ecotoxicology and Environmental Safety* 147: 494-499.

Ahuactzin-Pérez, M., Tlécuitl-Beristain, S., García-Dávila, J., Santacruz-Juárez, E., González-Pérez, M., Gutiérrez-Ruíz, M.C., Sánchez, C., 2018b. Kinetics and pathway of biodegradation of dibutyl phthalate by *Pleurotus ostreatus*. *Fungal Biology* 122: 991-997.

Ajay, K., Behera, D., Bhattacharya, S., Mishra, P.K., Ankit, Y., Anoop, A., 2021. Distribution and characteristics of microplastics and phthalate esters from a freshwater lake system in Lesser Himalayas. *Chemosphere* 283: 131132.

Bornehag, C.G., Sundell, J., Weschler, C.J., Sigsgaard, T., Lundgren, B., Hasselgren, M., Hägerhed-Engman, L., 2004. The association between asthma and allergic symptoms in children and phthalates in house dust: a nested case–control study. *Environmental Health Perspectives* 112: 1393-1397.

Cao, Y., Liu, J., Liu, Y., Wang, J., Hao, X., 2016. An integrated exposure assessment of phthalates for the general population in China based on both exposure scenario and biomonitoring estimation approaches. *Regulatory Toxicology and Pharmacology* 74: 34-41.

Chatterjee, S., Karlovsky, P., 2010. Removal of the endocrine disrupter butyl benzyl phthalate from the environment. *Applied Microbiology and Biotechnology* 87: 61-73.

Deierlein, A.L., Wu, H., Just, A.C., Kupsco, A.J., Braun, J.M., Oken, E., Baccarelli, A.A., 2022. Prenatal phthalates, gestational weight gain, and long-term weight changes among Mexican women. *Environmental Research* 209: 112835.

Ema, M., Miyawaki, E., 2002. Effects on development of the reproductive system in male offspring of rats given butyl benzyl phthalate during late pregnancy. *Reproductive Toxicology* 16: 71-76.

Frederiksen, H., Skakkebaek, N.E., Andersson, A.M., 2007. Metabolism of phthalates in humans. *Molecular Nutrition & Food Research* 51: 899-911.

Gani, K.M., Tyagi, V.K., Kazmi, A.A., 2017. Occurrence of phthalates in aquatic environment and their removal during wastewater treatment processes: a review. *Environmental Science and Pollution Research* 24: 17267-17284.

Gao, D.W., Wen. Z.D., 2016. Phthalate esters in the environment: A critical review of their occurrence, biodegradation, and removal during wastewater treatment processes. *Science of the Total Environment* 541: 986-1001.

Gao, X., Li, J., Wang, X., Zhou, J., Fan, B., Li, W., Liu, Z., 2019. Exposure and ecological risk of phthalate esters in the Taihu Lake basin, China. *Ecotoxicology and Environmental Safety* 171: 564-570.

Gao, K., Li, B., Xue, C., Dong, J., Qian, P., Lu, Q., Deng, X., 2021. Oxidative stress responses caused by dimethyl phthalate (DMP) and diethyl phthalate (DEP) in a marine diatom *Phaeodactylum tricornutum*. *Marine Pollution Bulletin* 166: 112222.

González-Sálamo, J., González-Curbelo, M.Á., Socas-Rodríguez, B., Hernández-Borges, J., Rodríguez-Delgado. M.Á., 2018. Determination of phthalic acid esters in water Samples by hollow fiber liquid-phase microextraction prior to gas chromatography tandem mass spectrometry. *Chemosphere* 201: 254-261.

Hassall, C., 2014. The ecology and biodiversity of urban ponds. *WIREs Water* 1: 187-206.

Hu, J., Xia, M., Wang, Y., Tian, F., Sun, B., Yang, M., Li, W., 2021. Paternal exposure to di-n-butyl-phthalate induced developmental toxicity in zebrafish (*Danio rerio*). *Birth Defects Research* 113: 14-21.

Huang, Y., Cui, C., Zhang, D., Li, L., Pan. D., 2015. Heterogeneous catalytic ozonation of dibutyl phthalate in aqueous solution in the presence of iron-loaded activated carbon. *Chemosphere* 119: 295-301.

Joensen, U.N., Frederiksen, H., Jensen, M.B., Lauritsen, M.P., Olesen, I.A., Lassen, T.H., Jørgensen, N., 2012. Phthalate excretion pattern and testicular function: a study of 881 healthy Danish men. *Environmental Health Perspectives* 120: 1397.

Jönander, C., Backhaus, T., Dahllöf, I., 2022. Single substance and mixture toxicity of dibutyl-phthalate and sodium dodecyl sulphate to marine zooplankton. *Ecotoxicology and Environmental Safety* 234: 113406.

Kaur, H., Hundal, S.S., 2018. Heavy metal accumulation in some selected ponds of district Ludhiana (Punjab), India. *International Journal of Chemical Studies* 6: 1739-1743.

Kay, V.R., Bloom, M.S., Foster, W.G., 2014. Reproductive and developmental effects of phthalate diesters in males. *Critical Reviews in Toxicology* 44: 467-498.

Kim, S.K., Kannan, K., 2007. Perfluorinated acids in air, rain, snow, surface runoff, and lakes: relative importance of pathways to contamination of urban lakes. *Environmental Science & Technology* 41: 8328-8334.

Kumari, A., Kaur, R., 2019. Modulation of biochemical and physiological parameters in *Hordeum vulgare* L. seedlings under the influence of benzyl-butyl phthalate. *PeerJ* 7: e6742.

Kumari, A., Kaur. R., 2020. Di-n-butyl phthalate-induced phytotoxicity in *Hordeum vulgare* seedlings and subsequent antioxidant defense response. *Biologia Plantarum* 64: 110-118.

Kumari, A., Sharma, R., Kaur, R., Rajput, S., Kaur, R., 2020a. Phthalates (emerging environmental pollutants): sources, fate and their toxicological consequences in animals. In: Pollutants and Protectants: Evaluation and Assessment Techniques. Sharma, A., Kumar, M. (Eds.). I. K. International Publishing House, Delhi, India. Chapter 3, pp. 53-74.

Kumari, A., Arora, S., Kaur. R., 2020b. Comparative cytotoxic and genotoxic potential of benzyl-butyl phthalate and di-n-butyl phthalate using *Allium cepa* assay. *Energy, Ecology and Environment* 5: 1-14.

Kumari, A., Kaur, R., 2021. Chromatographic methods for the determination of phthalic acid esters in different samples. *Journal of Analytical Chemistry* 76: 41-56.

Lee, Y.S., Lim, J.E., Lee, S., Moon, H.B., 2020. Phthalates and non-phthalate plasticizers in sediment from Korean coastal waters: Occurrence, spatial distribution, and ecological risks. *Marine Pollution Bulletin* 154: 111119.

Li, C., Chen, J., Wang, J., Han, P., Luan, Y., Ma, X., Lu, A., 2016. Phthalate esters in soil, plastic film, and vegetable from greenhouse vegetable production bases in Beijing, China: concentrations, sources, and risk assessment. *Science of the Total Environment* 568: 1037-1043.

Li, R., Liang, J., Duan, H., Gong, Z., 2017. Spatial distribution and seasonal variation of phthalate esters in the Jiulong River estuary, Southeast China. *Marine Pollution Bulletin* 122: 38-46.

Li, J., Li, H., Lin, D., Li, M., Wang, Q., Xie, S., Liu, F., 2021. Effects of butyl benzyl phthalate exposure on *Daphnia magna* growth, reproduction, embryonic development and transcriptomic responses. *Journal of Hazardous Materials* 404: 124030.

Linton, S., Goulder, R., 2000. Botanical conservation value related to origin and management of ponds. *Aquatic Conservation: Marine and Freshwater Ecosystems* 10: 77-91.

Liu, H., Liang, H., Liang, Y., Zhang, D., Wang, C., Cai, H., Shvartsev, S.L., 2010. Distribution of phthalate esters in alluvial sediment: a case study at JiangHan Plain, Central China. *Chemosphere* 78: 382-388.

Liu, H., Cui, K., Zeng, F., Chen, L., Cheng, Y., Li, H., Luan, T., 2014. Occurrence and distribution of phthalate esters in riverine sediments from the Pearl River Delta region, South China. *Marine Pollution Bulletin* 83: 358-365.

Liu, X., Sun, Z., Chen, G., Zhang, W., Cai, Y., Kong, R., You, J., 2015. Determination of phthalate esters in environmental water by magnetic Zeolitic Imidazolate Framework-8 solid-phase extraction coupled with high-performance liquid chromatography. *Journal of Chromatography A* 1409: 46-52.

Loraine, G.A., Pettigrove, M.E., 2006. Seasonal variations in concentrations of pharmaceuticals and personal care products in drinking water and reclaimed wastewater in southern California. *Environmental Science & Technology* 40: 687-695.

Luo, X., Shu, S., Feng, H., Zou, H., Zhang, Y., 2021. Seasonal distribution and ecological risks of phthalic acid esters in surface water of Taihu Lake, China. *Science of the Total Environment* 768: 144517.

Lyche, J.L., Gutleb, A.C., Bergman, Å., Eriksen, G.S., Murk, A.J., Ropstad, E., Skaare, J.U., 2009. Reproductive and developmental toxicity of phthalates. *Journal of Toxicology and Environmental Health, Part B* 12: 225-249.

Mathieu-Denoncourt, J., de Solla, S.R., Langlois, V.S., 2015. Chronic exposures to monomethyl phthalate in Western clawed frogs. *General and Comparative Endocrinology* 219: 53-63.

Mathieu-Denoncourt, J., Wallace, S.J., de Solla, S.R., Langlois, V.S., 2016. Influence of lipophilicity on the toxicity of bisphenol A and phthalates to aquatic organisms. *Bulletin of Environmental Contamination and Toxicology* 97: 4-10.

Meeker, J.D., Ferguson, K.K., 2014. Urinary phthalate metabolites are associated with decreased serum testosterone in men, women, and children from NHANES 2011–2012. The *Journal of Clinical Endocrinology & Metabolism* 99: 4346-4352.

Mendiola, J., Meeker, J.D., Jørgensen, N., Andersson, A.M., Liu, F., Calafat, A.M., Hauser, R., 2012. Urinary concentrations of di (2-ethylhexyl) phthalate metabolites and serum reproductive hormones: pooled analysis of fertile and infertile men. *Journal of Andrology* 33: 488-498.

Montuori, P., Jover, E., Morgantini, M., Bayona, J.M., Triassi, M., 2008. Assessing human exposure to phthalic acid and phthalate esters from mineral water stored in polyethylene terephthalate and glass bottles. *Food Additives and Contaminants* 25: 511-518.

Motohashi, M., Wempe, M.F., Mutou, T., Takahashi, H., Kansaku, N., Ikegami, M., Wakui, S., 2016. Male rats exposed in utero to di (n-butyl) phthalate: Age-related changes in Leydig cell smooth endoplasmic reticulum and testicular testosterone-biosynthesis enzymes/proteins. *Reproductive Toxicology* 59: 139-146.

Müller, A., Österlund, H., Nordqvist, K., Marsalek, J., Viklander, M., 2019. Building surface materials as sources of micropollutants in building runoff: A pilot study. *Science of the Total Environment* 680: 190-197.

Muneer, M., Theurich, J., Bahnemann, D., 2001. Titanium dioxide mediated photocatalytic degradation of 1, 2-diethyl phthalate. *Journal of Photochemistry and Photobiology A: Chemistry* 143: 213-219.

Net, S., Sempere, R., Delmont, A., Paluselli, A., Ouddane, B., 2015. Occurrence, fate, behavior and ecotoxicological state of phthalates in different environmental matrices. *Environmental Science & Technology* 49: 4019-4035.

NTP-CERHR (National Toxicology Program - Centre for the Evaluation of Risks to Human Reproduction US), 2003. NTP-CERHR Monograph on the Potential Human Reproductive and Developmental Effects of Di-n-butyl Phthalate (DBP) (No. 3). Research Triangle Park: US Department of Health and Human Services. Available at [Access date: 09.05.2022]: https://ntp.niehs.nih.gov/ntp/ohat/phthalates/dbp/dbp_monograph_final.pdf

Philips, E.M., Jaddoe, V.W., Deierlein, A., Asimakopoulos, A.G., Kannan, K., Steegers, E.A., Trasande, L., 2020. Exposures to phthalates and bisphenols in pregnancy and postpartum weight gain in a population-based longitudinal birth cohort. *Environment International* 144: 106002.

Pirsaheb, M., Nouri, M., Hossini, H., 2022. Advanced oxidation processes for the removal of phthalate esters (PAEs) in aqueous matrices: a review. *Reviews on Environmental Health*.

Posnack, N.G., 2014. The adverse cardiac effects of di (2-ethylhexyl) phthalate and bisphenol A. *Cardiovascular Toxicology* 14: 339-357.

Prevarić, V., Bureš, M.S., Cvetnić, M., Miloloža, M., Grgić, D.K., Markić, M., Ukić, Š., 2021. The problem of phthalate occurrence in aquatic environment: A review. *Chemical and Biochemical Engineering Quarterly* 35: 81-104.

Qu, R., Feng, M., Sun, P., Wang. Z., 2015. A comparative study on antioxidant status combined with integrated biomarker response in *Carassius auratus* fish exposed to nine phthalates. *Environmental Toxicology* 30: 1125-1134.

Rajput, S., Sharma, R., Kaur, R., Arora, S., 2017. Analysis of seasonal and temporal variation in physicochemical and microbial characteristics of surface water in Amritsar (Punjab*). Journal of Chemical and Pharmaceutical Research* 9: 242-248.

Rajput, S., Kumari, A., Arora, S., Kaur, R., 2018. Multi-residue pesticides analysis in water samples using reverse phase high performance liquid chromatography (RP-HPLC). *MethodsX* 5: 744-751.

Rajput, S., Kaur, T., Arora, S., Kaur, R., 2019. Heavy metal concentration and mutagenic assessment of pond water samples: a case study from India. *Polish Journal of Environmental Studies* 29: 789-798.

Rajput, S., Sharma, R., Kumari, A., Kaur, R., Sharma, G., Arora, S., Kaur, R., 2021. Pesticide residues in various environmental and biological matrices: distribution, extraction, and analytical procedures. *Environment, Development and Sustainability* 24: 6032–6052.

Ramzi, A., Gireeshkumar, T.R., Rahman, K.H., Manu, M., Balachandran, K.K., Chacko, J., Chandramohanakumar, N., 2018. Distribution and contamination status of phthalic acid esters in the sediments of a tropical monsoonal estuary, Cochin-India. *Chemosphere* 210: 232-238.

Rehan, M., Bharati, D.K., Banerjee, S., Gautam, R.K., Chattopadhyaya, M.C., 2017. Physicochemical and heavy metal analysis of pond water quality of Mau-aima vicinity, Allahabad (India). *Asian Journal of Research in Chemistry* 10: 29-32.

Roslev, P., Vorkamp, K., Aarup, J., Frederiksen, K., Nielsen, P.H., 2007. Degradation of phthalate esters in an activated sludge wastewater treatment plant. *Water Research* 41: 969–976.

Santos, S., Sol, C.M., van Zwol–Janssens, C., Philips, E.M., Asimakopoulos, A.G., Martinez-Moral, M.P., Trasande, L., 2021. Maternal phthalate urine concentrations, fetal growth and adverse birth outcomes. A population-based prospective cohort study. *Environment International* 151: 106443.

Schmidt, N., Castro-Jiménez, J., Oursel, B., Sempere, R., 2021. Phthalates and organophosphate esters in surface water, sediments and zooplankton of the NW Mediterranean Sea: Exploring links with microplastic abundance and accumulation in the marine food web. *Environmental Pollution* 272: 115970.

Semenov, A.A., Enikeev, A.G., Babenko, T.A., Shafikova, T.N., Gorshkov, A.G., 2021. Phthalates-a strange delusion of ecologists. *Theoretical and Applied Ecology* 1: 16-21.

Singh, S., Li, S.S.L., 2012. Epigenetic effects of environmental chemicals bisphenol A and phthalates. *International Journal of Molecular Sciences* 13: 10143-10153.

Sol, C.M., Santos, S., Asimakopoulos, A.G., Martinez-Moral, M.P., Duijts, L., Kannan, K., Jaddoe, V.W., 2020. Associations of maternal phthalate and bisphenol urine concentrations during pregnancy with childhood blood pressure in a population-based prospective cohort study. *Environment International* 138: 105677.

Staples, C.A., Peterson, D.R., Parkerton, T. F., Adams, W.J., 1997. The environmental fate of phthalate esters: a literature review. *Chemosphere* 35: 667-749.

Suresh, A., Jindal, T., 2022. Occurrence and toxicity of phthalates in different microenvironments. In: Jindal, T. (Ed.). New Frontiers in Environmental Toxicology. Springer, Cham. pp 15–21.

Tao, H., Wang, Y., Liang, H., Zhang, X., Liu, X., Li, J., 2020. Pollution characteristics of phthalate acid esters in agricultural soil of Yinchuan, northwest China, and health risk assessment. *Environmental Geochemistry and Health* 42: 4313-4326.

Tran, H.T., Lin, C., Bui, X.T., Nguyen, M.K., Cao, N.D.T., Mukhtar, H., Nghiem, L.D., 2022. Phthalates in the environment: characteristics, fate and transport, and advanced wastewater treatment technologies. *Bioresource Technology* 344: 126249.

van den Dries, M.A., Guxens, M., Spaan, S., Ferguson, K. K., Philips, E., Santos, S., Pronk, A., 2020. Phthalate and bisphenol exposure during pregnancy and offspring nonverbal IQ. *Environmental Health Perspectives* 128: 077009.

Wang, C., Huang, P., Qiu, C., Li, J., Hu, S., Sun, L., Wang, S., 2021. Occurrence, migration and health risk of phthalates in tap water, barreled water and bottled water in Tianjin, China. *Journal of Hazardous Materials* 408: 124891.

Wang, H., Liang, H., Gao, D., 2017. Occurrence and distribution of phthalate esters (PAEs) in wetland sediments. *Journal of Forestry Research* 28: 1241-1248.

Wang, L., Ying, G.G., Chen, F., Zhang, L.J., Zhao, J.L., Lai, H.J., Tao, R., 2012. Monitoring of selected estrogenic compounds and estrogenic activity in surface water and sediment of the Yellow River in China using combined chemical and biological tools. *Environmental Pollution* 165: 241-249.

Wang, P., Wang, S. L., Fan, C.Q., 2008. Atmospheric distribution of particulate-and gas-phase phthalic esters (PAEs) in a Metropolitan City, Nanjing, East China. *Chemosphere* 72: 1567-1572.

Wang, X., Lin, Q., Wang, J., Lu, X., Wang, G., 2013. Effect of wetland reclamation and tillage conversion on accumulation and distribution of phthalate esters residues in soils. *Ecological Engineering* 51: 10-15.

Wang, X., Tao, W., Xu, Y., Feng, J., Wang, F., 2014. Indoor phthalate concentration and exposure in residential and office buildings in Xi'an, China. *Atmospheric Environment* 87: 146-152.

Weizhen, Z., Xiaowei, Z., Peng, G., Ning, W., Zini, L., Jian, H., Zheng, Z., 2020. Distribution and risk assessment of phthalates in water and sediment of the Pearl River Delta. *Environmental Science and Pollution Research* 27: 12550-12565.

Wu, M.H., Liu, N., Xu, G., Ma, J., Tang, L., Wang, L., Fu, H.Y., 2011. Kinetics and mechanisms studies on dimethyl phthalate degradation in aqueous solutions by pulse radiolysis and electron beam radiolysis. *Radiation Physics and Chemistry* 80: 420-425.

Xu, B., Gao, N.Y., Cheng, H., Xia, S.J., Rui, M., Zhao, D.D., 2009. Oxidative degradation of dimethyl phthalate (DMP) by UV/H2O2 process. *Journal of Hazardous Materials* 162: 954-959.

Xu, D., Deng, X., Fang, E., Zheng, X., Zhou, Y., Lin, L., Huang, Z., 2014. Determination of 23 phthalic acid esters in food by liquid chromatography tandem mass spectrometry. *Journal of Chromatography A* 1324: 49-56.

Zeng, F., Wen, J., Cui, K., Wu, L., Liu, M., Li, Y., Zeng, Z., 2009. Seasonal distribution of phthalate esters in surface water of the urban lakes in the subtropical city, Guangzhou, China. *Journal of Hazardous Materials* 169: 719-725.

Zeng, L. S., Zhou, Z. F., Shi, Y.X., 2013. Effects of phthalic acid esters on the ecological environment and human health. *Applied Mechanics and Materials* 295: 640-643.

Zhang, Y., Jiao, Y., Li, Z., Tao, Y., Yang, Y., 2021. Hazards of phthalates (PAEs) exposure: A review of aquatic animal toxicology studies. *Science of the Total Environment* 771: 145418.

Zhou, L. J., Zhang, B. B., Zhao, Y. G., Wu, Q. L., 2016. Occurrence, spatiotemporal distribution, and ecological risks of steroids in a large shallow Chinese lake, Lake Taihu. *Science of the Total Environment* 557: 68-79.

Eurasian Journal of Soil Science 2023, 12(1), 28 - 36

Eurasian Journal of Soil Science

Journal homepage : http://ejss.fesss.org

Pores distribution influences the soil microorganism's response to changes in temperature and moisture

Efraín Francisco Visconti-Moreno *, Ibonne Geaneth Valenzuela-Balcázar

Universidad Francisco de Paula Santander, Faculty of Agricultural and Environmental Sciences. Research group on Environment and Life – GIAV, Cucuta, Colombia

Article Info

Received : 28.01.2022
Accepted : 22.09.2022
Available online : 30.09.2022

Author(s)

E.F.Visconti-Moreno *
I.G.Valenzuela-Balcázar

* Corresponding author

Abstract

Microorganisms are an essential fraction of soil organic matter, which presence and activity depend directly on soil physical conditions. This study aimed to address the effect of soil temperature and moisture under contrasting macroporosity conditions on soil biological properties. Soil physical-chemical characterization implicated the collection of composite samples and undisturbed surface soil samples (0 to 10 cm). Also, samples of undisturbed surface soil were extracted in 40 polyvinyl chloride cylinders of 18 cm diameter and 20 cm height for the arrangement of soil mesocosm as the experimental units of a completely randomized experiment with a 2x2x3 factorial arrangement. The experiment duration was 21 days, and the soil biological properties measured were microbial biomass (MB) and soil respiration (SR). Macroporosity showed a significant effect on MB, which indicates that aeration pore influences the number of microorganisms in the soil; for the SR, the macroporosity had a not significant effect. The temperature at the ranges established in the experiment did not significantly affect MB, whereas a highly significant effect of temperature over SR was observed. A highly significant effect of soil moisture was observed on MB and SR. Macroporosity, moisture, and temperature are determining factors in the presence of soil microorganisms, both directly and through the interaction between them. Herein the microorganisms have a wide range of thermal adaptation, and the effect of soil temperature can boost soil microorganisms. In turn, it was observed that the microorganisms present are significantly sensitive to the moisture deficit in soil.

Keywords: Microbial biomass, soil respiration, biological degradation, physical properties, climate change.

Introduction

Conserving the soil as the best habitat for organisms that occupy it is a role that corresponds fundamentally to soil microorganisms since they are responsible for the main biogeochemical processes through which the flow of energy and matter occurs; in terrestrial ecosystems (Pulleman et al., 2012; Mujtar et al., 2019).

Brevik et al. (2015) reported that microorganisms make up an important fraction of soil organic matter (SOM), together with the macro and mesofauna of the soil, and the roots, which constitute the living biomass of soils. Soil microorganisms are responsible for decomposing and transforming organic waste in soils. Through the intense activity of numerous and diverse microorganisms, SOM decomposes, transforms, and stabilizes the soil organic carbon (SOC) (Macías and Camps-Arbestain, 2010; Pulleman et al., 2012).

Soil microbial activity is considered to be an ecological indicator of fundamental importance since, on the one hand, it represents the level of biological activity involving the labile component of SOM and, on the other, it

: https://doi.org/10.18393/ejss.1182338
: http://ejss.fesss.org/10.18393/ejss.1182338
Publisher : Federation of Eurasian Soil Science Societies
e-ISSN : 2147-4249

integrates the factors of the environment with the soil use and management (Zagal et al., 2002). Indeed different use and management systems on the same soil can differentially affect soil microorganisms, thus modulating the ecosystem services provided by these organisms (Di Ciocco et al., 2014); consequently, it is necessary to know the behavior of the microorganisms in each situation.

Soil management practices are decisive since the agricultural use of soils generally causes a drastic decrease in the total microbial biomass of soils, together with a decrease in the total SOC. The latter is because the decomposition of SOM by microorganisms is strongly affected by the soil's chemical and physical conditions (Kaurin et al., 2018). For example, soil temperature, water content, and aeration are physical conditions that directly influence the activity of microorganisms. For this reason, soil management practices, such as tillage, irrigation and drainage, use of fire, and incorporation of organic fertilizer, can modify soil microorganism communities and affect soil quality (Brevik et al., 2015).

Soil microorganisms' activity will be determined by their sensitivity to temperature, the availability of substrates, their interactions with surface processes and other environmental factors such as soil moisture, and possible adaptations of microbial physiology (Schindlbacher et al., 2011). According to the IPCC (2007), climate change is expected to substantially impact soil moisture and temperature conditions with greater frequency and duration due to droughts. Furthermore, since soil warming is occurring, changes have been observed in the composition of the soil microbial community. The latter, in terms of an increase or decrease in the abundance of fungi. Also, because of an increase or decrease in the abundance of gram-positive or gram-negative bacteria (Rinnan et al., 2008). Also, Kaurin et al. (2018) mentioned that climate models project a 5 to 15% decrease in soil water content in the topsoil (10 cm) by the end of the century. It can mean that microbial communities and the biogeochemical cycles they control will be affected by extreme changes in soil water content. That is because soil microbial communities are susceptible to changes in soil moisture (Morugán-Coronado et al., 2019).

Scientists have increased their interest in the understanding of how drought can impact soil microbes. In this direction Siebielec et al. (2020) studied the impact of water stress on soil microbial activity and diversity. Their results proves the greater susceptibility of microbial communities to drought in sandy soils and the important role of exogenous organic matter in protecting microbial activity in drought periods. Also, Borowik and Wyszkowska (2016) proved that soil microbe's activity depends on the soil moisture level in dependence with the grain-size distribution of soil. They demonstrated that both excessively dry and wet soil create unfavorable conditions that may deplete the biomass of microorganisms. Since soil aeration pores (macroporosity) are a physical characteristic that can be modified by use and management practices (Bronick and Lal, 2005) and is directly involved with the water-air relationships necessary to favor the survival of soil microorganisms (Dexter, 2004). Ishak et al. (2016) studied the interactions between soil moisture and soil microbial activity at different soil compaction conditions, finding that microbial activity was higher in uncompact soils and decreased as soil compaction increased.

The effect of changes in soil temperature and moisture under contrasting aeration conditions on soil microorganisms must be studied. This research aims to evaluate the effect of the soil aeration pores (macroporosity), the soil temperature, and moisture content on the presence of microorganisms in agricultural soil in Norte de Santander, Colombia.

Material and Methods

Study site and soil sampling

The soil selected for this study is located in the Astilleros village of El Zulia municipality in Norte de Santander, Colombia. In an oil palm field 20 years old, with geographic coordinates of reference: 8º 12` 17" N and 72º 32` 52" W and 84 m above sea level altitude. The soil is classified as Fluventic Dystrudepts (Soil Survey Staff, 2010) under a humid tropical forest with an average annual temperature of 27.3 ºC and a mean annual rainfall of 2000 mm (IGAC, 2006a).

A soil sampling was carried out by tracing an imaginary cross of 50 meters on each side to mark five points (intersection and ends of the cross) to achieve soil physical-chemical characterization. At each point, a composite soil sample was collected consisting of five sub-samples of surface soil (0 to 10 cm depth), also arranged on the ends (04) and intersection (01) of a 2-meter-long cross (Valadares-Pereira et al., 2017). At these same five points, ten undisturbed surface soil samples (two at each point) were extracted in metallic cylinders of 5 cm in diameter and 5 cm in height for physical analysis. Also, samples of undisturbed surface soil (0 to 15 cm depth) were extracted in 40 polyvinyl chloride (PVC) cylinders of 18 cm in diameter and 20 cm in height (eight at each point) for the arrangement of experimental units (Schindlbacher et al., 2011; Lubbers et al., 2017).

Experimental Design

The evaluation was carried out through a completely randomized experiment with a 2x2x3 factorial arrangement with 3 repetitions, representing 36 experimental units. The experimental units consisted of soil and microorganism mesocosm, conformed by undisturbed soil extracted at a depth of 15 cm in the PVC cylinders indicated above (Figure 1). The duration of the experiment was 21 days, and the factors were: macroporosity (two levels), soil temperature (two levels), and soil moisture (three levels), as presented in Table 1.

A: cylinder buried up to 15 cm deep with 5 cm edge. B: extraction of the cylinder with an undisturbed soil sample. C: cylinder prepared with canvas and mesh in its lower part.

Figure 1. Images of the mesocosm design (experimental units) and construction process, with undisturbed soil at 15 cm depth in PVC cylinders of 18 cm in diameter and 20 cm in height.

Table 1. Organization of treatments to evaluate the effect of macroporosity, soil temperature and soil moisture on the presence of microorganisms.

Macroporosity	Temperature	Moisture
Compacted soil with macroposority <8%	Low temperature 16 - 20 ºC	<20% FC[b]
		FC[a]
		>80% Sat. [c]
	High temperature 36 - 40 ºC	<20% FC[b]
		FC[a]
		>80% Sat. [c]
Well aerated soil with macroporosity >10%	Low temperature 16 - 20 ºC	<20% FC[b]
		FC[a]
		>80% Sat. [c]
	High temperature 36 - 40 ºC	<20% FC[b]
		FC[a]
		>80% Sat. [c]

a: soil moisture at field capacity (FC), b: soil moisture less than 20% of field capacity (<20% FC), c: above 80% of soil saturation (>80% Sat.).

The soil was compacted with a hydraulic press for the treatments with aeration at the limiting level (macroporosity <8%) (Figure 2). The treatments with the non-limiting aeration level (macroporosity> 10%) were left with the natural aeration of the soil without disturbance. During the 21 days of the experiment, to achieve the low temperature (16 – 20 ^{0}C), a room with refrigeration was used, and for the high temperature in another room, the heat was generated with incandescent bulbs to raise the soil temperature (36 – 40 ^{0}C). Thermometers were used for daily monitoring of soil temperature in the experimental units. Distilled water was applied when daily measurements determined it to achieve soil moisture at the three established levels, using a Delta T Devices brand dielectric sensor.

D: preparation of treatments with aeration <8% E: soil temperature monitoring with a Hg thermometer, F: soil moisture monitoring with a dielectric sensor.

Figure 2. Images of the control process of the levels of each factor evaluated.

Soil Physical-chemical characterization.

In order to assess the general conditions offered by the soil to microorganisms in their first 10 cm of depth, the main chemical properties were determined: pH and electrical conductivity in soil/water suspension (1: 1), and the cation exchange capacity by the 1N ammonium acetate method, pH 7 (IGAC, 2006b). In addition, the acid digestion with potassium dichromate oxidation method determined the oxidizable soil organic carbon content (Lozano et al., 2005). Also, the following soil physical properties were measured: texture with the agitation and sedimentation method of modified Bouyoucos, total porosity and aeration pores (macroporosity) using the tension table method with undisturbed samples in metallic cylinders, and the bulk density in the same metallic cylinders of 5 cm in diameter and 5 cm in height, the moisture content at saturation and field capacity was measured in the field with the dielectric sensor, (Pla, 1983; 2010).

Measurement of the presence of soil microorganisms

Considering that the experimental units of undisturbed surface soil without vegetation constitute mesocosms of the soil with the microorganisms that inhabit it (Lubbers et al., 2017), the effect of the macroporosity, the soil temperature, and soil moisture was evaluated in each experimental unit, through indirect measurement of the presence of microorganisms in the soil, through soil microbial biomass (MB) and soil respiration (SR) determinations.

CO_2 emission can measure the presence of microorganisms in the soil due to their respiration. Therefore, at the end of the 21 days of the experiment, an alkali trap was placed in each experimental unit and covered with a hermetic chamber for 24 hours, thus achieving the measurement of soil respiration (SR) according to the static absorption in NaOH method (Anderson, 1982; Lozano et al. 2005).

At the end of the SR measurement, a 200g soil sample from 0 to 10 cm deep was extracted in each experimental unit. These samples were used to measure in the laboratory the carbon of the microbial biomass using the induced respiration method, which is an indirect way of measuring the microbial biomass; as a function of a microbial metabolic response (Dalal, 1998) as a result of adding an easily degradable substrate such as glucose. It is presumed that the respiratory activity of microorganisms is equivalent to the MB present in the soil (Jenkinson and Ladd, 1981; Anderson and Domsch, 1989).

Statistical analysis

The results were tabulated with Microsoft's Excel software to perform the descriptive statistical analysis. Then with the statistical program Minitab18, the statistical assumptions were reviewed, and an analysis of variance was carried out, which allowed interpretation of the relationship of the soil microorganism with the physical conditions: temperature, moisture, and macroporosity.

Results and Discussion

Soil chemical and physical characteristics

In general, the chemical properties analyzed showed the typical condition of a Dystrudept (Table 2), a strongly acid reaction, a low cation exchange capacity, medium organic carbon content, and a non-saline condition (IGAC, 2006b).

Table 2. Chemical characteristics of the surface soil from 0 to 10 cm deep (n=5).

pH	[a] EC, dS m^{-1}	[b] SOC, g kg^{-1}	[c] CEC, $cmol_c$ kg^{-1}
5.07 (±0.21)	0.31(±0.11)	14.0(±0.38)	11.84(±1.91)

a: electric conductivity (EC), b: soil organic carbon (SOC), c: cation exchange capacity (CEC)

The soil physical analysis has revealed (Table 3) that sand is the predominant mineral particle, and the textural class is sandy clay loam. In addition, an ideal bulk density consistent with the textural class (USDA, 1999) is observed as an appropriate total porosity and a favorable macroporosity (aeration pore space), which is interpreted as good physical conditions for the growth of plants and microorganisms (Dexter, 2004; Pla, 2010).

Table 3. Physical characteristics of the surface soil from 0 to 10 cm deep (n = 5).

Sand, g kg^{-1}	Clay, g kg^{-1}	Silt, g kg^{-1}	[a] Bd, Mg m^{-3}	Total Porosity, % v v^{-1}	Macroporosity, % v v^{-1}	[b] Moisture at FC, % v v^{-1}
604.3 (±76.4)	256.5 (±3.57)	139.2 (±5.29)	1.35 (±0.05)	47 (±4.18)	13.93 (±2.79)	29.07 (±5.86)

a: bulk density (Bd), b: field capacity (FC)

Effect of macroporosity, soil temperature and moisture

In order to evaluate the effect of the factors: macroporosity, soil temperate, and soil moisture, we carried out a three-way analysis of variance to the data recorded on MB and SR in the experiment (Table 4), revealing a significant effect of the macroporosity, which indicates that soil aeration pore space influences the quantity of microorganisms in the soil. However, for the SR, the macroporosity had a not significant effect.

Table 4. Statistical effects of soil macroporosity, soil temperature, and soil moisture on microbial biomass and soil respiration (3-way ANOVA with 95% confidence level).

Source of Variance	Microbial Biomass	Soil Respiration
Factor 1: Macroporosity	Significant*	Not significant
Factor 2: Soil Temperature	Not significant	Highly significant***
Factor 3: Soil moisture	Highly significant***	Highly significant***
Factor 1 x Factor 2	Not significant	Not significant
Factor 1 x Factor 3	Significant*	Not significant
Factor 2 x Factor 3	Significant*	Significant*
Factor 1 x Factor 2 x Factor 3	Significant*	Not significant

*p value<0,05 ; ***p value<0,001

It was found that the temperature in the ranges established in the experiment did not significantly affect the MB, suggesting the existence of adaptation mechanisms of microorganisms to changes in soil temperature, as Malcolm et al. (2008) indicated. On the other hand, in our experiment, we observed a highly significant effect of temperature over SR (Table 4), which coincides with Liua et al. (2018), who pointed out that the response of microbial respiration to changes in soil temperature has reported an exponential increase in SR with increasing soil temperature. As expected, a highly significant effect of soil moisture was observed on MB and SR due to the direct influence of soil moisture on the survival of microorganisms (Iglesias, 2008; Wang et al., 2019). Either excessively dry or wet soil conditions decrease the MB, by creating stress on most aerobic bacteria and fungi (Borowik and Wyszkowska, 2016).

When evaluating the effect of double or triple interactions of the studied factors over MB, we found significant effects for three interactions, which show that the response of microorganisms is due to possible adaptations of microbial physiology, as well as interactions with surface processes and environmental factors such as temperature (Schindlbacher et al., 2011). However, the interaction of soil temperature and soil moisture was the only one with a significant effect on the SR.

It was observed that the MB is significantly lower in the compacted soil with macroporosity <8% (Table 5), confirming that soil microbial presence depends on the pore structure and soil compaction conditions (Moráis-Lima do Nascimento et al., 2016). The variation in soil temperature from 16 ^{0}C to 40 ^{0}C did not cause a significant difference in the total amount of microorganisms present in the soil (MB). However, it did generate a significant difference in their activity, with high temperatures generating a significant increase in SR. Soil moisture is a very influential factor in soil microorganisms (Table 5). MB and SR are significantly lower when the soil has less moisture.

Table 5. Microbial biomass and soil respiration according to each factor after 21 days of experiment in the soil mesocosms with microorganisms.

Variable /Factor	Macoporosity		Soil Temperature		Soil moisture		
	<8% n= 18	>10% n= 18	16 – 20 ^{0}C n= 18	36 - 40 ^{0}C n= 18	<20% FC n= 12	FC n= 12	>80% Sat n= 12
Microbial Biomass (mg C kg^{-1})	50.64 a^x (±34.78)	66.70 b (±28.29)	62.70 (±34.60)	54.64 (±30.25)	25.37 a (±14.09)	77.11 b (±16.82)	73.54 b (±31.84)
Soil respiration (mg CO_2 m^{-2} h^{-1})	168.40 (±150.80)	212.20 (±143.40)	106.79 a (±81.70)	273.77 b (±151.30)	90.86 a (±44.10)	223.82b (±173.70)	256.16 b (±140.10)

x: comparison of means was made by Fisher LSD (95%); different letters indicate a significant difference at p<0,05.

Discussion

In agreement with other studies (Frey et al., 2009), reduced soil macroporosity can cause a decrease in MB due to O_2 depletion by aerobic microorganisms and CO_2 increase in the soil atmosphere. Nevertheless, the CO_2 evolved seems to stay trapped in the compacted soil since we found an insignificant effect of macroporosity on the SR. It may also correspond with the anaerobic respiration in compacted soils (Liu et al., 2018). So, the relationships between soil compaction and the growth characteristics of microorganisms are complex (Cui and Holden, 2015).

Similar interpretation was made by Ishak et al. (2016), who found that soils with low compaction contain more soil pores predominated with macropores that enhance soil capacity to retain soil water and provide soil oxygen diffusion, thereby increasing soil respiration. But in the compacted soils low microbial activity was observed, which is presumably because at higher levels of compaction and high moisture content, water is taking up all available pore space and creating anaerobic conditions.

Based on Luia et al. (2018) approach, the hypothesis is that the acclimatization or adaptation to different climates by soil microorganisms determines their growth and respiration response to temperature. Therefore, the optimum temperature should be positively correlated with ambient temperature. The study site presents maximum air temperatures of up to 35ºC as the annual average, so this may be the reason why our results show that the variability in temperature keeps the microbial biomass similar, whereas higher temperatures increase its metabolism, generating more respiration in correspondence with many studies that reported a significant increase of SR when soil temperature ascends (Bárcenas -Moreno et al., 2009; Lipson et al., 2009).

Regarding the interaction of macroporosity and moisture on soil microorganisms (Figure 3), we observed that when aeration is limiting (macroporosity <8%), there is a greater MB with the soil moisture at field capacity (FC). On the other hand, if the soil aeration is satisfactory (macroporosity >10%), there is a higher MB when the soil moisture is near saturation. The air-water ratio in soil explains it. In other words, when a limitation on soil aeration appears, microorganisms are affected in their survival in conditions of moisture close to saturation, but if the soil aeration is high, they can thrive in water excess.

Regarding the interaction of temperature and soil moisture on the soil MB (Figure 4), we observe that when the temperature is low, there is a higher MB with soil moisture near saturation, and when the temperature is high, there is a higher MB with the moisture at field capacity (FC). To understand this, we must consider that the temperature may influence the renewal of soil air because the air expansion within the pore space and the tendency of warm air to move upward may boost some air exchange between soil and atmosphere (Jury and Horton, 2004). In addition, besides soil, water affects aeration, so aerobic activity decreases as soil becomes wetter and eventually saturated due to restricted O_2 diffusion (Voroney and Heck, 2015). On the other hand, the thermal properties of water must be involved in boosting MB at cold soil temperature with water content near saturation.

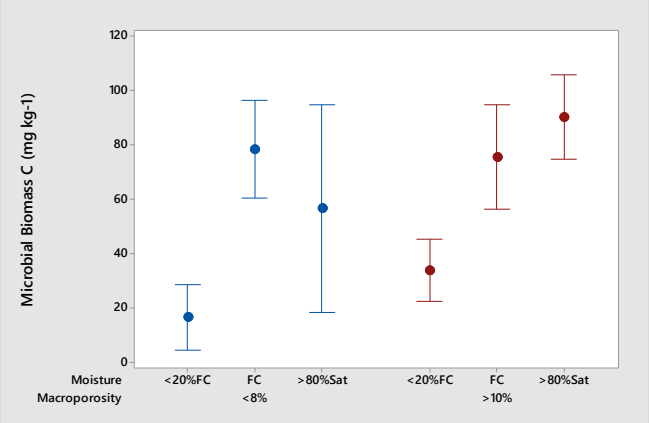

FC: field capacity, Sat: saturation. Intervals are the standard deviation.

Figure 3. Effect of the interaction between macroporosity and soil moisture on microbial biomass after 21 days of experiment in the soil mesocosms with microorganisms.

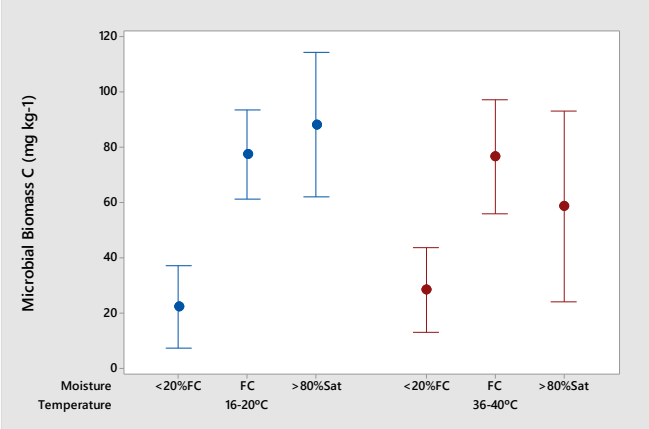

Figure 4. Effect of soil moisture and temperature interaction on microbial biomass after 21 days of experiment in the soil mesocosms with microorganisms.

The analysis of the effect of the triple interaction of factors (Figure 5) allowed the finding that the combination of factors that favored the highest total MB is when the soil has high macroporosity, low temperature, and soil moisture from field capacity to saturation. Demonstrating that a higher macroporosity is necessary for suitable moisture conditions to allow aeration; therefore increasing the availability of O_2 for microorganisms (Dexter, 2004; Voroney and Heck, 2015). While the most limiting condition for the soil MB is limiting aeration with dry soil in any temperature condition.

For the interaction of soil temperature and soil moisture on SR (Figure 6), it was found that the highest SR occurred when the soil temperature was high and the soil moisture was ideal or near saturation. It expresses that these conditions accelerated the microbial activity of soil. In contrast, low temperature with moisture at field capacity or dry soil is the most limiting condition for the microbial activity of the soil and generates an SR decrease.

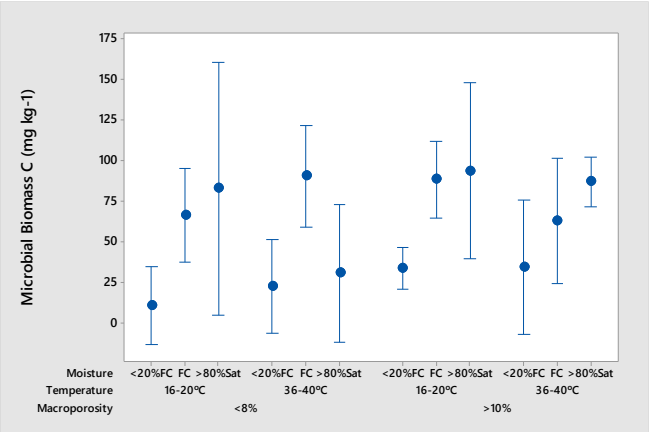

Figure 5. Effect of the triple interaction of factors on microbial biomass after 21 days of experiment in the soil mesocosms with microorganisms

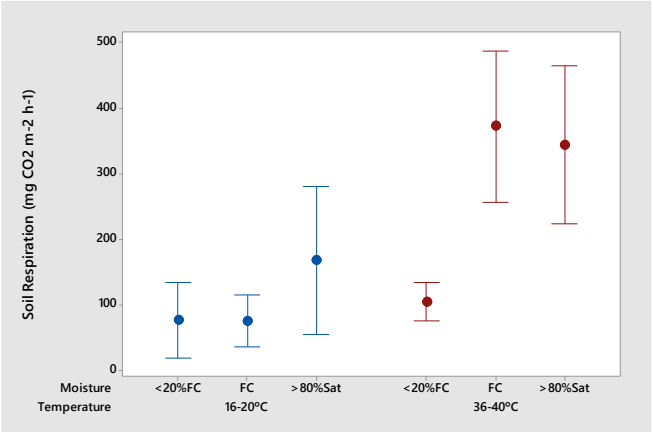

FC: field capacity, Sat: saturation. Intervals are the standard deviation

Figure 6. Effect of soil moisture and temperature interaction on soil respiration after 21 days of experiment in the soil mesocosms with microorganisms

In the experiment, it was observed that water content had a highly significant effect on the MB and SR, which indicates that soil water content is decisive for the soil microorganism's survival. Field capacity or a condition near saturation appears to be suitable for microorganisms, coinciding with the various studies that have indicated this (Harris, 1981; Barros et al., 1995; Prado and Airoldi, 1999; Chen et al., 2007). However, the marked effect of the scarcity of soil water on microorganism's survival found in this study is also due to the absence of growing plants since these, through their exudates, can help in the survival of microorganisms (Chen et al., 2007).

The temperature significantly affects SR, but on MB, the effect of temperature is conditioned by the soil water content. It implies that temperature alone does not alter the presence of microorganisms in this soil but indeed increases their activity level, which has also been reported in other studies (Barcenas-Moreno et al., 2009; Vimal et al., 2017; Liu et al., 2018). It is imperative to highlight that soil moisture deficit seriously affects microorganisms at temperatures above 36ºC. Therefore, in high temperatures conditions ideal water content in soil is necessary to promote MB.

Conclusion

This study confirms the need to bear in mind the distribution of soil's pore space, the state of water content and temperature, to favor the survival of soil microorganisms. The microorganisms present in the studied soil have a wide range of thermal adaptation, and the increase in soil temperature is confirmed as a factor that intensifies the activity of soil microorganisms. In turn, it was observed that the microorganisms present are significantly sensitive to the moisture deficit in soil.

Acknowledgements

Our thanks to the technical staff of the Francisco de Paula Santander University Environmental Quality Laboratory. Also, a special acknowledgment to Dr. Deyanira Lobo Lujan for her contribution to this paper.

References

Anderson, J.P.E., 1982. Soil respiration. In. Methods of soil analysis, Part 2- Chemical and Microbiological Properties. Page, A.L., Keeney, D. R., Baker, D.E., Miller, R.H., Ellis, R. Jr., Rhoades, J.D. (Eds.). ASA-SSSA, Madison, Wisconsin, USA. pp. 831-871.

Anderson, T.H., Domsch, K.H., 1989. Ratios of microbial biomass carbon to total organic carbon in arable soils. *Soil Biology and Biochemistry* 21(4): 471-479.

Bárcenas-Moreno, G., Gómez-Brandón, M., Rousk, J., Bååth, E., 2009. Adaptation of soil microbial communities to temperature: comparison of fungi and bacteria in a laboratory experiment. *Global Change Biology* 15: 2950 – 2957.

Barros, N., Gomez-Orellana, I., Feijóo, S., Balsa, R., 1995. The effect of soil moisture on soil microbial activity studied by microcalorimetry. *Thermochimica Acta* 249: 161–168.

Borowik, A., Wyszkowska, J., 2016. Soil moisture as a factor affecting the microbiological and biochemical activity of soil. *Plant Soil and Environment* 62: 250-255.

Brevik, E., Cerdà, A., Mataix-Solera, J., Pereg, L., Quinton, J., Six, J., Van Oost, K., 2015. The interdisciplinary nature of soil. *Soil* 1(1): 117–129.

Bronick, C., Lal, R., 2005. Soil structure and management: a review. *Geoderma* 124(1-2): 3–22.

Chen, M., Zhu, Y., Su, Y., Chen, B., Fu, B., Marschner, P., 2007. Effects of soil moisture and plant interactions on the soil microbial community structure. *European Journal of Soil Biology* 43(1): 31–38.

Cui, J., Holden, N.M., 2015. The relationship between soil microbial activity and microbial biomass, soil structure and grassland management. *Soil and Tillage Research* 146: 32–38.

Dalal, R., 1998. Soil microbial biomass—what do the numbers really mean? *Australian Journal of Experimental Agriculture* 38(7): 649 - 665.

Dexter, A., 2004. Soil physical quality: Part I. Theory, effects of soil texture, density, and organic matter, and effects on root growth. *Geoderma* 120(3-4): 201-214.

Di Ciocco, C., Sandler, R., Falco, L., Coviella, C., 2014. Microbiological activity of a soil under different uses and its relation with physico-chemical variables. *Revista de la Facultad de Ciencias Agrarias. Universidad Nacional de Cuyo* 41: 73-85. [in Spanish]

Frey, B., Kremer, J., Rüdt, A., Sciacca, S., Matthies, D., Lüscher, P., 2009. Compaction of forest soils with heavy logging machinery affects soil bacterial community structure. *European Journal of Soil Biology* 45: 312–320.

Harris, R., 1981. Effect of water potential on microbial growth and activity. In: Water Potential Relations in Soil Microbiology, Volume 9, Parr, J.F., Gardner, W.R., Elliott, L.F. (Eds.). Soil Science Society of America Inc. USA. pp.23–95.

IGAC, 2006a. Estudio general de suelos y zonificación de tierras del departamento Norte de Santander. Instituto Geográfico Agustín Codazzi (IGAC). Bogotá. 304 p. [in Spanish]

IGAC, 2006b. Métodos analíticos de laboratorio de suelos. Instituto Geográfico Agustín Codazzi (IGAC). Bogotá. 547 p. [in Spanish]

Iglesias, M., 2008. Estudio del carbono de la biomasa microbiana en suelos alterados. *Lazaroa* 29: 117–123. [in Spanish]

IPCC, 2007. Intergovernmental Panel on Climate Change (IPCC). Uso de la tierra, cambio de uso de la tierra y silvicultura. Informe especial del grupo de trabajo III del IPCC. Publicado Por el Grupo Intergubernamental de Expertos sobre el Cambio Climático, OMM-PNUMA. 128 p. [in Spanish]

Ishak, L., McHenry, M.T., Brown, P.H., 2016. Soil compaction and its effects on soil microbial communities in Capsicum growing soil. *Acta Horticulturae* 1123: 123-130.

Jacinthe, P.A., Lal, R., Kimble, J.M., 2002. Carbon budget and seasonal carbon dioxide emission from a central Ohio Luvisol as influenced by wheat residue amendment. *Soil and Tillage Research* 67: 147–157.

Jenkinson, D., Ladd, J., 1981. Microbial biomass in soil: Measurement and turnover. In: Soil Biochemistry, Volume 5. Paul, E.A., Ladd, J.N. (Eds.). CRC Press. pp. 415- 471.

Jury, W., Horton, R., 2004. Soil Physics. Sixth edition. John Wiley & Sons Inc., USA. 359 p.

Kaurin, A., Mihelič, R., Kastelec, D., Grčman, H., Bru, D., Philippot, L., Suhadolc, M., 2018. Resilience of bacteria, archaea, fungi and N-cycling microbial guilds under plough and conservation tillage, to agricultural drought. *Soil Biology and Biochemistry* 120: 233–245.

Lipson, D.A., Monson, R.K., Schmidt, S.K., Weintraub, M.N., 2009. The trade-off between growth rate and yield in microbial communities and the consequences for under-snow soil respiration in a high elevation coniferous forest. *Biogeochemistry* 95: 23-35.

Liu, S., Zhang, Y., Zong, Y., Hu, Z., Wu, S., Zhou, J., Jin, Y., Zou, J., 2018. Response of soil carbon dioxide fluxes, soil organic carbon and microbial biomass carbon to biochar amendment: a meta-analysis. *GCB Bioenergy* 8: 392-406.

Liu, Y., He, N., Wen, X., Xu, L., Sun, X., Yu, G., Liang, L., Schipperd, L.A., 2018. The optimum temperature of soil microbial respiration: Patterns and controls. *Soil Biology and Biochemistry* 121: 35–42.

Lozano, Z., Hernández, R., Ojeda, A., 2005. Manual de métodos para la evaluación de la calidad física, química y biológica de los suelos. Facultad de Agronomía, Universidad Central de Venezuela. 45 p.

Lubbers, I.M., Pulleman, M.M., Van Groenigen, J.W., 2017. Can earthworms simultaneously enhance decomposition and stabilization of plant residue carbon? *Soil Biology and Biochemistry* 105: 12 – 24.

Macías, F., Camps-Arbestain, M., 2010. Soil carbon sequestration in a changing environment. *Mitigation and Adaptation Strategies for Global Change* 15: 511-529.

Malcolm, G.M., López-Gutiérrez, J.C., Koide, R.T., Eissenstat, D.M., 2008. Acclimation to temperature and temperature sensitivity of metabolism by ectomycorrhizal fungi. *Global Change Biology* 14(5): 1-12.

Moráis-Lima do Nascimento, P.G., da Cruz, B.L.S., Dantas, A.M.M., Freitas, F.C.L., Ambrósio, M.M.Q., Júnior, R.S., 2016. Microbial communities in soil cultivated with muskmelon under different management systems. *Revista Brasilera do Ciencia do Solo* 40: e0160130.

Morugán-Coronado, A., García-Orenes, F., McMillan, M., Pereg, L., 2019. The effect of moisture on soil microbial properties and nitrogen cyclers in Mediterranean sweet orange orchards under organic and inorganic fertilization. *Science of the Total Environment* 655: 158–167.

Mujtar, V., Muñoz, N., Prack Mc Cormick, B., Pulleman, M., Tittonell, P., 2019. Role and management of soil biodiversity for food security and nutrition; where do we stand? *Global Food Security* 20: 132–144.

Pla, S.I., 1983. Metodología para la caracterización física con fines de diagnóstico de problemas de manejo y conservación de suelos en condiciones tropicales. Revista de la Facultad de Agronomía. Alcance 32. 91p. [in Spanish]

Pla, S.I., 2010. Medición y evaluación de propiedades físicas de los suelos: dificultades y errores más frecuentes. I – Propiedades mecánicas. *Suelos Ecuatoriales* 40: 75-93. [in Spanish]

Prado, A.G.S., Airoldi, C., 1999. The influence of moisture on microbial activity of soils. *Thermochima Acta* 332: 71-74.

Pulleman, M., Creamer, R., Hamer, U., Helder, J., Pelosi, C., Peres, G., Rutgers, M., 2012. Soil biodiversity, biological indicators and soil ecosystem services an overview of European approaches. *Current Opinion in Environmental Sustainability* 4(5): 529–538.

Rinnan, R., Michelsen, A., Jonasson, S., 2008. Effects of litter addition and warming on soil carbon, nutrient pools and microbial communities in a subarctic heath ecosystem. *Applied Soil Ecology* 39: 271-281.

Schindlbacher, A., Rodler, A., Kuffner, M., Kitzler, B., Sessitsch, A., Zechmeister-Boltenstern, S., 2011. Experimental warming effects on the microbial community of a temperate mountain forest soil. *Soil Biology and Biochemistry* 43: 1417–1425.

Siebielec, S., Siebielec, G., Klimkowicz-Pawlas, A., Gałązka, A., Grządziel, J., Stuczyński, T. 2020. Impact of water stress on microbial community and activity in sandy and loamy soils. *Agronomy* 10(9): 1429.

Soil Survey Staff 2010. Keys to Soil Taxonomy, 11th Edition. United States Department of Agriculture (USDA), Natural Resources Conservation Service, Washington, DC. 939p. Available at [Access date: 28.01.2022]: https://www.nrcs.usda.gov/wps/PA_NRCSConsumption/download?cid=nrcs142p2_053110&ext=pdf

USDA, 1999. Guía para la evaluación de la calidad y salud del suelo. Departamento de Agricultura, Servicio de Investigación Agricola, Servicio de Conservación de Recursos Naturales, 249 p. Available at [Access date: 28.01.2022]: https://www.nrcs.usda.gov/Internet/FSE_DOCUMENTS/nrcs142p2_051284.pdf [in Spanish]

Valadares-Pereira, A.A., Oliveira, E.C.A.M., Navarrete, A.A., Junior, W.P.O., Tsai, S.M., Peluzio, J.M., Morais, P.B., 2017. Fungal community structure as an indicator of soil agricultural management effects in the Cerrado. *Revista Brasileira do Ciencia do Solo* 41: e0160489.

Vimal, S.R., Singh, S.J., Arora, N.K., Singh, S., 2017. Soil-plant-microbe ınteractions in stressed agriculture management: A review. *Pedosphere* 27(2): 177–192.

Voroney, R.P., Heck, R.J., 2015. The Soil Habitat. In: Soil Microbiology, Ecology and Biochemistry. 4th Edition. Paul, E.A. (Ed.). Elsevier, p. 15– 39.

Wang, G., Huang, W., Mayes, M., Liu, X., Zhang, D., Zhang, Q., Han, T., Zhou, G., 2019. Soil moisture drives microbial controls on carbon decomposition in two subtropical forests. *Soil Biology and Biochemistry* 130: 185 – 194.

Zagal, E., Rodríguez, N., Vidal, I., Quezada, L., 2002. Microbial activity in a volcanic ash soil under different agricultural management. Agricultura Técnica 62: 297-309. [in Spanish]

Eurasian Journal of Soil Science 2023, 12(1), 37- 62

Eurasian Journal of Soil Science

Journal homepage : http://ejss.fesss.org

Identification of species of the genus *Quercus* L. with different responses to soil and climatic conditions according to hyperspectral survey data

Pavel Dmitriev, Boris Kozlovsky, Anastasiya Dmitrieva, Vladimir Lysenko, Vasily Chokheli, Tatiana Minkina, Saglara Mandzhieva, Svetlana Sushkova*, Tatyana Varduni

Southern Federal University, Rostov-on-Don, Russia

Article Info

Received : 15.05.2022
Accepted : 01.10.2022
Available online : 03.10.2022

Author(s)

P.Dmitriev
B.Kozlovsky
A.Dmitrieva
V.Lysenko
V.Chokheli
T.Minkina
S.Mandzhieva
S.Sushkova *
T.Varduni

* Corresponding author

Abstract

Soil standing may be studied indirectly using remote sensing through an assessment of state of the plants growing on it. The ability to evaluate the physiological state of plants using the hyperspectral survey data also provides a tool to characterize vegetation cover and individual samples of woody plants. In the present work the hyperspectral imaging was applied to identify the species of the woody plants evaluating the differences in their physiological state. Samples of *Quercus macrocarpa* Michx., *Q. robur* L. and *Q. rubra* L. were studied using Cubert UHD-185 hyperspectral camera over five periods with an interval of 7-10 days. In total, 80 vegetation indices (VIs) were calculated. Sample sets of values of VIs were analyzed using analysis of variance (ANOVA), principal component analysis (PCA), decision tree (DT), random forest (RF) methods. It was shown using the ANOVA, that the following VIs are the most dependent on the species affiliation of the samples: Carter2, Carter3, Carter4, CI, CI2, CRI4, Datt, Datt2, GMI2, Maccioni, mSR2, MTCI, NDVI2, OSAVI2, PRI, REP_Li, SR1, SR2, SR6, Vogelmann, Vogelmann2, Vogelmann4. VIs that are effective for the separation of oak species, were also revealed using the DT method – these are Boochs, Boochs2, CARI, CRI1, CRI3, D1, D2, Datt, Datt3; Datt4, Datt5, DD, DDn, EGFN, Gitelson, MCARI2, MTCI, MTVI, NDVI3, PRI, PSND, PSRI, RDVI, REP_Li, SPVI, SR4, Vogelmann, Vogelmann2, Vogelmann3. PCA and RF methods reliably differentiated *Q. rubra* from *Q. robur* and *Q. macrocarpa*. *Q. rubra*, unlike other species, was under stress from the impact of soil pH against the background of drought. This was manifested in leaf chlorosis. Influence of the environmental stress factors on the reliability and efficiency of species identification was demonstrated. *Q. robur* and *Q. macrocarpa*were were poorly separated by PCA and RF methods all over the five periods of the experiment.

Keywords: Hyperspectral imaging, vegetation indices, *Quercus macrocarpa*, *Quercus robur*, *Quercus rubra*, environmental stress, drought stress, reflection spectra.

Introduction

Remote sensing of Earth's surface allows to assess the state of vegetation and its species composition. The number of works devoted to establishing the species affiliation of woody plant samples using remote sensing methods has been steadily growing in recent years (Dainelli et al., 2021; Fassnachtet al., 2016).Various technologies and types of sensors are used to identify tree species, with great interest being shown in the possibilities of hyperspectral imaging (Cao et al., 2018; Tuominen et al., 2018; Saarinen et al., 2018; Nezami et

: https://doi.org/10.18393/ejss.1183524
: http://ejss.fesss.org/10.18393/ejss.1183524
Publisher : Federation of Eurasian Soil Science Societies
e-ISSN : 2147-4249

al., 2020; Miyoshi et al., 2020a,b; Sothe et al., 2020). However, many questions regarding the reliability of tree species identification by remote sensing remain open.

In addition, the remote monitoring of soil, as a component of biogeocenoses, is a more complicated and difficult since it is hidden by vegetation in many areas. However, the assessment of the soil standing can be achieved indirectly through the state of plants growing on it. The values of vegetation indices (VIs) and spectral channels data primarily depend on the physiological state of plants (Oppelt and Mauser 2004; Ronay et al., 2021). Therefore, it is of great interest to study the spectral characteristics of a group of the related plant species having different responses to the specific soil and climatic conditions, varying from optimum to stress. Particularly, oak species *Quercus macrocarpa* Michx., *Q. robur* L. and *Q. rubra* L. are of interest considering their wide distribution and occurrence in the central and southern regions of Russia (Kozlovsky et al., 2009).

In the Rostov region, oak forests from *Q. robur* L. are considered the most valuable formations of ravine and floodplain forests (Zozulin, 1992). *Q. robur* is the leading species in protective forest belts and plantations of settlements in the Rostov region of Russia (Kozlovsky et al., 2009). *Q. macrocarpa* Michx. – the most promising species from the genus *Quercus* for the regional culture according to the results of the introduction test. *Q. rubra* L. in its biological properties does not correspond to the climatic and soil conditions of the steppe zone - it does not tolerate drought well and needs the acidic soils (Kozlovsky et al., 2016).

We propose that hyperspectral imaging can distinguish stressed *Q. rubra* from *Q. robur* and *Q. macrocarpa*, which grow under optimal conditions, but having differences in their physiological state. We evaluated the possibilities of using hyperspectral survey data (VIs values) to identify woody plant samples based on differences in their physiological state using the species of the genus *Quercus* as a test plants. Influence of soil pH and drought, as environmental stress factors, were studied in regard of such an identification. Performance of the studied VIs was discussed in the context of the various spectral ranges on the basis of which they are calculated.

Material and Methods

The research was performed in the Botanic Garden of the Southern Federal University (SFedU), Rostov-on-Don, Russia (Figure 1). The climate of the Rostov region is temperate continental, arid, average annual rainfall – 548 mm, and most of the precipitation falls in the frost-free period. The summer is hot, the average temperature of July month is + 22 ... + 23 ºC., maximum +40 ºC. Winter is moderately mild, the average air temperature in January is -5 ºC, the average absolute temperature minimum is -20 ...- 25 ºC, the absolute minimum is -32 ºC. The growing season lasts 216 days (from April 1 to November 4), the frost-free period is 258 days.

Figure 1. Research region

The objects of study were *Q. macrocarpa*, *Q. robur* and *Q. rubra*. The ecological and biological properties of these species under local culture conditions are given below (Kozlovsky et al., 2016).

Q. robur is a species of native flora. In the regional culture, it reaches a height of 26 m. It grows relatively fast. The plant is winter-hardy and drought-resistant, leaves can be strongly affected by insects and fungal diseases. It bears fruit abundantly and regularly. The duration of ontogeny is on average 90 years. *Q. robur* is widely used in regional culture.

Q. macrocarpa is a species of North American flora. In the Botanical Garden of Southern Federal University it reaches a height of 26 m. In terms of ecological and biological properties, it is not inferior to the species of the local flora, *Q. robur*, while it is resistant to diseases and pests. Fruiting occurs with a frequency of 3-4 years. The duration of ontogeny is on average 90 years. It is a promising species for the creation of protective forest belts, artificial forests, and landscaping of settlements.

Q. rubra is a species of North American flora. In the Botanical Garden it reaches a height of 15 m, growing slowly. This species is highly winter-hardy, but weakly drought-resistant – against the background of drought the growth processes are stopped, and the plant needs watering at the initial stages of ontogenesis. The tree is disease and pest resistant. It rarely bears fruit and grows poorly on the neutral and alkaline chernozems needing acidic soils. This species may often suffer from leaf chlorosis, especially during the drought period. The duration of ontogeny is about 60 years.

All the studied oak seedlings were grown under the same soil and solar illumination conditions and according to one agricultural technique at the introduction nursery of the Botanical Garden. Their landings were oriented from north to south. At the time of the experiment, all seedlings of *Q. macrocarpa*, *Q. robur*, *Q. rubra* were at the same stage of ontogeny (virginile stage).

For the experiment, five specimens of each species of oak were selected from the plantations. The crown section of each specimen was filmed 3 to 5 times.

Hyperspectral images were obtained using a Cubert UHD-185 video camera in accordance with Aasen et al. (2015), Bareth et al. (2015). The shooting was carried out from 12 to 14 hours in sunny and cloudless weather. For shooting, the most sunlit part of the crown of the plant was chosen. The camera was located on the southeast side of the object at 90 cm. The light reflected from leaves was recorded in the range of 450-950 nm. Each image was represented as a single black-and-white image, 1000 × 1000 pixels in size. All the studied 125 hyperspectral images, 50 × 50 pixels in size, had the square resolution up to 35 mm^2.

The experiment was repeated five times in 2021: Aug 22, Sept 05, Sept 13, Sept 20, and Sept 30.

60 to 100 spectral profiles were randomly selected from each hyperspectral image. The number of spectral profiles were from 1500 to 2500 spectral profiles per one variant of the experiment.

A Savitsky-Golay filter (length 12 nm) was used as a preprocessing step to reduce the measurement error and remove artifacts in the spectral data.

For each variant of the experiment, 80 VIs were calculated (Dmitriev et al., 2022a,b).

Sample sets of VIs values were analyzed using analysis of variance (ANOVA), principal component analysis (PCA), decision tree (DT), random forest (RF) methods. The data was processed in the environment for statistical calculations R (R Core Team) using the «hsdar» package (Lehnert et al., 2019).

Results and Discussion

ANOVA was used to determine the contribution of experimentally controlled factors («species», «sample», «snapshot») to the vegetation index (VI) value. The strength of the influence of factors (the ratio between deviation of the factor and the total deviation) of 80 VIs is shown in Figure 2. VI should be considered suitable for identification of oak species, if the value of the deviation of the factor «species» significantly exceeds the values of the deviation of «sample» and «snapshot», with a low value of the deviation of random factors (Table 1 and Supplementary Table 1). This means that the value of the index depends more on species characteristics than on other factors. It should be noted that the results of the analysis of variance vary depending on the timing of the survey. For all survey periods, effective VIs were Carter2, Carter3, Carter4, CI, CI2, CRI4, Datt, Datt2, GMI2, Maccioni, mSR2, MTCI, NDVI2, OSAVI2, PRI, REP_Li, SR1, SR2, SR6, Vogelmann, Vogelmann2, Vogelmann4. As a positive fact, it should be noted the low value of the deviation of the «snapshot» factor for most VIs, as far as this value includes the operation errors of the instrument and errors of the operator's work when selecting spectral profiles from the snapshot.

Table 1. Results of a three-way ANOVA analysis of the statistical complex «species-sample-snapshot» for the Maccioni value

ANOVA	Df	SumSq	MeanSq	F value	Pr(>F)
Species	2	51.044	25.522	12211.401	<2e-16*
Sample	12	10.397	0.866	414.539	<2e-16*
Snapshot	37	0.527	0.014	6.812	<2e-16*
Intragroupvariance	3875	8.099	0.002		

Note: * significancelevel< 0.001

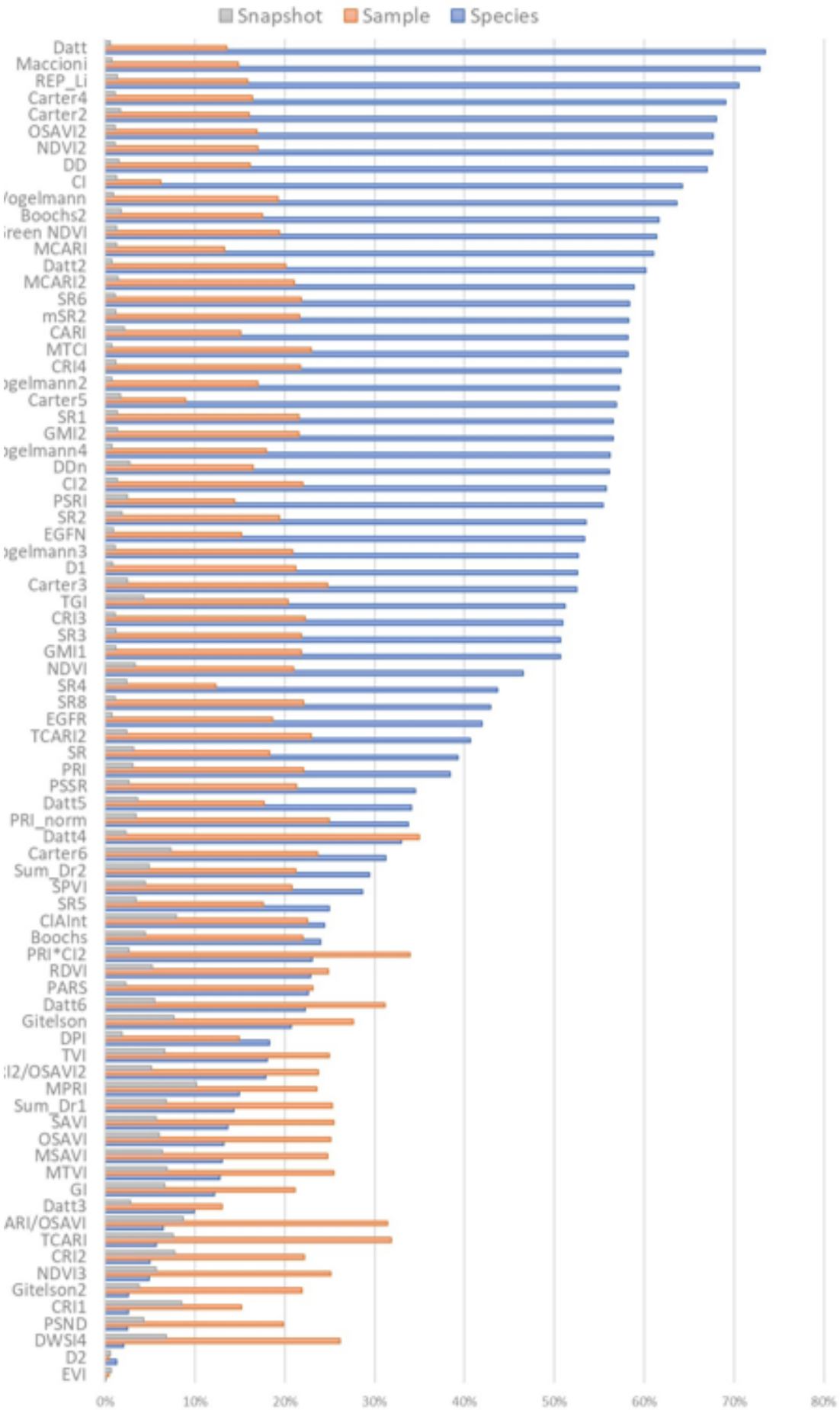

Figure 2. Strength of influence of the factors «species», «sample», «snapshot» on the VIs values of Acer species, Aug 22)

Thus, a set of VIs has been selected to be suitable for the identification of plant species in accordance with the aims of the present work.

An important criterion for the objectivity of the data obtained is the reproducibility of the results of their processing over a time scale. Figure 3 presents the results of data analysis carried out by the PCA method for the five studied time periods. Projections of the values of 80 VIs on the main components showed that the location of oak species coincides in all periods (in some cases, the images are inverted mirrorwise about the first or second component). Projection of *Q. rubra* data is the most isolated, may be explained by its ecological and biological features (Kozlovsky et al., 2016).

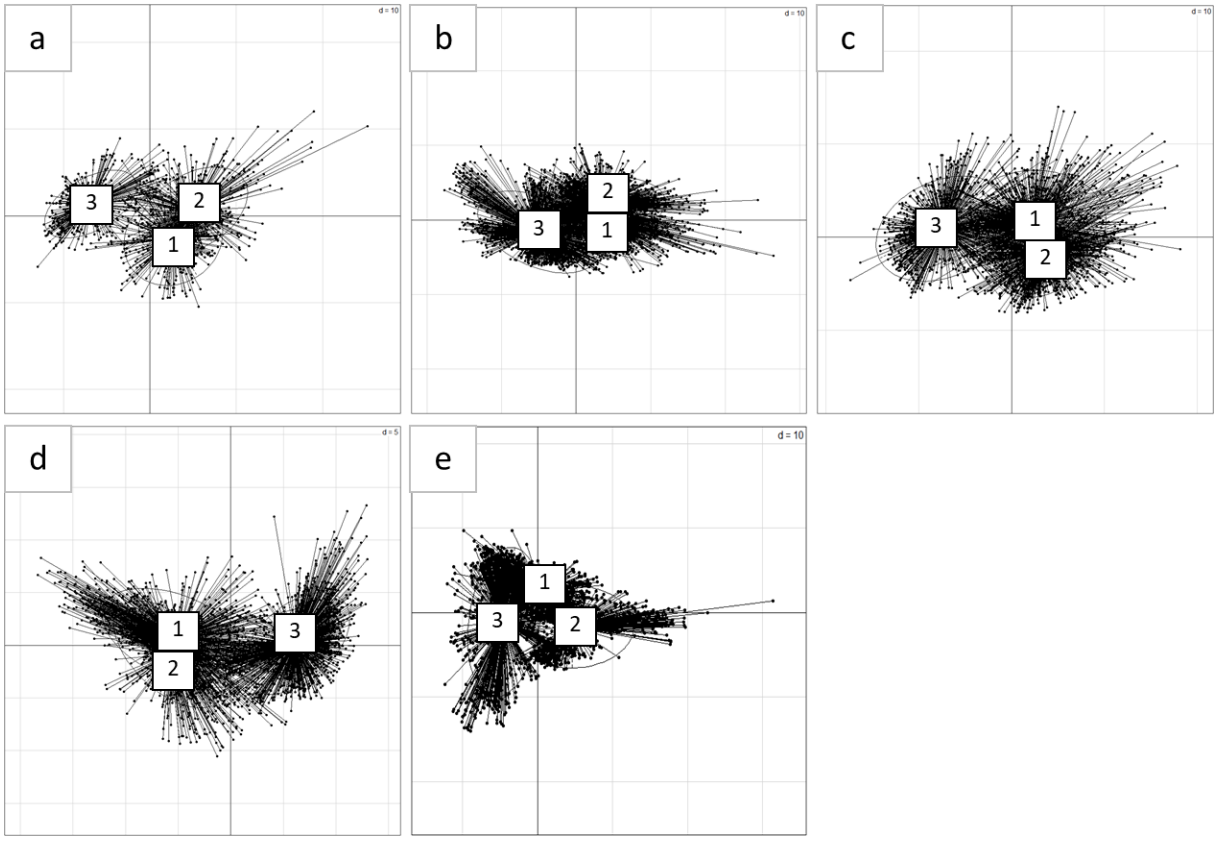

Figure 3. PCA of the 80 VIs values for Q. macrocarpa (1), Q. robur (2), Q. rubra (3) at different survey times. Dates of the experiments: a – Aug 22, b – Sept 05, c – Sept 13, d – Sept 20, e – Sept 30

The proportion of dispersion of the first and second main components varies from 70.4 to 71.5%, the number of significant components (according to the Kaiser criterion) is from 6 to 7 (Table 2).

Factor loads (by analogy with the value of the correlation coefficient) can be considered very weak in the range from 0 to 0.3, weak – from 0.3 to 0.5, medium - from 0.5 to 0.7 and high – from 0.7 to 0.9. VIs Factor loads on the main component are very weak and do not exceed 0.150. They change little depending on the VIs (Aug 22 – Table 3, for other dates – Supplementary Table 2).

Due to the large number of the statisticaly significant components and low factor loads, the PCA results cannot be considered to be satisfactory for the experiment.This problem can be solved by reducing the number of VIs, and by selecting indices that have the largest dispersion by oak species.In order to avoid a subjective approach when choosing such VIs, the DT method was used (Figure 4-8).

The decision tree method divided samples of oak species by VI values in five levels. The division of oak samples into clades is not witout alternative. At the same time, most of the *Q. rubra* samples are grouped in one of the two clusters of the higher hierarchy, while *Q. macrocarpa* and *Q. robur* are grouped mainly in the alternative cluster. As a result, the DT method divided the oak samples at different survey times according to the following indices:

- Aug 22 – Boochs2, Carter5, CRI3, Datt, Datt5, DPI, MCARI2, MTVI, PRI, SR8, TGI;
- Sept 05 – Boochs2, CRI3, Datt4, Maccioni, MTCI, NDVI3, PSRI, RDVI, RDVI, REP_Li, SPVI, TCARI2;
- Sept 13 – Boochs2, CRI3, CRI4, Datt5, DD, DWSI4, Gitelson, MCARI, PRI;
- Sept 20 – Boochs, Carter3, D1, Datt, Datt3, Datt5, Gitelson2, MCARI2, Sum_Dr1, Vogelmann;
- Sept 30 – Boochs2, Carter6, Datt5, NDVI3, PRI_norm, SPVI, SR5, Sum_Dr1, TCARI2, Vogelmann2.

Table 2. Dispersion values calculated for the main components of the projection of 80 VIs for *Q. robur*, *Q. macrocarpa*, *Q. rubra*

Experimentdates	Aug 22			Sept 05			Sept 13			Sept 20			Sept 30		
Statistics	Standard deviation	ProportionofVariance	CumulativeProportion	Standard deviation	ProportionofVariance	CumulativeProportion	Standard deviation	ProportionofVariance	CumulativeProportion	Standard deviation	ProportionofVariance	CumulativeProportion	Standard deviation	ProportionofVariance	CumulativeProportion
Comp.1	6.595	0.544	0.544	6.704	0.562	0.562	6.503	0.529	0.529	6.954	0.605	0.605	5.482	0.376	0.376
Comp.2	3.571	0.160	0.704	3.501	0.153	0.715	3.835	0.184	0.713	3.302	0.136	0.741	4.466	0.249	0.625
Comp.3	3.083	0.119	0.823	2.895	0.105	0.820	3.392	0.144	0.856	2.886	0.104	0.845	2.972	0.110	0.736
Comp.4	1.650	0.034	0.857	2.166	0.059	0.879	1.549	0.030	0.886	1.672	0.035	0.880	2.400	0.072	0.808
Comp.5	1.444	0.026	0.883	1.381	0.024	0.902	1.229	0.019	0.905	1.339	0.022	0.902	2.053	0.053	0.860
Comp.6	1.256	0.020	0.903	1.110	0.015	0.918	1.080	0.015	0.920	1.176	0.017	0.920	1.515	0.029	0.889
Comp.7	1.058	0.014	0.917	1.000	0.012	0.930	1.000	0.013	0.932	1.000	0.013	0.932	1.049	0.014	0.903
Comp.8	0.999	0.012	0.929				0.920	0.011	0.943				1.011	0.013	0.916
Comp.9													1.000	0.012	0.928

Table 3. VI factor loads on significant components for *Q. robur*, *Q. macrocarpa*, *Q. rubra* (Aug 22)

Factors	Comp.1	Comp.2	Comp.3	Comp.4	Comp.5	Comp.6	Comp.7	Comp.8
Boochs		0.239	0.133					0.209
Boochs2	0.101	0.189			0.1			
CARI	-0.131		0.112	0.152	-0.118			
Carter2	-0.146							
Carter3	-0.137				-0.183			
Carter4	-0.15							
Carter5		-0.101	0.21	0.106				-0.106
Carter6	-0.125	0.133			-0.174	-0.111		
CI	0.121			-0.163				0.194
CI2	0.148				-0.111			
ClAInt	-0.113	0.168		0.11	-0.118			
CRI1		-0.194	0.176					
CRI2		-0.206	0.105					0.181
CRI3	-0.144			-0.145				-0.112
CRI4	-0.147				0.115			
D1	0.116				-0.241		0.184	
D2						-0.102	0.168	-0.96
Datt	0.145					0.112		
Datt2	0.144				-0.147			
Datt3						-0.311	-0.609	-0.123
Datt4	0.106	-0.114	-0.16					
Datt5			-0.254	0.169	0.106	0.132		0.107
Datt6	0.115	-0.124			-0.188			0.175
DD	0.145							
DDn		-0.211						
DPI					0.265	-0.302	-0.302	-0.354
DWSI4			0.227	-0.382				
EGFN	0.127			0.17			-0.123	
EGFR	0.12			0.189			-0.147	
EVI							0.114	0.987
GI			0.255	-0.321	-0.112			
Gitelson	0.121	-0.136			-0.117			
Gitelson2		0.172				0.324		-0.557
GMI1	0.144			0.138				0.108

Table 3. Continue

Factors	Comp.1	Comp.2	Comp.3	Comp.4	Comp.5	Comp.6	Comp.7	Comp.8
GMI2	0.148				-0.114			
Green NDVI	0.145					0.114		
Maccioni	0.148							
MCARI	-0.124		0.143	0.151	-0.112			
MCARI2	0.131	0.126						-0.147
MPRI		0.176				-0.152		
MSAVI	0.104		0.218					
mSR2	0.148				-0.103			
MTCI	0.145				-0.106			-0.101
MTVI		0.256		0.109	-0.12			
NDVI	0.137		0.117					
NDVI2	0.15							
NDVI3			-0.187	0.404				
OSAVI	0.105		0.219					
OSAVI2	0.15							
PARS	0.115		0.171	0.138				
PRI	0.116				0.201	-0.3	0.305	
PRI_norm	-0.117				-0.15	0.319	-0.316	
PRI*CI2	0.106					-0.393	0.307	0.135
PSRI	-0.128			0.203	-0.129			-0.113
PSSR	0.129		0.12					0.123
PSND		-0.101	0.237	0.185	-0.13			
RDVI		0.232	0.131	0.132				
REP_Li	0.142				0.147	0.103		
SAVI	0.105		0.22					
SPVI		0.248		0.141				
SR	0.138		0.109					
SR1	0.148				-0.114			
SR2	0.147				-0.119			
SR3	0.144			0.138				0.108
SR4		-0.1	0.247					
SR5			-0.277					-0.113
SR6	0.148				-0.113			
SR8	0.102		-0.2		0.112		0.106	
Sum_Dr1		0.255		0.139	-0.126			
Sum_Dr2		0.253						
TCARI		0.175	-0.134	-0.131	-0.171		-0.104	0.153
TCARI/OSAVI		0.161	-0.146	-0.121	-0.164			0.163
TCARI2		0.219		-0.107	0.237	0.126		
TCARI2/OSAVI2		0.187			0.118			0.187
TGI	-0.134				-0.215	-0.129		
TVI		0.257	0.103	0.102				
Vogelmann	0.145				-0.135			
Vogelmann2	-0.133				0.207			0.129
Vogelmann3	0.13					-0.149	-0.103	-0.156
Vogelmann4	-0.133				0.212			0.128

It should be noted that the VIs that are significant for clustering coincide at many times (for example, Boochs2, Datt5, CRI3) or are derived from the same index (for example, Carter3, Carter5, Carter6 or CRI3, CRI4, Vogelmann, Vogelmann2) or are close in the used spectral channels.

Visualization of the results of species differentiation using PCA according to the value of VIs selected using DT is shown in Figure 9. The dispersion values of the first two principal components in all survey periods are from 74 to 80% (Table 4). Factor loads of VI on the main components are on average doubled (in some cases they exceeded 0.4), but for most of the VI they remained low (Table 5).

In more detail, the separation of oak species by PCA can be demonstrated by their samples. Projection of VI values Boochs2, Carter5, CRI3, Datt, Datt5, DPI, MCARI2, MTVI, PRI, SR8, TGI by main components for samples of oak species on the first survey date is shown in Figure 10, for other dates in Supplementary Table 3.

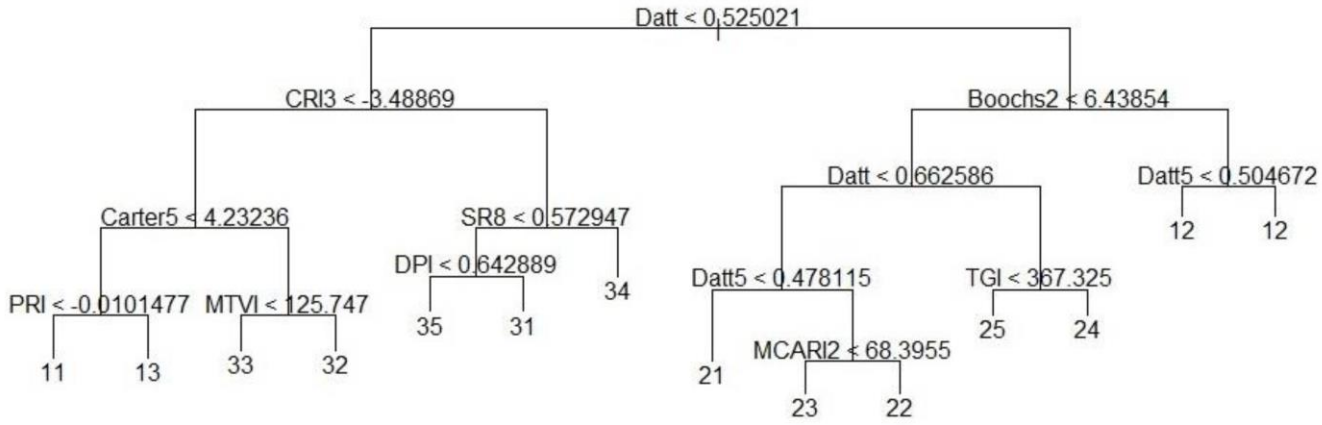

Figure 4. Decision tree of the 80 VIs values for Q. macrocarpa (1), Q. robur (2), Q. rubra (3) (Aug 22). Numerical designation, bottom digits: the first digit indicates the species; the second is the sample of the species.

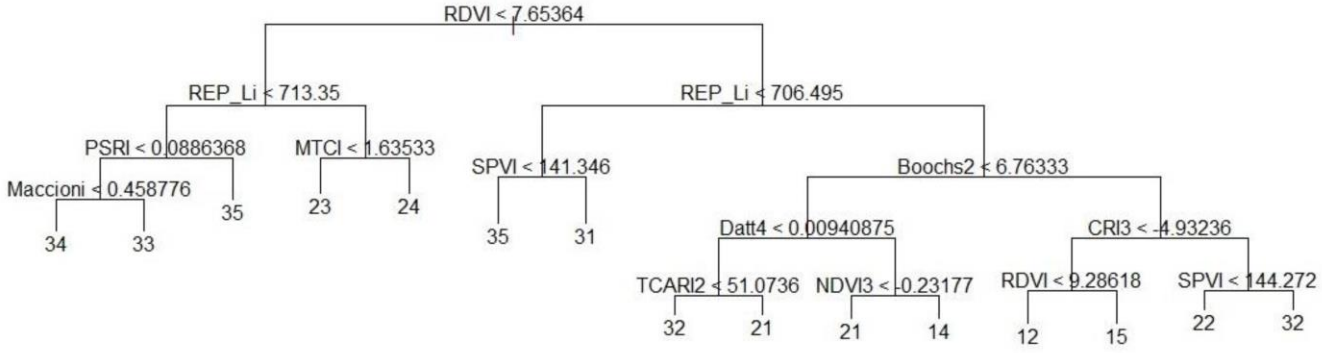

Figure 5. Decision tree of the 80 VIs values for Q. macrocarpa (1), Q. robur (2), Q. rubra (3) (Sept 05). Numerical designation, bottom digits: the first digit indicates the species; the second is the sample of the species.

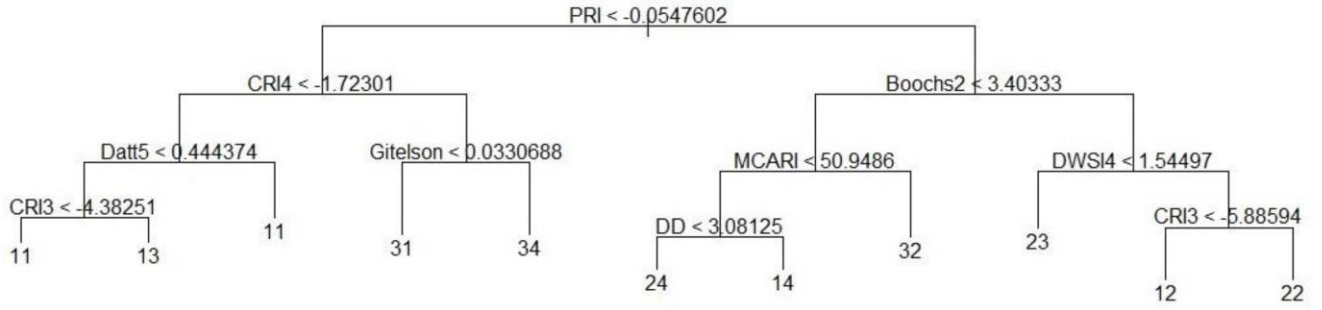

Figure 6. Decision tree of the 80 VIs values for Q. macrocarpa (1), Q. robur (2), Q. rubra (3) (Sept 13). Numerical designation, bottom digits: the first digit indicates the species; the second is the sample of the species.

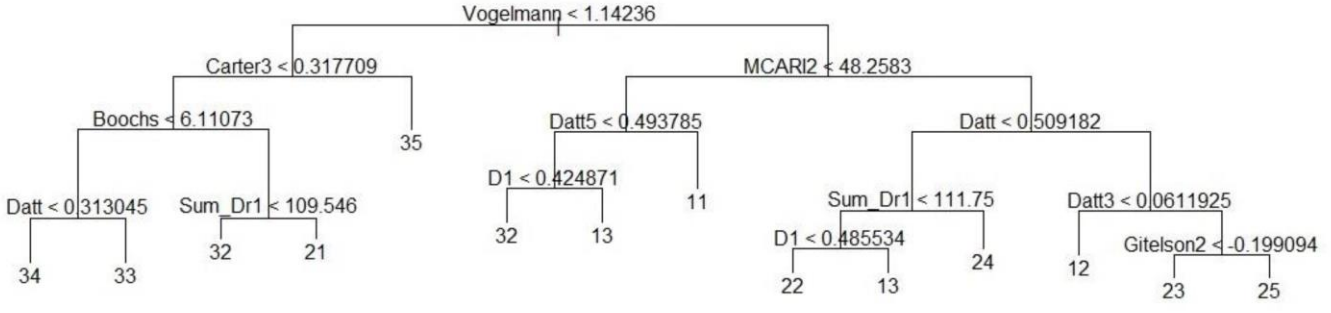

Figure 7. Decision tree of the 80 VIs values for Q. macrocarpa (1), Q. robur (2), Q. rubra (3) (Sept 20). Numerical designation, bottom digits: the first digit indicates the species; the second is the sample of the species.

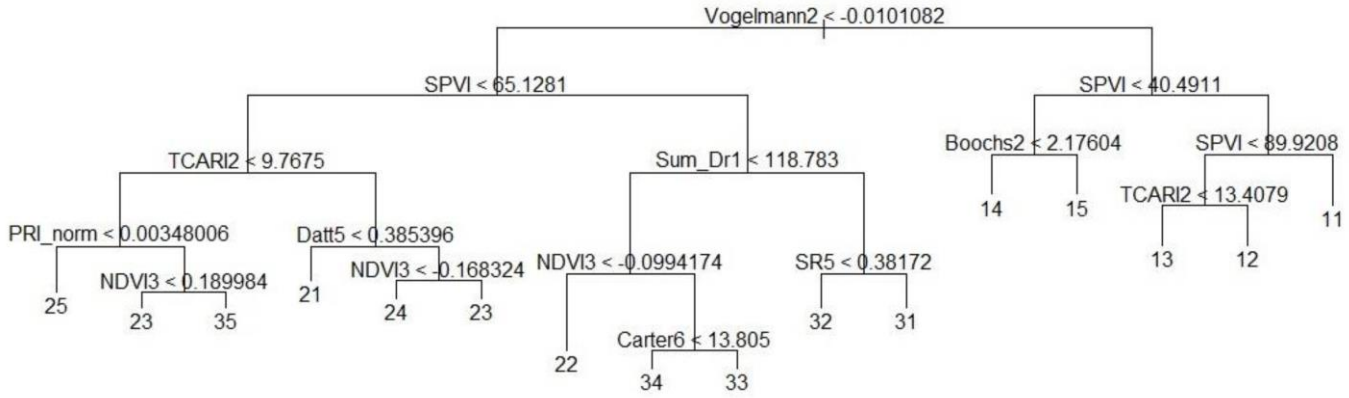

Figure 8. Decision tree of the 80 VIs values for Q. macrocarpa (1), Q. robur (2), Q. rubra (3) (Sept 30). Numerical designation, bottom digits: the first digit indicates the species; the second is the sample of the species.

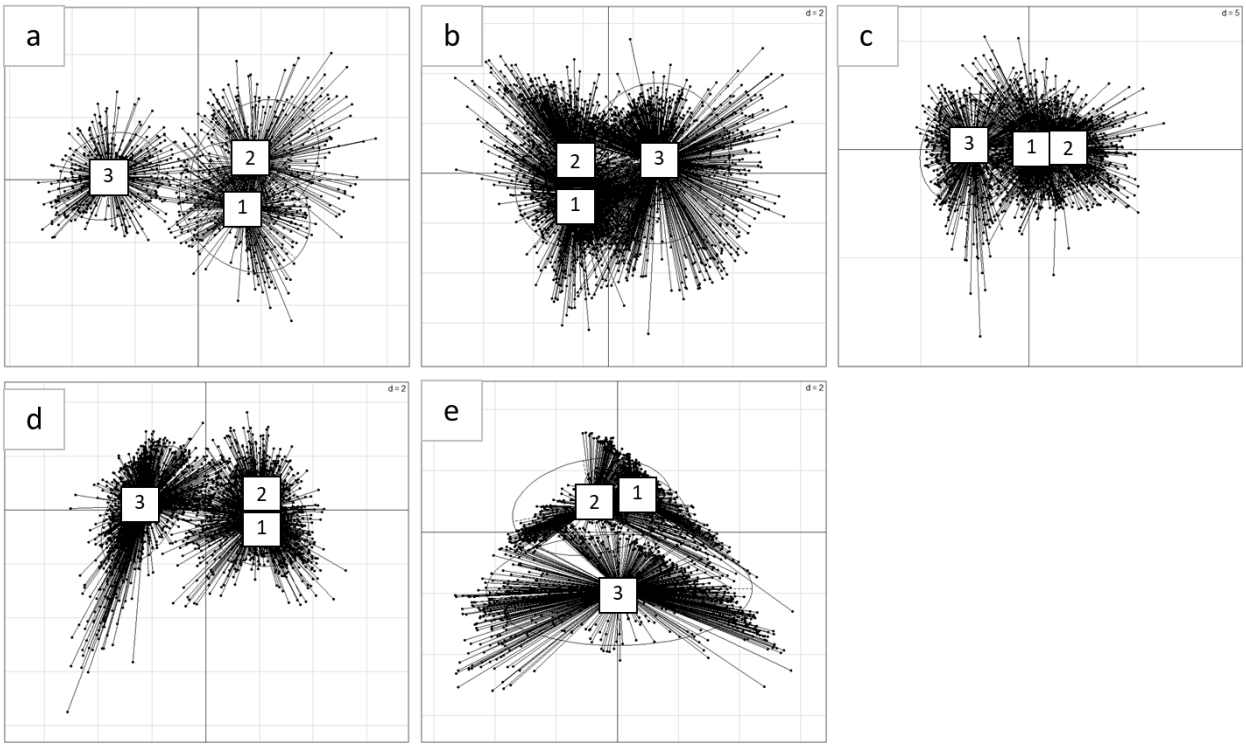

Figure 9. PCA of the VIs values selected by the DT method, Q. macrocarpa (1), Q. robur (2), Q. rubra (3) VIs at different survey times. Experiment dates: a – Aug 22, b – Sept 05, c – Sept 13, d – Sept 20, e – Sept 30.

Table 4. Dispersions of the principal components of the projection of the values selected by the DT method, VI for *Q. robur*, *Q. macrocarpa*, *Q. rubra*

Experimentdates	Aug 22			Sept 05			Sept 13			Sept 20			Sept 30		
Statistics	Standard deviation	ProportionofVariance	CumulativeProportion	Standard deviation	ProportionofVariance	CumulativeProportion	Standard deviation	ProportionofVariance	CumulativeProportion	Standard deviation	ProportionofVariance	CumulativeProportion	Standard deviation	ProportionofVariance	CumulativeProportion
Comp.1	2.510	0.573	0.573	2.283	0.434	0.434	2.247	0.561	0.561	2.365	0.559	0.559	2.130	0.454	0.454
Comp.2	1.345	0.165	0.738	2.071	0.357	0.792	1.484	0.245	0.806	1.342	0.180	0.740	1.696	0.288	0.742
Comp.3	1.087	0.108	0.845	1.221	0.124	0.916	1.005	0.112	0.918	1.118	0.125	0.865	1.069	0.114	0.856
Comp.4	0.872	0.069	0.914	0.775	0.050	0.966	0.571	0.036	0.955	0.766	0.059	0.923	0.893	0.080	0.936

Table 5. Factor loads selected by the DT method, VI for significant components for *Q. robur*, *Q. macrocarpa*, *Q. rubra*

Factors	Comp.1	Comp.2	Comp.3	Comp.4
		Aug 22		
Boochs2	0.296	0.465		
Carter5	-0.318		-0.472	
CRI3	-0.343		0.280	-0.251
Datt	0.372			0.253
Datt5	0.269	-0.276	0.489	-0.213
DPI	0.188		-0.401	-0.855
MCARI2	0.351	0.293		0.146
MTVI		0.687	0.303	
PRI	0.312	0.140	-0.293	
SR8	0.335	-0.214	0.243	-0.188
TGI	-0.339	0.256	0.241	-0.170
		Sept 05		
RDVI		0.467	0.141	0.211
Boochs2	-0.267	0.363		-0.170
CRI3	0.357		-0.340	-0.403
Datt4	-0.304	-0.275	0.275	-0.151
Maccioni	-0.430			
MTCI	-0.416		0.187	
NDVI3	0.176		0.635	-0.557
PSRI	0.358		0.406	
RDVI.1		0.467	0.141	0.211
REP_Li	-0.423			-0.200
SPVI		0.440	0.264	
TCARI2		0.390	-0.277	-0.573
		Sept 13		
Boochs2	0.319	0.178	0.616	0.173
CRI3	-0.394		0.223	-0.665
CRI4	-0.430			-0.238
Datt5		-0.641	0.235	
DD	0.430			-0.180
DWSI4	0.154	0.600		-0.306
Gitelson	0.313	-0.104	-0.673	
MCARI	-0.313	0.420		0.474
PRI	0.391		0.215	-0.329
		Sept 20		
Boochs	0.352	0.313	0.177	0.153
Carter3	-0.394		0.149	-0.219
D1	0.325	-0.345	-0.200	-0.285
Datt	0.347	-0.406		
Datt3	-0.178	-0.431	0.294	0.786
Datt5	-0.272	-0.413	0.125	-0.369
Gitelson2	0.103	-0.210	0.754	-0.292
MCARI2	0.405	-0.117		
Sum_Dr1	0.238	0.400	0.463	
Vogelmann	0.396	-0.207	-0.137	
		Sept 30		
Boochs2	0.288		0.548	0.537
Carter6	0.303	-0.414		-0.198
Datt5	-0.360	-0.325	0.175	
NDVI3	-0.337	-0.307	0.290	-0.197
PRI_norm	-0.306	-0.366		0.246
SPVI	0.328	-0.399		-0.219
SR5	-0.297	-0.351		0.398
Sum_Dr1	0.325	-0.390	0.130	-0.266
TCARI2	0.406	-0.107		0.447
Vogelmann2	-0.146	0.208	0.741	-0.296

It can be seen on the projection (Figure 10), as well as in Figure.3 and 9, Q. *rubra* is well separated from *Q. robur* and *Q. macrocarpa*. At the same time, *Q. robur* and *Q. macrocarpa* are poorly separated by PCA. The good differentiation of *Q. rubra* is associated with its physiological state – soil pH stress, enhanced by drought, that is manifested by leaf chlorosis (Figure 11) (Dmitriev et al., 2022a). Stress may be detected by the configuration of the spectral profiles of oak crowns, which are built using the average values of the reflection coefficient (Figure 12).

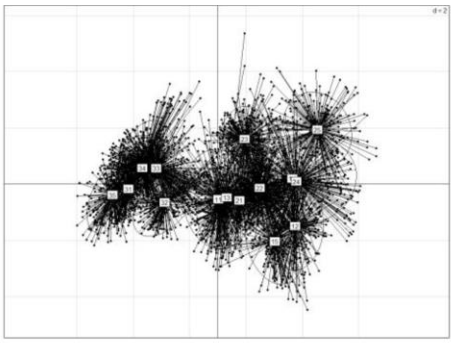

Figure 10. PCA of the values for Boochs2, Carter5, CRI3, Datt, Datt5, DPI, MCARI2, MTVI, PRI, SR8, TGI for Q. macrocarpa (1), Q. robur (2), Q. rubra (3) samples in first shooting time (Aug 22). Numerical designation, bottom digits: the first digit indicates the species; the second is the sample of the species.

Figure 11. Fragments of crowns Q. macrocarpa (1), Q. robur (2), Q. rubra (3). Sept 13

This configuration of the arrangement of objects on the projections persists throughout the period studied (in some cases, the images are inverted mirrorwise about the first or second component).

RF is the next method used to separate species. In total, 500 trees have been analysed. (Figure 13). The number of variables tried at each separation was – 8.

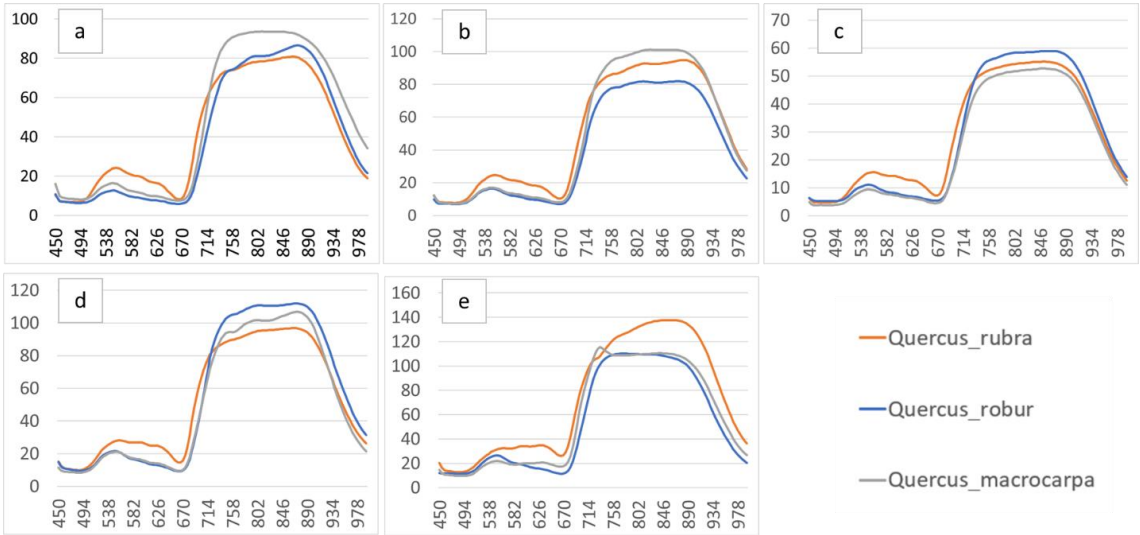

Figure 12. Spectral profiles of crowns of Q. macrocarpa, Q. robur and Q. rubra plants. Dates of the experiments: a – Aug 22, b – Sept 05, c – Sept 13, d – Sept 20, e – Sept 30. Y-scales – reflectance, percent; X-scales – wavelength, nm.

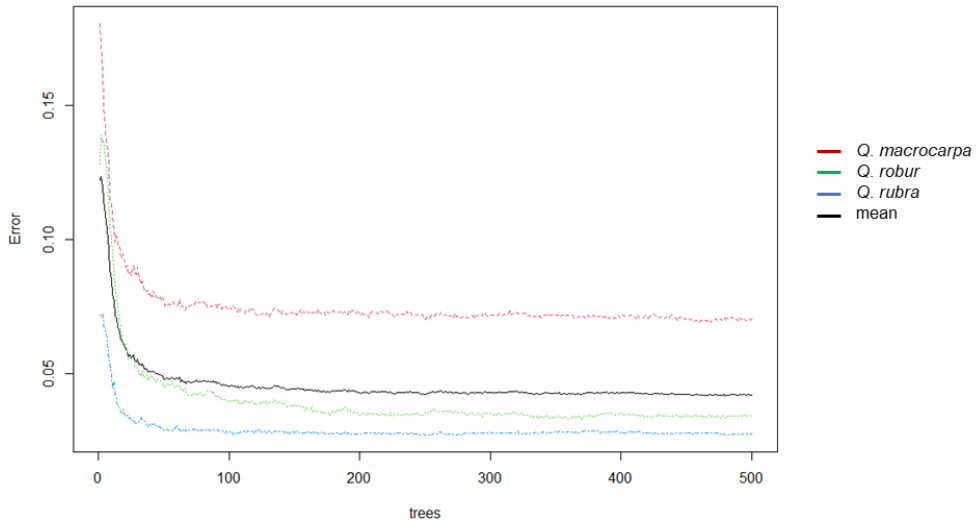

Figure 13. Random forest matrix error depending on the number of trees

OOB estimate of the matrix values error calculated for the 80 VIs of three oak species is low – 4.19%. This indicates a good differentiation of all three oak species by the RF method (Table 6).

The RF method also makes it possible to determine what VIs are the most suitable for species identification. In Figure 14, VIs are arranged depending on their influence on the error value (Mean Decrease Accuracy) and the Gini criterion.

As a result of the RF analysis, it was found that out of 80 VIs, the following VIs have the greatest influence on the accuracy of identification of *Quercus* species and the Gini index:

- D1 D_{730} / D_{706} (Zarco-Tejada et al., 2003)
- Datt3 D_{754} / D_{704} (Datt, 1999)
- DPI D_{688}× D_{710} / D^2_{697} (Zarco-Tejada et al., 2003)
- Vogelmann R_{740} / R_{720} (Vogelmann et al., 1993),

where Rxxx: Reflectance at the wavelength "xxx", Dxxx: First derivation of reflectance values at the wavelength "xxx".

Table 6. Error rates of the matrix of RF values of 80 VIs for *Q. robur*, *Q. macrocarpa*, *Q. rubra*

Species	*Quercusmacrocarpa*	*Quercusrobur*	*Quercusrubra*	class.error
Quercusmacrocarpa	3857	230	61	0.070154
Quercusrobur	110	4610	51	0.033746
Quercusrubra	41	107	5269	0.027321

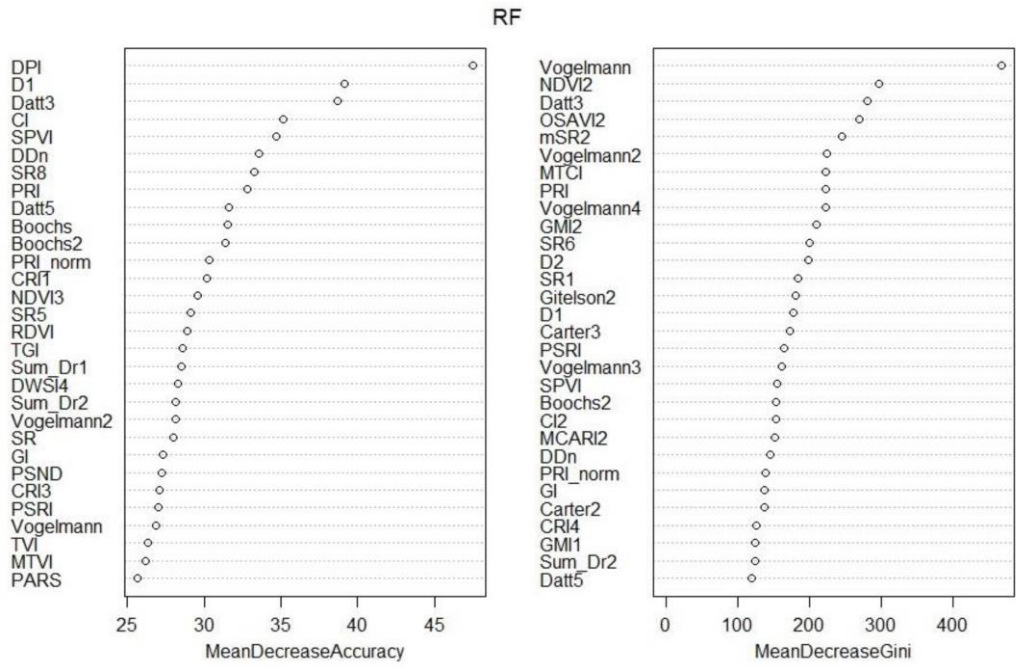

Figure 14. RF: Mean Decrease Accuracy and Mean Decrease Gini calculated for the 80 VIs of Acer species.

These VIs make it possible to separate quite well the stressed *Q. rubra* from *Q. robur* and *Q. macrocarpa*, which are found to be in our region under optimal conditions. At the same time, *Q. robur* and *Q. macrocarpa* are poorly separated. The following wavelengths are used in calculating these VIs: 698 nm,704 nm, 706 nm, 710 nm, 720 nm, 730 nm, 740 nm, 754 nm.

In order to find out how repeatable the result is at different shooting times, the scheme for forming the training and testing samples was as follows:

1. The training sample is the data of 2 (Sept 05), 3 (Sept 13), 4 (Sept 20) and 5 (Sept 30) survey dates. The tested sample – data of the 1st (Aug 22) survey period;
2. The training sample is the data of the 1st, 3rd, 4th, and 5th survey dates. The test sample – data from the 2nd survey period;
3. The training sample is the data of the 1st, 2nd, 4th, and 5th survey dates. The test sample – data from the 3rd survey period;
4. The training sample is the data of the 1st, 2nd, 3rd, and 5th survey dates. The test sample – data of the 4th survey period;
5. The training sample is the data of the 1st, 2nd, 3rd and 4th survey dates. The test sample – data of the 5th survey period.

According to the presented scheme the training sample matrices have a low OOB estimate of error rate (Table 7). Despite the fact that it is not possible to simultaneously identify all three species by VIs values (Table 8), the result obtained should be considered good for field surveys with a hyperspectral camera of tree crowns. *Q. rubra* was well identified in all five terms. *Q. robur* was well identified in the second and third terms of survey, satisfactorily – in the first and fifth and was not identified in the 4th survey. *Q. macrocarpa* was satisfactorily identified only in the second survey period.Good reproducibility of the results (both positive and negative) in terms of timing was obtained, that can be seen from the values of the classification errors of the trained matrices (Table 7) and from the test results (Table 8).The results obtained with the RF method and the PCA method are similar.

Table 7. Error rates of RF matrix of 80 VI values for *Q. robur*, *Q. macrocarpa*, *Q. rubra*, training samples. Number of trees: 500; Number. of variables tried at each split: 8

Training set 1				
Species	*Q. macrocarpa*	*Q. robur*	*Q. rubra*	class.error
Q. macrocarpa	3672	157	41	0.051163
Q. robur	84	4256	50	0.030524
Q. rubra	48	98	4884	0.029026
	OOB estimate of error rate			3.60%
Training set 2				
Species	*Q. macrocarpa*	*Q. robur*	*Q. rubra*	class.error
Q. macrocarpa	2832	209	35	0.079324
Q. robur	79	3477	24	0.028771
Q. rubra	17	62	3857	0.020071
	OOB estimate of error rate			4.02%
Training set 3				
Species	*Q. macrocarpa*	*Q. robur*	*Q. rubra*	class.error
Q. macrocarpa	3096	130	35	0.050598
Q. robur	75	3372	37	0.032147
Q. rubra	23	59	4490	0.017935
	OOB estimate of error rate			3.17%
Training set 4				
Species	*Q. macrocarpa*	*Q. robur*	*Q. rubra*	class.error
Q. macrocarpa	3003	194	63	0.078834
Q. robur	66	3562	47	0.030748
Q. rubra	36	94	3544	0.035384
	OOB estimate of error rate			4.71%
Training set 5				
Species	*Q. macrocarpa*	*Q. robur*	*Q. rubra*	class.error
Q. macrocarpa	2847	212	66	0.08896
Q. robur	107	3806	42	0.037674
Q. rubra	39	80	4337	0.026706
	OOB estimate of error rate			4.73%

Table 8. Error rates of the matrix of RF values of 80 VIs for *Q. robur*, *Q. macrocarpa*, *Q. rubra*, tested samples

Test sample 1			
Species	*Q. macrocarpa*	*Q. robur*	*Q. rubra*
Q. macrocarpa	112	156	10
Q. robur	143	219	10
Q. rubra	23	6	367
Test sample 2			
Species	*Q. macrocarpa*	*Q. robur*	*Q. rubra*
Q. macrocarpa	632	225	133
Q. robur	382	963	405
Q. rubra	58	3	943
Test sample 3			
	Q. macrocarpa	*Q. robur*	*Q. rubra*
Q. macrocarpa	32	1	0
Q. robur	658	1214	184
Q. rubra	197	72	661
Test sample 4			
Species	*Q. macrocarpa*	*Q. robur*	*Q. rubra*
Q. macrocarpa	422	611	57
Q. robur	122	167	4
Q. rubra	344	318	1682
Test sample 5			
Species	*Q. macrocarpa*	*Q. robur*	*Q. rubra*
Q. macrocarpa	395	146	124
Q. robur	0	464	60
Q. rubra	628	206	777

All methods of the data analysis used in the experiment clearly separate *Q. rubra* from *Q. robur* and *Q. macrocarpa*. This can be associated with a significant difference between the ecological and biological properties of *Q. rubra* and *Q. robur*, *Q. macrocarpa*.When using VI, it is not possible to reliably separate *Q. robur* and *Q. macrocarpa*.These species differ significantly in morphology, but are similar in ecological and biological properties. Most VIs have been developed to quantify the state (primarily the physiological state associated with photosynthetic pigments) of plants (Tucker, 1979; Blackburn 1998; Datt 1999; leMaireetal 2004; Zarco-Tejada et al. 2003; Bolca et al., 2012). Therefore, in a specific period, species that differ significantly in physiology can be successfully separated using VIs. For woody plants that differ in phenology, it is possible to propose a search for VIs with unique seasonal dynamics, by analogy with the NDVI signature.

Conclusion

The ANOVA method applied to the hyperspectral data allows to reveal VI, whose variation significantly depends on the species belonging to the sample.This also confirms the possibility of identifying oak species using VI.PCA and RF methods reliably differentiating *Q. rubra* from *Q. robur* and *Q. macrocarpa*.

The results obtained suggest the possibility that droubt and impact of soil pH, being a factor of environmental stress, may influence the realibility of such an identification. It may be a consequence of a droubt-induced and pH-induced chlorosis that evidently influence leaf pigment composition and, therefore, VIs. It means that changes in the hyperspectral data caused by stress should be considered as a reflectance spectral "signature of stress" and should be an object of attention in the future researches.

Acknowledgements

The project was supported by the Russian Science Foundation under grant No. 22-14-00338 and performed in Southern Federal University (Rostov-on-Don, Russian Federation).

References

Aasen, H., Burkart, A., Bolten, A., Bareth, G., 2015. Generating 3D hyperspectral information with lightweight UAV snapshot cameras for vegetation monitoring: From camera calibration to quality assurance. *ISPRS Journal of Photogrammetry and Remote Sensing* 108: 245–259.

Bareth, G., Aasen, H., Bendig, J., Gnyp, M.L., Bolten, A., Jung, A., Michels, R., Soukkamäki, J., 2015. Low-weight and UAV-based hyperspectral full-frame cameras for monitoring crops: Spectral comparison with portable spectroradiometer measurements. *Photogrammetrie - Fernerkundung - Geoinformation* 1: 69–79.

Blackburn, G.A., 1998. Quantifying Chlorophylls and Caroteniods at Leaf and Canopy Scales: An Evaluation of Some Hyperspectral Approaches. *Remote Sensing of Environment* 66: 273–285.

Bolca, M., Kurucu, Y., Altınbaş, Ü., Esetlili, M.T., Özen, F., 2012. A study on the determination of electromagnetic reflection values of agricultural crop pattern to improve accuracy of land use map by remote sensing technique. *Eurasian Journal of Soil Science* 1(2): 116 - 126.

Cao, J., Leng, W., Liu, K., Liu, L., He, Z., Zhu, Y., 2018. Object-Based mangrove species classification using unmanned aerial vehicle hyperspectral images and digital surface models. *Remote Sensing* 10(1): 89.

Dainelli, R., Toscano, P., Di Gennaro, S.F., Matese, A., 2021. Recent advances in unmanned aerial vehicles forest remote sensing - A systematic review. Part II: Research applications. *Forests* 12(4): 397.

Datt, B., 1999. Visible/near infrared reflectance and chlorophyll content in eucalyptus leaves. *Remote Sensing*. 20: 2741–2759.

Dmitriev, P., Kozlovsky, B., Minkina, T., Rajput, V.D., Dudnikova, T., Barbashev, A., Ignatova, M.A., Kapralova, O.A., Varduni, T.V., Tokhtar, V.K., Tarik, E.P., Akça, İ., Sushkova, S., 2022a. Hyperspectral imaging for small-scale analysis of Hordeum vulgare L. leaves under the benzo[a]pyrene effect. *Environmental Science and Pollution Research*

Dmitriev, P.A., Kozlovsky, B.L., Kupriushkin, D.P., Lysenko, V.S., Rajput, V.D., Ignatova, M.A., Tarik, E.P., Kapralova, O.A., Tokhtar, V.K., Singh, A.K., Minkina, T.M., Varduni, T.V., Sharma, M., Taloor, A.K., Thapliyal, A., 2022b. Identification of species of the genus Acer L. using vegetation indices calculated from the hyperspectral images of leaves. *Remote Sensing Applications: Society and Environment* 25, 100679.

Fassnacht, F.E., Latifi, H., Stereńczak, K., Modzelewska, A., Lefsky, M., Waser, L.T., Straub, C., Ghosh, A., 2016. Review of studies on tree species classification from remotely sensed data. *Remote Sensing of Environment* 186: 64–87.

Kozlovskiy, B.L., Kuropyatnikov, M.V., Fedorinova, O.I., 2016. Results of introduction testing of species of the genus Quercus L. In the botanical garden of the Southern Federal. *Bulletin of the Udmurt University. Series Biology. Earth Sciences* 26(2):53–58.

Kozlovsky, B.L., Ogorodnikova, T.K., Kuropyatnikov, M.V., Fedorinova, O.I., 2009. An assortment of woody plants for green building in the Rostov region. Rostov-on-D.: Publishing House of Southern Federal University. 416p.

Lehnert, L.W., Meyer, H., Obermeier, W.A., Silva, B., Regeling, B., Thies, B., Bendix, J., 2019. Hyperspectral Data Analysis in R: The hsdar Package. *Journal of Statistical Software* 89 (12): 1–23.

Lemaire, C., Kohn, S.C., Brooker, R.A., 2004. The effect of silica activity on the incorporation mechanisms of water in synthetic forsterite: a polarised infrared spectroscopic study. *Contributions to Mineralogy and Petrology* 147: 48–57.

Miyoshi, G.T., Arruda, Md.S., Osco, L.P., Junior, J.M., Gonçalves, D.N., Imai, N.N., Tommaselli, A.M.G., Honkavaara, E., Gonçalves, W.N., 2020b. A novel deep learning method to identify single tree species in UAV-based hyperspectral images. *Remote Sensing* 12(8): 1294.

Miyoshi, G.T., Imai, N.N., Tommaselli, A.M.G., Honkavaara, E., 2020a. Spectral differences of tree species belonging to atlantic forest obtained from UAV hyperspectral images. 2020 IEEE Latin American GRSS & ISPRS Remote Sensing Conference (LAGIRS) pp. 60-65.

Nezami, S., Khoramshahi, E., Nevalainen, O., Pölönen, I., Honkavaara, E., 2020. Tree species classification of drone hyperspectral and RGB imagery with deep learning convolutional neural networks. *Remote Sensing* 12(7): 1070.

Oppelt, N., Mauser, W., 2004. Hyperspectral monitoring of physiological parameters of wheat during a vegetation period using AVIS data. *International Journal of Remote Sensing* 25(1): 145–159.

Ronay, I., Ephrath, J.E., Eizenberg, H., Blumberg, D.G., Maman, S., 2021. Hyperspectral reflectance and indices for characterizing the dynamics of crop–weed competition for water. *Remote Sensing* 13(3): 513.

Saarinen, J., Rogerson, C.M., Hall, C.M., 2017. Geographies of tourism development and planning. *Tourism Geographies* 19(3): 307–3017.

Sothe, C., Dalponte, M., Almeida, C.M., Schimalski, M.B., Lima, C.L., Liesenberg, V., Miyoshi, G.T., Tommaselli, A.M.G., 2019. Tree species classification in a highly diverse subtropical forest integrating UAV-based photogrammetric point cloud and hyperspectral data. *Remote Sensing* 11(11): 1338.

Tucker, C.J., 1979. Red and photographic infrared linear combinations for monitoring vegetation. *Remote Sensing of Environment* 8: 127–150.

Tuominen, S., Balazs, A., Honkavaara, E., Pölönen, I., Saari, H., Hakala, T., Viljanen, N., 2017. Hyperspectral UAV-imagery and photogrammetric canopy height model in estimating forest stand variables. *Silva Fennica* 51(5): 7721.

Vogelmann, J.E., Rock, B.N., Moss, D.M., 1993. Red edge spectral measurements from sugar maple leaves. *International Journal of Remote Sensing* 14: 1563–1575.

Zarco-Tejada, P.J., Pushnik, J.C., Dobrowski, S., Ustin, S.L., 2003. Steady-state chlorophyll a fluorescence detection from canopy derivative reflectance and double-peak red-edge effects. *Remote Sensing of Environment* 84: 283–294.

Zozulin, G.M., 1992. Forests of the Lower Don. Rostov-on-Don: Publishing of Rostov University. 200p.

Supplementary Tables

Supplementary Table 1. Results of a three-way ANOVA of the statistical complex «species-sample-snapshot»

ANOVA		Df				Sum Sq				Mean Sq				F value			Pr(>F)		
	date	Species	Sample	Snapshot	Residuals	Species	Sample	Snapshot	Residuals	Species	Sample	Snapshot	Residuals	Species	Sample	Snapshot	Species	Sample	Snapshot
Boochs	Aug 22	2	12	37	3875	2193.00	2014.26	406.36	4524.16	1096.50	167.85	10.98	1.17	939.17	143.77	9.41	0.00	0.00	0.00
Boochs2	Aug 22	2	12	37	3875	9790.69	2787.88	279.72	3021.54	4895.35	232.32	7.56	0.78	6278.07	297.95	9.70	0.00	0.00	0.00
CARI	Aug 22	2	12	37	3875	16285038.71	4233062.50	609240.12	6844569.28	8142519.35	352755.21	16465.95	1766.34	4609.82	199.71	9.32	0.00	0.00	0.00
Carter2	Aug 22	2	12	37	3875	48.24	11.38	1.21	10.10	24.12	0.95	0.03	0.00	9250.81	363.71	12.55	0.00	0.00	0.00
Carter3	Aug 22	2	12	37	3875	11.14	5.25	0.52	4.31	5.57	0.44	0.01	0.00	5004.38	393.01	12.74	0.00	0.00	0.00
Carter4	Aug 22	2	12	37	3875	51.64	12.24	0.82	10.06	25.82	1.02	0.02	0.00	9950.55	393.04	8.53	0.00	0.00	0.00
Carter5	Aug 22	2	12	37	3875	2944.09	462.64	89.75	1681.34	1472.05	38.55	2.43	0.43	3392.63	88.85	5.59	0.00	0.00	0.00
Carter6	Aug 22	2	12	37	3875	57927.56	43888.64	13528.71	69993.91	28963.78	3657.39	365.64	18.06	1603.49	202.48	20.24	0.00	0.00	0.00
CI	Aug 22	2	12	37	3875	38.19	3.67	0.77	16.84	19.10	0.31	0.02	0.00	4395.05	70.48	4.77	0.00	0.00	0.00
CI2	Aug 22	2	12	37	3875	2093.44	827.14	51.91	780.45	1046.72	68.93	1.40	0.20	5197.07	342.24	6.97	0.00	0.00	0.00
ClAInt	Aug 22	2	12	37	3875	55760841.02	51330191.70	18017116.95	103144026.53	27880420.51	4277515.97	486949.11	26617.81	1047.43	160.70	18.29	0.00	0.00	0.00
CRI1	Aug 22	2	12	37	3875	0.05	0.32	0.18	1.58	0.03	0.03	0.00	0.00	67.16	66.29	12.10	0.00	0.00	0.00
CRI2	Aug 22	2	12	37	3875	0.31	1.36	0.48	4.01	0.15	0.11	0.01	0.00	148.61	109.94	12.52	0.00	0.00	0.00
CRI3	Aug 22	2	12	37	3875	6293.42	2744.00	133.20	3175.41	3146.71	228.67	3.60	0.82	3839.97	279.05	4.39	0.00	0.00	0.00
CRI4	Aug 22	2	12	37	3875	2158.92	817.37	44.37	739.89	1079.46	68.11	1.20	0.19	5653.41	356.73	6.28	0.00	0.00	0.00
D1	Aug 22	2	12	37	3875	125.40	50.54	2.08	60.37	62.70	4.21	0.06	0.02	4024.81	270.33	3.61	0.00	0.00	0.00
D2	Aug 22	2	12	37	3875	715.03	235.15	348.60	55820.56	357.51	19.60	9.42	14.41	24.82	1.36	0.65	0.00	0.18	0.95
Datt	Aug 22	2	12	37	3875	48.67	9.00	0.40	8.21	24.33	0.75	0.01	0.00	11490.34	354.21	5.11	0.00	0.00	0.00
Datt2	Aug 22	2	12	37	3875	699.46	233.92	9.31	219.15	349.73	19.49	0.25	0.06	6183.95	344.68	4.45	0.00	0.00	0.00
Datt3	Aug 22	2	12	37	3875	5.07	6.68	1.47	38.09	2.53	0.56	0.04	0.01	257.82	56.60	4.04	0.00	0.00	0.00
Datt4	Aug 22	2	12	37	3875	0.07	0.07	0.00	0.06	0.03	0.01	0.00	0.00	2154.09	380.72	8.23	0.00	0.00	0.00
Datt5	Aug 22	2	12	37	3875	13.89	7.22	1.46	18.14	6.95	0.60	0.04	0.00	1483.64	128.42	8.42	0.00	0.00	0.00
Datt6	Aug 22	2	12	37	3875	26.14	36.48	6.46	48.15	13.07	3.04	0.17	0.01	1051.62	244.63	14.05	0.00	0.00	0.00
DD	Aug 22	2	12	37	3875	673467.61	162326.10	15672.72	153366.25	336733.80	13527.17	423.59	39.58	8508.02	341.78	10.70	0.00	0.00	0.00
DDn	Aug 22	2	12	37	3875	1682277.16	493490.66	82878.48	737351.69	841138.58	41124.22	2239.96	190.28	4420.43	216.12	11.77	0.00	0.00	0.00
DPI	Aug 22	2	12	37	3875	15.69	12.84	1.61	55.71	7.85	1.07	0.04	0.01	545.83	74.42	3.02	0.00	0.00	0.00
DWSI4	Aug 22	2	12	37	3875	7.23	89.98	23.52	223.63	3.62	7.50	0.64	0.06	62.68	129.93	11.01	0.00	0.00	0.00
EGFN	Aug 22	2	12	37	3875	22.43	6.37	0.39	12.83	11.22	0.53	0.01	0.00	3386.58	160.39	3.17	0.00	0.00	0.00
EGFR	Aug 22	2	12	37	3875	4666.65	2072.45	86.27	4298.31	2333.33	172.70	2.33	1.11	2103.53	155.70	2.10	0.00	0.00	0.00
EVI	Aug 22	2	12	37	3875	3301959.86	76119639.64	132664613.35	18873071318.70	1650979.93	6343303.30	3585530.09	4870470.02	0.34	1.30	0.74	0.71	0.21	0.88
GI	Aug 22	2	12	37	3875	69.03	120.46	37.98	341.27	34.51	10.04	1.03	0.09	391.89	113.98	11.66	0.00	0.00	0.00
Gitelson	Aug 22	2	12	37	3875	0.37	0.50	0.14	0.79	0.19	0.04	0.00	0.00	910.58	202.58	18.36	0.00	0.00	0.00
Gitelson2	Aug 22	2	12	37	3875	138.25	1162.95	201.29	3807.58	69.13	96.91	5.44	0.98	70.35	98.63	5.54	0.00	0.00	0.00
GMI1	Aug 22	2	12	37	3875	5570.06	2400.85	128.87	2901.56	2785.03	200.07	3.48	0.75	3719.37	267.19	4.65	0.00	0.00	0.00
GMI2	Aug 22	2	12	37	3875	1953.98	744.20	47.90	709.67	976.99	62.02	1.29	0.18	5334.61	338.63	7.07	0.00	0.00	0.00
Green NDVI	Aug 22	2	12	37	3875	24.49	7.76	0.51	7.11	12.25	0.65	0.01	0.00	6670.78	352.21	7.55	0.00	0.00	0.00
Maccioni	Aug 22	2	12	37	3875	51.04	10.40	0.53	8.10	25.52	0.87	0.01	0.00	12211.40	414.54	6.81	0.00	0.00	0.00
MCARI	Aug 22	2	12	37	3875	9173726.93	1998338.78	196442.24	3667841.75	4586863.47	166528.23	5309.25	946.54	4845.93	175.93	5.61	0.00	0.00	0.00
MCARI2	Aug 22	2	12	37	3875	3691166.89	1319532.30	91721.79	1166900.04	1845583.44	109961.02	2478.97	301.14	6128.75	365.15	8.23	0.00	0.00	0.00
MPRI	Aug 22	2	12	37	3875	8646.65	13605.30	5870.69	29659.57	4323.33	1133.77	158.67	7.65	564.84	148.13	20.73	0.00	0.00	0.00
MSAVI	Aug 22	2	12	37	3875	0.44	0.85	0.22	1.90	0.22	0.07	0.01	0.00	452.27	143.29	11.89	0.00	0.00	0.00
mSR2	Aug 22	2	12	37	3875	1091.50	405.21	21.99	354.92	545.75	33.77	0.59	0.09	5958.57	368.67	6.49	0.00	0.00	0.00
MTCI	Aug 22	2	12	37	3875	811.58	320.44	11.03	251.10	405.79	26.70	0.30	0.06	6262.28	412.09	4.60	0.00	0.00	0.00
MTVI	Aug 22	2	12	37	3875	378600.26	755411.41	205469.61	1624652.50	189300.13	62950.95	5553.23	419.27	451.50	150.15	13.25	0.00	0.00	0.00
NDVI	Aug 22	2	12	37	3875	12.29	5.54	0.90	7.71	6.15	0.46	0.02	0.00	3089.31	232.10	12.17	0.00	0.00	0.00
NDVI2	Aug 22	2	12	37	3875	42.96	10.78	0.73	9.07	21.48	0.90	0.02	0.00	9179.40	383.85	8.41	0.00	0.00	0.00
NDVI3	Aug 22	2	12	37	3875	1.24	6.37	1.44	16.30	0.62	0.53	0.04	0.00	147.12	126.29	9.23	0.00	0.00	0.00
OSAVI	Aug 22	2	12	37	3875	1.62	3.08	0.74	6.82	0.81	0.26	0.02	0.00	460.08	145.90	11.31	0.00	0.00	0.00
OSAVI2	Aug 22	2	12	37	3875	57.61	14.44	0.97	12.13	28.81	1.20	0.03	0.00	9204.31	384.39	8.39	0.00	0.00	0.00
PARS	Aug 22	2	12	37	3875	5120.71	5246.32	534.94	11770.63	2560.36	437.19	14.46	3.04	842.89	143.93	4.76	0.00	0.00	0.00
PRI	Aug 22	2	12	37	3875	4.85	2.79	0.39	4.60	2.43	0.23	0.01	0.00	2042.82	195.81	8.84	0.00	0.00	0.00
PRI_norm	Aug 22	2	12	37	3875	0.00	0.00	0.00	0.00	0.00	0.00	0.00	0.00	1722.84	212.29	9.56	0.00	0.00	0.00
PRI*CI2	Aug 22	2	12	37	3875	7.93	11.67	0.91	13.91	3.97	0.97	0.02	0.00	1104.48	270.80	6.82	0.00	0.00	0.00
PSRI	Aug 22	2	12	37	3875	2.48	0.64	0.11	1.24	1.24	0.05	0.00	0.00	3882.80	168.45	9.43	0.00	0.00	0.00
PSSR	Aug 22	2	12	37	3875	22069.13	13615.17	1701.62	26467.92	11034.57	1134.60	45.99	6.83	1615.50	166.11	6.73	0.00	0.00	0.00
PSND	Aug 22	2	12	37	3875	0.14	1.12	0.24	4.14	0.07	0.09	0.01	0.00	66.53	87.52	6.16	0.00	0.00	0.00
RDVI	Aug 22	2	12	37	3875	886.87	965.62	203.02	1822.97	443.44	80.47	5.49	0.47	942.59	171.05	11.66	0.00	0.00	0.00
REP_Li	Aug 22	2	12	37	3875	292006.24	65821.24	5778.70	50166.73	146003.12	5485.10	156.18	12.95	11277.63	423.68	12.06	0.00	0.00	0.00
SAVI	Aug 22	2	12	37	3875	2.76	5.14	1.15	11.12	1.38	0.43	0.03	0.00	480.01	149.25	10.83	0.00	0.00	0.00
SPVI	Aug 22	2	12	37	3875	672661.70	488123.86	105021.17	1083712.39	336330.85	40676.99	2838.41	279.67	1202.61	145.45	10.15	0.00	0.00	0.00
SR	Aug 22	2	12	37	3875	20945.52	9750.46	1697.66	20981.71	10472.76	812.54	45.88	5.41	1934.16	150.06	8.47	0.00	0.00	0.00
SR1	Aug 22	2	12	37	3875	1953.98	744.20	47.90	709.67	976.99	62.02	1.29	0.18	5334.61	338.63	7.07	0.00	0.00	0.00
SR2	Aug 22	2	12	37	3875	8764.54	3181.62	315.10	4123.26	4382.27	265.13	8.52	1.06	4118.42	249.17	8.00	0.00	0.00	0.00
SR3	Aug 22	2	12	37	3875	5570.06	2400.85	128.87	2901.56	2785.03	200.07	3.48	0.75	3719.37	267.19	4.65	0.00	0.00	0.00
SR4	Aug 22	2	12	37	3875	3248.87	915.73	181.32	3088.59	1624.44	76.31	4.90	0.80	2038.05	95.74	6.15	0.00	0.00	0.00
SR5	Aug 22	2	12	37	3875	3.41	2.41	0.47	7.38	1.71	0.20	0.01	0.00	895.52	105.32	6.69	0.00	0.00	0.00
SR6	Aug 22	2	12	37	3875	416.23	155.93	7.63	133.40	208.12	12.99	0.21	0.03	6045.33	377.46	5.99	0.00	0.00	0.00
SR8	Aug 22	2	12	37	3875	11.72	6.03	0.31	9.23	5.86	0.50	0.01	0.00	2460.03	211.05	3.51	0.00	0.00	0.00

Supplementary Table 1. (Continue)

Sum_Dr1	Aug 22	2	12	37	3875	170031.32	300589.34	81413.49	638392.98	85015.66	25049.11	2200.36	164.75	516.04	152.05	13.36	0.00	0.00	0.00
Sum_Dr2	Aug 22	2	12	37	3875	346229.68	249445.24	57355.91	522347.34	173114.84	20787.10	1550.16	134.80	1284.24	154.21	11.50	0.00	0.00	0.00
TCARI	Aug 22	2	12	37	3875	54784.50	306775.46	73268.28	529436.68	27392.25	25564.62	1980.22	136.63	200.49	187.11	14.49	0.00	0.00	0.00
TCARI/OSAVI	Aug 22	2	12	37	3875	84992.63	414303.17	115308.92	703397.81	42496.31	34525.26	3116.46	181.52	234.11	190.20	17.17	0.00	0.00	0.00
TCARI2	Aug 22	2	12	37	3875	307381.33	173483.92	18482.17	256733.96	153690.67	14456.99	499.52	66.25	2319.72	218.21	7.54	0.00	0.00	0.00
TCARI2/OSAVI2	Aug 22	2	12	37	3875	734622.32	978028.74	211345.54	2190815.04	367311.16	81502.39	5712.04	565.37	649.68	144.16	10.10	0.00	0.00	0.00
TGI	Aug 22	2	12	37	3875	510038280.27	202975582.60	42948154.37	240219205.71	255019140.13	1691463188	1160760.93	61992.05	4113.74	272.85	18.72	0.00	0.00	0.00
TVI	Aug 22	2	12	37	3875	807271016.04	1116504714.24	298690843.08	2260397886.42	403635508.02	93042059.52	8072725.49	583328.49	691.95	159.50	13.84	0.00	0.00	0.00
Vogelmann	Aug 22	2	12	37	3875	54.06	16.34	0.81	13.73	27.03	1.36	0.02	0.00	7626.03	384.29	6.17	0.00	0.00	0.00
Vogelmann2	Aug 22	2	12	37	3875	2.51	0.75	0.03	1.10	1.26	0.06	0.00	0.00	4439.55	219.65	3.12	0.00	0.00	0.00
Vogelmann3	Aug 22	2	12	37	3875	117.16	46.49	2.53	56.15	58.58	3.87	0.07	0.01	4042.91	267.37	4.72	0.00	0.00	0.00
Vogelmann4	Aug 22	2	12	37	3875	3.08	0.99	0.04	1.37	1.54	0.08	0.00	0.00	4345.21	231.55	3.14	0.00	0.00	0.00
Boochs	Sept 05	2	12	17	8368	588.58	22332.75	430.87	8690.64	294.29	1861.06	25.35	1.04	283.37	1791.97	24.40	0.00	0.00	0.00
Boochs2	Sept 05	2	12	17	8368	15597.31	13039.20	155.74	5704.33	7798.66	1086.60	9.16	0.68	11440.28	1593.99	13.44	0.00	0.00	0.00
CARI	Sept 05	2	12	17	8368	18824201.91	39505963.71	281520.83	15120414.53	9412100.96	3292163.64	16560.05	1806.93	5208.88	1821.96	9.16	0.00	0.00	0.00
Carter2	Sept 05	2	12	17	8368	49.69	34.43	0.23	28.69	24.84	2.87	0.01	0.00	7244.85	836.67	3.99	0.00	0.00	0.00
Carter3	Sept 05	2	12	17	8368	18.50	15.42	0.14	13.87	9.25	1.28	0.01	0.00	5580.04	775.24	5.05	0.00	0.00	0.00
Carter4	Sept 05	2	12	17	8368	66.86	36.91	0.30	33.11	33.43	3.08	0.02	0.00	8448.11	777.34	4.42	0.00	0.00	0.00
Carter5	Sept 05	2	12	17	8368	1399.63	835.02	69.75	4152.22	699.82	69.59	4.10	0.50	1410.34	140.24	8.27	0.00	0.00	0.00
Carter6	Sept 05	2	12	17	8368	104365.13	537378.48	6812.02	252252.05	52182.57	44781.54	400.71	30.14	1731.06	1485.55	13.29	0.00	0.00	0.00
CI	Sept 05	2	12	17	8368	13.94	8.42	0.45	36.29	6.97	0.70	0.03	0.00	1606.80	161.70	6.10	0.00	0.00	0.00
CI2	Sept 05	2	12	17	8368	2901.45	1429.45	17.10	2289.64	1450.72	119.12	1.01	0.27	5301.99	435.35	3.68	0.00	0.00	0.00
ClAInt	Sept 05	2	12	17	8368	162071817.41	958283436.21	11725030.84	362775479.47	81035908.71	79856953.02	689707.70	43352.71	1869.22	1842.03	15.91	0.00	0.00	0.00
CRI1	Sept 05	2	12	17	8368	0.06	1.59	0.07	2.86	0.03	0.13	0.00	0.00	84.73	388.11	11.22	0.00	0.00	0.00
CRI2	Sept 05	2	12	17	8368	0.26	4.76	0.14	6.51	0.13	0.40	0.01	0.00	164.58	509.25	10.43	0.00	0.00	0.00
CRI3	Sept 05	2	12	17	8368	8142.25	4503.24	75.26	9190.27	4071.13	375.27	4.43	1.10	3706.88	341.69	4.03	0.00	0.00	0.00
CRI4	Sept 05	2	12	17	8368	2931.99	1347.41	15.28	2194.92	1466.00	112.28	0.90	0.26	5589.01	428.08	3.43	0.00	0.00	0.00
D1	Sept 05	2	12	17	8368	173.58	115.51	1.30	166.99	86.79	9.63	0.08	0.02	4348.97	482.37	3.84	0.00	0.00	0.00
D2	Sept 05	2	12	17	8368	2252.60	2315.05	16.74	6877.34	1126.30	192.92	0.98	0.82	1370.43	234.74	1.20	0.00	0.00	0.26
Datt	Sept 05	2	12	17	8368	47.85	29.38	0.23	26.10	23.92	2.45	0.01	0.00	7670.65	784.93	4.40	0.00	0.00	0.00
Datt2	Sept 05	2	12	17	8368	706.94	437.15	4.40	614.37	353.47	36.43	0.26	0.07	4814.44	496.18	3.53	0.00	0.00	0.00
Datt3	Sept 05	2	12	17	8368	22.29	12.79	0.65	60.45	11.14	1.07	0.04	0.01	1542.50	147.57	5.30	0.00	0.00	0.00
Datt4	Sept 05	2	12	17	8368	0.05	0.11	0.00	0.07	0.02	0.01	0.00	0.00	2993.04	1142.50	6.76	0.00	0.00	0.00
Datt5	Sept 05	2	12	17	8368	6.25	14.18	0.58	60.72	3.13	1.18	0.03	0.01	431.01	162.83	4.68	0.00	0.00	0.00
Datt6	Sept 05	2	12	17	8368	17.06	38.18	0.65	46.82	8.53	3.18	0.04	0.01	1524.57	568.72	6.88	0.00	0.00	0.00
DD	Sept 05	2	12	17	8368	1105377.34	1149439.95	5973.37	601045.98	552688.67	95786.66	351.37	71.83	7694.75	1333.58	4.89	0.00	0.00	0.00
DDn	Sept 05	2	12	17	8368	1880593.74	3552501.67	52204.70	1097081.26	940296.87	296041.81	3070.86	131.10	7172.13	2258.06	23.42	0.00	0.00	0.00
DPI	Sept 05	2	12	17	8368	60.43	17.12	1.30	140.44	30.22	1.43	0.08	0.02	1800.38	84.99	4.55	0.00	0.00	0.00
DWSI4	Sept 05	2	12	17	8368	56.31	214.30	10.59	716.17	28.16	17.86	0.62	0.09	328.99	208.66	7.28	0.00	0.00	0.00
EGFN	Sept 05	2	12	17	8368	26.41	12.88	0.18	33.34	13.20	1.07	0.01	0.00	3314.48	269.46	2.61	0.00	0.00	0.00
EGFR	Sept 05	2	12	17	8368	7121.47	2921.16	36.09	8503.78	3560.74	243.43	2.12	1.02	3503.88	239.54	2.09	0.00	0.00	0.01
EVI	Sept 05	2	12	17	8368	21706773.90	81809408.68	73113515.07	58524901349.89	10853386.95	6817450.72	4300795.00	6993893.56	1.55	0.97	0.61	0.21	0.47	0.88
GI	Sept 05	2	12	17	8368	113.92	280.86	16.24	1164.89	56.96	23.40	0.96	0.14	409.16	168.13	6.86	0.00	0.00	0.00
Gitelson	Sept 05	2	12	17	8368	0.45	1.20	0.02	0.83	0.22	0.10	0.00	0.00	2269.07	1015.43	9.62	0.00	0.00	0.00
Gitelson2	Sept 05	2	12	17	8368	440.15	4933.03	178.34	6446.16	220.07	411.09	10.49	0.77	285.68	533.65	13.62	0.00	0.00	0.00
GMI1	Sept 05	2	12	17	8368	6769.05	4067.21	66.85	8156.58	3384.52	338.93	3.93	0.97	3472.25	347.72	4.03	0.00	0.00	0.00
GMI2	Sept 05	2	12	17	8368	2569.04	1289.68	15.06	2010.55	1284.52	107.47	0.89	0.24	5346.23	447.31	3.69	0.00	0.00	0.00
Green NDVI	Sept 05	2	12	17	8368	23.31	18.32	0.30	22.87	11.66	1.53	0.02	0.00	4265.75	558.51	6.42	0.00	0.00	0.00
Maccioni	Sept 05	2	12	17	8368	63.55	34.22	0.26	27.34	31.77	2.85	0.02	0.00	9724.07	872.81	4.69	0.00	0.00	0.00
MCARI	Sept 05	2	12	17	8368	7714381.83	11040022.16	88953.27	7691461.46	3857190.92	920001.85	5232.55	919.15	4196.47	1000.92	5.69	0.00	0.00	0.00
MCARI2	Sept 05	2	12	17	8368	6397725.80	3408072.37	10086.13	2763762.31	3198862.90	284006.03	593.30	330.28	9685.38	859.90	1.80	0.00	0.00	0.02
MPRI	Sept 05	2	12	17	8368	19362.51	128741.34	3040.06	99877.73	9681.25	10728.44	178.83	11.94	811.12	898.86	14.98	0.00	0.00	0.00
MSAVI	Sept 05	2	12	17	8368	1.47	3.17	0.11	7.77	0.73	0.26	0.01	0.00	790.74	284.67	7.00	0.00	0.00	0.00
mSR2	Sept 05	2	12	17	8368	1509.95	748.04	7.98	1053.01	754.98	62.34	0.47	0.13	5999.60	495.37	3.73	0.00	0.00	0.00
MTCI	Sept 05	2	12	17	8368	1227.66	574.96	5.28	695.14	613.83	47.91	0.31	0.08	7389.22	576.77	3.74	0.00	0.00	0.00
MTVI	Sept 05	2	12	17	8368	485487.16	9807356.78	134203.45	2403161.69	242743.58	817279.73	7894.32	287.18	845.25	2845.83	27.49	0.00	0.00	0.00
NDVI	Sept 05	2	12	17	8368	11.53	14.65	0.25	23.32	5.77	1.22	0.01	0.00	2068.98	438.08	5.17	0.00	0.00	0.00
NDVI2	Sept 05	2	12	17	8368	54.15	28.71	0.24	28.49	27.07	2.39	0.01	0.00	7951.73	702.58	4.10	0.00	0.00	0.00
NDVI3	Sept 05	2	12	17	8368	4.64	12.45	0.41	40.65	2.32	1.04	0.02	0.00	477.22	213.64	4.92	0.00	0.00	0.00
OSAVI	Sept 05	2	12	17	8368	4.96	11.01	0.36	26.52	2.48	0.92	0.02	0.00	783.34	289.65	6.75	0.00	0.00	0.00
OSAVI2	Sept 05	2	12	17	8368	72.63	38.44	0.32	38.16	36.31	3.20	0.02	0.00	7963.69	702.43	4.09	0.00	0.00	0.00
PARS	Sept 05	2	12	17	8368	11612.29	10448.90	505.65	35132.43	5806.14	870.74	29.74	4.20	1382.93	207.40	7.08	0.00	0.00	0.00
PRI	Sept 05	2	12	17	8368	9.55	6.89	0.06	7.59	4.78	0.57	0.00	0.00	5267.86	632.89	3.74	0.00	0.00	0.00
PRI*CI2	Sept 05	2	12	17	8368	12.09	9.00	0.22	27.31	6.04	0.75	0.01	0.00	1851.71	229.91	4.03	0.00	0.00	0.00
PRI_norm	Sept 05	2	12	17	8368	0.01	0.01	0.00	0.01	0.00	0.00	0.00	0.00	3915.89	483.09	2.19	0.00	0.00	0.00
PSND	Sept 05	2	12	17	8368	0.54	2.16	0.36	15.88	0.27	0.18	0.02	0.00	141.68	94.84	11.23	0.00	0.00	0.00
PSRI	Sept 05	2	12	17	8368	1.91	3.00	0.02	2.92	0.95	0.25	0.00	0.00	2733.94	715.79	3.59	0.00	0.00	0.00
PSSR	Sept 05	2	12	17	8368	31728.93	26135.96	472.16	57970.23	15864.47	2178.00	27.77	6.93	2290.04	314.39	4.01	0.00	0.00	0.00
RDVI	Sept 05	2	12	17	8368	1210.09	6589.88	82.78	1652.50	605.04	549.16	4.87	0.20	3063.85	2780.85	24.66	0.00	0.00	0.00
REP_Li	Sept 05	2	12	17	8368	241752.79	200363.29	666.22	121244.60	120876.40	16696.94	39.19	14.49	8342.59	1152.38	2.70	0.00	0.00	0.00
SAVI	Sept 05	2	12	17	8368	8.31	17.77	0.59	43.55	4.15	1.48	0.03	0.01	798.13	284.48	6.68	0.00	0.00	0.00
SPVI	Sept 05	2	12	17	8368	742008.04	5940866.07	92649.04	1237382.85	371004.02	495072.17	5449.94	147.87	2508.97	3348.00	36.86	0.00	0.00	0.00
SR	Sept 05	2	12	17	8368	19771.78	26786.02	704.32	68103.45	9885.89	2232.17	41.43	8.14	1214.70	274.27	5.09	0.00	0.00	0.00
SR1	Sept 05	2	12	17	8368	2569.04	1289.68	15.06	2010.55	1284.52	107.47	0.89	0.24	5346.23	447.31	3.69	0.00	0.00	0.00

Supplementary Table 1. (Continue)

SR2	Sept 05	2	12	17	8368	9984.10	5980.35	92.03	11777.42	4992.05	498.36	5.41	1.41	3546.91	354.09	3.85	0.00	0.00	0.00
SR3	Sept 05	2	12	17	8368	6769.05	4067.21	66.85	8156.58	3384.52	338.93	3.93	0.97	3472.25	347.72	4.03	0.00	0.00	0.00
SR4	Sept 05	2	12	17	8368	1637.01	1572.51	135.37	7919.73	818.50	131.04	7.96	0.95	864.83	138.46	8.41	0.00	0.00	0.00
SR5	Sept 05	2	12	17	8368	3.26	5.58	0.27	22.05	1.63	0.46	0.02	0.00	617.96	176.37	6.08	0.00	0.00	0.00
SR6	Sept 05	2	12	17	8368	593.85	299.88	2.99	405.53	296.92	24.99	0.18	0.05	6126.98	515.67	3.63	0.00	0.00	0.00
SR8	Sept 05	2	12	17	8368	5.21	6.29	0.26	18.95	2.61	0.52	0.02	0.00	1150.47	231.45	6.66	0.00	0.00	0.00
Sum_Dr1	Sept 05	2	12	17	8368	254695.73	4046985.61	53143.94	887190.47	127347.86	337248.80	3126.11	106.02	1201.15	3180.94	29.49	0.00	0.00	0.00
Sum_Dr2	Sept 05	2	12	17	8368	326174.85	2699617.33	41312.32	612100.65	163087.42	224968.11	2430.14	73.15	2229.56	3075.53	33.22	0.00	0.00	0.00
TCARI	Sept 05	2	12	17	8368	314958.10	2600267.16	37845.61	1500340.97	157479.05	216688.93	2226.21	179.30	878.32	1208.56	12.42	0.00	0.00	0.00
TCARI/OSAVI	Sept 05	2	12	17	8368	596403.18	3695502.12	55775.93	2346231.45	298201.59	307958.51	3280.94	280.38	1063.56	1098.36	11.70	0.00	0.00	0.00
TCARI2	Sept 05	2	12	17	8368	229569.86	997886.29	17583.84	794682.01	114784.93	83157.19	1034.34	94.97	1208.69	875.65	10.89	0.00	0.00	0.00
TCARI2/OSAVI2	Sept 05	2	12	17	8368	1081438.21	8332367.67	221786.83	7950771.87	540719.11	694363.97	13046.28	950.14	569.09	730.80	13.73	0.00	0.00	0.00
TGI	Sept 05	2	12	17	8368	608053573.98	2027738698.66	12833859.91	832733580.37	304026786.99	168978224.89	754932.94	99514.05	3055.11	1698.03	7.59	0.00	0.00	0.00
TVI	Sept 05	2	12	17	8368	593379687.41	13288776732.81	184256273.45	3377877060.50	296689843.71	1107398061.07	10838604.32	403666.00	734.99	2743.35	26.85	0.00	0.00	0.00
Vogelmann	Sept 05	2	12	17	8368	62.95	35.03	0.41	43.36	31.48	2.92	0.02	0.01	6073.99	563.28	4.70	0.00	0.00	0.00
Vogelmann2	Sept 05	2	12	17	8368	1.89	1.33	0.02	2.01	0.94	0.11	0.00	0.00	3919.53	461.21	4.80	0.00	0.00	0.00
Vogelmann3	Sept 05	2	12	17	8368	245.55	110.01	0.99	143.34	122.77	9.17	0.06	0.02	7167.40	535.19	3.39	0.00	0.00	0.00
Vogelmann4	Sept 05	2	12	17	8368	2.42	1.69	0.02	2.59	1.21	0.14	0.00	0.00	3901.08	455.33	4.70	0.00	0.00	0.00
Boochs	Sept 13	2	12	18	7001	341.71	3202.29	23.74	3623.94	170.85	266.86	1.32	0.52	330.07	515.54	2.55	0.00	0.00	0.00
Boochs2	Sept 13	2	12	18	7001	3260.64	4346.08	7.98	2211.15	1630.32	362.17	0.44	0.32	5161.96	1146.72	1.40	0.00	0.00	0.12
CARI	Sept 13	2	12	18	7001	5204848.19	4413204.21	39919.43	5341026.39	2602424.09	367767.02	2217.75	762.89	3411.25	482.07	2.91	0.00	0.00	0.00
Carter2	Sept 13	2	12	18	7001	55.64	26.57	0.15	18.24	27.82	2.21	0.01	0.00	10679.51	849.98	3.22	0.00	0.00	0.00
Carter3	Sept 13	2	12	18	7001	19.90	12.40	0.07	8.54	9.95	1.03	0.00	0.00	8156.16	847.38	3.38	0.00	0.00	0.00
Carter4	Sept 13	2	12	18	7001	52.49	24.79	0.22	19.79	26.24	2.07	0.01	0.00	9281.77	730.52	4.37	0.00	0.00	0.00
Carter5	Sept 13	2	12	18	7001	929.66	1741.12	60.98	3954.13	464.83	145.09	3.39	0.56	823.01	256.90	6.00	0.00	0.00	0.00
Carter6	Sept 13	2	12	18	7001	38353.48	47737.51	544.43	70945.99	19176.74	3978.13	30.25	10.13	1892.37	392.56	2.98	0.00	0.00	0.00
CI	Sept 13	2	12	18	7001	18.29	12.61	0.29	23.17	9.14	1.05	0.02	0.00	2762.91	317.63	4.91	0.00	0.00	0.00
CI2	Sept 13	2	12	18	7001	1836.30	1468.92	20.49	1372.74	918.15	122.41	1.14	0.20	4682.57	624.29	5.80	0.00	0.00	0.00
ClAInt	Sept 13	2	12	18	7001	60620802.47	84700336.82	621845.54	106063204.82	30310401.23	7058361.40	34546.97	15149.72	2000.72	465.91	2.28	0.00	0.00	0.00
CRI1	Sept 13	2	12	18	7001	2.06	1.46	0.17	14.10	1.03	0.12	0.01	0.00	511.03	60.30	4.66	0.00	0.00	0.00
CRI2	Sept 13	2	12	18	7001	4.79	3.54	0.36	31.76	2.39	0.30	0.02	0.00	527.76	65.12	4.46	0.00	0.00	0.00
CRI3	Sept 13	2	12	18	7001	4495.16	3266.51	86.89	6395.14	2247.58	272.21	4.83	0.91	2460.51	298.00	5.28	0.00	0.00	0.00
CRI4	Sept 13	2	12	18	7001	1770.63	1460.06	19.27	1130.65	885.31	121.67	1.07	0.16	5481.88	753.39	6.63	0.00	0.00	0.00
D1	Sept 13	2	12	18	7001	83.47	50.94	1.48	89.76	41.73	4.24	0.08	0.01	3254.90	331.05	6.43	0.00	0.00	0.00
D2	Sept 13	2	12	18	7001	646.90	308.77	6.56	516.84	323.45	25.73	0.36	0.07	4381.43	348.54	4.94	0.00	0.00	0.00
Datt	Sept 13	2	12	18	7001	44.43	16.25	0.25	17.24	22.22	1.35	0.01	0.00	9021.74	550.02	5.57	0.00	0.00	0.00
Datt2	Sept 13	2	12	18	7001	482.98	253.06	6.18	343.49	241.49	21.09	0.34	0.05	4921.97	429.82	7.00	0.00	0.00	0.00
Datt3	Sept 13	2	12	18	7001	1.63	4.83	0.58	48.88	0.82	0.40	0.03	0.01	116.74	57.67	4.62	0.00	0.00	0.00
Datt4	Sept 13	2	12	18	7001	0.05	0.26	0.00	0.28	0.03	0.02	0.00	0.00	645.54	539.80	4.79	0.00	0.00	0.00
Datt5	Sept 13	2	12	18	7001	0.23	40.22	0.47	61.19	0.11	3.35	0.03	0.01	13.13	383.47	2.99	0.00	0.00	0.00
Datt6	Sept 13	2	12	18	7001	27.54	28.90	1.34	118.23	13.77	2.41	0.07	0.02	815.52	142.59	4.39	0.00	0.00	0.00
DD	Sept 13	2	12	18	7001	348711.82	172997.26	1248.64	127628.70	174355.91	14416.44	69.37	18.23	9564.19	790.81	3.81	0.00	0.00	0.00
DDn	Sept 13	2	12	18	7001	432853.59	794814.59	1859.40	640901.42	216426.79	66234.55	103.30	91.54	2364.18	723.52	1.13	0.00	0.00	0.32
DPI	Sept 13	2	12	18	7001	12.66	12.78	0.79	80.34	6.33	1.07	0.04	0.01	551.80	92.83	3.80	0.00	0.00	0.00
DWSI4	Sept 13	2	12	18	7001	32.49	341.48	2.23	413.67	16.25	28.46	0.12	0.06	274.93	481.61	2.10	0.00	0.00	0.00
EGFN	Sept 13	2	12	18	7001	10.03	15.74	0.37	19.44	5.02	1.31	0.02	0.00	1806.98	472.55	7.45	0.00	0.00	0.00
EGFR	Sept 13	2	12	18	7001	2496.65	5139.67	189.85	5527.82	1248.33	428.31	10.55	0.79	1581.01	542.45	13.36	0.00	0.00	0.00
EVI	Sept 13	2	12	18	7001	127706.18	618711.10	301288.22	938588152.30	63853.09	51559.26	16738.23	134064.87	0.48	0.38	0.12	0.62	0.97	1.00
GI	Sept 13	2	12	18	7001	2.88	536.30	3.97	714.67	1.44	44.69	0.22	0.10	14.09	437.80	2.16	0.00	0.00	0.00
Gitelson	Sept 13	2	12	18	7001	0.66	0.90	0.03	2.57	0.33	0.07	0.00	0.00	898.64	204.09	4.16	0.00	0.00	0.00
Gitelson2	Sept 13	2	12	18	7001	378.15	802.25	37.87	4179.91	189.07	66.85	2.10	0.60	316.68	111.98	3.52	0.00	0.00	0.00
GMI1	Sept 13	2	12	18	7001	4212.58	3030.47	81.00	6302.37	2106.29	252.54	4.50	0.90	2339.78	280.53	5.00	0.00	0.00	0.00
GMI2	Sept 13	2	12	18	7001	1706.18	1367.82	17.10	1225.69	853.09	113.98	0.95	0.18	4872.77	651.07	5.43	0.00	0.00	0.00
Green NDVI	Sept 13	2	12	18	7001	20.36	9.98	0.21	16.41	10.18	0.83	0.01	0.00	4342.13	354.68	4.92	0.00	0.00	0.00
Maccioni	Sept 13	2	12	18	7001	48.40	20.10	0.22	16.20	24.20	1.68	0.01	0.00	10454.43	723.78	5.17	0.00	0.00	0.00
MCARI	Sept 13	2	12	18	7001	2046851.95	1969201.35	23113.53	2960860.44	1023425.98	164100.11	1284.09	422.92	2419.91	388.02	3.04	0.00	0.00	0.00
MCARI2	Sept 13	2	12	18	7001	1514925.63	1697780.83	5016.15	773859.74	757462.81	141481.74	278.67	110.54	6852.66	1279.97	2.52	0.00	0.00	0.00
MPRI	Sept 13	2	12	18	7001	7398.78	9453.66	213.50	28329.76	3699.39	787.81	11.86	4.05	914.21	194.69	2.93	0.00	0.00	0.00
MSAVI	Sept 13	2	12	18	7001	2.53	2.77	0.05	5.77	1.27	0.23	0.00	0.00	1535.04	280.05	3.14	0.00	0.00	0.00
mSR2	Sept 13	2	12	18	7001	973.92	721.09	9.35	626.55	486.96	60.09	0.52	0.09	5441.22	671.45	5.81	0.00	0.00	0.00
MTCI	Sept 13	2	12	18	7001	735.17	535.62	8.75	413.11	367.59	44.63	0.49	0.06	6229.51	756.43	8.24	0.00	0.00	0.00
MTVI	Sept 13	2	12	18	7001	100502.32	1277215.82	5881.29	1303815.52	50251.16	106434.65	326.74	186.23	269.83	571.51	1.75	0.00	0.00	0.02
NDVI	Sept 13	2	12	18	7001	18.84	12.52	0.13	16.99	9.42	1.04	0.01	0.00	3880.11	429.88	3.00	0.00	0.00	0.00
NDVI2	Sept 13	2	12	18	7001	43.90	23.54	0.20	17.86	21.95	1.96	0.01	0.00	8607.03	769.27	4.31	0.00	0.00	0.00
NDVI3	Sept 13	2	12	18	7001	6.15	23.65	0.20	31.67	3.07	1.97	0.01	0.00	679.18	435.68	2.43	0.00	0.00	0.00
OSAVI	Sept 13	2	12	18	7001	8.38	9.57	0.16	19.60	4.19	0.80	0.01	0.00	1496.28	284.95	3.26	0.00	0.00	0.00
OSAVI2	Sept 13	2	12	18	7001	58.79	31.55	0.26	23.80	29.39	2.63	0.01	0.00	8647.39	773.36	4.30	0.00	0.00	0.00
PARS	Sept 13	2	12	18	7001	10207.35	7501.06	575.65	38715.72	5103.68	625.09	31.98	5.53	922.90	113.04	5.78	0.00	0.00	0.00
PRI	Sept 13	2	12	18	7001	10.74	9.37	0.06	5.51	5.37	0.78	0.00	0.00	6827.65	992.98	4.11	0.00	0.00	0.00
PRI_norm	Sept 13	2	12	18	7001	0.02	0.02	0.00	0.02	0.01	0.00	0.00	0.00	4935.57	737.90	3.34	0.00	0.00	0.00
PRI*CI2	Sept 13	2	12	18	7001	6.35	19.92	0.28	16.59	3.18	1.66	0.02	0.00	1339.73	700.44	6.53	0.00	0.00	0.00
PSRI	Sept 13	2	12	18	7001	4.57	2.74	0.02	2.38	2.28	0.23	0.00	0.00	6730.77	673.70	2.58	0.00	0.00	0.00
PSSR	Sept 13	2	12	18	7001	23632.90	25370.15	489.14	48130.20	11816.45	2114.18	27.17	6.87	1718.82	307.53	3.95	0.00	0.00	0.00
PSND	Sept 13	2	12	18	7001	1.16	1.74	0.17	11.66	0.58	0.15	0.01	0.00	348.55	87.34	5.56	0.00	0.00	0.00

Supplementary Table 1. (Continue)

RDVI	Sept 13	2	12	18	7001	448.03	2375.89	8.32	1882.90	224.02	197.99	0.46	0.27	832.94	736.17	1.72	0.00	0.00	0.03
REP_Li	Sept 13	2	12	18	7001	295797.63	113759.87	565.78	66788.17	147898.82	9479.99	31.43	9.54	15503.34	993.73	3.29	0.00	0.00	0.00
SAVI	Sept 13	2	12	18	7001	13.82	15.94	0.27	31.64	6.91	1.33	0.01	0.00	1528.78	293.85	3.26	0.00	0.00	0.00
SPVI	Sept 13	2	12	18	7001	114725.93	834836.15	3249.36	794730.30	57362.97	69569.68	180.52	113.52	505.33	612.86	1.59	0.00	0.00	0.05
SR	Sept 13	2	12	18	7001	19131.21	20186.48	418.48	50989.63	9565.61	1682.21	23.25	7.28	1313.38	230.97	3.19	0.00	0.00	0.00
SR1	Sept 13	2	12	18	7001	1706.18	1367.82	17.10	1225.69	853.09	113.98	0.95	0.18	4872.77	651.07	5.43	0.00	0.00	0.00
SR2	Sept 13	2	12	18	7001	7207.68	6425.51	68.86	7601.46	3603.84	535.46	3.83	1.09	3319.16	493.16	3.52	0.00	0.00	0.00
SR3	Sept 13	2	12	18	7001	4212.58	3030.47	81.00	6302.37	2106.29	252.54	4.50	0.90	2339.78	280.53	5.00	0.00	0.00	0.00
SR4	Sept 13	2	12	18	7001	1035.18	3091.11	116.07	7678.66	517.59	257.59	6.45	1.10	471.91	234.86	5.88	0.00	0.00	0.00
SR5	Sept 13	2	12	18	7001	2.07	10.34	0.27	21.26	1.03	0.86	0.01	0.00	340.52	283.72	4.93	0.00	0.00	0.00
SR6	Sept 13	2	12	18	7001	370.18	260.84	3.54	235.68	185.09	21.74	0.20	0.03	5498.08	645.70	5.84	0.00	0.00	0.00
SR8	Sept 13	2	12	18	7001	8.27	15.39	0.39	18.70	4.14	1.28	0.02	0.00	1549.19	480.16	8.12	0.00	0.00	0.00
Sum_Dr1	Sept 13	2	12	18	7001	34269.59	511467.39	2336.59	505181.61	17134.80	42622.28	129.81	72.16	237.46	590.68	1.80	0.00	0.00	0.02
Sum_Dr2	Sept 13	2	12	18	7001	71172.44	446055.65	1484.72	393379.92	35586.22	37171.30	82.48	56.19	633.33	661.54	1.47	0.00	0.00	0.09
TCARI	Sept 13	2	12	18	7001	174396.01	250778.89	4182.17	423862.44	87198.01	20898.24	232.34	60.54	1440.26	345.18	3.84	0.00	0.00	0.00
TCARI/OSAVI	Sept 13	2	12	18	7001	301288.91	362239.78	5378.47	597390.46	150644.46	30186.65	298.80	85.33	1765.45	353.77	3.50	0.00	0.00	0.00
TCARI2	Sept 13	2	12	18	7001	179269.02	181648.71	2180.29	249301.91	89634.51	15137.39	121.13	35.61	2517.15	425.09	3.40	0.00	0.00	0.00
TCARI2/OSAVI2	Sept 13	2	12	18	7001	200253.68	1031940.53	20576.04	2385333.30	100126.84	85995.04	1143.11	340.71	293.87	252.40	3.36	0.00	0.00	0.00
TGI	Sept 13	2	12	18	7001	210217683.16	231672136.51	2513182.04	240285856.67	105108841.58	19306011.38	139621.22	34321.65	3062.46	562.50	4.07	0.00	0.00	0.00
TVI	Sept 13	2	12	18	7001	150098347.48	1974985826.02	9294804.47	1857147078.06	75049173.74	164582152.17	516378.03	265268.83	282.92	620.44	1.95	0.00	0.00	0.01
Vogelmann	Sept 13	2	12	18	7001	44.82	26.77	0.41	25.94	22.41	2.23	0.02	0.00	6046.60	601.89	6.21	0.00	0.00	0.00
Vogelmann2	Sept 13	2	12	18	7001	1.77	0.87	0.02	1.41	0.89	0.07	0.00	0.00	4392.65	358.30	4.86	0.00	0.00	0.00
Vogelmann3	Sept 13	2	12	18	7001	106.40	68.49	0.72	83.77	53.20	5.71	0.04	0.01	4445.93	476.97	3.32	0.00	0.00	0.00
Vogelmann4	Sept 13	2	12	18	7001	2.15	1.13	0.02	1.78	1.08	0.09	0.00	0.00	4235.74	370.54	5.28	0.00	0.00	0.00
Boochs	Sept 20	2	12	13	7083	10140.77	5441.77	59.95	4525.05	5070.39	453.48	4.61	0.64	7936.60	709.83	7.22	0.00	0.00	0.00
Boochs2	Sept 20	2	12	13	7083	19980.15	4279.23	34.00	4034.52	9990.08	356.60	2.62	0.57	17538.56	626.05	4.59	0.00	0.00	0.00
CARI	Sept 20	2	12	13	7083	8029116.69	11359679.46	324744.11	18994144.15	4014558.35	946639.96	24980.32	2681.65	1497.05	353.01	9.32	0.00	0.00	0.00
Carter2	Sept 20	2	12	13	7083	119.28	32.14	0.13	22.51	59.64	2.68	0.01	0.00	18769.65	843.00	3.20	0.00	0.00	0.00
Carter3	Sept 20	2	12	13	7083	34.22	14.09	0.07	10.52	17.11	1.17	0.01	0.00	11519.72	790.87	3.82	0.00	0.00	0.00
Carter4	Sept 20	2	12	13	7083	72.70	16.37	0.10	15.89	36.35	1.36	0.01	0.00	16208.75	608.09	3.58	0.00	0.00	0.00
Carter5	Sept 20	2	12	13	7083	3.77	1548.18	46.43	3795.86	1.89	129.02	3.57	0.54	3.52	240.74	6.66	0.03	0.00	0.00
Carter6	Sept 20	2	12	13	7083	69031.46	92121.05	2379.35	172450.68	34515.73	7676.75	183.03	24.35	1417.65	315.30	7.52	0.00	0.00	0.00
CI	Sept 20	2	12	13	7083	19.23	10.08	0.22	18.95	9.62	0.84	0.02	0.00	3594.31	314.09	6.21	0.00	0.00	0.00
CI2	Sept 20	2	12	13	7083	1451.60	438.42	3.08	532.62	725.80	36.53	0.24	0.08	9652.04	485.86	3.15	0.00	0.00	0.00
ClAInt	Sept 20	2	12	13	7083	182300788.67	152754157.89	1109978.03	207006661.23	91150394.33	12729513.16	85382.93	29225.85	3118.83	435.56	2.92	0.00	0.00	0.00
CRI1	Sept 20	2	12	13	7083	0.06	0.13	0.01	0.65	0.03	0.01	0.00	0.00	345.56	120.52	4.25	0.00	0.00	0.00
CRI2	Sept 20	2	12	13	7083	0.23	0.60	0.02	1.99	0.11	0.05	0.00	0.00	405.99	176.85	4.80	0.00	0.00	0.00
CRI3	Sept 20	2	12	13	7083	4987.34	2669.84	36.76	5143.46	2493.67	222.49	2.83	0.73	3434.00	306.38	3.89	0.00	0.00	0.00
CRI4	Sept 20	2	12	13	7083	1446.57	427.38	3.02	501.24	723.28	35.62	0.23	0.07	10220.68	503.28	3.28	0.00	0.00	0.00
D1	Sept 20	2	12	13	7083	115.63	12.97	0.27	44.59	57.81	1.08	0.02	0.01	9183.41	171.67	3.31	0.00	0.00	0.00
D2	Sept 20	2	12	13	7083	5222.80	2211.15	13.21	47797.74	2611.40	184.26	1.02	6.75	386.97	27.31	0.15	0.00	0.00	1.00
Datt	Sept 20	2	12	13	7083	46.67	13.55	0.22	16.83	23.33	1.13	0.02	0.00	9820.01	475.10	7.04	0.00	0.00	0.00
Datt2	Sept 20	2	12	13	7083	359.44	121.68	0.88	129.14	179.72	10.14	0.07	0.02	9856.80	556.11	3.71	0.00	0.00	0.00
Datt3	Sept 20	2	12	13	7083	15.53	7.76	1.60	35.61	7.76	0.65	0.12	0.01	1544.23	128.55	24.50	0.00	0.00	0.00
Datt4	Sept 20	2	12	13	7083	0.00	0.02	0.00	0.03	0.00	0.00	0.00	0.00	41.09	278.06	14.28	0.00	0.00	0.00
Datt5	Sept 20	2	12	13	7083	34.49	52.22	2.49	99.06	17.25	4.35	0.19	0.01	1233.13	311.14	13.71	0.00	0.00	0.00
Datt6	Sept 20	2	12	13	7083	4.07	3.61	0.05	6.14	2.04	0.30	0.00	0.00	2347.89	347.18	4.11	0.00	0.00	0.00
DD	Sept 20	2	12	13	7083	1032505.76	300155.35	5205.55	423573.49	516252.88	25012.95	400.43	59.80	8632.79	418.27	6.70	0.00	0.00	0.00
DDn	Sept 20	2	12	13	7083	1967143.09	550071.25	10019.56	772498.76	983571.55	45839.27	770.74	109.06	9018.32	420.30	7.07	0.00	0.00	0.00
DPI	Sept 20	2	12	13	7083	28.94	8.07	1.54	79.37	14.47	0.67	0.12	0.01	1291.29	60.04	10.58	0.00	0.00	0.00
DWSI4	Sept 20	2	12	13	7083	239.12	163.85	2.23	200.52	119.56	13.65	0.17	0.03	4223.20	482.31	6.07	0.00	0.00	0.00
EGFN	Sept 20	2	12	13	7083	5.74	12.76	0.34	23.32	2.87	1.06	0.03	0.00	871.50	322.93	7.98	0.00	0.00	0.00
EGFR	Sept 20	2	12	13	7083	1499.09	2985.74	71.42	6217.48	749.55	248.81	5.49	0.88	853.89	283.45	6.26	0.00	0.00	0.00
EVI	Sept 20	2	12	13	7083	15416094.24	92395213.79	151349235.23	41228880996.79	7708047.12	7699601.15	11642248.86	5820821.83	1.32	1.32	2.00	0.27	0.20	0.02
GI	Sept 20	2	12	13	7083	255.47	252.51	3.90	357.73	127.74	21.04	0.30	0.05	2529.12	416.63	5.93	0.00	0.00	0.00
Gitelson	Sept 20	2	12	13	7083	0.10	0.07	0.00	0.10	0.05	0.01	0.00	0.00	3473.87	392.58	3.45	0.00	0.00	0.00
Gitelson2	Sept 20	2	12	13	7083	589.62	929.98	49.80	2640.59	294.81	77.50	3.83	0.37	790.78	207.88	10.28	0.00	0.00	0.00
GMI1	Sept 20	2	12	13	7083	4826.67	2525.94	33.89	4849.40	2413.34	210.49	2.61	0.68	3524.90	307.45	3.81	0.00	0.00	0.00
GMI2	Sept 20	2	12	13	7083	1428.72	425.90	3.00	503.54	714.36	35.49	0.23	0.07	10048.45	499.23	3.25	0.00	0.00	0.00
Green NDVI	Sept 20	2	12	13	7083	24.17	9.88	0.19	16.40	12.08	0.82	0.01	0.00	5217.89	355.54	6.19	0.00	0.00	0.00
Maccioni	Sept 20	2	12	13	7083	60.85	12.30	0.16	14.46	30.43	1.03	0.01	0.00	14901.92	502.13	5.90	0.00	0.00	0.00
MCARI	Sept 20	2	12	13	7083	1162679.17	7180017.23	223926.90	12653482.05	581339.58	598334.77	17225.15	1786.46	325.41	334.93	9.64	0.00	0.00	0.00
MCARI2	Sept 20	2	12	13	7083	4540426.24	1087785.83	10681.29	1279225.29	2270213.12	90648.82	821.64	180.61	12570.05	501.92	4.55	0.00	0.00	0.00
MPRI	Sept 20	2	12	13	7083	19525.96	23855.20	862.88	83956.03	9762.98	1987.93	66.38	11.85	823.66	167.71	5.60	0.00	0.00	0.00
MSAVI	Sept 20	2	12	13	7083	10.16	6.18	0.14	8.22	5.08	0.52	0.01	0.00	4378.64	444.18	9.29	0.00	0.00	0.00
mSR2	Sept 20	2	12	13	7083	847.02	234.39	1.62	270.54	423.51	19.53	0.12	0.04	11087.97	511.39	3.25	0.00	0.00	0.00
MTCI	Sept 20	2	12	13	7083	532.41	137.76	1.29	167.87	266.21	11.48	0.10	0.02	11232.22	484.38	4.19	0.00	0.00	0.00
MTVI	Sept 20	2	12	13	7083	1223931.79	1046870.91	44801.43	1604666.40	611965.89	87239.24	3446.26	226.55	2701.22	385.07	15.21	0.00	0.00	0.00
NDVI	Sept 20	2	12	13	7083	68.08	23.89	0.15	20.88	34.04	1.99	0.01	0.00	11544.78	675.12	3.86	0.00	0.00	0.00
NDVI2	Sept 20	2	12	13	7083	56.72	13.36	0.08	12.72	28.36	1.11	0.01	0.00	15792.67	619.96	3.42	0.00	0.00	0.00
NDVI3	Sept 20	2	12	13	7083	42.05	25.11	0.40	31.48	21.03	2.09	0.03	0.00	4731.18	470.89	6.99	0.00	0.00	0.00
OSAVI	Sept 20	2	12	13	7083	31.65	17.80	0.34	23.88	15.82	1.48	0.03	0.00	4693.95	440.02	7.68	0.00	0.00	0.00
OSAVI2	Sept 20	2	12	13	7083	76.15	17.93	0.11	17.07	38.08	1.49	0.01	0.00	15803.54	620.15	3.42	0.00	0.00	0.00
PARS	Sept 20	2	12	13	7083	11366.22	5137.63	109.24	17598.04	5683.11	428.14	8.40	2.48	2287.38	172.32	3.38	0.00	0.00	0.00

Supplementary Table 1. (Continue)

PRI	Sept 20	2	12	13	7083	15.85	7.76	0.07	6.41	7.93	0.65	0.01	0.00	8752.54	713.77	5.69	0.00	0.00	0.00
PRI_norm	Sept 20	2	12	13	7083	0.02	0.02	0.00	0.01	0.01	0.00	0.00	0.00	5744.44	699.99	21.30	0.00	0.00	0.00
PRI*CI2	Sept 20	2	12	13	7083	8.11	5.36	0.07	10.12	4.05	0.45	0.01	0.00	2836.15	312.19	3.83	0.00	0.00	0.00
PSRI	Sept 20	2	12	13	7083	20.84	11.69	0.08	7.05	10.42	0.97	0.01	0.00	10469.71	978.65	6.57	0.00	0.00	0.00
PSSR	Sept 20	2	12	13	7083	43164.70	16674.60	169.57	33939.73	21582.35	1389.55	13.04	4.79	4504.10	289.99	2.72	0.00	0.00	0.00
PSND	Sept 20	2	12	13	7083	2.33	1.88	0.12	11.63	1.16	0.16	0.01	0.00	708.90	95.22	5.61	0.00	0.00	0.00
RDVI	Sept 20	2	12	13	7083	3799.27	1334.33	40.54	1678.77	1899.63	111.19	3.12	0.24	8014.84	469.14	13.16	0.00	0.00	0.00
REP_Li	Sept 20	2	12	13	7083	1267269.57	425400.41	1846.85	279475.60	633634.78	35450.03	142.07	39.46	16058.77	898.44	3.60	0.00	0.00	0.00
SAVI	Sept 20	2	12	13	7083	52.72	29.49	0.56	39.51	26.36	2.46	0.04	0.01	4725.31	440.48	7.71	0.00	0.00	0.00
SPVI	Sept 20	2	12	13	7083	1150265.20	388029.67	13082.17	662658.95	575132.60	32335.81	1006.32	93.56	6147.45	345.63	10.76	0.00	0.00	0.00
SR	Sept 20	2	12	13	7083	25737.48	8929.11	53.08	14885.78	12868.74	744.09	4.08	2.10	6123.25	354.06	1.94	0.00	0.00	0.02
SR1	Sept 20	2	12	13	7083	1428.72	425.90	3.00	503.54	714.36	35.49	0.23	0.07	10048.45	499.23	3.25	0.00	0.00	0.00
SR2	Sept 20	2	12	13	7083	6037.78	2027.97	12.51	2550.76	3018.89	169.00	0.96	0.36	8382.91	469.27	2.67	0.00	0.00	0.00
SR3	Sept 20	2	12	13	7083	4826.67	2525.94	33.89	4849.40	2413.34	210.49	2.61	0.68	3524.90	307.45	3.81	0.00	0.00	0.00
SR4	Sept 20	2	12	13	7083	343.02	2507.23	71.98	6253.54	171.51	208.94	5.54	0.88	194.26	236.65	6.27	0.00	0.00	0.00
SR5	Sept 20	2	12	13	7083	5.51	9.50	0.29	19.31	2.75	0.79	0.02	0.00	1010.19	290.41	8.07	0.00	0.00	0.00
SR6	Sept 20	2	12	13	7083	306.91	81.89	0.56	95.83	153.45	6.82	0.04	0.01	11341.80	504.40	3.20	0.00	0.00	0.00
SR8	Sept 20	2	12	13	7083	1.39	4.44	0.25	16.81	0.70	0.37	0.02	0.00	293.80	155.94	8.24	0.00	0.00	0.00
Sum_Dr1	Sept 20	2	12	13	7083	261562.05	289941.05	12602.45	525997.53	130781.02	24161.75	969.42	74.26	1761.08	325.36	13.05	0.00	0.00	0.00
Sum_Dr2	Sept 20	2	12	13	7083	1052457.50	348589.65	5920.17	355350.11	526228.75	29049.14	455.40	50.17	10489.03	579.02	9.08	0.00	0.00	0.00
TCARI	Sept 20	2	12	13	7083	364017.71	719820.07	18023.62	1569172.22	182008.86	59985.01	1386.43	221.54	821.56	270.76	6.26	0.00	0.00	0.00
TCARI/OSAVI	Sept 20	2	12	13	7083	1168010.81	1624606.20	19027.76	2442807.06	584005.40	135383.85	1463.67	344.88	1693.34	392.55	4.24	0.00	0.00	0.00
TCARI2	Sept 20	2	12	13	7083	2356153.91	553763.83	3485.52	345074.39	1178076.96	46146.99	268.12	48.72	24181.22	947.21	5.50	0.00	0.00	0.00
TCARI2/OSAVI2	Sept 20	2	12	13	7083	11508981.30	9551785.06	28326.06	9175077.28	5754490.65	795982.09	2178.93	1295.37	4442.37	614.48	1.68	0.00	0.00	0.06
TGI	Sept 20	2	12	13	7083	185651654.87	457038424.73	22358919.45	762632748.10	92825827.43	38086535.39	1719916.88	107670.87	862.13	353.73	15.97	0.00	0.00	0.00
TVI	Sept 20	2	12	13	7083	1947880637.93	1725764970.75	59222353.13	2341229121.16	973940318.97	143813747.56	4555565.63	330542.02	2946.49	435.08	13.78	0.00	0.00	0.00
Vogelmann	Sept 20	2	12	13	7083	44.28	9.21	0.06	9.94	22.14	0.77	0.00	0.00	15778.70	546.88	3.03	0.00	0.00	0.00
Vogelmann2	Sept 20	2	12	13	7083	1.14	0.32	0.00	0.48	0.57	0.03	0.00	0.00	8313.74	396.20	3.24	0.00	0.00	0.00
Vogelmann3	Sept 20	2	12	13	7083	140.67	38.96	1.12	78.63	70.33	3.25	0.09	0.01	6335.44	292.44	7.75	0.00	0.00	0.00
Vogelmann4	Sept 20	2	12	13	7083	1.31	0.39	0.00	0.57	0.66	0.03	0.00	0.00	8162.96	401.59	3.12	0.00	0.00	0.00
Boochs	Sept 30	2	12	14	6641	9853.51	48597.14	1234.53	5725.00	4926.76	4049.76	88.18	0.86	5715.04	4697.73	102.29	0.00	0.00	0.00
Boochs2	Sept 30	2	12	14	6641	452.71	12556.79	796.12	5173.31	226.35	1046.40	56.87	0.78	290.57	1343.27	73.00	0.00	0.00	0.00
CARI	Sept 30	2	12	14	6640	7723068.42	113295496.40	1589870.30	20901423.12	38615341.21	9441291.37	113562.16	3147.80	12267.39	2999.33	36.08	0.00	0.00	0.00
Carter2	Sept 30	2	12	14	6640	61.86	30.55	0.51	33.76	30.93	2.55	0.04	0.01	6083.87	500.79	7.11	0.00	0.00	0.00
Carter3	Sept 30	2	12	14	6640	13.00	12.90	0.28	15.65	6.50	1.07	0.02	0.00	2757.92	455.82	8.45	0.00	0.00	0.00
Carter4	Sept 30	2	12	14	6640	50.52	18.55	0.35	22.66	25.26	1.55	0.02	0.00	7402.28	452.92	7.26	0.00	0.00	0.00
Carter5	Sept 30	2	12	14	6640	248.23	2653.40	76.45	4309.62	124.12	221.12	5.46	0.65	191.23	340.68	8.41	0.00	0.00	0.00
Carter6	Sept 30	2	12	14	6641	577561.61	849171.57	15769.85	253759.18	288780.80	70764.30	1126.42	38.21	7557.53	1851.94	29.48	0.00	0.00	0.00
CI	Sept 30	2	12	14	6640	18.93	7.88	0.27	28.67	9.46	0.66	0.02	0.00	2192.36	152.09	4.53	0.00	0.00	0.00
CI2	Sept 30	2	12	14	6640	1344.02	697.56	14.81	609.06	672.01	58.13	1.06	0.09	7326.31	633.74	11.54	0.00	0.00	0.00
ClAInt	Sept 30	2	12	14	6641	1876414580.28	1803351580.23	21333103.67	461216678.32	938207290.14	150279298.35	1523793.12	69449.88	13509.13	2163.85	21.94	0.00	0.00	0.00
CRI1	Sept 30	2	12	14	6640	19.02	60.41	4.28	261.74	9.51	5.03	0.31	0.04	241.28	127.72	7.75	0.00	0.00	0.00
CRI2	Sept 30	2	12	14	6640	36.65	142.03	6.32	308.41	18.33	11.84	0.45	0.05	394.57	254.82	9.72	0.00	0.00	0.00
CRI3	Sept 30	2	12	14	6640	681.90	3217.57	211.23	5416.02	340.95	268.13	15.09	0.82	418.00	328.73	18.50	0.00	0.00	0.00
CRI4	Sept 30	2	12	14	6640	854.91	298.48	19.60	638.70	427.46	24.87	1.40	0.10	4443.87	258.58	14.56	0.00	0.00	0.00
D1	Sept 30	2	12	14	6640	68.41	118.50	2.64	162.80	34.20	9.87	0.19	0.02	1395.12	402.77	7.69	0.00	0.00	0.00
D2	Sept 30	2	12	14	6640	15508.19	52121.00	8905.77	23052209.99	7754.09	4343.42	636.13	3471.72	2.23	1.25	0.18	0.11	0.24	1.00
Datt	Sept 30	2	12	14	6640	62.76	12.57	1.05	33.62	31.38	1.05	0.07	0.01	6196.76	206.85	14.78	0.00	0.00	0.00
Datt2	Sept 30	2	12	14	6640	242.96	83.39	6.43	162.80	121.48	6.95	0.46	0.02	4954.61	283.44	18.74	0.00	0.00	0.00
Datt3	Sept 30	2	12	14	6640	414.52	65.97	4.99	144.34	207.26	5.50	0.36	0.02	9534.40	252.91	16.39	0.00	0.00	0.00
Datt4	Sept 30	2	12	14	6640	0.23	1.82	0.08	0.68	0.12	0.15	0.01	0.00	1127.21	1472.83	54.85	0.00	0.00	0.00
Datt5	Sept 30	2	12	14	6640	323.51	324.00	5.17	225.22	161.76	27.00	0.37	0.03	4768.85	796.02	10.89	0.00	0.00	0.00
Datt6	Sept 30	2	12	14	6640	110.72	399.05	8.56	133.85	55.36	33.25	0.61	0.02	2746.33	1649.65	30.33	0.00	0.00	0.00
DD	Sept 30	2	12	14	6641	1123462.24	1303548.35	10623.27	376266.56	561731.12	108629.03	758.80	56.66	9914.40	1917.27	13.39	0.00	0.00	0.00
DDn	Sept 30	2	12	14	6641	6125111.30	6841598.81	172983.79	1282826.45	3062555.65	570133.23	12355.98	193.17	15854.39	2951.49	63.97	0.00	0.00	0.00
DPI	Sept 30	2	12	14	6640	66.97	132.59	3.96	341.30	33.48	11.05	0.28	0.05	651.41	214.96	5.50	0.00	0.00	0.00
DWSI4	Sept 30	2	12	14	6640	1086.23	433.45	13.53	299.11	543.11	36.12	0.97	0.05	12056.65	801.85	21.46	0.00	0.00	0.00
EGFN	Sept 30	2	12	14	6640	32.13	9.76	1.83	27.45	16.06	0.81	0.13	0.00	3885.63	196.81	31.57	0.00	0.00	0.00
EGFR	Sept 30	2	12	14	6640	8363.66	3451.02	383.39	7884.13	4181.83	287.59	27.38	1.19	3521.93	242.20	23.06	0.00	0.00	0.00
EVI	Sept 30	2	12	14	6641	180347.66	2324671.11	5392491.41	2099469161.69	90173.83	193722.59	385177.96	316137.50	0.29	0.61	1.22	0.75	0.83	0.25
GI	Sept 30	2	12	14	6640	1421.88	692.52	19.45	585.81	710.94	57.71	1.39	0.09	8058.37	654.14	15.75	0.00	0.00	0.00
Gitelson	Sept 30	2	12	14	6640	10.03	20.88	0.74	3.24	5.01	1.74	0.05	0.00	10284.27	3569.57	108.89	0.00	0.00	0.00
Gitelson2	Sept 30	2	12	14	6640	81438.65	44660.93	2187.96	28533.52	40719.33	3721.74	156.28	4.30	9475.74	866.08	36.37	0.00	0.00	0.00
GMI1	Sept 30	2	12	14	6640	1706.00	4095.50	174.17	5976.15	853.00	341.29	12.44	0.90	947.75	379.20	13.82	0.00	0.00	0.00
GMI2	Sept 30	2	12	14	6640	1251.97	688.15	13.29	580.90	625.98	57.35	0.95	0.09	7155.38	655.50	10.85	0.00	0.00	0.00
Green NDVI	Sept 30	2	12	14	6640	1.76	12.48	0.85	20.70	0.88	1.04	0.06	0.00	281.84	333.62	19.46	0.00	0.00	0.00
Maccioni	Sept 30	2	12	14	6640	57.88	14.08	0.47	27.70	28.94	1.17	0.03	0.00	6936.76	281.22	8.04	0.00	0.00	0.00
MCARI	Sept 30	2	12	14	6640	16371961.33	41731768.89	696512.14	8779402.00	8185980.66	3477647.41	49750.87	1322.20	6191.19	2630.20	37.63	0.00	0.00	0.00
MCARI2	Sept 30	2	12	14	6640	363231.03	1347439.08	68919.71	384265.59	181615.52	112286.59	4922.84	57.87	3138.26	1940.28	85.07	0.00	0.00	0.00
MPRI	Sept 30	2	12	14	6640	211775.21	246302.47	4724.11	101526.83	105887.61	20525.21	337.44	15.29	6925.20	1342.38	22.07	0.00	0.00	0.00
MSAVI	Sept 30	2	12	14	6640	9.76	14.51	0.19	16.26	4.88	1.21	0.01	0.00	1992.28	493.67	5.55	0.00	0.00	0.00
mSR2	Sept 30	2	12	14	6640	726.25	384.71	5.96	315.42	363.13	32.06	0.43	0.05	7644.25	674.89	8.96	0.00	0.00	0.00
MTCI	Sept 30	2	12	14	6640	465.49	220.68	3.07	206.74	232.74	18.39	0.22	0.03	7474.97	590.63	7.04	0.00	0.00	0.00
MTVI	Sept 30	2	12	14	6640	12795954.57	24646406.29	596811.16	3337074.35	6397977.29	2053867.19	42629.37	502.57	12730.48	4086.72	84.82	0.00	0.00	0.00

Supplementary Table 1. (Continue)

NDVI	Sept 30	2	12	14	6640	37.25	30.43	0.54	33.56	18.63	2.54	0.04	0.01	3684.96	501.74	7.61	0.00	0.00	0.00
NDVI2	Sept 30	2	12	14	6640	37.77	17.44	0.24	16.02	18.89	1.45	0.02	0.00	7827.93	602.21	7.08	0.00	0.00	0.00
NDVI3	Sept 30	2	12	14	6640	154.70	72.07	1.88	42.92	77.35	6.01	0.13	0.01	11965.41	929.03	20.78	0.00	0.00	0.00
OSAVI	Sept 30	2	12	14	6640	26.64	37.55	0.65	42.78	13.32	3.13	0.05	0.01	2066.88	485.63	7.25	0.00	0.00	0.00
OSAVI2	Sept 30	2	12	14	6640	50.00	22.94	0.32	21.34	25.00	1.91	0.02	0.00	7778.17	594.83	7.16	0.00	0.00	0.00
PARS	Sept 30	2	12	14	6639	9547.95	14054.63	767.50	31617.97	4773.98	1171.22	54.82	4.76	1002.42	245.93	11.51	0.00	0.00	0.00
PRI	Sept 30	2	12	14	6639	14.50	7.94	0.19	8.04	7.25	0.66	0.01	0.00	5985.82	546.66	11.44	0.00	0.00	0.00
PRI_norm	Sept 30	2	12	14	6639	0.05	0.08	0.00	0.05	0.02	0.01	0.00	0.00	3107.85	858.02	9.19	0.00	0.00	0.00
PRI*CI2	Sept 30	2	12	14	6639	9.84	15.37	0.35	18.78	4.92	1.28	0.02	0.00	1739.19	452.78	8.83	0.00	0.00	0.00
PSRI	Sept 30	2	12	14	6639	21.93	16.74	0.26	9.27	10.96	1.40	0.02	0.00	7854.23	999.62	13.28	0.00	0.00	0.00
PSSR	Sept 30	2	12	14	6639	19673.41	22382.38	1130.06	28044.96	9836.70	1865.20	80.72	4.22	2328.61	441.54	19.11	0.00	0.00	0.00
PSND	Sept 30	2	12	14	6639	0.08	4.67	0.38	14.11	0.04	0.39	0.03	0.00	18.93	183.22	12.86	0.00	0.00	0.00
RDVI	Sept 30	2	12	14	6639	11326.21	24994.63	877.40	2168.06	5663.11	2082.89	62.67	0.33	17341.49	6378.19	191.91	0.00	0.00	0.00
REP_Li	Sept 30	2	12	14	6639	265738.63	131930.69	1919.70	317092.54	132869.31	10994.22	137.12	47.76	2781.90	230.19	2.87	0.00	0.00	0.00
SAVI	Sept 30	2	12	14	6639	39.51	61.13	1.20	69.48	19.75	5.09	0.09	0.01	1887.49	486.70	8.22	0.00	0.00	0.00
SPVI	Sept 30	2	12	14	6639	10084591.18	15585576.69	364172.04	1927776.37	5042295.59	1298798.06	26012.29	290.37	17364.98	4472.88	89.58	0.00	0.00	0.00
SR	Sept 30	2	12	14	6639	22179.79	18668.98	572.28	20234.69	11089.90	1555.75	40.88	3.05	3638.59	510.44	13.41	0.00	0.00	0.00
SR1	Sept 30	2	12	14	6639	1248.40	684.18	13.10	577.26	624.20	57.02	0.94	0.09	7178.91	655.73	10.76	0.00	0.00	0.00
SR2	Sept 30	2	12	14	6639	5754.30	3566.67	103.10	3397.74	2877.15	297.22	7.36	0.51	5621.79	580.76	14.39	0.00	0.00	0.00
SR3	Sept 30	2	12	14	6639	1710.79	4072.57	173.65	5942.70	855.39	339.38	12.40	0.90	955.62	379.15	13.86	0.00	0.00	0.00
SR4	Sept 30	2	12	14	6639	1009.84	4806.80	146.50	7621.00	504.92	400.57	10.46	1.15	439.86	348.95	9.12	0.00	0.00	0.00
SR5	Sept 30	2	12	14	6639	14.94	28.40	0.36	26.93	7.47	2.37	0.03	0.00	1841.74	583.47	6.31	0.00	0.00	0.00
SR6	Sept 30	2	12	14	6639	270.69	141.75	2.20	117.62	135.35	11.81	0.16	0.02	7639.55	666.75	8.85	0.00	0.00	0.00
SR8	Sept 30	2	12	14	6639	3.17	11.16	0.26	18.68	1.59	0.93	0.02	0.00	564.01	330.46	6.72	0.00	0.00	0.00
Sum_Dr1	Sept 30	2	12	14	6639	5927009.38	9697362.85	256841.09	1402258.25	2963504.69	808113.57	18345.79	211.22	14030.73	3826.02	86.86	0.00	0.00	0.00
Sum_Dr2	Sept 30	2	12	14	6639	3589447.99	6734517.00	167789.13	661540.69	1794724.00	561209.75	11984.94	99.64	18011.25	5632.11	120.28	0.00	0.00	0.00
TCARI	Sept 30	2	12	14	6639	1925079.98	2820026.13	43213.95	2027091.91	962539.99	235002.18	3086.71	305.33	3152.45	769.66	10.11	0.00	0.00	0.00
TCARI/OSAVI	Sept 30	2	12	14	6639	3829097.82	5382640.25	46713.44	3549515.49	1914548.91	448553.35	3336.67	534.65	3580.96	838.97	6.24	0.00	0.00	0.00
TCARI2	Sept 30	2	12	14	6639	231814.82	1351391.30	45166.43	386082.49	115907.41	112615.94	3226.17	58.15	1993.12	1936.52	55.48	0.00	0.00	0.00
TCARI2/OSAVI2	Sept 30	2	12	14	6639	5573196.69	18237286.44	589483.11	19916473.51	2786598.35	1519773.87	42105.94	2999.92	928.89	506.60	14.04	0.00	0.00	0.00
TGI	Sept 30	2	12	14	6639	984393027.60	2852603562.57	60855938.56	873517904.49	492196513.80	237716963.55	4346852.75	131573.72	3740.84	1806.72	33.04	0.00	0.00	0.00
TVI	Sept 30	2	12	14	6639	12794442412.98	31390104790.64	710763336.72	3167684374.16	6397221206.49	2615842065.89	50768809.77	477132.76	13407.63	5482.42	106.40	0.00	0.00	0.00
Vogelmann	Sept 30	2	12	14	6639	30.69	17.97	0.24	17.05	15.34	1.50	0.02	0.00	5975.81	583.31	6.66	0.00	0.00	0.00
Vogelmann2	Sept 30	2	12	14	6639	7.82	0.83	0.03	1.07	3.91	0.07	0.00	0.00	24263.99	428.37	12.42	0.00	0.00	0.00
Vogelmann3	Sept 30	2	12	14	6639	113.86	139.32	2.24	136.40	56.93	11.61	0.16	0.02	2770.91	565.10	7.77	0.00	0.00	0.00
Vogelmann4	Sept 30	2	12	14	6639	8.74	0.95	0.03	1.19	4.37	0.08	0.00	0.00	24294.49	441.18	11.97	0.00	0.00	0.00

Supplementary Table 2. VI factor loads on significant components for *Q. robur*, *Q. macrocarpa*, *Q. rubra*

VI	Comp.1	Comp.2	Comp.3	Comp.4	Comp.5	Comp.6	Comp.7	Comp.8	Comp.9
				Sept 05					
Boochs		0.202	0.126					-	-
Boochs2		0.233			0.134			-	-
CARI	0.124		0.119	0.156				-	-
Carter2	0.140							-	-
Carter3	0.138				-0.137			-	-
Carter4	0.144							-	-
Carter5		-0.169	0.243		0.145	0.113		-	-
Carter6	0.127	0.119			-0.159			-	-
CI		0.112		-0.101	-0.182	-0.309		-	-
CI2	-0.142							-	-
ClAInt	0.123	0.129		0.135				-	-
CRI1	-0.102	-0.133		0.162		-0.107		-	-
CRI2	-0.108	-0.128		0.187				-	-
CRI3	0.133			-0.181				-	-
CRI4	0.141							-	-
D1	-0.133				-0.114			-	-
D2				0.152	-0.127	0.150		-	-
Datt	-0.142							-	-
Datt2	-0.143							-	-
Datt3				0.134		-0.132		-	-
Datt4	-0.114		-0.177		-0.100			-	-
Datt5		0.109	-0.292	0.122	0.104			-	-
Datt6	-0.127			0.170	-0.146			-	-
DD	-0.136			-0.143				-	-
DDn		-0.278						-	-
DPI					0.232	0.208		-	-
DWSI4			0.260	-0.189	-0.243			-	-
EGFN	-0.102	0.115		0.155				-	-
EGFR	-0.103			0.180				-	-
EVI							-0.990	-	-
GI			0.283	-0.136	-0.168			-	-
Gitelson	-0.131				-0.191			-	-
Gitelson2		0.176			0.206	-0.106		-	-
GMI1	-0.134			0.174				-	-
GMI2	-0.142				-0.104			-	-
Green NDVI	-0.140				0.156			-	-
Maccioni	-0.142							-	-
MCARI	0.113		0.176	0.139		0.120		-	-
MCARI2	-0.109	0.181						-	-
MPRI	0.123	0.140			-0.133			-	-
MSAVI	-0.119		0.182		0.105			-	-
mSR2	-0.143							-	-
MTCI	-0.140							-	-
MTVI		0.215	0.122					-	-
NDVI	-0.134		0.133					-	-
NDVI2	-0.144							-	-
NDVI3			-0.238	0.224	0.259			-	-
OSAVI	-0.121		0.181					-	-
OSAVI2	-0.144							-	-
PARS	-0.121		0.102	0.210				-	-
PRI	-0.114			-0.177		0.346		-	-
PRI_norm	0.108			0.177		-0.38		-	-
PRI*CI2					-0.168	0.573		-	-
PSRI	0.106			0.254				-	-
PSSR	-0.135			0.126				-	-
PSND			0.177	0.193	0.140			-	-
RDVI		0.238	0.162					-	-
REP_Li	-0.133			-0.141				-	-
SAVI	-0.120		0.183		0.101			-	-
SPVI		0.245		0.114				-	-
SR	-0.131		0.118	0.106				-	-
SR1	-0.142				-0.104			-	-
SR2	-0.140				-0.126			-	-
SR3	-0.134			0.174				-	-
SR4		-0.159	0.260		0.129			-	-
SR5		0.149	-0.277		-0.101			-	-
SR6	-0.143							-	-
SR8			-0.234	-0.115		0.226		-	-
Sum_Dr1		0.215	0.105	0.110				-	-
Sum_Dr2		0.250	0.111					-	-
TCARI	0.124	0.130			-0.179			-	-
TCARI/OSAVI	0.125	0.118			-0.188			-	-
TCARI2		0.198		-0.259	0.169			-	-
TCARI2/OSAVI2	0.114	0.132						-	-
TGI	0.126		0.107		-0.171			-	-
TVI		0.221	0.123					-	-
Vogelmann	-0.143				-0.104			-	-
Vogelmann2	0.138				0.157			-	-
Vogelmann3	-0.133							-	-
Vogelmann4	0.138				0.165			-	-

Supplementary Table 2. (Continue)

	Sept 13								
Boochs		0.247			0.126				-
Boochs2		0.190							-
CARI	0.117		0.136	-0.141					-
Carter2	0.148			-0.104					-
Carter3	0.144				-0.134	-0.120			-
Carter4	0.151								-
Carter5			0.265			0.159			-
Carter6	0.116	0.155			-0.148				-
CI				0.107		-0.306		0.285	-
CI2	-0.149				-0.100				-
ClAInt	0.116	0.149		-0.171					-
CRI1		-0.156	0.173			-0.144			-
CRI2		-0.177	0.136	-0.116					-
CRI3	0.143			0.185					-
CRI4	0.146				0.105				-
D1	-0.133							-0.137	-
D2	0.132			-0.101	-0.106			0.106	-
Datt	-0.144				0.106				-
Datt2	-0.149								-
Datt3				-0.195		-0.226		-0.692	-
Datt4		-0.158	-0.165						-
Datt5			-0.269	-0.12	0.180				-
Datt6	-0.117	-0.135		-0.125					-
DD	-0.145			0.101					-
DDn		-0.222							-
DPI						0.286		-0.249	-
DWSI4			0.220	0.184	-0.164	-0.197			-
EGFN	-0.111			-0.234				0.249	-
EGFR	-0.112			-0.246		0.116		0.218	-
EVI							-0.998		-
GI			0.259	0.151	-0.153	-0.134			-
Gitelson	-0.117	-0.148			-0.145				-
Gitelson2		0.112			0.274				-
GMI1	-0.143			-0.177				0.114	-
GMI2	-0.149				-0.101				-
Green NDVI	-0.145				0.202				-
Maccioni	-0.148								-
MCARI			0.191	-0.109		0.146			-
MCARI2	-0.125	0.137							-
MPRI		0.165			-0.148				-
MSAVI	-0.115		0.182						-
mSR2	-0.150								-
MTCI	-0.144								-
MTVI		0.251		-0.101					-
NDVI	-0.137		0.116						-
NDVI2	-0.151								-
NDVI3		-0.102	-0.188	-0.211	0.172	0.215			-
OSAVI	-0.116		0.185						-
OSAVI2	-0.151								-
PARS	-0.108		0.167	-0.198	0.109				-
PRI	-0.126			0.156	-0.160	0.255			-
PRI_norm	0.121			-0.154	0.194	-0.300			-
PRI*CI2					-0.390	0.350			-
PSRI	0.124			-0.259					-
PSSR	-0.138			-0.11				0.101	-
PSND			0.226	-0.165	0.105				-
RDVI		0.236		-0.1					-
REP_Li	-0.141			0.177	0.158				-
SAVI	-0.115		0.185						-
SPVI		0.248		-0.142	0.132				-
SR	-0.131		0.130			-0.122			-
SR1	-0.149				-0.101				-
SR2	-0.147								-
SR3	-0.143			-0.177				0.114	-
SR4			0.274			0.130			-
SR5			-0.285					-0.102	-
SR6	-0.150								-
SR8			-0.249	0.105		0.181			-
Sum_Dr1		0.247		-0.151					-
Sum_Dr2		0.252							-
TCARI	0.104	0.159			-0.131	-0.172			-
TCARI/OSAVI	0.113	0.132			-0.145	-0.182			-
TCARI2		0.210		0.219	0.233				-
TCARI2/OSAVI2		0.193		0.131					-
TGI	0.116	0.122			-0.195				-
TVI		0.253							-
Vogelmann	-0.149								-
Vogelmann2	0.143								-
Vogelmann3	-0.138							-0.135	-
Vogelmann4	0.143								-

Supplementary Table 2. (Continue)

	Sept 20								
Boochs	0.104	0.167						-	-
Boochs2	0.134							-	-
CARI		0.204	-0.102	0.168				-	-
Carter2	-0.142							-	-
Carter3	-0.138							-	-
Carter4	-0.141							-	-
Carter5		0.168	-0.269					-	-
Carter6	-0.103	0.137	0.158		-0.111	-0.154		-	-
CI	0.105		0.186			-0.119		-	-
CI2	0.141							-	-
ClAInt	-0.121		0.124	0.170	-0.128			-	-
CRI1			-0.248		-0.220	-0.123		-	-
CRI2		-0.106	-0.239		-0.121			-	-
CRI3	-0.126			-0.147				-	-
CRI4	-0.140							-	-
D1	0.110			-0.108				-	-
D2				0.182		-0.152		-	-
Datt	0.123	-0.105		-0.107	-0.102			-	-
Datt2	0.135							-	-
Datt3		-0.123			-0.297	0.172		-	-
Datt4		-0.293						-	-
Datt5		-0.210		0.118				-	-
Datt6	0.118	-0.128				-0.123		-	-
DD	0.132			-0.102				-	-
DDn	-0.108		-0.209		0.130			-	-
DPI						0.415		-	-
DWSI4	0.112	0.149		-0.148		-0.122		-	-
EGFN		-0.141		0.373	0.138			-	-
EGFR		-0.141		0.371	0.130			-	-
EVI							0.995	-	-
GI	0.101	0.177		-0.154				-	-
Gitelson	0.127	-0.106				-0.107		-	-
Gitelson2			0.163		-0.359	0.407		-	-
GMI1	0.127			0.147				-	-
GMI2	0.141							-	-
Green NDVI	0.130			0.103		0.130		-	-
Maccioni	0.134							-	-
MCARI		0.238	-0.165	0.121				-	-
MCARI2	0.138							-	-
MPRI			0.215			-0.104		-	-
MSAVI	0.122	0.110	-0.104		0.102			-	-
mSR2	0.141							-	-
MTCI	0.137							-	-
MTVI		0.223	0.119	0.138				-	-
NDVI	0.139							-	-
NDVI2	0.142							-	-
NDVI3	-0.113	-0.141		0.170		0.130		-	-
OSAVI	0.125	0.103	-0.105					-	-
OSAVI2	0.142							-	-
PARS	0.121		-0.144	0.101	-0.148			-	-
PRI	0.129				0.166			-	-
PRI_norm	-0.116	-0.116			-0.276			-	-
PRI*CI2	0.115			0.147		-0.247		-	-
PSRI	-0.126				-0.194			-	-
PSSR	0.134					-0.114		-	-
PSND			-0.230		-0.231			-	-
RDVI	0.117	0.155		0.121				-	-
REP_Li	0.131			-0.163		0.130		-	-
SAVI	0.126	0.104	-0.104					-	-
SPVI		0.127	0.136	0.234				-	-
SR	0.139					-0.121		-	-
SR1	0.141							-	-
SR2	0.140					-0.122		-	-
SR3	0.127			0.147				-	-
SR4		0.158	-0.249					-	-
SR5		-0.163	0.180					-	-
SR6	0.140							-	-
SR8		-0.132	0.188	0.133	0.416	0.149		-	-
Sum_Dr1		0.203	0.132	0.262	-0.130			-	-
Sum_Dr2	0.112	0.139	0.120	0.114				-	-
TCARI			0.239			-0.200		-	-
TCARI/OSAVI	-0.102		0.213		-0.130	-0.206		-	-
TCARI2	0.125		0.118			0.112		-	-
TCARI2/OSAVI2		0.138		-0.246		0.163		-	-
TGI		0.226			-0.174	-0.159		-	-
TVI		0.222	0.114	0.152				-	-
Vogelmann	0.138							-	-
Vogelmann2	-0.131				0.112			-	-
Vogelmann3	0.127							-	-
Vogelmann4	-0.131				0.110			-	-

Supplementary Table 2. (Continue)

	Sept 30								
Boochs		0.195							
Boochs2		0.106	0.103		0.306		0.173		
CARI		0.166							
Carter2	0.163								
Carter3	0.147		-0.144						
Carter4	0.155		0.130						
Carter5			0.208		-0.213	-0.171			
Carter6	0.103	0.174				0.129			
CI				-0.167	0.242	0.298	0.214		
CI2	-0.166								
ClAInt	0.127	0.138				0.152			
CRI1	-0.108				-0.258	0.205	0.239		
CRI2	-0.115				-0.245	0.206	0.210		
CRI3			-0.100	-0.309	-0.154				
CRI4	0.133		0.109		-0.147		0.150		
D1	-0.110						0.281		
D2								0.219	-0.947
Datt			-0.255	0.186		-0.140			
Datt2	-0.121		-0.200	0.145					
Datt3			-0.231	0.212		-0.131			
Datt4		-0.140			-0.128	0.144	0.124		
Datt5		-0.142		0.170					
Datt6	-0.134				-0.206	0.208			
DD	-0.123	-0.129			0.103	-0.135			
DDn		-0.170							
DPI			-0.122	0.108			-0.288	0.208	0.159
DWSI4	-0.121	0.135		-0.151					
EGFN			0.179	0.167	0.246	0.182	-0.133		
EGFR			0.159	0.180	0.250	0.189	-0.151		
EVI								-0.901	-0.188
GI	-0.116	0.139		-0.124	-0.111				
Gitelson	-0.137				-0.220	0.191			
Gitelson2		0.139	-0.114	0.127					
GMI1			0.137	0.255	0.111				
GMI2	-0.170								
Green NDVI				0.322					
Maccioni	-0.106		-0.235	0.120		-0.105			
MCARI		0.175							
MCARI2		0.173			0.228		0.136		
MPRI	0.110	0.159				0.153			
MSAVI	-0.123	0.122	0.126			-0.134			
mSR2	-0.171								
MTCI	-0.149		-0.180						
MTVI		0.194							
NDVI	-0.149	0.108							
NDVI2	-0.172								
NDVI3	0.112	-0.137		0.198					
OSAVI	-0.126	0.123	0.122			-0.133			
OSAVI2	-0.171								
PARS	-0.111		0.179	0.174			0.230		
PRI	-0.139			-0.145		0.105	-0.169		
PRI_norm	0.107	-0.108	-0.135				0.311		
PRI*CI2	-0.131				-0.101	0.250	-0.231		
PSRI	0.122	-0.117		0.143					
PSSR	-0.158								
PSND			0.130	0.235	-0.120	-0.142	0.110		
RDVI		0.194							
REP_Li	-0.134		-0.139		0.130	-0.148	0.169		
SAVI	-0.121	0.128	0.125			-0.142			
SPVI		0.184							
SR	-0.162								
SR1	-0.170								
SR2	-0.169					0.119			
SR3			0.137	0.255	0.111				
SR4			0.205		-0.186	-0.142			
SR5		-0.108	-0.221						
SR6	-0.169								
SR8		-0.111	-0.144		0.192		-0.316		
Sum_Dr1		0.179				0.101			
Sum_Dr2		0.192							
TCARI	0.103	0.140				0.207			
TCARI/OSAVI	0.115	0.112	-0.112			0.240			
TCARI2		0.190			0.172		0.194		
TCARI2/OSAVI2		0.189					0.185		
TGI		0.197							
TVI		0.195							
Vogelmann	-0.170								
Vogelmann2		-0.111	0.245	-0.137					
Vogelmann3	-0.129								
Vogelmann4		-0.109	0.246	-0.134					

Supplementary Table 3. Projections of VI values for *Q. robur, Q. macrocarpa, Q. rubra*

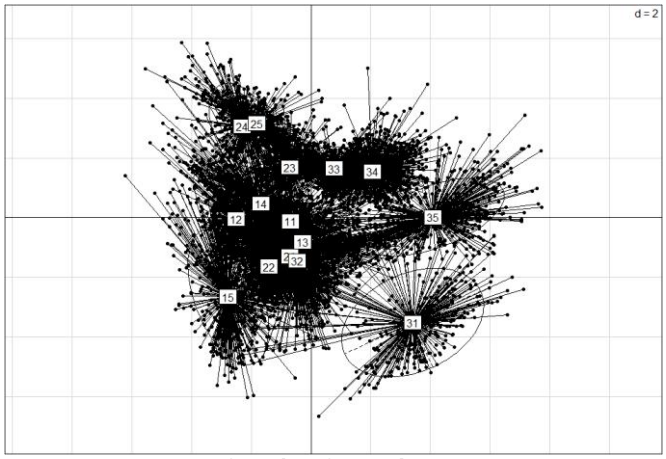

Figure 1. Projections of VI values for Boochs2, CRI3, Datt4, Maccioni, MTCI, NDVI3, PSRI, RDVI, RDVI, REP_Li, SPVI, TCARI2 for Q. macrocarpa (1), Q. robur (2), Q. rubra (3) samples (Sept 05). Numerical designation on the projection: the first digit indicates the view; the second is the sample of the species

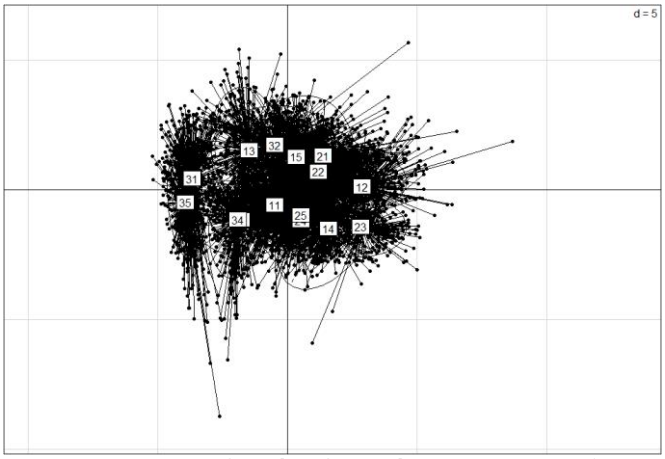

Figure 2. Projections of VI values for Boochs2, CRI3, CRI4, Datt5, DD, DWSI4, Gitelson, MCARI, PRI for Q. macrocarpa (1), Q. robur (2), Q. rubra (3) samples (Sept 13). Numerical designation on the projection: the first digit indicates the view; the second is the sample of the species

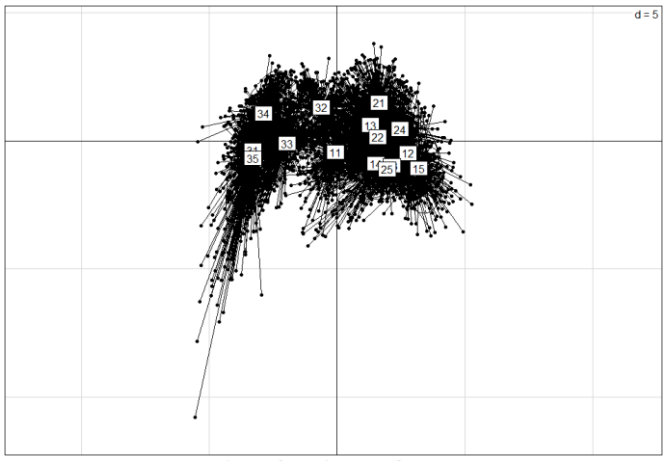

Figure 3. Projections of VI values for Boochs, Carter3, D1, Datt, Datt3, Datt5, Gitelson2, MCARI2, Sum_Dr1, Vogelmann for Q. macrocarpa (1), Q. robur (2), Q. rubra (3) samples (Sept 20). Numerical designation on the projection: the first digit indicates the view; the second is the sample of the species

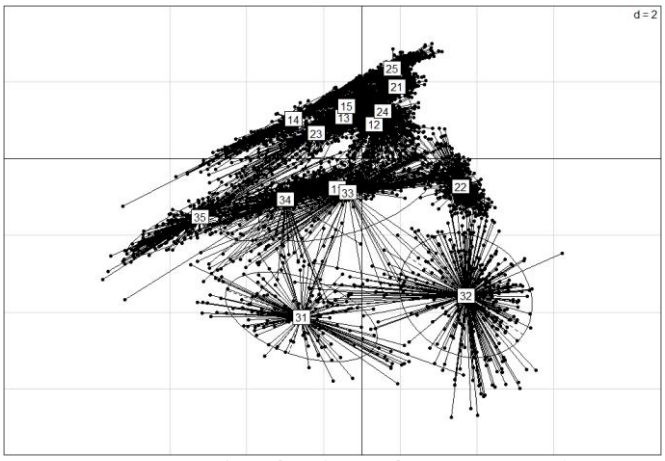

Figure 4. Projections of VI values for Boochs2, Carter6, Datt5, NDVI3, PRI_norm, SPVI, SR5, Sum_Dr1, TCARI2, Vogelmann2 for Q. macrocarpa (1), Q. robur (2), Q. rubra (3) samples (Sept 30). Numerical designation on the projection: the first digit indicates the view; the second is the sample of the species

Eurasian Journal of Soil Science 2023, 12(1), 63- 78

Eurasian Journal of Soil Science

Journal homepage : http://ejss.fesss.org

Salt accumulation in soils under furrow and drip irrigation using modified waters in Central Iran

Leila Jahanbazi [a] , Ahmad Heidari [a,*], Mohammad Hossein Mohammadi [a], Maria Kuniushkova [b]

[a] Soil Science Department, College of Agriculture and Natural Resources, University of Tehran, Karaj, Iran
[b] Lomonosov Moscow State University, Leninskie gory GSP-1, 119991 Moscow, Russia

Article Info

Received : 01.02.2022
Accepted : 04.10.2022
Available online : 09.10.2022

Author(s)

L.Jahanbazi
A.Heidari *
M.H.Mohammadi
M.Kuniushkova

* Corresponding author

Abstract

The objectives of this study were i) to characterize the water and soils under different managements, ii) to evaluate the sustainability of using hypersaline soils and water, and iii) to assess possible solutions to prevent more degradation of soil and water resources. Field and laboratory analysis of the samples using eight pedons and 128 surface samples taken from grid in four pre-determined land uses; pistachio orchard abandoned, pistachio orchard with furrow irrigation, wheat and maize cropping with furrow irrigation, pistachio orchard with drip irrigation. The study area, 170 ha, comprised two distinct soil parent materials including marls (max. ECe >100 dS/m) and alluviums (max. ECe >60 dS/m). Abandoning lands caused salinity increasing due to lack of leaching by irrigation water. The maximum increase of soil salinity was in the abandoned land use (EC e =98 dS/m), where trees had been removed and there is no irrigation, followed by pistachio plantation land use (EC=11 to 34 dS/m), and wheat and maize cropping land use (EC=11-19 dS/m). The minimum rise in soil salinity was in the drip irrigation due to mixing freshwater with saline water and therefore better water quality (EC=3 dS/m at surface layer and 17 dS/m in next layer). Land use change to agriculture increased the need for irrigation and because of arid climate it mainly supplied by groundwater from deep wells. Using deep groundwater due to rock-water reaction and increasing salinity, decreased water quality in furrow irrigation and therefore it had more significant effect on soil salinity compare to drip. Comparison of the mean values of soil salinity indicators in 2018 showed that salinity has increased by 3-6 times in the furrow irrigation and at least two-fold in the drip irrigation, compared to 2002. The calculated salinity indicators also proved the soil and water resources had been degraded and present land use types are not sustainable. Possible solutions could be to minimize land use change to agriculture, to use drip irrigation with mixed saline and freshwater, and to remove salt crusts from the soil surface.

Keywords: Land degradation, Arid climate, Solute dynamics, Saline soils, Saline water, Irrrigation.

Introduction

Soil and water salinity are the most important progressive factors of soil degradation which limit food production and sustainable agriculture spatially in arid regions. Saline soils are one of the most extensive soil types found in arid and semi-arid regions, and they severely limit water availability, temporally and spatially, due to high salt accumulation (Bouaziz et al., 2020).

Although the salinity of hypersaline soils is much higher than that of saline soils, the chemical characteristics separating saline and hypersaline soils are not precisely defined (Dion and Nautiyal, 2008). Hypersaline soils include soils that contain salt accumulation at lower ranges (4–8 dS/m), that restrict the yield of many crops,

: https://doi.org/10.18393/ejss.1186388
: http://ejss.fesss.org/10.18393/ejss.1186388
Publisher : Federation of Eurasian Soil Science Societies
e-ISSN : 2147-4249

in moderate ranges (8–16 dS/m), where only tolerant crops may yield satisfactorily, and highly hypersaline soils (ECe>16 dS/m), in which only a few very tolerant crops may yield satisfactorily (USDA, 1954).

More than 90% of Iran, which has a total area of about 1.65 Mha, is located in arid and semiarid regions where producing crops without irrigation is impossible. The use of saline groundwater to irrigate saline soils with different levels of salinity, especially in central Iran, has led to accelerated environmental degradation (Al-Muaini et al., 2019). Long term use of hypersaline water for agriculture purposes has led to further accumulation of salts in soils and conversion of salt-affected soils into hypersaline soils. Such a relationship between changes in salinity parameter associated with different types of land use has been reported in many studies (Pasternak and De Malach, 1995; Hanson et al., 2008).

The quality of irrigation water is one of the most critical factors in the management of salt-affected soils (Acar and Yilmaz, 2019). Irrigation water quality not only affects crop yield and physical soil conditions but also influences plant nutrition, irrigation system usability, and water application (Minhas et al., 2020). Therefore, analysis of irrigation water quality is essential to support suitable management for maximum crop productivity. Several parameters, including total dissolved solute content, the relative proportion of sodium to calcium and magnesium ions, pH, carbonate and bicarbonate, specific ions such as chloride, sulfate, and boron, and nitrate concentration are involved in the determination of irrigation water quality (Bauder et al., 2010). Hypersaline water is water where salinity hazard is high (0.75–2.25 dS/m) to very high (>2.25 dS/m) and this cannot be used on soils with restricted drainage. Even for salt tolerant crops, using hypersaline water requires special management (USDA, 1954). High pH, above 8.5, with high concentrations of HCO_3^- and CO_3^{2-}, causes precipitation of calcium and magnesium ions, leaving excess sodium in the soil solution. Small amounts of chloride are essential for plants, but in high concentrations it is toxic to sensitive crops (Geilfus, 2019). Low concentrations of sulfate ion in irrigation water benefit soil fertility (Bauder et al., 2010).

Soil texture diversity in vertical profile is an effective factor on soil water movement, nutrients, soil solute migrations, primary and secondary salinity. Particle size distribution (PSD) is an useful tool for soil classification. Investigation of PSD effects on soil salinity is necessary to estimate the intensity and extent of soil degradation. The more dominant fine part in particle size distribution, the higher increase in salinity ions due to the high specific level of these fine particles (Yang and Yanful, 2002; Zhao et al., 2016).

Finding crops which are resistant to salinity and are also valuable commercially is one of the important management challenges in hypersaline agriculture (Mustafa and Akhtar, 2019). Pistachio is one of the strategic crops that play a key role in people's livelihoods in arid and semi-arid regions (Moazzzam Jazi et al., 2019). Suitable EC for pistachio trees is less than 4 dS/m however, up to 8 dS/m, a suitable product is produced. Although pistachio has been produced conventionally in arid regions for a long time, a recent increase in soil and water salinity problems has caused the crop cultivation strategy used in pistachio plantations to change (Crane, 1978; Bodaghabadi et al., 2019).

The use of hypersaline soil and water for agriculture, and associated problems such as soil and water degradation in arid and semi-arid regions, has led to a variety of research focused on hypersaline agriculture and soil and water resources management (e.g. see Rhoades et al. 1992; Minhas, 1996; Tanji and Kielen, 2002; Hoffman and Shalhevet, 2007; Grattan et al., 2002; Pereira et al., 2014, Gebremeskel et al., 2018). As various studies have shown, it is not possible to use hypersaline soils and water for agriculture without taking into account sustainability and the salt balance in the root zone (Gebremeskel et al., 2018; Minhas et al., 2020). However, despite the numerous studies in the field of salinity, no study has yet been conducted on the application of hypersaline water to hypersaline soils and its long-term sustainability. This study examines the hypothesis of instability of hypersaline agriculture in arid zones. The main mechanisms involved in salt accumulation are using hypersaline waters in the arid climate and irrelevant irrigation methods. The objectives of this study were i) to characterize the water and soils quality under different managements in the studied arid region, ii) to evaluate the soils quality sustainability of using hypersaline soils and water in the arid region under study, and iii) to assess possible solutions to prevent rapid degradation of soil and water resources.

Material and Methods

Site description

The study area comprises about 170 ha located in the south west of Eyvanekey county (Semnan province) in central Iran, between latitudes 35° 19´ 39.186" to 35° 21´ 11.204" N and longitudes 51° 57´ 55.402" to 52° 02´ 4.316" E (Figure 1). Common crops in the study region are pistachio, wheat, and maize. The main section of the study area was 135 ha of pistachio orchard under five- to 60-year-old pistachio trees in different patches and two kinds of furrow and drip irrigation methods, with about 17 ha of cropland with cultivated agricultural crops of wheat and maize.

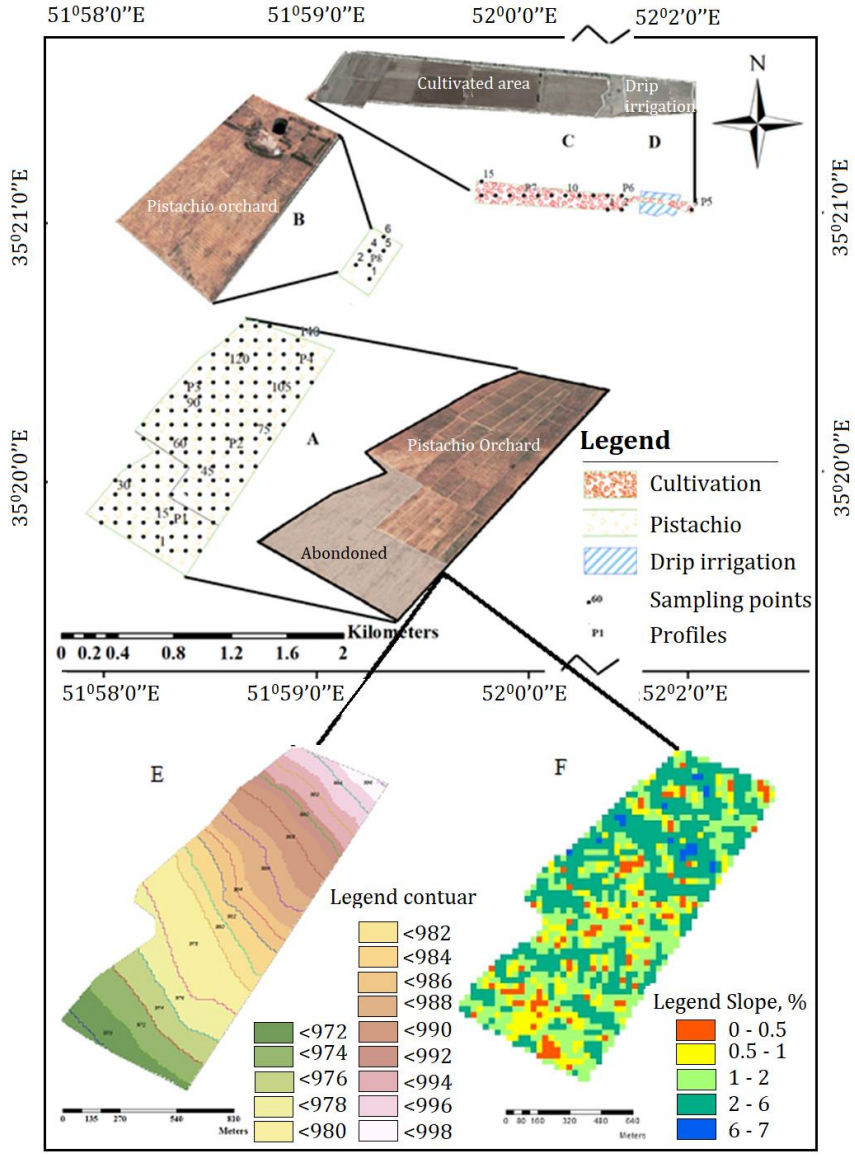

Figure 1. Soil samples location and land use (21 Oct. 2018) (above); Land use 1 & 2 in two different fields: A &B left above; Land use 3&4: C&D right above, slope (below left) and elevation (below right) maps

The geology comprises an admixture of coarse igneous and pyroclastic rock fragments in the north-western section of the Eyvanekey alluvial fan, originating from the Alborz Mountain Chain, along with the remnants of eroded marls originating from the southern Neogene formations. Patches of the alluviums have overlaid the marls in the middle parts of the area where they meet. The overall slope (about 1.5%) of the study area is flat with no effective slope aspect direction. There are some artificially established slopes in the opposite direction to the direction of the main slope, created to lead rainwater into the irrigation channels under the pistachio trees. Based on the Köppen climate classification system, the study area is classified as having a dry (B) climate (Köppen, 1931). The coldest month was January with 2.9 degrees and the warmest month was July, with 29.7 degrees. The average Min. T was recorded in January as -3.4 °C and the Avg. Max. T was recorded as 38.7 °C in July. The spring and summer rainfall in the study area is between 30% and 70% of the mean annual precipitation, which is less than 50% of the threshold (mean annual precipitation +140 mm), which, in combination with temperature of less than 18 °C, is classified as BWk. The reference evapotranspiration of the study area is 944.53 mm, which is much higher than its annual precipitation (127 mm), and the mean annual temperature is 16.6 °C. The annual aridity index (AI) in the region is equal to 0.135, which has caused it to be classified as an arid region. According to the mean annual soil temperature at a depth of 50 cm (17.6 °C), based on the climatic data and using The Natural System Model (NSM) software, soil moisture and temperature regimes were identified as Aridic and Thermic, respectively (Newhall and Berdanier, 1996; Table 1). The soil thermal regime was characterized as thermic (> 270 days soil temperature at a depth of 50 cm was >8 ^{0}C). Also, due to the long period that the soil moisture control section was recorded to be dry during the year, the soil moisture regime was determined as subdivision of aridic regime; weakly aridic which means that Soil Moisture Control Section is dry for more than half of the time that T > 5 ^{0}C (Soil Survey Staff, 2014).

Table 1. Monthly climatic data, soil climate and aridity index of Eyvanekey for Year (2018)

	Jan.	Feb.	Mar.	Apr.	May	Jun.	Jul.	Aug.	Sep.	Oct.	Nov.	Dec.	Year
Avg. T (°C)	2.9	5.8	10.2	15.8	22.3	26.9	29.7	28.4	24	18.1	10.4	4.9	16.6
Min. T (°C)	-3.4	-0.9	3	8.2	14	18.1	20.7	19.4	15.1	10	3.1	-1.5	8.8
Max. T (°C)	9.3	12.6	17.5	23.5	30.6	35.8	38.7	37.4	33	26.3	17.8	11.3	24.48
P (mm)	28	20	20	14	11	1	0	0	2	8	11	12	127
ET (mm)	1.6	7.0	24.0	56.7	118.6	163.4	195.5	171.5	115.6	64.8	20.8	5.2	944.5
P – ET (mm)	26	13	-4	-43	-108	-162	-196	-172	-114	-57	-10	7	-818
Aridity Index	17.50	2.86	0.83	0.25	0.09	0.01	0.00	0.00	0.02	0.12	0.53	2.31	0.13
Soil Temp. regime	Thermic (>270 days soil temperature at the depth of 50 cm is > 8 ^{0}C)												
Soil Mois. Regime	Weak Aridic (Soil Moisture Control Section is dry for more than one half of the time that T> 5 ^{0}C)												

Soil and water sampling

After the study area had been selected, in order to understand the existing problems in the study area and determine sampling strategy four field observations were carried out to check for the existence of salt crusting and the presence of rock fragments during November, 2018. Soil survey showed that there is high variation of EC in furrow irrigation, 4-70 dS/m and a narrow variation range of EC in drip irrigation method, 3-16 dS/m. Also salt crusting was observed clearly in the abandon area (about 30 percent of study area) and its margin with pistachio trees. Amount and also size of rock fragments was completely different in the different sites. Portable devices were used to evaluate the initial spatial distribution of moisture content, pH, and EC along the transecting and traversing areas. Before laboratory analysis and profile description the spatial and temporal sampling design was prepared, based on the results of field observations combined with information on land use, climate, management, and the geology of the area (Geological Survey and Mineral Exploration of Iran, 2011). We decided to go to the field in wet season to investigate salt movement and its interaction with rain and a grid design soil sampling used as a tool to find salt spatial changes in the study area. A sampling strategy was produced so that all the factors influencing soil salinity dynamics (irrigation methods, crop types, and land use) were included.

Sampling was performed using two complementary approaches. The first approach comprised surface sampling to investigate spatial changes in salinity, in which five samples were taken, with about 4 kg of soil being taken from the four corners and centre of a square with sides of 4 m (making five samples in total), using a grid design with 100 m intervals between the sampled squares. The subsamples were thoroughly mixed, and then a 3 kg sample of the mixture was transferred to the laboratory. In the second approach, in order to investigate variation in soil properties by depth, eight profiles (P1 – P8) were dug and described from four different pre-determined land use examples (a pistachio orchard abandoned due to water scarcity (P1 in Figure1 A), a more than 20-year-old pistachio orchard with a furrow irrigation system (P2, P3 and P4 in Figure1 A, plus P8 in Figure 1 B), farms of wheat and maize with a furrow irrigation system (P6 and P7 in Figure1 C), a five-year-old pistachio orchard with a drip irrigation system (P5 in Figure1 D)). Sampling was carried out at 10 cm intervals, with consideration soil genetic layers, to a depth of 1 m from the soil surface. In total, 128 samples from the upper 20 cm of sampling points, plus 80 samples from eight soil profiles, were collected for laboratory analysis. The soil horizons described in each profile and the soil profiles were classified following Keys to Soil Taxonomy (Soil Survey Staff, 2014). Additionally, ARC GIS software was used to design a grid based on 100 m intervals in the study area to collect soil samples and it was also used to map soil salinity spatial variability using inverse distance weighing. Furthermore, irrigation water sources, including three very deep wells (>200 m depth), were sampled in November 2018 for detailed laboratory analysis after several field measurements. The fresh surface water (EC < 1 dS/m) for mixing with saline water in drip irrigation is provided from a small river near to the study area. The mixing ratio varies between 20 to 50% depending on fresh water availability. In addition to annual rainfall approximately 200 to 300 mm irrigation water is used to sustain the pistachio and other crops.

Laboratory Analysis

All soil samples were air dried and passed through a 2 mm sieve in preparation for processing in the laboratory. ECe and pHe and pHsp were determined by using an EC/pH meter (Jenway 3540). Concentrations of Na^+ and K^+ in the saturated extracts were determined using a flame-photometer. Mg^{2+} and Ca^{2+} were measured by complexometry, and Cl^-, HCO_3^-, and CO_3^{2-} were measured using the titration method (Zhao et al., 2016). Soil saturation percentage was determined by oven drying the saturated soil paste. In-situ soil water content was measured using a portable soil moisture meter (PMS-714). The same methods were used to analyse the water samples. Particle size distribution was measured using the hydrometer method after the removal of soluble salts (Gee and Bauder, 1986). Rock fragments (with diameter >2 mm) were determined by weighing samples before and after sieving. Soil organic carbon (SOC) was measured using the wet combustion

method (Walkley and Black, 1934). $CaCO_3$ was determined using calcimetry analysis (Dreimanis, 1962) and gypsum was measured by using precipitation with acetone and reading the EC of the precipitated gypsum (USDA, 1954).

Calculation of Salinity and Sodicity indices

Table 2 summarizes the different indicators of salinity and sodicity for soil extracts and water, including the Sodium Adsorption Ratio (SAR), Magnesium Adsorption Ratio (MAR), Residual Sodium Carbonate (RSC), Residual Sodium Bicarbonate (RSBC), the Permeability Index (PI), and the Kelly Ratio (KR), which were calculated to assess the suitability of the soil and water for agricultural use. Also in order to compare soil quality changes with reference year, salinity and sodicity factors along with soil organic carbon used as soil quality parameters (Table 2).

Table 2. Salinity parameters with formulas, units, recommendation salinity parameters ranges for agricultural using and sources

Parameters	Symbol	Formula	Units	Limits	Water/Soil	References
Electrical Conductivity	EC	-	dS/m	0.25-3	Water	Fipps (2003)
Electrical conductivity (saturation extract)	EC	-	dS/m	0-4	Soil	Ayers and Westcot (1985)
Calcium	Ca^{2+}	-	meq/l	0-20	Both	Ayers and Westcot (1985)
Magnesium	Mg^{2+}	-	meq/l	0-5	Both	Ayers and Westcot (1985)
Sodium	Na^{+}	-	meq/l	0-40	Both	Ayers and Westcot (1985)
Sodium adsorption ratio	SAR	$SAR=\frac{Na^{+}}{\sqrt{Ca^{2+}+Mg^{2+}}}$	-	0-9	Soil	Ayers and Westcot (1985)
Sodium adsorption ratio	SAR	$SAR=\frac{Na^{+}}{\sqrt{Ca^{2+}+Mg^{2+}}}$	-	1-26	Water	Fipps (2003)
Bicarbonate	HCO_3^-	-	meq/l	0-10	Both	Ayers and Westcot (1985)
Chloride	Cl^-	-	meq/l	0-30	Both	Ayers and Westcot (1985)
Alkalinity/ Basicity	pH	-	-	6.5-8.4	Both	Ayers and Westcot (1985)
Magnesium adsorption ratio	MAR	$MAR=\frac{Mg^{2+}}{Ca^{2+}+Mg^{2+}}\times 100$	%	<50	Soil	Raghunath (1987)
Residual sodium carbonate	RSC	$RSC=(HCO_3^-+CO_3^{2-})-(Ca^{2+}Mg^{2+})$	meq/l	<2.5	Soil	CFC (1975)
Residual sodium bicarbonate	RSBC	$RSBC=(HCO_3^-+Ca^{2+})$	meq/l	<1.25	Soil	Eaton (1950)
Permeability index	PI	$PI=\frac{Na++\sqrt{HCO3-}}{Ca^{2+}+Mg^{2+}+Na^{+}}\times 100$	%	>6.5	Both	Doneen (1964)
Kelly ratio	KR	$KR=\frac{Na^{+}}{Ca^{2+}+Mg^{2+}}$	meq/l	<1	Both	Sundaray et al. (2009)

Statistical Analysis

A Completely Randomized Design (CRD) was used to investigate the effects of land-use type on soil salinity and Duncan's multiple range test (DMRT) performed to indicate the significance of the differences between the land use types. Also, a one sample t-test, was performed to statistically compare surface soil salinity (0-20 cm) between the sample and reference year (2002) and changes in water salinity compared to the reference year (2008). Comparison of the means and standard deviations of the measured parameters in different land use areas and different irrigation methods were carried out using SPSS software (Ver. 26, George and Mallery, 2019).

Results

Groundwater Depth and Variation in Quality

Three very deep wells, 200 m provide the irrigation water in the study region. In 2002 the groundwater table in study area was 50 meters and over time, due to the imbalance between low re-charges (precipitation) and high discharge (water pumping from the groundwater), the groundwater table fell to below 200 m. Comparisons of the irrigation water soluble ions measured in 2008 and 2018 are given in Table 3. According to the Wilcox irrigation classification diagram (based on EC and SAR) (USDA, 1954), the water used for irrigation was classified as very high salinity water, 6.31-7.08 dS/m (C4) that is not suitable for irrigation in the study area (Table 3). Regarding SAR, the water was classified as S1 and S2 (9.33-11.12), which refers to low to medium sodium levels that are hazardous in fine textured soils with high CEC. In drip irrigation the extracted groundwater is mixed with fresh water, resulting in a 50% reduction in the EC and SAR of drip irrigation water, compared to irrigation water sources used currently, and to 2008. The salinity hazard attributed to all water resources other than drip irrigation has increased significantly (7.27%, 14.38%, and 1.9%) relative to the average EC in 2008. However, the overall classification (C4) has remained constant and the sodium hazard (SAR) has reduced considerably (about 13% in Well No. 2 and about 1.59% in Well No. 3 Table 3).

In respect of concentrations of anions and cations in the analysed samples, considerable changes were observed relative to 2008. Concentrations of calcium and sulphate have increased, 17%–49% and 39%–51%,

respectively, in the case of furrow irrigation water sources (Wells 1, 2, and 3) while concentrations of sodium, magnesium, bicarbonate, and chloride have mainly decreased (between 1.5% and 18%) or show only a small increase (between 1.35% and 4.55%) in some cases (Table 3). Of course, in the case of drip irrigation water the concentrations of all cations and anions have decreased, between 2% and 68%, due to mixing with fresh water (Table 3), and the maximum decreases were associated with sodium (68%) and chloride (60%). One-sample t-test was used to compare the irrigation water salinity indicators and soluble ions in 2018 to the 2008 and the results showed significant difference for HCO_3^-compared (Table 3).

Table 3. Laboratory Analysis and the Salinity Indicators of the Irrigation Water Sources in 20 Nov. 2018 (groundwater depth 230 m) and 19 Oct. 2008 (groundwater depth 180 m)

Indicators	Na^+	K^+	Ca^{2+}	Mg^{2+}	HCO_3^-	CO_3^{2-}	Cl^-	SO_4^{2-}	Class
Furrow Irrigation water well 1	41.22	0.15	18.5	9.0	1.90	0	40.0	24.5	C_4S_2
Furrow Irrigation water well 2	39.03	0.15	23.5	11.5	1.90	0	45.0	23.9	C_4S_1
Furrow Irrigation water well 3	41.22	0.15	19.5	11.0	2.10	0	40.5	20.5	C_4S_2
Drip irrigation	12.67	0.09	11.5	4.5	2.25	0	17.5	7.5	C_4S_1
Averages of Reported results for 2008	39.27	-	15.8	11.0	2.30	0	44.4	19.37	C_4S_2
Changes of water salinity parameters relative to year 2008 %									
Indicators	Na^+	K^+	Ca^{2+}	Mg^{2+}	HCO_3^-	CO_3^{2-}	Cl^-	SO_4^{2-}	Class
Furrow Irrigation water well 1	3.78		17.09	-18.18	-17.39	0	-9.91	39.24	-
Furrow Irrigation water well 2	-1.74		48.73	4.55	-17.39	0	1.35	40.84	
Furrow Irrigation water well 3	3.78		23.42	0	-8.70	0	-8.78	51.11	
Drip irrigation	-68.10		-27.22	-59.09	-2.17	0	-60.59	-53.48	

Indicators	EC	pH	SAR	PI	KR
Furrow Irrigation water well 1	6.64	7.76	11.12	61.99	1.50
Furrow Irrigation water well 2	7.08	7.55	9.33	54.58	1.12
Furrow Irrigation water well 3	6.31	7.58	10.56	59.49	1.35
Drip irrigation	2.73	7.57	4.48	49.43	0.79
Averages of Reported results for 2008	6.19	7.64	10.73	61.73	1.47
Changes of water salinity parameters relative to year 2008 %					
Indicators	EC	pH	SAR	PI	KR
Furrow Irrigation water well 1	7.27	1.57	3.63	0.42	2.04
Furrow Irrigation water well 2	14.38	-1.18	-13.05	-11.58	-23.81
Furrow Irrigation water well 3	1.94	-0.79	-1.58	-3.63	-8.16
Drip irrigation	-55.9	-0.92	-58.25	-19.93	-46.26

The measured pH also decreased, (0.79% – 1.18%) in the water of Wells 2 and 3 and drip irrigation water, compared to the value reported for 2008. Furthermore, all other indicators of irrigation water quality such as SAR, PI, and PK decreased between 1.58% and 58.25% compared to 2008, except for Well No. 1.

Soil Salinity Profiles

Table 4 shows the soil horizons described in each profile and the classification of the studied profiles. The highest values of EC and the ions of Na^+, Ca^{2+}, Mg^{2+}, Cl^-, and SO_4^{2-} were measured in the surface layer of the profile located in an abandoned area (P1) but values decreased with depth (Table 4). The ECe and the Na^+, Ca^{2+}, Mg^{2+}, Cl^-, and SO_4^{2-} ions in profiles P2 and P3 were considerably lower (10% to more than 90%) than P1 but, they showed similar trends in profiles P5 and P6, which were located under pistachio trees and in maize cultivation using a furrow irrigation system. Irregular trends of variations were observed in the case of the other profiles (P3, P4, P5, P7, and P8) (Figure 1 and Table 4). Although, Na^+ was the predominant cation in all profiles, the predominant anion changed between SO_4^{2-} and Cl^- in different layers of the profiles (Table 4).

Soil Salinity Indicators

The mean values of the results of the soil laboratory analysis and the calculated salinity and sodicity indicators in the surface soil samples (0-20 cm) from four land uses are presented in Table 5. Comparison of the mean values of the measured ECe (in 2018) with those of 2002 indicated that it increased by at least two to more than eight times in areas with drip irrigation and abandoned areas. The consequences of increasing salinity are reduced yields and soil and water quality in the study area. Pistachio orchards yield 500 kg/ha up to 2000 kg/ha depending on productive year or non-productive year of pistachio.

In spite of the increase in the ECe values, the pH of different land use areas showed decreases between 0.2 and 0.5. The SOC in topsoil decreased by more than 2.5 times compared to the average content in 2008, although the calcium carbonate equivalent (CCE) increased (23% – 40%), irrespective of land use type, (Table 6).

Furthermore, the results obtained from a one sample t-test to compare the changes in soil salinity under two irrigation methods with 2002 showed that there was a significant difference between both irrigation methods and the year 2002 ($p < 0.05$).

Table 4. Morphological and physiochemical results of soil profiles.

Horizon	Depth cm	pHe	EC mS/cm	OC %	$CaCO_3$ %	Na^+	K^+	Ca^{2+}	Mg^{2+}	HCO_3^- (meq/l)	CO_3^{2-}	Cl^-	SO_4^{2-}	SP
P1: Loamy-skeletal, mixed, active, thermic Gypsic Haplosalids														
^Apyz	0-17	7.00	98	0.73	15	1120	5	497	272	1	0	1573	321	37
^ACyz	17-32	7.04	55	0.47	15	587	6	88	215	1	0	715	180	33
^C1z	32-42	7.44	27	0.27	14	396	32	15	40	1	0	261	221	27
2C2z	42-61	7.39	18	0.15	15	234	20	18	15	1	0	148	139	31
2C3z	61-105	7.43	12	1.32	14	168	13	34	12	1	0	86	140	24
P2: Fine-loamy, mixed, active, thermic Gypsic Haplosalids														
Apyz	0-35	7.95	34	1.01	13	496	16	43	89	11	0	303	330	37
Bw1	35-55	7.80	12	0.37	13	176	3	29	9	2	0	60	155	32
Bw2	55-85	7.69	7	0.27	16	92	1	20	13	1	0	35	89	37
Bk1	85-100	7.66	9	0.27	19	114	1	34	13	1	0	58	104	43
P3: Coarse-loamy, mixed, superactive, calcareous, thermic Typic Torrifluvents														
Ap1	0-20	7.81	11	0.49	14	129	2	41	33	2	0	67	136	30
Ap2	20-40	7.34	8	0.60	15	95	1	31	14	2	0	32	108	34
2O	40-55	7.60	15	>50	13	178	1	59	26	5	0	100	158	63
3C1	55-70	7.44	13	0.44	13	178	1	47	27	2	0	75	174	38
4C2	70-100	7.21	12	0.19	11	137	2	40	18	1	0	82	115	26
P4: Coarse-loamy, mixed, superactive, calcareous, thermic Typic Torriorthents														
Ap	0-30	7.66	5	0.30	11	73	1	17	7	1	0	29	68	26
AC	30-60	7.45	5	0.19	12	61	1	11	7	1	0	28	52	26
C	60-110	7.57	5	0.18	11	101	1	11	3	1	0	27	88	28
P5: Loamy-skeletal, mixed, active , calcareous, thermic Typic Torriorthents														
Ap	0-30	8.10	3	0.35	17	26	1	10	6	2	1	9	32	21
C1	30-43	7.22	17	0.27	18	179	1	50	50	1	0	139	140	31
C2	43-64	7.18	15	0.21	18	156	1	59	36	1	0	121	130	29
2BAb	64-100	7.22	14	0.14	20	147	1	65	28	0	0	132	109	49
P6: Fine-loamy, mixed, superactive, thermic Sodic Haplocambids														
Ap1	0-25	7.52	19	0.45	19	223	2	54	47	2	0	168	155	36
Ap2	25-50	7.53	15	0.38	20	184	2	46	35	7	0	127	132	37
AB	50-60	7.61	8	0.25	21	138	1	28	20	1	0	41	144	44
Bw1	60-80	7.44	8	0.20	21	127	1	28	10	0	0	34	131	40
Bw2	80-110	7.42	7	0.19	21	127	0	27	13	1	0	27	139	35
P7: Fine-loamy, mixed, superactive, thermic Sodic Haplocambids														
Ap	0-40	7.43	11	0.46	17	138	1	37	19	1	0	66	127	38.6
Bw	40-73	7.45	7	0.21	20	90	1	31	16	0	0	36	101	35.9
2C	73-80	7.37	8	0.18	21	86	1	41	5	0	0	41	91	32.8
3C	80-110	7.47	8	0.20	22	90	1	25	38	1	0	40	113	40.5
P8: Loamy-skeletal, mixed, superactive , calcareous, thermic Typic Torrifluvents														
Ap	0-30	7.50	11	0.28	12	146	1	27	6	0	1	66	113	27.3
2C1	30-51	7.40	12	0.15	12	141	1	44	10	0	1	83	112	21.8
3C2	51-67	7.23	11	0.24	12	119	1	44	17	0	1	82	99	24.6
4C3	67-110	7.45	9	0.19	13	88	1	34	15	1	0	55	82	24.1

The calculated indicators for soil salinity showed that, as for ECe, the highest values of SAR, MAR, RSBC, PI, and KR were observed in the abandoned land, which was followed by pistachio orchards, cultivated lands, and drip irrigation. SAR, RSBC, and KR indicators were very high in all types of land use, but MAR, RSC, and PI indicators were in the suitable range for all land uses. Concentrations of all anions and cations were very much higher than their applicable range for agricultural use (Table 5). The standard deviations for the measured parameters are very high in some cases, which demonstrates very high variability in the measured parameters (Table 5) and as expected, the standard deviation is low for the parameters that have low variability.

Considering the changes in ECe compared to 2002, during the 16 years to 2018 the largest increase has been observed in the area of abandoned land. In agreement with the increased means of ECe, the maximum values for the means of Ca^{2+}, Na^+, and Cl^- ion concentrations and SAR, MAR, RSBC, PI, and KR were all obtained in the abandoned land. Conversely, the minimum values of the parameters mentioned were determined in the land under drip irrigation.

Table 5. Comparison the means and standard deviations of some soil properties and salinity indicators in surface soil samples under different land-uses and different irrigation methods.

	OC	CCE	K^+	Ca^{2+}	Mg^{2+}	Na^+	Cl^-	HCO^-_3	CO_3^{2-}
	%					meq/l			
					Land use 1 Abandoned				
Mean	0.20	16.1	4.9	101.4	24.4	523.8	829.3	3.1	0.6
Std.dev	0.11	1.8	4.3	98.7	50.9	461.5	843.9	3.2	1.5
					Land use 2 Pistachio				
Mean	0.22	13.7	10.9	94.9	18.2	372.9	497.5	5.6	1.1
Std.dev	0.15	2.0	13.1	60.7	33.4	506.1	970.5	3.7	1.6
					Land use 3 Crop land				
Mean	0.19	17.5	2.2	73.4	15.0	205.2	35.1	1.1	0.6
Std.dev	0.09	1.1	1.8	46.2	8.3	129.4	49.4	0.3	0.5
					Mean of Total furrow land uses 1,2 and 3				
Mean	0.19	15.3	7.58	20.86	97.9	434.0	630.2	4.16	0.11
Std.dev	0.13	2.4	9.56	41.42	80.3	471.4	903.8	3.59	0.18
					Land use 4 Drip irrigation				
Mean	0.15	18.8	0.7	51.9	7.0	121.7	44.5	1.3	0.8
Std.dev	0.11	0.8	0.3	21.3	3.7	81.1	93.5	1.2	0.3
					Mean of the reported results for soil analyses 2002 (reference year)				
Mean	0.50	10.5							
Std.dev									

Continued	EC	pH	SAR	MAR	RSC	RSBC	PI	KR
	dS/m			%		meq/l	%	meq/l
					Land use 1 Abandoned			
Mean	57.3	7.3	74.3	16.4	-127.6	96.6	73.1	6.1
Std.dev	39.2	0.3	71.5	10.2	138.0	101.7	17.0	8.2
					Land use 2 Pistachio			
Mean	43.8	7.5	58.1	12.5	-109.6	59.0	64.7	5.3
Std.dev	40.6	0.4	106.2	18.6	43.2	56.2	18.8	13.0
					Land use 3 Crop land			
Mean	24.2	7.6	28.7	8.2	-86.0	37.3	68.8	2.3
Std.dev	16.8	0.22	10.8	8.6	21.8	2.0	5.8	0.5
					Mean of Total furrow land uses 1,2 and 3			
Mean	49.2	7.4	63.7	14.1	-117.6	76.5	68.7	5.5
Std.dev	39.8	0.4	88.0	14.8	99.1	82.5	17.8	10.5
					Land use 4 Drip irrigation			
Mean	17.4	7.6	22.9	10.8	-90.6	33.4	54.9	2.3
Std.dev	9.5	0.4	14.5	7.7	30.2	8.1	26.1	1.5
					Mean of the reported results for soil analyses 2002 (reference year)			
Mean	8.02	7.8						
Std.dev								

Table 6. One-sample t-test comparison of the means of salinity indicators and soluble ions in irrigation water samples to the reference year, 2008.

Water Sources	Test Value (Reference Year)	t	df	Sig. (2-tailed)	Mean Difference	Confidence Interval of the Difference 95%	
						Lower	Upper
EC	6.19	2.182	2	0.161	0.48667	-0.4730	1.4463
Na^+	39.27	1.671	2	0.237	1.22000	-1.9209	4.3609
Ca^{2+}	15.80	3.077	2	0.091	4.70000	-1.8724	11.2724
Mg^{2+}	11.00	-0.655	2	0.580	-0.50000	-3.7862	2.7862
HCO_3^-	2.30	-5.000	2	0.038*	-0.33333	-0.6202	-0.0465
CL^-	44.40	-1.614	2	0.248	-2.56667	-9.4074	4.2741
SO_4^{2-}	19.37	2.888	2	0.102	3.59667	-1.7620	8.9553
pH	7.64	-0.152	2	0.893	-0.01000	-0.2921	0.2721
SAR	10.73	-0.744	2	0.534	-0.39333	-2.6680	1.8813
PI	61.73	-1.398	2	0.297	-3.04333	-12.4079	6.3213
KR	1.47	-1.327	2	0.316	-0.14667	-0.6221	0.3288

Comparison of the mean values for types of land use (abandoned, pistachio furrow, and crop land), with the mean values of ECe in 2002 also showed they increased more than six times (Table 5). The results of univariate analysis of ECe under different land uses showed that there was a significant difference between the ECe of different land uses (sig = 0.004 and $p< 0.05$). Because the difference between land uses was significant, Duncan's multiple range test (DMRT) used to indicate the significance of the differences between the land use types. The results showed that the difference between the mean values of ECe for land use 1 (abandoned) compared to land use 2 (pistachio orchard) was not significant but the mean value of ECe in land use 4 (drip

irrigation) differed significantly from the ECe in abandoned and pistachio orchard land-uses. The mean of ECe in furrow irrigation on all land uses was intermediate (p=0.05, Figure 2). To assess the sustainability of the agriculture in the study area, we compared data obtained in 2018 with the data from soil and water analyses over the past 16 years (Tables 3 and 6). During these years ECe increased sharply, while pH and OC decreased, demonstrating that salinity is tending to increase, a trend which can cause soil degradation over time.

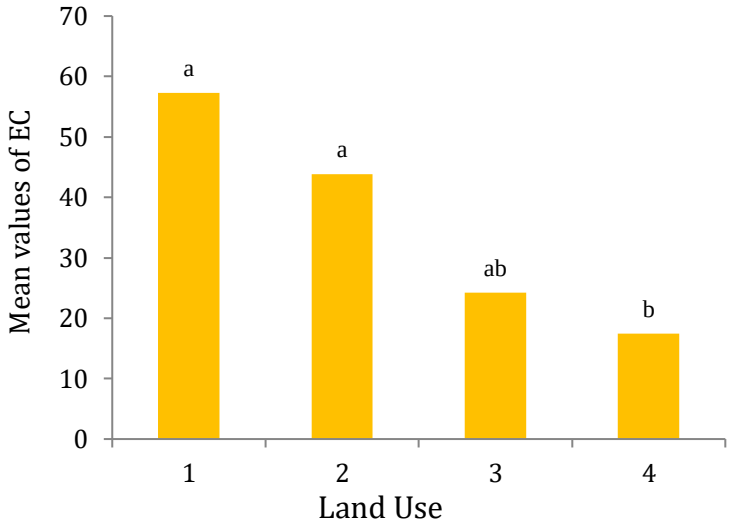

Figure 2. Comparison of EC mean values (128 samples, 0-20 cm) between different land uses by using Duncan's Post Hock test, at %5 level confidence, 2018. Land use 1: abandoned, 2: Pistachio, 3: Cultivated land, 4: Drip irrigation

Spatial variability in surface soil

Figure 3 illustrates the spatial variability of ECe (as the basic indicator of salinity) in the surface soil samples (upper 20 cm) of the pistachio orchards (Figure 1 A and B). All of the study area was classified as hypersaline soil (ECe > 4 dS/m). The highest values of ECe were observed at the middle of the orchard, which is under planted pistachio trees, followed by the abandoned area located on the downward slope that receives the runoff water which has passed through the higher saline area. The area with salinity class of 4–8 dS/m covers about 33% of the studied plot (~ 35 ha). About 20% of the land (21 ha) was found to contain 8–16 dS/m and about 15% of land (16 ha) was classified with salinity of 16–32 dS/m. Areas with salinity greater than 32 dS/m occupied about 8% to less than 1% of the land (Figure 3).

In addition, a comparison of the mean values of surface soil samples analysed for different land uses in 2018 with the mean of the reported results 2002 demonstrates that SOC decreased by at least two to more than three times in all land use types. While the CCE increased in all land use types (Table 5), this is possibly the result of the precipitation of carbonates from irrigation water or from CO_2 deposition in the soil solution. However, mean values of ECe in 2018 increased more than two to seven times in different land use types, compared to 2002. Statistical comparison of the measured ECe in surface soil samples, under both irrigation methods, was significant (p = 0.0, p= 0,023 and p< 0,05).

Discussion

Environmental characteristics

Classification of the study area as an arid region (based on AI classes) means that annual precipitation can only compensate for 13% of potential evapotranspiration (UNEP, 1997). The highest ET occurred in the summer season and exceeded more than 195.5 mm in July. Intensifying agricultural use of the land around the study area and land-use change from dry rangelands to cropping lands and extension of fruit tree plantations, the area that is pistachio cultivated and under drip irrigation is about 5 years old, has increased the need for water, but this can only be obtained from the groundwater. The amount of rainfall slightly exceeds evapotranspiration in three months only (January, February, and December) of each year. Lack of rainfall, along with increased abstraction of groundwater, has depleted groundwater, falling water table from 50 m under 200 m during 20 years, and reduced water quality (Tables 2 and 3). Furthermore, the existence of saline marl formations leads to excessive salinization of groundwater and an increased accumulation of surface salt by irrigation water, diffusion and also capillary movement (Table 3). The hot and arid climate combined with other environmental parameters demonstrate the unsuitability of the study area for agricultural purposes.

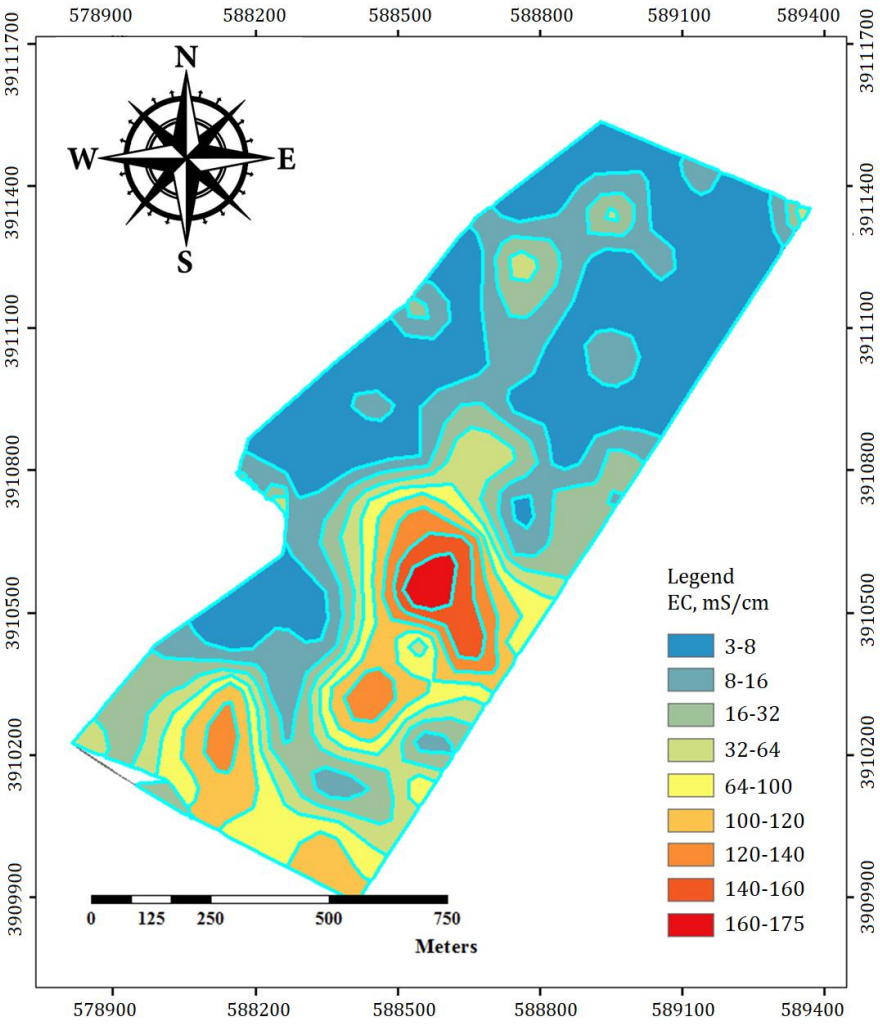

Figure 3. Map of spatial variability of surface soil salinity (0-20 cm) in the studied pistachio orchard, 21 Oct. 2019.

Water Quality

Based on the standards cited in Table 2, the EC of all the water sources was more than twice that of the standards defined by Fipps (2003). The concentrations of Ca^{2+} and Na^{+} in furrow irrigation water were close to the upper limits of the standards with maximum values of 23.5 meq/l for Ca^{2+} and 41.22 meq/l for Na^{+} (Table 3). Mg^{2+} concentration was double the standard limit for irrigation water (9 to 11.5 meq/l), but among the anions HCO_3^- was below the standard limit while the Cl^- concentration was much higher (40 to 45 meq/l) than the upper limit (30 meq/l) (Ayers and Wescot, 1985). Although the calculated SAR values were relatively high, all were in the standard range defined by Fipps (2003), not an acute water quality problem. The PI in the water was in the normal range (Doneen, 1964) but the KR index that should be <1 (Sundaray et al., 2009) was very high (Table 3). However, in the case of drip irrigation water, which is a mix of fresh and saline water, all of the measured and calculated parameters were within the standard range so using it for irrigation does not pose a serious risk.

Except for HCO_3^-, there was no significant difference in the salinity indicators and soluble ions of irrigation water samples taken from Wells 1, 2, and 3 compared to 2008 (Table 3 and 6). The values of EC, Na^{+}, and Mg^{2+} remained relatively constant (Sig > 0.05, Tables 6). However comparison of the concentrations of Ca^{2+}, SO_4^{2-} and Cl^- values with 2008 in Table 3 showed that Ca^{2+} and SO_4^{2-} concentrations have increased while Cl^- concentration has decreased. Dominant anion changed from chloride to sulfate compounds possibly due to the fall in the water table and changes in the composition of the water that is passing through the deeper geological formations. The increased Ca^{2+} and SO_4^{2-} may account for the small decrease in pH values caused by sulfate (Ahmed et al., 2013, Table 3). Evaporation, the water-rock reaction and the weathering of carbonate and silicate minerals are the main factors that changed the chemical quality of ground water in study area. Saline marl formations parent material could be the cause of the predominance of calcium and ground water salinity. Saline alluviums parent material could be the main source of chlorine ions in soil and water system. Calcium is largely responsible for water hardness and decreasing ground water quality. The amount of Ca^{2+}

increased in ground water compare to reference year due to water contact with certain rocks and minerals, especially limestone and gypsum. Also soil $CaCO_3$ increased compare to reference year but as it is insoluble in water so it does not cause hardness whereas calcium bicarbonate is readily soluble in water and causes the hardness of the water by dissolving Ca^{2+} ions in it. Although the contribution of groundwater to soil salinization depends on its depth from soil surface and groundwater near the soil surface contributes effectively to salinization, arid climate and high evaporation could change this fact. The depth of ground water in study area is near 230 m but still there is strong linear relation between groundwater and soil salinity due to high evaporation and capillary movement. In land use 1 this correlation is even stronger than other land uses due to lack of irrigation no water is added from above and interaction between ground water and soil salinity is more. Also, the capillary movement and the existence of texture discontinuity caused more salinity in this land use. In land use 4 the relationship is weak due to mixed irrigation water with fresh water. In land use 4 even if there was a good relationship between ground water and soil salinity it is gone because modified irrigation water is added from above. The result showed positive relationship between the increase in soil salinity and the increase in salinity in groundwater and irrigation water, and as a result, the amount of salinity ions. There is high connection between soil and water ion chemistry and the order of abundance of cations and anions in both soil and water was same (Na^{+}> Ca^{2+}> Mg^{2+}, Cl^{-}> SO_4^{2-}> HCO_3^{-}). Demir et al. (2009) stated that the results of studies of the depth and quality of groundwater should be made available to producers so that decisions can be made to maintain the stability of current minimum soil and water characteristics before the development of agriculture in affected areas.

Soil Quality

The studied soils were classified as soil orders Aridisols and Entisols in the first category of the American soil classification system (Table 4, Soil Survey Staff, 2014). The presence of salic and gypsic horizons is characteristic of arid zone soils and restricts many common agricultural uses. The layered sedimentary characteristic, also indicates that several discontinuities exist between parent materials in different soil layers, which may contain large amounts of coarse fragments which limit capillary movement of water within the soil. However, the main sources of water in the furrow irrigation system are hypersaline, the use of which will intensify soil salinization, as has been emphasized in various studies (Pereira et al. 2002, 2009; Qadir and Oster, 2004; Hoffman and Shalhevet, 2007). Considering the extent of study area (170 ha), the depth of irrigation water used (at least 200 mm), EC of irrigation water (7 dS/m) and high evapotranspiration (> 944 mm) a total amount of about 90 kg/ha salt is adding to soil. Regarding that drainage, runoff and leaching are very scarce due to limited rainfall and low slope almost all of the added salt accumulates in soils and due to increase in osmotic pressure restricts water availability for plants.

Dissolved salt variation had different pattern in soil profiles due to different land use, management factors, parent materials and irrigation methods. Table 4 shows the changes of anions and cations for soil profile horizons. This help us to determine the depth of salt accumulation, the mobility of anions and cations, the most mobile ions and the salt transfer agent, which can be the result of upward movement of salt by the capillary movement of groundwater or downward movement through leaching. Particle size distribution is a distinctive feature that separates soil families. Although the fine fraction of the studied soil is loamy, a large amount of coarse fragments shows a sharp difference between the profiles of the marl formation and those of the alluvial formation. These differences have led to higher salt accumulation in the finer particle size classes due to there being less leaching and high capillary rise. The worst case scenario happened in P1 in land use 1 with high amount of clay and without irrigation. Due to high specific surface of fine particle size more saline ions absorbed and the highest amount of EC was observed in this soil profile. The subsoil horizons have coarse texture and high gravel percentage than surface horizon. The maximum accumulation of soluble salts due to high evaporation and capillary rise has occurred near the soil surface that layers are fine texture and have low gravel percentage and after depth of 40 cm, values show a sharp decrease trend due to coarse texture and more gravel percentage. Numerous coarse and fine sediment layers and also high gravel percentage in the subsoil layers observed in profile 8, Land use 1. Against Continuous evaporation, the most amounts of soluble anions and cations were observed in the fine texture horizon which is located under the surface layers with coarse texture and high rate of salt leaching. Furrow Irrigation in P2 in land use 2 with fine loamy texture and without gravels has caused the maximum accumulation of anion chlorine and sodium cation to be about 10 to 20 cm deep instead of the soil surface. Of course, calcium and magnesium cations, as well as anion sulfate after chlorine and sodium, have significant amounts, which did not show many changes with depth and this is expected due to their lower solubility and mobility compared to sodium and chlorine. P 3 in land use 1 and P4 in land use 2 are similar in terms of soil characteristics and classification. Soil texture in both profiles is coarse loamy but in P3, lack of irrigation had led to accumulation of salts and increased salinity compared to P 4 and

the total amount of soluble cations and anions in P4 with coarse-textured soils and furrow irrigation is much less than in fine-textured soils. Profiles 6 and 7 inland use 3 with furrow irrigation are located on marl materials, but alluvial materials are also partially mixed. With Attention to fine soil texture, low gravel percentage, agricultural operations, such as soil plowing and irrigation, distribution of salts is mainly at the surface or in the depth of water infiltration. Profile 5 is located in land use 4 and due to continuous wetness by drip irrigation salt leached from surface layers and from a depth of 30 cm onwards a sharp increase in Sodium and chlorine concentrations are observed.

The results of Zhao et al. (2016) showed that there is a significant linear relationship between particle size distribution and soil salinity; different soil textures and their combination in the soil profile play an important role in soil salinity changes. Likewise, many studies of water in abandoned areas (Demir et al., 2009; Qian et al., 2017; Yu et al., 2018) have found that the highest accumulations of Na^+ and Cl^- occurred in the surface layers (Table 4), but they wash out easily with irrigation.

The soil organic carbon content had low amounts in all land uses and irrigation methods. Although OC amount changed slowly compare to reference year but it had large effect on soil physical properties that are important for soil fertility and therefore soil quality. Decreasing OC had negative effect on the soil pore structure, water dynamics, soil hydraulic properties and soluble ion movements and therefor soil quality decreased compare to reference year. Also, Loss of soil organic carbon content limited the soil's ability to provide nutrients for sustainable plant production and led lower yields compare to reference year. The potential effects of SOC in arable topsoil on soil PSDs and soil pore structure which may influence soil hydraulic properties, plant water supply and the physical conditions for root growth was mentioned in other studies (Fukumasu et al., 2022) .

To assess the interaction between different types of land use and changes in salinity, the relations between land use and management should be considered (Taghadosi and Hassanlou, 2017). The study area was under four different types of land use, and results of the analysis of representative soil pedons from each land use type are given in Table 4. The significant differences found showed that changes in land use affect variations in ECe and the result of Taghadosi and Hassanlou (2017) also showed that soils under different land uses have different degrees of sensitivity to salinity. Drip irrigation Land-use was distinctly different from abandoned land and pistachio orchards land uses (Figure 2). Among the land use types in the current study, the highest values of ECe, anions, and cations, were obtained from the abandoned land, which was followed by pistachio orchards, cropland, and drip irrigation produced the lowest values. Qian et al. (2017) examined the most important factors affecting salinity in different land uses and cover types and found that soil salinity in the region was most affected by groundwater salinity and vegetation cover; the least important factor was the distance to the nearest irrigation canal. Comparison of the means of the measured and calculated parameters of all land use types under furrow irrigation with those under drip irrigation revealed that furrow irrigation has led to more severe soil degradation than drip irrigation. This has been identified in many studies of the relationship between salinity and different irrigation management systems (Pereira et al., 2007; Devkota et al., 2015; Miao et al., 2015; Gebremeskel et al., 2018).

Sodium and chloride, which are predominant in all the water samples, were present in lower amounts in this irrigation system. By attention to ECe spot variation in the area under drip irrigation, the problem of salt movement from highly saline areas and therefore the spread of salinity through the whole study area is not observed attributed to water being sprayed near the roots. In drip irrigation, salinity increased between rows of plants due to lack of irrigation, but constant wetting of the area around the roots maintains lower salinity thereby saving water and increasing crop yield. Regardless of the salinity of the soil and the type of crop, there is a generally positive relationship between water use efficiency and the drip irrigation method, and applying drip irrigation in many cases increased crop production in hypersaline soils (Phene, 1986; Pasternak and De Malach, 1995; Burt and Isbell, 2005; Hillel, 2000; Dudley et al., 2008; Hanson et al., 2008; Minhas et al., 2020). It should be noted that, contrary to the findings of this study, there are studies that believe that furrow irrigation can be very efficient if additional measures, such as land levelling and improvements to soil structure, are undertaken (Pereira et al., 2002; Darouich et al., 2014).

It seems that convincing farmers to increase water quality by mixing saline water from wells with fresh water, replacing the furrow method with drip irrigation, as well as using ice to wash off surface salts and direct them out of the root zone will improve conditions.

Increasing salinity parameters (such as ECe, SAR, KR, RSCB) and generally high concentrations of cations and anions, compared to the normal range for agricultural use and 2008, indicate a progressive trend of degradation and decrease of soil quality in the study area. High values of SAR in some parts were associated with poor water infiltration and increased water loss by evaporation due to waterlogging. However, RSC

showed a reverse trend, with a negative value in all land uses, demonstrating that there no excess HCO_3^- or CO_3^{2-} anions are available to react with Na^+ and produce sodium carbonate, which causes a rapid increase of soil pH. The decrease in means of pH values compared to 2002 can be attributed to these negative values of RSC, which may be the result of the changing composition of irrigation water from sodium- and chloride-dominated to calcium- and sulfate-dominated water, due to the extraction of water from increasingly deeper levels.

Although all segments of the soils in the pistachio orchard were hypersaline, salt was not evenly distributed through the different locations. The uneven salt distribution is mainly due to the difference in the composition of parent materials; fine-textured saline and gypseous marls contain high accumulations of salt but less salt accumulates in gravelly alluvial deposits inter-bedded between eroded marls (Table 4). There is an area with extremely high salinity in the central part of the pistachio orchard that acts as a salt source for the surrounding areas, and needs to be managed to prevent the movement of salt into adjacent regions.

As mentioned above, saline soils and water have predetermined definitions, but these do not work for hypersaline soils and water. In arid regions such as Iran, hypersaline environments have existed for centuries and saline agriculture has been established on them for many years. In the study area, during the last 60 years, some areas of the land have been abandoned due to severe reductions in yield, but in other parts farmers still continue with saline agriculture as in the past, without special changes in management. Salinity tolerance pistachios is 8.4 dS/m and pistachio is sensitive spatially in early vegetative growth. With increasing the average salinity of the root zone (ECe) from 4 to 10 dS/m, the pistachio yield potential percentage decreases from 100 to 50. According to our studies, farmers will face severe declines in yield in all parts of the country in the near future, due to soil and water degradation, and if they do not change their ways they will be forced to abandon more areas. In many parts of the world that are located in arid regions and faced with problems of hypersalinity these definitions have been examined and land use type, land suitability, yield, and irrigation methods have been assessed or changed in order to develop the best management methods (Pasternak and De Malach, 1995; Hanson et al., 2008; Minhas et al., 2020). Changing land use in the study area is very difficult due to farmers' heavy dependence on their lands to meet their needs and, indeed, their very survival (Cheraghi, 2004; Taghadosi and Hassanlou, 2017).

Conclusion

The sustainability of hypersaline agriculture around the world is not very well studied. The availability of land suitable for agriculture in the studied arid region is scarce. Mismanagement of the saline and hypersaline soils and water accelerates the degradation and abandonment of agriculture. To improve the existing fragile conditions, and to develop adequate management methods, it is essential to characterize soils and irrigation water quality and to monitor changes. Due to the high sensitivity of the economic and social conditions in these arid regions, special management is needed to sustain agriculture. Using hypersaline water in hypersaline soils should be controlled precisely, using scientific approaches. Full characterization of the environment, soils, and water play the most important role in achieving suitable management approaches. Taking into consideration all the measured characteristics in the soils along with the calculated soil salinity indicators, all of the soils have become severely degraded, especially in the abandoned and pistachio plantation areas. Increasing salinity parameters (such as ECe, SAR, KR, RSCB) and generally high concentrations of cations and anions, compared to reference year indicate a progressive trend of soil. High values of SAR in soil were associated with poor water infiltration and increased water loss by evaporation due to waterlogging. The parent material of the soil are saline marl and alluviums therefore soil is contain considerable amount of saline ions. Although all segments of the soils in the pistachio orchard were hypersaline, salt was not evenly distributed through the different locations. The uneven salt distribution is mainly due to the difference in the composition of parent materials; fine-textured saline and gypseous marls contain high accumulations of salt but less salt accumulates in gravelly alluvial deposits inter-bedded between eroded marls. Among the types of land use, abandonment of the land was associated with the worst degradation while the best was drip irrigation water, pistachio plantations had the next highest level of salt accumulation after the abandoned areas. Maize and barley cultivation systems were less saline than pistachio plantations due to their use of more irrigation water. Land use change from dry rangelands to cropping lands has increased the need for irrigation water. The study area is located in arid climate which the amount of rainfall slightly exceeds evapotranspiration and irrigation water is mainly supplied by groundwater from deep wells. Using deep well irrigation led to sink water table, besides degrading the water quality. A large amount of residual salt in the soil becomes active and the high rate of evaporation caused soil salinization reaches the surface by capillary movement. The analysis result indicated a gradual change of salinity and chemical

composition of irrigation water from sodium- and chloride-dominated to calcium- and sulfate-dominated water, due to the extraction of water from increasingly deeper levels. All of the measured and calculated parameters for water sources were far from the standard range for irrigation and in the opposite in the case of drip irrigation water, which is a mix of fresh and saline water, all of them were within the standard range. Comparison of the means of the measured and calculated parameters of all land use types under furrow irrigation with those under drip irrigation revealed that furrow irrigation has led to more severe soil degradation than drip irrigation. The land use status quo intensifies the hazard of irreversible land degradation in the not so distant future. Possible solutions to this challenge, which would prevent rapid degradation, could include reconsidering the present forms of land use, limiting the further change of rangelands to conventional agriculture, and changing irrigation systems to drip irrigation. Removal of salt crusts from the soil surface at the end of the dry season may also help to reduce the hazard of salinization. Introducing other agricultural systems, such as greenhouse crops that have lower water requirement along with producing higher incomes for farmers, may be another solution. Providing management solutions appropriate to the conditions found in arid regions needs much more detailed studies.

References

Acar, B., Yilmaz, A.M., 2019. Irrigation techniques and plant growth strategies in salt-affected soils. *International Journal of Agriculture and Economic Development* 7(1): 1-9.

Ahmed, M.N., Abdel Samie, S.G., Badawy, H.A., 2013. Factors controlling mechanisms of groundwater salinization and hydrogeochemical processes in the Quaternary aquifer of the Eastern Nile Delta, Egypt. *Environmental Earth Sciences* 68: 369-394.

Al-Muaini, A., Green, S., Dakheel, A., Abdullah, A.H., Abou Dahr, W.A., Dixon, S., Clothier, B., 2019. Irrigation management with saline groundwater of a date palm cultivar in the hyper-arid United Arab Emirates. *Agricultural Water Management* 211: 123-131.

Ayers, R.S., Westcot, D.W., 1985. Water quality for agriculture. Food and Agriculture Organization of the United Nations. Vol. 29. Rome, Italy. Available at [Access date: 01.02.2022]: http://www.fao.org/docrep/003/t0234e/t0234e00.HTM

Bauder, T.A., Waskom, R.M., Davis, J.G., 2010. Irrigation water quality criteria, Colorado State University Extension. Fact Sheet No. 0.506. Available at [Access date: 01.02.2022]: https://extension.colostate.edu/docs/pubs/crops/00506.pdf

Bodaghabadi, M.B., Faskhodi, A.A., Salehi, M.H., Hosseinifard, S.J., Heydari, M., 2019. Soil suitability analysis and evaluation of pistachio orchard farming, using canonical multivariate analysis. *Scientia Horticulturae* 246: 528-534.

Bouaziz, M., Hihi, S., Chtourou, M.Y., Osunmadewa, B., 2020. Soil salinity detection in semi-arid region using spectral unmixing, remote sensing and ground truth measurements. *Journal of Geographic Information System* 12(4): 372-386.

Burt, C.M., Isbell, B., 2005. Leaching of accumulated soil salinity under drip irrigation. *American Society of Agricultural Engineers* 48 (6): 2115-2121.

Cheraghi, S.A.M., 2004. Institutional and scientific profiles of organizations working on saline agriculture in Iran. Prospects of saline agriculture in the Arabian Peninsula: Proceedings of the International Symposium on "Prospects of Saline Agriculture in the GCC Countries" 18–20 March 2001, Dubai, United Arab Emirates. Taha, F.K., Ismail, S., Jaradat, A. (Eds.). Amherst Scientific Publishers. pp.399–412.

Crane, J.C., 1978. Pistachio Tree Nuts. Avipublishing Co., Westport, California, USA.

Darouich, H.M., Pedras, C.M., Gonçalves, J.M., Pereira, L.S., 2014. Drip vs. surface irrigation: A comparison focussing on water saving and economic returns using multicriteria analysis applied to cotton. *Biosystems Engineering* 122: 74-90.

Demir, Y., Erşahin, S., Güler, M., Cemek, B., Günal, H., Arslan, H., 2009. Spatial variability of depth and salinity of groundwater under irrigated ustifluvents in the Middle Black Sea Region of Turkey. *Environmental Monitoring and Assessment* 158: 279-294.

Devkota, M., Gupta, R.K., Martius, C., Lamers, J.P.A., Devkota, K.P., Sayre, K.D., Vlek, P.L.G., 2015. Soil salinity management on raised beds with different furrow irrigation modes in salt-affected lands. *Agricultural Water Management* 152: 243-250.

Dion, P., Nautiyal, C.S., 2008. Microbiology of extreme soils. Springer Berlin, Heidelberg. 369p.

Doneen, L.D., 1964. Notes on water quality in agriculture published as a water science and engineering paper 4001. Department of Water Science and Engineering, University of California, Davis, Oakland, CA, USA.

Dreimanis, A., 1962. Quantitative gasometric determination of calcite and dolomite by using Chittick apparatus. *Journal of Sedimentary Research* 32: 520-529.

Dudley, L.M., Ben-Gal, A., Lazarovitch, N., 2008. Drainage water reuse: Biological, physical, and technological considerations for system management. *Journal of Environmental Quality* 37 (S5): S 25 – S 35.

Eaton, F.M., 1950. Significance of carbonates in irrigation waters. *Soil Science* 69 (2): 123–134.

Fipps, G., 2003. Irrigation water quality standards and salinity management strategies. Texas Cooperative Extension, Texas A&M University System. Available at [Access date: 01.02.2022]: https://twon.tamu.edu/wp-content/uploads/sites/3/2021/06/irrigation-water-quality-standards-and-salinity-management-strategies-1.pdf

Fukumasu, J., Jarvis, N., Koestel, J., Kätterer, T., Larsbo, M., 2022. Relations between soil organic carbon content and the pore size distribution for an arable topsoil with large variations in soil properties. *European Journal of Soil Science* 73(1): e13212.

Gebremeskel, G., Gebremicael, T.G., Ki, M., Meresa, E., Gebremedhin, T., Girmay, A., 2018. Salinization pattern and its spatial distribution in the irrigated agriculture of Northern Ethiopia: An integrated approach of quantitative and spatial analysis. *Agricultural Water Management* 206: 147–157.

Gee, G.W., Bauder, J.W., 1986. Particle-size Analysis. In: Methods of Soil Analysis. Part 2, Chemical and Microbiological Properties. Page, A.L., Miller, R.H., Keeney, D.R. (Eds.), 2nd Edition. Agronomy Monograph No. 9, American Society of Agronomy, Soil Science Society of America. Madison, Wisconsin, USA. pp. 383-411.

Geilfus, C.M., 2019. Chloride in soil: From nutrient to soil pollutant. *Environmental and Experimental Botany* 157: 299-309.

Geological Survey and Mineral Exploration of Iran, 2011. Geological map of Semnan, 1:100000, Sheet N0.:6661.

George, D., Mallery, P., 2019. IBM SPSS statistics 26 step by step: A simple guide and reference. 16th Edition. Routledge, New York, USA. 402p. .

Ghazali, M.F., Wikantika, K., Harto, A.B., Kondoh, A., 2020. Generating soil salinity, soil moisture, soil pH from satellite imagery and its analysis. *Information Processing in Agriculture* 7(2): 294-306.

Grattan, S., Zeng, L., Shannon, M., Roberts, S., 2002. Rice is more sensitive to salinity than previously thought. *California Agriculture* 56 (6): 189-198.

Hanson, B., Hopmans, J.W., Simunek, J., 2008. Leaching with subsurface drip irrigation under saline, shallow groundwater conditions. *Vadose Zone Journal* 7 (2): 810-818.

Hillel, D., 2000. Salinity management for sustainable irrigation. Integrating Science, Environment, and Economics. The international bank for reconstruction and development. The World Bank, USA. Available at [Access date: 01.02.2022]: https://documents.worldbank.org/en/publication/documents-reports/downloadstats?docid=687661468741583380

Hoffman, G.J., Shalhevet, J., 2007. Controlling salinity. In: Design and Operation of Farm Irrigation Systems (2nd Edition). Hoffman, G.J., Evans, R.G., Jensen, M.E., Martin, D.L., Elliot, R.L. (Eds.). American Society of Agricultural and Biological Engineers, St Joseph, MI, USA. pp. 160–207.

Köppen, W., 1931. Grundriss der Klimakunde. Walter de Gruyter, Berlin, Germany. 388p. [in German]

Miao, Q., Shi, H., Goncalves, J.M., Pereira, L.S., 2015. Field assessment of basin irrigation performance and water saving in Hetao, Yellow River basin: Issues to support irrigation systems modernisation. *Biosystems Engineering* 136: 102-116.

Minhas, P.S., 1996. Saline water management for irrigation in India. *Agricultural Water Management* 30: 1–24.

Minhas, P.S., Ramos, T.B., Ben-Gal, A., Pereira, L.S., 2020. Coping with salinity in irrigated agriculture: Crop evapotranspiration and water management issues. A*gricultural Water Management* 227: 105832.

Moazzzam Jazi, M., Seyedi, S.M., Ebrahimie, E., De Moro, G., 2017. A genome-wide transcriptome map of pistachio (Pistacia vera L.) provides novel insights into salinity-related genes and marker discovery. *BMC Genomics* 18: 627.

Mustafa, G., Akhtar, M.S., 2019. Crops and methods to control soil salinity. In: Salt Stress, Microbes, and Plant Interactions: Mechanisms and Molecular Approaches. Akhtar, M.S., (Ed.). Springer, Singapore pp. 237-251.

Newhall, F., Berdanier, C.R., 1996. Calculation of soil moisture regimes from the climatic record. Soil Survey Investigation Reports No. 46. Natural Resources Conservation Service, USDA, Lincoln, Nebraska, USA. Available at [Access date: 01.02.2022]: https://www.nrcs.usda.gov/Internet/FSE_DOCUMENTS/nrcs142p2_052248.pdf

Pasternak, D., De Malach, Y., 1995. Irrigation with brackish water under desert conditions X. Irrigation management of tomatoes (Lycopersicon esculentum Mills) on desert sand dunes. *Agricultural Water Management* 28(2): 121-132.

Pereira, L.S., Cordery, I., Iacovides, I., 2009. Coping with water scarcity: Addressing the challenges. Springer Dordrecht. 382p.

Pereira, L.S., Duarte, E., Fragoso, R., 2014. Water use: Recycling and desalination for agriculture. In: Encyclopedia of Agriculture and Food Systems. van Alfen, N.K. (Ed.), Vol. 5. Elsevier, San Diego, pp. 407–424.

Pereira, L.S., Gonçalves, J.M., Dong, B., Mao, Z., Fang, S.X., 2007. Assessing basin irrigation and scheduling strategies for saving irrigation water and controlling salinity in the upper Yellow River Basin, China. *Agricultural Water Management* 93(3): 109-122.

Pereira, L.S., Oweis, T., Zairi, A., 2002. Irrigation management under water scarcity. *Agricultural Water Management* 57(3): 175-206.

Phene, C.J., 1986. Automation. In: Trickle Irrigation for Crop Production: Design, Operation and Management. Nakayama, F.S., Bucks, D.A. (Eds.), Vol. 9, Elsevier, Amsterdam. pp.188-215.

Qadir, M., Oster, J.D., 2004. Crop and irrigation management strategies for saline-sodic soils and waters aimed at environmentally sustainable agriculture. *Science of the Total Environment* 323 (1-3): 1-19.

Qian, T., Tsunekawa, A., Masunaga, T., Wang, T., 2017. Analysis of the spatial variation of soil salinity and its causal factors in China's Minqin Oasis. *Mathematical Problems in Engineering* Article ID 9745264.

Raghunath, I.M., 1987. Groundwater, 2nd edn. New Age International (P) Limited Publishers, New Delhi, India. 570p.

Rhoades, J.D., Kandiah, A., Mashali, A.M., 1992. The use of saline waters for crop production. FAO irrigation and drainage Paper 48, The Food and Agriculture Organization of United Nations. Rome, Italy. 134p. Available at [Access date: 01.02.2022]: http://www.fao.org/3/a-t0667e.pdf

Soil Science Division Staff, 2017. Soil survey manual. C Ditzler, K Scheffe, and HC Monger (eds.). USDA Handbook 18. Government Printing Office, Washington, D.C.

Soil Survey Staff, 2014. Keys to soil taxonomy. 12rd Edition. United States Department of Agriculture (USDA), Natural Resources Conservation Service. Washington DC, USA. 360p. Available at [Access date: 01.02.2022]: https://www.nrcs.usda.gov/wps/PA_NRCSConsumption/download?cid=stelprdb1252094&ext=pdf

Sundaray, S.K., Nayak, B.B., Bhatta, D., 2009. Environmental studies on river water quality with reference to suitability for

agricultural purposes: Mahanadi river estuarine system, India – a case study. *Environmental Monitoring and Assessment*, 155(1-4): 227-243.

Taghadosi, M.M., Hasanlou, M., 2017. Trend analysis of soil salinity in different land cover types using Landsat time series data (case study Bakhtegan salt lake). *The International Archives of the Photogrammetry, Remote Sensing and Spatial Information Sciences* XLII-4/W4, 251–257.

Tanji, K.K., Kielen, N.C., 2002. Agricultural drainage water management in arid and semi-arid areas. FAO irrigation and drainage Paper 61, The Food and Agriculture Organization of United Nations. Rome, Italy. 190p. Available at [Access date: 01.02.2022]: http://www.fao.org/3/a-ap103e.pdf

UNEP, 1997. World Atlas of Desertification (2nd Edition), United Nations Environment Programme. Arnold, London. Available at [Access date: 01.02.2022]: https://wedocs.unep.org/20.500.11822/30300.

USDA, 1954. Diagnosis and improvement of saline and alkali soils. Agriculture Handbook No:60, United States Department of Agriculture (USDA), Washington DC, USA. 160p. Available at [access date: 01.02.2022]: https://www.ars.usda.gov/ARSUserFiles/20360500/hb60_pdf/hb60complete.pdf

Walkley, A., Black, I.A., 1934. An examination of the Degtjareff method for determining soil organic matter, and a proposed modification of the chromic acid titration method. *Soil Science* 37(1): 29-38.

Yang, M., Yanful, E.K., 2002. Water balance during evaporation and drainage in cover soils under different water table conditions. *Advances in Environmental Research* 6: 505–521.

Yu, P., Liu, S., Yang, H., Fan, G., Zhou, D., 2018. Short-term land use conversions influence the profile distribution of soil salinity and sodicity in northeastern China. *Ecological Indicators* 88: 79-87.

Zhao, Y., Feng, Q., Yang, H., 2016. Soil salinity distribution and its relationship with soil particle size in the lower reaches of Heihe River, Northwestern China. *Environmental Earth Sciences* 75: 810.

Eurasian Journal of Soil Science 2023, 12(1), 79 - 84

Eurasian Journal of Soil Science

Journal homepage : http://ejss.fesss.org

Evaluating the potential for multicropping in SE Kazakhstan : Double-cropping corn after winter triticale and winter oilseed rape

Tastanbek Atakulov, Sagynbai Kaldybayev, Kenzhe Yerzhanova *, Kuanysh Zholamanov, Ashirali Smanov, Ainash Seytzhan

Kazakh National Agrarian Research University, Almaty, Kazakhstan

Article Info

Received : 12.02.2022
Accepted : 09.10.2022
Available online : 12.10.2022

Author(s)

T.Atakulov
S.Kaldybaev
K.Yerzhanova *
K.Zholamanov
A.Smanov
A.Seytzhan

* Corresponding author

Abstract

Double cropping is not presently a common practice in Kazakhstan. The long-term climate averages, however, suggest that the practice should be possible in the most southern portions of the country. The study described herein represents the first simultaneous evaluation of silage and grain corn crops sowing in SE Kazakhstan. Germplasm was chosen such that physiological maturity could theoretically be reached if seeded following winter triticale and winter oilseed rape. Results indicate that, considering the effect of climate change, it has been determined that even if the silage and grain yields are low, the corn grown as a second product has reached the harvest maturity and the product can be obtained. These results clearly demonstrate that with the appropriate selection of cultivar and watering possibility, there is a seeding date window where silage and grain corn can be expected to reach physiological maturity as a double crop in SE Kazakhstan.

Keywords: Double cropping, corn, Kazakhstan, winter triticale, winter oilseed rape.

Introduction

In agriculture, multiple cropping or multicropping is the practice of growing two or more crops in the same piece of land during one year, instead of just one crop. When multiple crops are grown simultaneously, this is also known as intercropping. Multiple cropping refers to growing two crops on the same field during the same year. One method of multiple cropping is double cropping, which is when one crop is grown after the first crop is harvested (Borchers et al., 2014). Compared with mono-cropping, double-cropping used climatic, land, labor, and equipment resources more efficiently and produced more total grain (Crabtree et al., 1990). This system involves the harvesting of one species followed immediately by the planting of another. Double-cropping increases the amount of time land is used for crop production and can increase potential profit (Pullins et al., 1997).

Double cropping system is interesting worldwide attentions both in developed and in developing countries (Lamessa et al., 2015). It will also advantageous for the increase of annual production (Yamane et al., 2016). Farmers would have improved demand for their products, double cropping would guarantee the land was not bare and exposed to erosive forces between crops (Moore and Karlen, 2013). However, the economic return per unit area and time are the main considerations for acceptances of a certain cropping system and yield is the primary agronomic parameter in any category of cropping system (Lamessa et al., 2015). Besides the direct benefit for crop production by increasing the number of harvest and the amount of biomass extracted, multiple cropping can improve the functioning of agricultural systems and reduce the environmental consequences sometimes associated with crop production (Gaba et al., 2015).

Agriculture plays an essential role in Kazakhstan's economic, social and environmental development. Once considered the breadbasket of the Soviet Union, Kazakhstan still suffers from the effects of agricultural and

: https://doi.org/10.18393/ejss.1187439
: http://ejss.fesss.org/10.18393/ejss.1187439
Publisher : Federation of Eurasian Soil Science Societies
e-ISSN : 2147-4249

environmental mismanagement during the Soviet era. Over a third of Kazakhstanis' livelihoods depend directly or indirectly on the country's extensive rangelands for food, fodder, fuel and medicinal plants. Double-cropping system is not common product in Kazakhstan. Some farmers in Kazakhstan, in the Southeast Region, who used to plant milling wheat or barley as a first crop and corn as a second crop, want to double cropping to corn instead of mono-cropping. After Russian – Ukrainian war, due to crisis of cereals increased in the world, many farmers in SE Kazakhstan want to harvest the second-crop corn. Agro-climatic conditions of the SE Kazakhstan, where irrigated agriculture is developed, quite allows for an effective use of irrigated land throughout the year. However, in practice, farmers and peasant farms do not use these opportunities. Thus, after harvesting of early spring crops and winter wheat there is quite a lot of time (90-120 days) for cultivation of intermediate crops.

As in the whole world, Kazakhstan is one of the countries affected by climate change. Kazakhstan's hydro-meteorological service has observed a temperature increase in Kazakhstan over the last seventy years of weather observations. They observed not only a yearly average increase but also an increase in temperature during each season of the year. The average annual temperature increase is about 0.27°C every ten years. The highest increase has been observed for the autumn months (0.32°C/decade), the lowest in the summer months (0.2°C/decade) (Islyami et al., 2020). So far, there has been no scenario-based research on climate-change effects on agriculture in Kazakhstan.

To date, much of the information on the environmental, agronomic, and physiological constraints associated with double cropping has come from studies conducted in the US, South America, Turkey and China. We are unaware of any study that has explored the potential for double cropping for grain in SE Kazakhstan during the changing climate. The research described herein represents the first evaluation of the potential for double cropping in continental climate of SE Kazakhstan.

As the major limiting factor to double cropping in SE Kazakhstan is likely to be the interaction of seeding date and relative maturity for the summer seeded crop, this research aimed to evaluate the permissive window in late summer for seeding silage and grain corn crops. We hypothesized that, if the attainment of physiological maturity is primarily governed by seeding date, relative maturity, and their interaction, then with the appropriate selection of germplasm, silage and grain corn crops have the potential to be seeded as a double crop in SE Kazakhstan.

Material and Methods

Site and soil

The experiment was carried out on a light chestnut soil (65% sand, 2% silt and 33% clay fraction and soil textural class was named as Sandy clay loam. The pH was 7.2, soil organic matter content was 2,52%, $CaCO_3$ content was 5.80%, total N was 0.122%. Available nitrogen ($NH_4 + NO_3$) was 125 mg kg^{-1}, available phosphorus was 31 mg kg^{-1} and available potassium was 311 mg kg^{-1}), the field experiment was located on peasant farm " Bayserke Agro LLP farm " of Almaty Province of SE Kazakhstan 15 km from the city of Almaty, in the village of Ili Bayserke rafona Almaty region, Kazakhstan (Figure 1).

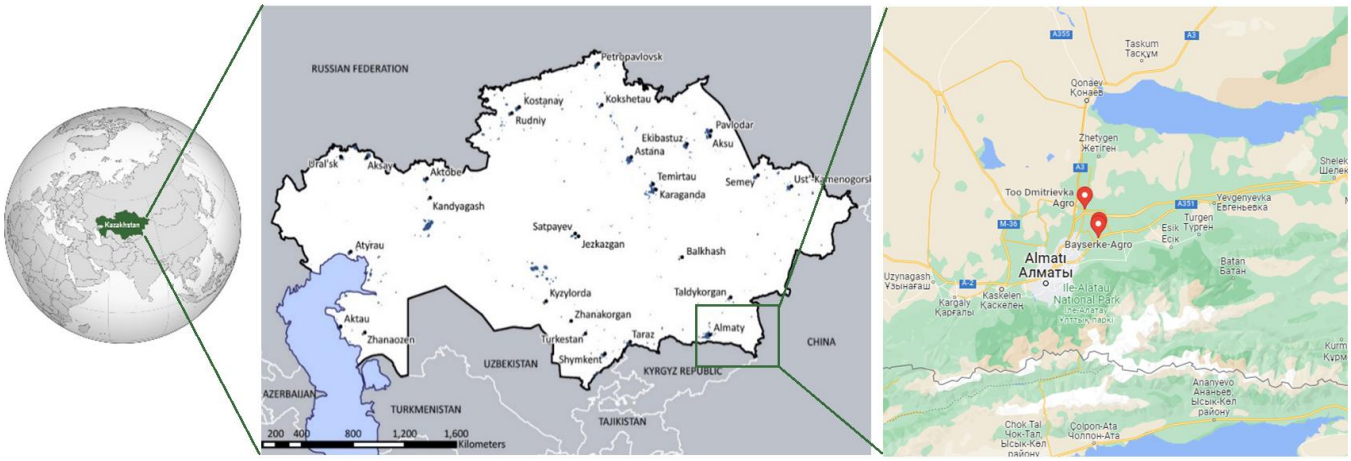

Figure 1. Study area

Climatic conditions

In study field, the summers are warm, dry, and mostly clear and the winters are freezing, snowy, and partly cloudy. Based on the Köppen climate classification system, the study area is classified as warm continental

climate/humid continental climate (Köppen, 1931) with mild winters and long hot summers, with a daily average air temperature of 19-20°C and an annual precipitation of 215 mm at the experimental site.. The altitude of the study site is 850 m. The average temperature is –7°C in January and +28°C in July. Over the course of the year, the temperature typically varies from -11°C to 30°C and is rarely below -18°C or above 34°C. The hot season lasts for 3.8 months, from May 25 to September 18, with an average daily high temperature above 23°C. The hottest month of the year in Almaty is July, with an average high of 29°C and low of 16°C. The cold season lasts for 3.4 months, from November 24 to March 5, with an average daily high temperature below 4°C. The coldest month of the year in Almaty is January, with an average low of -10°C and high of -2°C (Figure 2).

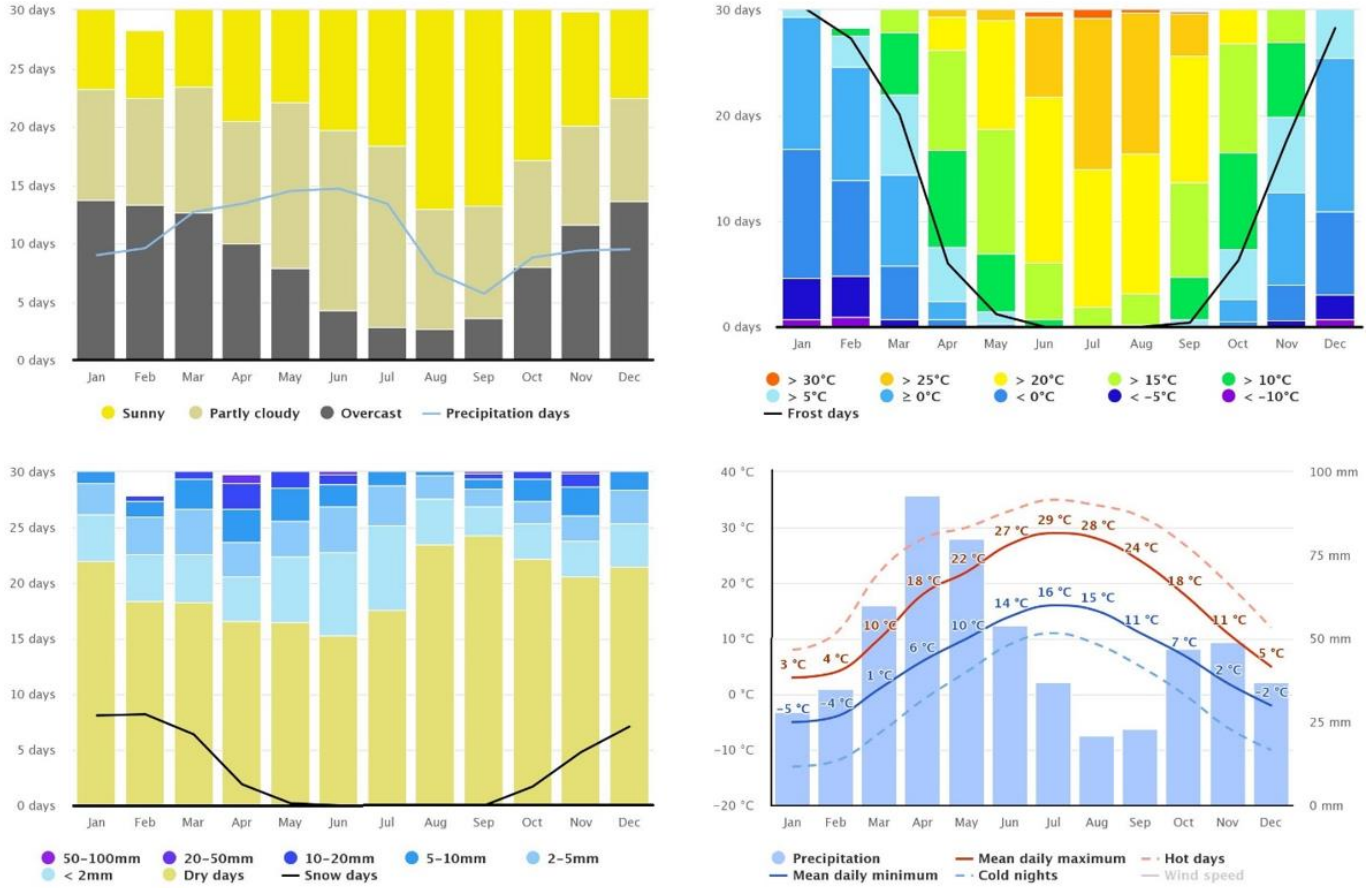

Figure 2. Climate conditions of the experimental area, Almaty, SE Kazakhstan

Experimental design

The experiment was carried out in "Bayserke Agro LLP" farm of Almaty Province of SE Kazakhstan. The trial started in September 2020 and consisted of 4 different double-cropping. These included winter barley (*Hordeum vulgare* L.), winter triticale (*Triticosecale*) and winter oilseed rape (*Brassica napus* L.), and ranged from monocultures to double corn crops for silage and grain (Table 1).

Table 1. Experimental design

No		The first crop	Second crop corn
1	WB	Monoculture winter barley	-
2	WT + SC	Winter triticale for grain	Silage corn
3	WT + GC	Winter triticale for green mass	Grain corn
4	SR + SC	Winter oilseed rape for grain	Silage corn
5	SR + GC	Winter oilseed rape for green mass	Grain corn

Practical constraints required the field trial design to be a split-plot design with one level of splitting. Fifteen experimental plots of 300 m^2 area (30m x 10m) separated by 1 m cement barriers were set in completely randomized block design with five treatments and three replications. The husbandry treatments were main plots; the crop rotations were sub-plots split within main plots. Sub-plot size was 15 m×9 m (plus 1m uncropped margin to avoid interactions due to soil movement). All crops (barley, triticale and seed rape) received 100 kg N ha^{-1} and 80 kg P ha^{-1} each year. The sources of fertilizers used were urea 46% N and double superphosphate 47% P_2O_5. Fertilizer applications are indicated in Table 2.

Table 2. Fertilizer applied to the different crops during the experiment

Crop	WB	WT + SC	WT + GC	SR + SC	SR + GC
	Winter barley	**Winter triticale**	**Winter triticale**	**Winter oilseed rape**	**Winter oilseed rape**
Fertilizer type	Double superphosphate (47% P2O5) Urea (46% N)	Double superphosphate (47% P2O5) Urea (46% N)	Double superphosphate (47% P2O5) Urea (46% N)	Double superphosphate (47% P2O5) Urea (46% N)	Double superphosphate (47% P2O5) Urea (46% N)
Fertilization rate	80 kg P_2O_5 ha^{-1} 100 kg N ha^{-1}	80 kg P_2O_5 ha^{-1} 100 kg N ha^{-1}	80 kg P_2O_5 ha^{-1} 100 kg N ha^{-1}	80 kg P_2O_5 ha^{-1} 100 kg N ha^{-1}	80 kg P_2O_5 ha^{-1} 100 kg N ha^{-1}
Fertilization date	10.Sep 2020 for DSP 10 Apr 2021 for Urea	10.Sep 2020 for DSP 10 Apr 2021 for Urea	10.Sep 2020 for DSP 10 Apr 2021 for Urea	10.Sep 2020 for DSP 10 Apr 2021 for Urea	10.Sep 2020 for DSP 10 Apr 2021 for Urea
Crop		**Silage corn**	**Grain corn**	**Silage corn**	**Grain corn**
Fertilizer type	-	Superphosphate (42% P2O5)	Superphosphate (42% P2O5)	Superphosphate (42% P2O5)	Superphosphate (42% P2O5)
Fertilization rate	-	40 kg P_2O_5 ha^{-1}	40 kg P_2O_5 ha^{-1}	40 kg P_2O_5 ha^{-1}	40 kg P_2O_5 ha^{-1}
Fertilization date	-	30 July 2021	20 June 2021	30 July 2021	20 June 2021

The sowing was done after the main crop monoculture winter barley was harvested in 25 May 2021, winter triticale was harvested in 25 May 2021 and winter seed rape was harvested in 26 May 2021. Grain corn was planted on 27 May 2021 and silage corn was planted on 08 July 2021 using a precision plot planter with variable seeding rate and row spacing capability. While 70 cm between rows were used in pure corn plantings, corn grain was planted 8 cm soil depth. Sowing and harvest dates, sowing rates and cultivar names per crop in each crop sequence are provided in Table 3.

Table 3. Sowing and harvest dates, sowing rate and cultivar name for each crop included in each sequence for the trial

Crop	WB Winter barley	WT + SC Winter triticale	WT + GC Winter triticale	SR + SC Winter oilseed rape	SR + GC Winter oilseed rape
Sowing date	25 Sep 2020	25 Sep 2020	25 Sep 2020	25 Sep 2020	25 Sep 2020
Sowing rate	120 kg ha^{-1}	120 kg ha^{-1}	120 kg ha^{-1}	20 kg ha^{-1}	20 kg ha^{-1}
Cultivar name	Zhuldyz	Taza	Taza	Kuban	Kuban
Harvest date	25 May 2021	25 May 2021	25 May 2021	26 May 2021	26 May 2021
Crop		**Silage corn**	**Grain corn**	**Silage corn**	**Grain corn**
Sowing date	-	08 July 2021	27 May 2021	08 July 2021	27 May 2021
Sowing rate	-	35 kg ha^{-1}	35 kg ha^{-1}	35 kg ha^{-1}	35 kg ha^{-1}
Cultivar name	-	Kazakhstan 43TB	Kazakhstan 43TB	Kazakhstan 43TB	Kazakhstan 43TB
Harvest date	-	10 Oct 2021	25 Sep 2021	10 Oct 2021	25 Sep 2021

With the planting 40 kg/ha pure phosphorus (superphosphate 42% P_2O_5) was used. In single corn and mixed planting, when the corn became 30 - 40 cm, ammonium sulfate fertilizer was added at a rate of 50 kg/ha pure nitrogen. After the last fertilization, weeds removal and covering roots with soil were carried out. Crop management not involving the treatments (e.g. seed date, application of herbicides or insecticides) was the same in all plots of a single crop and according to standard farm practice. Straw remained on the plots. At maturity, an area of 15×9 m was combine harvested and yield was standardized to t ha^{-1} based on the moisture content of a grain or seed subsamples and biomass of plants. The harvest stage of forages was done according to the dough period of corn. In the field experiment of the study; plant height, green herbage yield, hay yield, and protein ratios were determined.

Results and Discussion

The yield and yield component results of the plants grown as the first crop in the experiment are given in the Table 3. According to the results obtained, the yields of winter barley, winter triticale and winter oilseed rape were determined to be 5.76 t ha^{-1}, 6.38 t ha^{-1} and 2.52 t ha^{-1}, respectively (Table 3). In European countries, the product yield of winter barley is around 3.75 t ha^{-1}. In European countries, the highest winter barley yield is in Belgium with 7.82 t ha^{-1}, and the lowest winter barley yield is in Estonia with 1.30 t ha^{-1} (Garstang et al., 2010). There are many factors affecting the production of winter barley, such as climatic factors, barley variety and cultural practices (tillage, weed control, fertilization etc). On the other hand, it can be said that the yield results obtained for the winter barley from this study are above the European average. The yield of winter

triticale in this study was 6.38 t ha^{-1}, which is much higher than the yield results (1.59-2.43 t ha^{-1}, Sukhanberdina et al., 2022) obtained from studies of different triticale varieties grown in Kazakhstan conditions. In this study, the yield of winter oilseed rape was determined to be 2.52 t ha^{-1}. Similarly, the yield of winter oilseed rape was determined as 1.62-2.64 t ha^{-1} in Türkiye by Başalma (2004).

Table 3. At harvest yields of first crops

Plants	Plant Height (cm)	Biomass yield (t ha^{-1})	Grain or seed yield (t ha^{-1})	Yield of green mass, t/ha	Dry matter of yield (t/ha)	Crude Protein Content (%)
Winter barley	97	57.0	5.76	-	28.9	15
Winter triticale	110	64.8	6.38	64.8	31.4	13
Winter oilseed rape	118	67.6	2.52	67.6	32.1	30

The yield and yield component results of the silage corn as the second crop in the experiment are given in the Table 4. It was determined that the yield and plant height of silage corn grown as the second crop after oilseed rape (SR+SC) was higher than the silage maize grown after triticale (WT+SC). On the other hand, no difference was determined between the crude protein contents of the trials. In this study, it was determined that the height of the silage corn in the WT+SC and SR+SC trials varied between 70-80 cm, the yield of herbage varied between 9.4-10.5 t ha^{-1}, the dry yield between 4.6-4.8 t ha^{-1}, and crude protein content 6%. When compared with other studies, it was determined that the yield of silage corn obtained in this study was very low compared to the yield results obtained from other studies (Güneş and Acar, 2016; Güneş and Öner, 2019). Öztürk and Orak (2020) determined that the average plant height of different silage corn varieties (Calcio, Colonia, DK-743, Mas 74G, Pasha) plant height was 237 cm, herbage yield is 74.65 t ha^{-1} and dry yield was 6.83 t ha^{-1} in Türkiye. There are many factors affecting yield and quality in silage corn production. Geographical and climatic conditions (temperature, photoperiod and exposure time), cultural processes (planting time, harvest period, plant density and irrigation conditions), genetic characteristics of the variety are the factors that determine yield and quality (Cox et al., 1994). In this study, it was determined that some ecological factors limit the product yield, despite the growing of silage corn in Almaty ecological conditions.

Table 4. At harvest, silage corn yield and yield quality

Trials	Plant Height (cm)	Herbage yield (t ha^{-1})	Dry yield (t ha^{-1})	Crude Protein Content (%)
WT + SC	70	9,4	4,6	6
SR + SC	80	10,5	4,8	6

The yield and yield component results of the grain corn as the second crop in the experiment are given in the Table 5. It was determined that the yield and plant height of grain corn grown as the second crop after oilseedrape (SR+SC) was higher than the silage maize grown after triticale (WT+SC). On the other hand, no difference was determined between the crude protein contents of the trials. In this study, it was determined that the height of the grain corn in the WT+GC and SR+GC trials varied between 230-235 cm, the yield of biomass varied between 70.2-71 t ha^{-1}, grain yield 7.3-7.4 t ha^{-1}, the dry yield between 36-36.5 t ha^{-1}, and crude protein content 10%. When compared with other studies, it was determined that the yield of grain corn obtained in this study was very low compared to the yield results obtained from other studies (Bozkalfa et al., 2004; Idikut et al., 2012). Just like in silage corn grown as a second crop, the low yield of corn grown as a second crop may be due to the non-optimal geographical conditions. On the other hand, even if the geographical and climatic conditions are not optimal, corn for grain can be grown as a second crop in Almaty, SE Kazakhstan climatic conditions. Kazakhstan has a continental climate and therefore cold winters and hot summers are observed. Agricultural areas in SE Kazakhstan experience a shortage of precipitation and climate change scenario shows the negative consequences of global warming in SE Kazakhstan. And also, climate change in SE Kazakhstan affects both the amount of water, water quality, corn yield and affect new technology adaptation. Even if the yield is low in changing climatic conditions, maize can be grown and yield can be obtained in SE Kazakhstan, even if it is low. However, production planning carried out in suitable climatic conditions with most productive varieties should be made by analyzing corn varieties and application areas. Water use efficiency in corn production could be increased by better water management using new irrigation and agronomic techniques.

Table 5. At harvest, grain corn yield and yield quality

Trials	Plant Height (cm)	Biomass yield (t ha-1)	Grain or seed yield (t ha^{-1})	Dry matter of yield (t ha^{-1})	Crude Protein Content (%)
WT + GC	230	70,2	7,3	36,0	10
SR + GC	235	71,0	7,4	36,5	10

In summary, the results of this research demonstrate that double cropping following winter triticale and winter oilseed rape are already possible in SE Kazakhstan. While season length still represents the most significant limitation to double cropping in SE Kazakhstan, our results clearly demonstrate that with the appropriate selection of variety or cultivar, there is a seeding date window where silage or grain corn can be expected to reach physiological maturity as a double crop.

Acknowledgments

Funding for this research was provided by Kazakhstan Agricultural Ministry (Project No. IRN: AP09259400 Selection of non-traditional crops for intensive use of irrigated lands and creation of green conveyor depending on the bioclimatic potential of growing areas). We would like to thank "Bayserke Agro LLP" for in-kind contribution and anonymous reviewers for their constructive comments.

References

Başalma, D., 2004. Comparision of yield and yield components of winter rapeseed (Brassica napus ssp. oleifera L.) cultivars in Ankara conditions. *Tarım Bilimleri Dergisi* 10 (2): 211-217. [in Turkish]

Borchers, A., Truex-Powell, E., Wallander, S., Nickerson, C., 2014. Multi-Cropping Practices: Recent Trends in Double Cropping, USDA-ERC, Economic Information Bulletin Number 125. Available at [Access date : 12.02.2021]: https://www.ers.usda.gov/webdocs/publications/43862/46871_eib125.pdf?v=36.6

Bozkalfa, M.K., Eşiyok, D., Uğur, A., 2004. Determination of yield quality and plant characteristic of some sweet corn (Zea mays L. var. saccharata) varieties as main and second crop in Ege Region. *Ege Üniversitesi Ziraat Fakültesi Dergisi* 41(1):11- 19.

Cox W.J., Chemey, J.H., Chemey, D.J.R., Pardee, W.D., 1994. Forage quality and harvest index of corn hybrids under different growing conditions. *Agronomy Journal* 86(2): 277-282.

Crabtree, R.J., Prater, J.D., Mbolda, P., 1990. Long-term wheat, soybean, and grain sorghum double-cropping under rainfed conditions. *Agronomy Journal* 82(4): 683-686.

Gaba, S., Lescourret, F., Boudsocq, S., Enjalbert, J., Hinsinger, P., Journet, E.P., Navas, M.L., Wery, J., Louarn, G., Malézieux, E., Pelzer, E., Prudent, M., Ozier-Lafontaine, H., 2015. Multiple cropping systems as drivers for providing multiple ecosystem services: from concepts to design. *Agronomy for Sustainable Development* 35: 607–623.

Garstang, J.R., Spink, J.H., Suleimenov, M., Schillinger, W.F., McKenzie, R.H., Tanaka, D.L., Ceccarelli, S., Grando, S., Paynter, B.H., Fettell, N.A., 2010. Cultural Practices: Focus on Major Barley-Producing Regions. In: Barley. Ulrich, S.E. (Ed.). John Wiley & Sons, Ltd. pp.221-281.

Güneş A, Acar R 2006. The determination of growing possibilities of silage hybrid maize cultivars as second crop under Karaman ecological conditions. *Selçuk Tarım ve Gıda Bilimleri Dergisi* 20(39): 84-92. [in Turkish]

İdikut, L., Nesrin, S., Kara, A., 2012. Determination of some yield components with grain starch ratios of second crop corn for grain growing. *KSÜ Doğa Bilimleri Dergisi* 16(1): 8-15. [in Turkish]

Islyami, A., Aldashev, A., Thomas, T.S., Dunston, S., 2020. Impact of climate change on agriculture in Kazakhstan. *Silk Road: A Journal of Eurasian Development* 2(1): 66–88.

Köppen, W., 1931. Grundriss der Klimakunde. Walter de Gruyter, Berlin, Germany. 388p. [in German]

Lamessa, K., Sharma, J.J., Tessema, T., 2015. Influence of cowpea and soybean intercropping pattern and time of planting on yield and gross monetary value of sorghum. *Science, Technology and Arts Research Journal* 4(3): 38-46.

Moore, K.J., Karlen, D.L., 2013. Double cropping opportunities for biomass crops in the north central USA. *Biofuels* 4(6): 605–615.

Öner, F., Güneş, A., 2019. Determination of silage yield and quality characteristics of some maize (Zea mays L.) varieties. *Journal of Tekirdag Agricultural Faculty* 16(1): 42-50. [in Turkish]

Öztürk, Y., Orak, A., 2020. Determination of the yield and yield components of some corn varieties as a second crop in Tekirdag conditions. Kahramanmaraş *Sütçü İmam Üniversitesi Tarım ve Doğa Dergisi* 23 (6): 1634-1646. [in Turkish]

Pullins, E.E., Myers, R.L., Minor, H.C., 1997. Alternative crops in double-crop systems for Missouri. Outreach & Extension, University of Missouri, Colombia G40090. USA. Available at [Access date: 12.02.2021]: https://extension.missouri.edu/media/wysiwyg/Extensiondata/Pub/pdf/agguides/crops/g04090.pdf

Sukhanberdina, L.K., Tulegenova, D.K., Kaliyeva, L.T., Turbayev, A.Z., Mussina, M.K., 2022. Influence of elements of cultivation technology on yield and grain quality of winter triticale in the conditions of the Urals. IOP Conference Series: Earth and Environmental Science 979: 012057.

Yamane, K., Ikoma, A., Iijima, M., 2016. Performance of double cropping and relay intercropping for black soybean production in small-scale farms. *Plant Production Science* 19(4): 449-457.

Eurasian Journal of Soil Science 2023, 12(1), 85 - 91

Eurasian Journal of Soil Science

Journal homepage : http://ejss.fesss.org

Reducing soluble lead and cadmium in contaminated soils using dairy cattle waste based vermicompost

Zainal Muktamar [a,*], Bandi Hermawan [a], Wulandari [a], Priyono Prawito [a], Fahrurrozi Fahrurrozi [b], Nanik Setyowati [b], Sigit Sudjatmiko [b], Mohammad Chozin [b]

[a] Department of Soil Science, University of Bengkulu, Indonesia
[b] Department of Crop Production, University of Bengkulu, Indonesia

Article Info

Received : 04.06.2022
Accepted : 09.10.2022
Available online : 12.10.2022

Author(s)

Z.Muktamar *
B.Hermawan
Wulandari
P.Prawito
F.Fahrurrozi
N.Setyowati
S.Sudjatmiko
M.Chozin

* Corresponding author

Abstract

Continuous use of synthetic fertilizer can lead to the accumulation of heavy metals in the soil. The use of organic amendment can reduce the solubility of heavy metals such as Pb and Cd in soil. The experiment was undertaken to determine the decline of soluble Pb and Cd in polluted soils treated with dairy cattle waste-based vermicompost. The study used two soil samples; Inceptisols collected from Air Duku Village and Entisol from Beringin Raya Village, Bengkulu, Indonesia. Entisols and Inceptisols contained 2.0 and 0.4 mg kg^{-1} soluble Pb and 0.7 and 0.8 mg kg^{-1}soluble Cd, respectively. The samples were pretreated with either 100 ppm Pb or Cd. Vermicompost was applied at the rate of 0, 10, 20, and 30 Mg ha^{-1} on samples of Inceptisols and Entisol, arranged in Completely Randomized Design (CRD). The mixture was incubated for eight weeks. After the incubation ended, the soil sample was analyzed for soluble Pb and Cd using DTPA extraction before detection using Atomic Absorption Spectroscopy. The study resulted that the soluble Pb and Cd significantly reduced with vermicompost treatment, being the lowest was at the rate of 30 Mg ha^{-1}. Furthermore, the decreased soluble Pb and Cd was more substantial in Inceptisols than Entisols. Soluble Pb in both soils was lower than Cd, suggesting a higher retention affinity of the former. This study summarizes that vermicompost at the rate of 30 Mg ha^{-1} effectively immobilizes Pb and Cd in contaminated soils.

Keywords: Vermicompost, cadmium, lead, Inceptisols, Entisol.

Introduction

As an integral part of farming practices, fertilizers and pesticides have a high contribution to the productivity of agricultural crops. FAO (2021) reported that the use of pesticides increased by 39% for a decade (2000-2019), while in the same period, the consumption of N, P, K fertilizer rose from 134.7 million tones in 2000 to 188.5 million tones in 2019 (40%). On average, N, P, K fertilizer per cropland was 122 kg/ha in 2019, rising from 91.3 kg/ha in 2000. As a result, the production of agricultural crops, including cereals, sugar crops, vegetables, oil crops, fruits, roots and tubers, and others, reached 9,356 million tonnes in 2019. This uplifted consumption of these agrochemicals resulted in soil degradation and water pollution. Moreover, the long-term application of inorganic fertilizers and pesticides in agriculture has led to the contamination of soils by heavy metals (AlKhader, 2015; Gebeyehu and Bayissa, 2020; Kinuthia et al., 2020, Wei et al., 2020; Mng'ong'o et al., 2021a).

Phosphate fertilizers, among inorganic fertilizers, are a primary source of heavy metal contaminants in agricultural soils (Kelepertzis, 2014). During the production of certain inorganic phosphate fertilizers from phosphate rocks, inadvertently has added heavy metals such as cadmium (Cd), lead (Pb), arsenic (As), zinc (Zn), strontium (Sr), etc. to the soil (Khan et al., 2018). Phosphate fertilizer contains 11 ppm Cd and 12.5 ppm Pb (Gimeno-García et al., 1996; Setyorini et al., 2003). According to Atafar et al. (2010), the application of

: https://doi.org/10.18393/ejss.1187452
: http://ejss.fesss.org/10.18393/ejss.1187452
Publisher : Federation of Eurasian Soil Science Societies
e-ISSN : 2147-4249

fertilizer and pesticides significantly increased the concentration of Pb, As, and Cd in soils compared to non-wheat fertilized fields. Mng'ong'o et al. (2021b) detected Cu, Zn, Cd, Pb, and nickel (Ni) in plant samples leading to the possible risk to human and animal health.

In the last few decades, several techniques have been developed to immobilize heavy metals in contaminated soils, such as the use of organic materials. A review by Lwin et al. (2018) indicated that the application of organic amendment could reduce the solubility of heavy metals in soils. A previous study by Wang et al. (2020) revealed that soil treated with 1% organic matter had higher soil pH and lowered soluble Zn, Pb, and Cd than control (without treatment), leading to lower concentration in corn tissues. We have produced vermicompost from dairy cattle wastes for the organic farming system for the last ten years. Our previous study detected that vermicompost improved soil chemical properties. However, the effectiveness of vermicompost on the reduction of soluble heavy metals has not been evaluated intensively. Therefore, our current study aimed to determine the decline of soluble Pb and Cd in polluted soils treated with dairy cattle waste-based vermicompost.

Material and Methods

Soil Sample Collection and Experimental Design

The study used two soil samples collected to represent those from high and low altitudes in the humid tropical environment. The first soil sample was collected from Closed Agricultural Production System (CAPS) Research Station, Air duku Village, Selupu Rejang SubDistrict, Rejang Lebong Regency, Province of Bengkulu at 102◦36' 54.96" E and 3◦27' 34.26" S, the elevation of 1054 m above sea level. According to USDA Classification, the soil at the location was Andept, the order of Inceptisols. The second soil was sampled from Beringin Raya Village, Muara Bangkahulu SubDistrict, City of Bengkulu, Province of Bengkulu at 102◦15'42.0" E, 3◦45'20.9" S, elevation of 15 m above sea level. The soil was Psamment, the order of Entisols. The initial sample of Entisols had 0.7 mg kg^{-1} Cd, while Inceptisols 0.8 mg kg^{-1} (Table 1). Sukarjo et al. (2019) reported that soil contained Cd concentration above 9.3 mg $kg^{-1}$was considered a Cd contaminated soil. Likewise, the initial concentration of Pb in Entisols and Inceptisols was 2.0 and 0.4 mg kg^{-1}, respectively. According to Ericson et al. (2019) critical level of Pb in soil is 140 ppm. Composite soil samples were collected from 0-20 cm depths using a soil probe. The sample was air-dried and sieved using 2 mm screen. An undisturbed soil sample was also collected using a ring sample to determine field capacity (FC) moisture content. The initial characteristics of both soils are presented in Table 1.

Table 1. Initial characteristics of soil samples of Inceptisols and Entisols (Muktamar et al., 2021)

Soil Characteristics	Inceptisols	Entisols
Great Group	Andept	Psamment
Clay (%)	11.10	8.48
Silt (%)	34.94	10.54
Sand (%)	53.96	80.98
Organic-C (%)	2.86	2.34
Total-N (%)	0.19	0.32
Available P (ppm)	4.97	5.27
Exchangeable K (mmol kg^{-1})	1.90	2.41
Exchangeable Ca (mmol kg^{-1})	0.55	0.45
Exchangeable Mg (mmol kg^{-1})	1.17	0.17
Soluble Cd (mg kg^{-1})	0.80	0.70
Soluble Pb (mg kg^{-1})	0.40	2.00
CEC (cmol kg^{-1})	10.33	8.54
pH H_2O (1:1)	5.12	4.47

The study consisted of two set of experiments conducted at the Laboratory of Soil Science, Faculty of Agriculture, University of Bengkulu. Soil samples were pretreated with lead (Pb) or cadmium (Cd) using $Pb(NO_3)_2$ or $Cd(NO_3)_2$ solution, respectively. The study used a Completely Randomized Design (CRD) with two factors and three replications. The first factor was the rate of vermicompost, i.e., 0, 10, 20, and 30 Mg ha^{-1}, equivalent to 0, 5, 10, 15 mg g^{-1}, while the second factor was soil sample, consisting of Inceptisols and Entisols. Vermicompost was collected from CAPS Research Station and prepared using a method developed by Muktamar et al. (2017). The chemical properties of vermicompost were 7.98% C, 3.06% N, 5.96% P_2O_5, 1.27% K_2O, 1.79% Ca, 0.97% Mg, and pH of 5.47 (Muktamar et al., 2021).

Experimental Procedure

Vermicompost was homogeneously mixed with 0.3 kg of soil and placed in a 0.5 l transparent plastic bottle. The mixture was pretreated with 100 ppm Pb or Cd using $Pb(NO_3)_2$ or $Cd(NO_3)_2$ solution. The sample was

watered to field capacity (FC) and weighed as a basal weight for field capacity moisture content. Each experiment set was randomly positioned on a 150 cm wooden table and incubated for eight weeks. Distilled water was added to the mixture every day to reach a similar basal weight. Soil pH and temperature were measured for a week, four weeks of incubation, and at the end of the experiment. Soil pH measurement used pH meter at a 1:1 soil and distilled water ratio. Soil temperature measurement used a soil thermometer at 5 cm below the surface. At the end of the incubation, the soil was homogeneously incorporated and air-dried, ground, and passed through a 0.5 mm screen. The soil sample was analyzed for Pb or Cd using AAS after extraction with DTPA to determine their soluble form.

Data Analysis

Data were assessed using ANOVA using SAS University Edition at 5% level. Means among treatments were compared using DMRT at a 5% level.

Results

Treatment of Pb on continuously lowered soil pH during the incubation, as shown in Figure 1. Soil pH of Inceptisols at 4 and 8 weeks of the incubation was 9% and 14% lower than the first week, respectively, when the soil was treated with Pb (Figure 1a), while those of Entisols decreased by 2% and 9%. A similar fashion was observed at Cd treatment (Figure 1b). The soil pH of Entisols decreased by 2% and 12% at the 4 and 8 weeks of incubation, respectively, compared to the first week, while those of Inceptisols were 14% and 24%, respectively. Soil pH decline is more substantial in weeks 4 to 8 than previous one. The decrease in soil pH is more significant when soil is treated with Pb than with Cd.

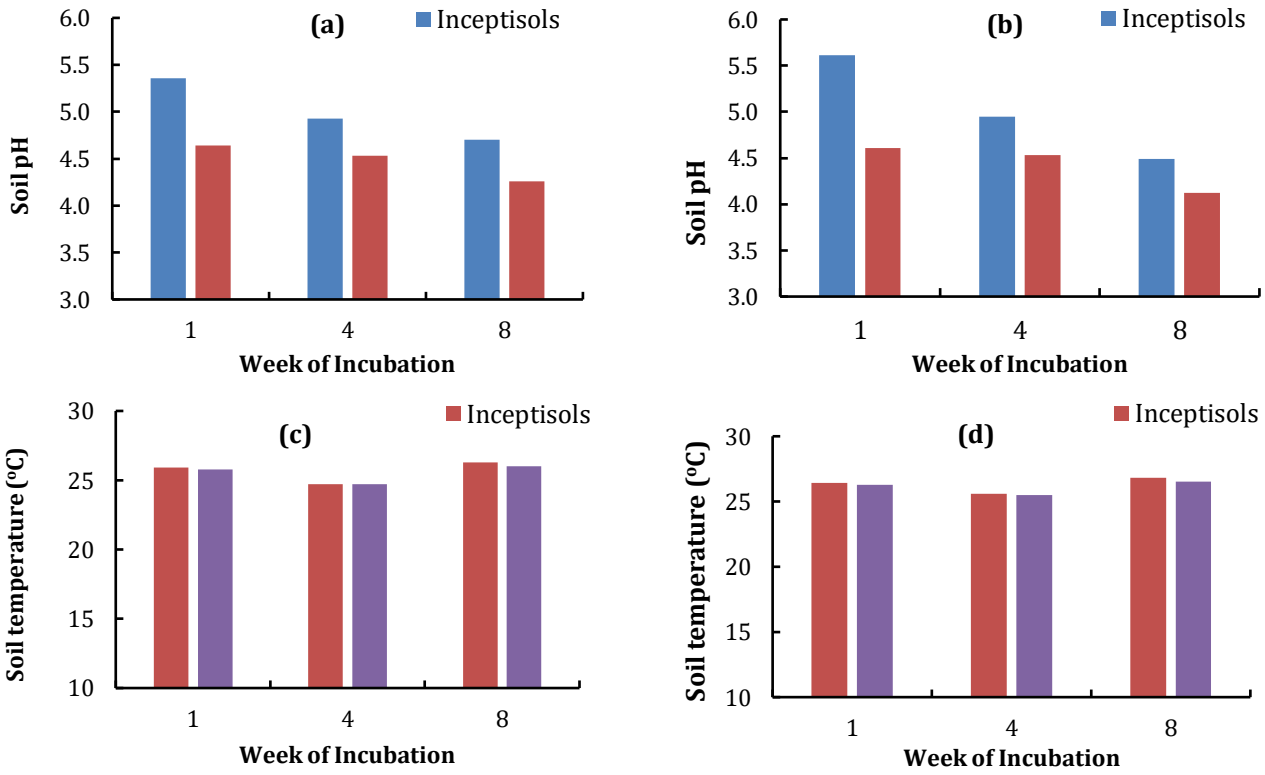

Figure 1. (a) pH of Pb treated soil at 1, 4, and 8 weeks of the incubation; (b) pH of Cd treated soil at 1, 4, and 8 weeks of the incubation; (c) Temperature of Pb treated soil at 1, 4, and 8 weeks of the incubation; (d) Temperature of Cd treated soil at 1, 4, and 8 weeks of the incubation.

Treatment of Pb or Cd did not significantly affect the temperature for both soil samples (Figures 1c and 1d). On average, the temperature of Inceptisols ranged from 24.7 °C to 26.3 °C for Pb treated soil, and 25.6 °C to 26.8 °C for Cd treated soils. Likewise, the temperature of Pb treated Entisols was 24.7 °C to 26.0 °C, while that of treated Cd was 25.5 °C to 26.5 °C. These results indicate that temperature has a similar effect on the vermicompost mineralization for soils treated with Pb or Cd.

Even though the soil pH continuously declined for the period of the incubation, vermicompost considerably increased the pH of Pb or Cd treated soils (Table 2). Treatment of vermicompost at a dose of 30 Mg ha^{-1} raised Pb treated soil by approximately 7% at week 1 and 8% at week 4 of the incubation compared to control, but

the effect was insignificant at week 8. Table 2 also shows that the pH of Cd-treated soil increased significantly at the first, fourth, and eighth weeks of the incubation as the vermicompost rate increased. Soil pH increased by 8% in the first week and by 7% in the fourth week when the vermicompost rate increased by 30 Mg ha^{-1} compared to control. However, the pH of Cd treated soil at week eight was continuously expanded by applying 30 Mg ha^{-1}vermicompost as compared to control. This result indicates that neutrality of the acidity is faster for Pb than in Cd-treated soils.

Table 2. pH of Pb and Cd treated soil as affected by vermicompost.

Vermicompost (ton/ha)	Pb treated soil			Cd treated soil		
	Week 1	Week 4	Week 8	Week 1	Week 4	Week 8
0	4.81 a	4.51 a	4.48 b	4.84 a	4.56 a	4.11 a
10	4.97 ab	4.69 b	4.43 b	5.11 b	4.69 b	4.29 b
20	5.09 b	4.85 c	4.54 b	5.24 bc	4.82 c	4.33 b
30	5.14 b	4.87 c	4.57 b	5.25 c	4.88 c	4.50 c

Note: Numbers followed by the same letter in the same column are not significantly different using DMRT at 5%

Temperatures for both Pb and Cd treated soils were not affected by the application of vermicompost, as shown in Table 3. On average, soil temperatures of Pb treated soil during the incubation ranged from 24.3 ^{o}C to 26.7 ^{o}C. Meanwhile, the average soil temperatures of Cd-treated soil were 25.5 ^{o}C to 26.8 ^{o}C. These results indicate that vermicompost decomposition does not significantly release the heat during the incubation.

Table 3. The temperature of Pb and Cd treated soil as affected by vermicompost

Vermicompost (ton/ha)	Soil Temperature (^{o}C)					
	Pb treated soil			Cd treated soil		
	Week 1	Week 4	Week 8	Week 1	Week 4	Week 8
0	26.0	24.7	26.0	26.3	25.5	26.5
10	25.8	24.8	26.0	26.5	25.3	26.7
20	25.5	24.8	26.0	26.5	25.7	26.8
30	26.0	24.3	26.7	26.0	25.7	26.7

Note: Numbers followed by the same letter in the same column are not significantly different using DMRT at 5%

The application of vermicompost substantially lowered soluble Pb of the soils treated with lead (Figure 2). The reduction of soluble Pb in Inceptisols was approximately 72% when treated with 30 Mg ha^{-1} vermicompost compared to the control; however, a rate of 10 or 20 had not been able to lower the soluble metal in the soil. A similar trend was observed in Entisols, where the application of 30 Mg ha^{-1} vermicompost reduced soluble Pb by as much as 26% compared to the control. There was no significant reduction of soluble Pb at the rate of 10 or 20 Mg ha^{-1}. Figure 2 also indicates that Inceptisols had lower soluble Pb than Entisols, suggesting that Entisols are more vulnerable to Pb contamination.

Similar to Pb treated soil, vermicompost treatment also lowered soluble Cd, as indicated in Figure 3. It was found that soluble Cd was significantly lower by treating 30 Mg ha^{-1} vermicompost than other rates. Soluble Cd in Inceptisols treated with 30 Mg ha^{-1} is 25.7% lower than the control, but both rates of 10 and 20 Mg ha^{-1} have not affected the reduction of the soluble Cd. Figure 3 also shows that Entisols treated with 30 Mg ha^{-1} had 24.7% lower soluble Cd than the control but were not different from that of 20 Mg ha^{-1}.

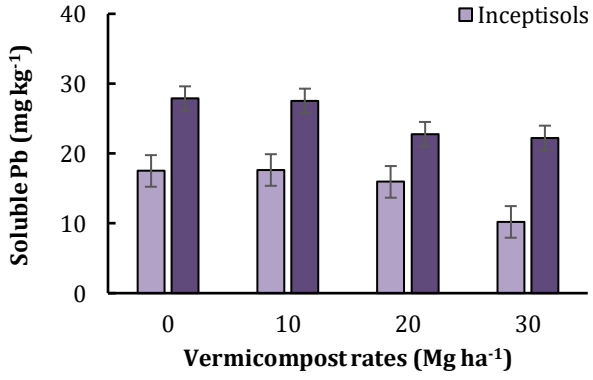

Figure 2. Soluble Pb as affected by vermicompost in Inceptisols and Entisols

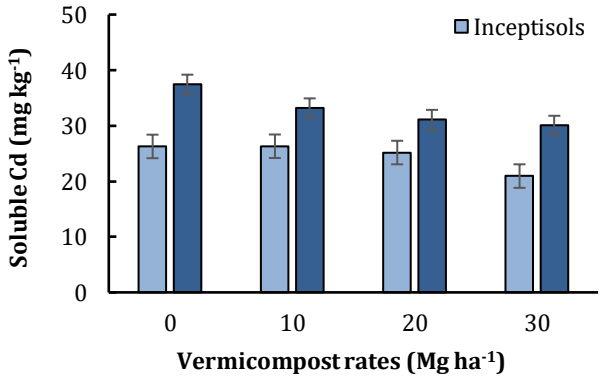

Figure 3. Soluble Cd as affected by vermicompost in Inceptisols and Entisols

A comparison between soluble Pb and Cd is presented in Figure 4. The figure shows that soluble Cd is always higher than soluble Pb at each rate of vermicompost. As the vermicompost rate is higher, the difference between both metals increases. At the control, soluble Pb is 40.4% higher than soluble Cd, while at the highest rate is more than 57%. This result indicates the different characteristics of both heavy metals.

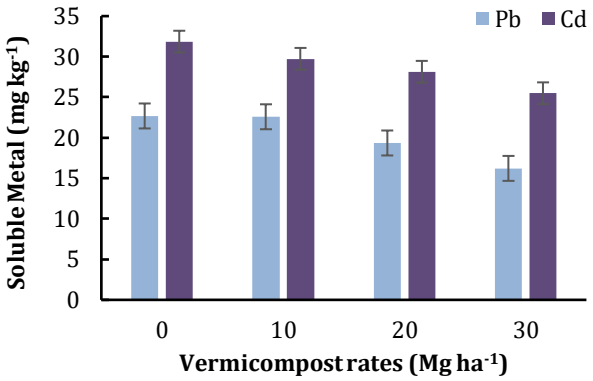

Figure 4. Soluble Pb and Cd as influenced by vermicompost

Correlation analysis shows that soil pH significantly correlates to soluble Pb with an r of 0.75 (Figure 5a). As soil pH is higher, soluble Pb declines. Likewise, soluble Cd decreases with increasing the soil pH, as shown in Figure 5b. Soluble Pb lowers by 59.2% as pH increases from 4.0- to 4.5, while soluble Cd decreases by 22.2% at the same pH range. These results suggest that the solubility of both Pb and Cd in the soil is dependent on the pH of the system.

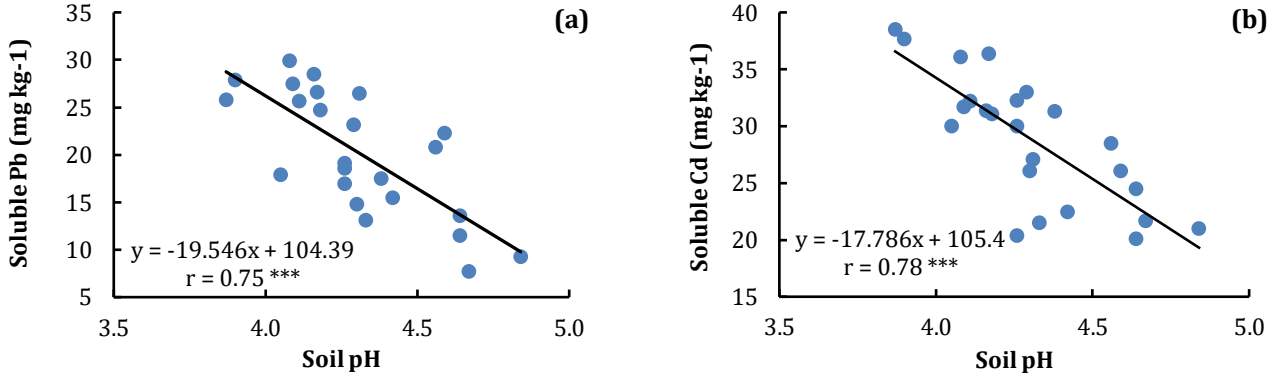

Figure 5. Correlation between soil pH and soluble Pb (a) and soluble Cd (b)

Discussion

In general, soil pH continuously decreases during eight weeks of the incubation, and the application of vermicompost significantly increases soil pH each week for both samples of Inceptisols and Entisols (Figures 1, Table 2). The decline in the pH of Pb or Cd treated soils is associated with the hydrolysis of the heavy metal as follows $M^{2+} + H_2O \rightarrow M(OH)_2 + 2\ H^+$ (Cruywagen and Van der Water, 1993; Barysz et al. 2004); M denotes Pb or Cd. As hydrolysis proceeds, higher proton release will lower soil pH. Meanwhile, the increase in soil pH by adding vermicompost is associated with the formation of organo-metal complexes, reducing their hydrolysis. Consequently, lower Pb and Cd hydrolysis will raise the soil pH.

Application of vermicompost significantly decreased the soluble Pb and Cd in both Inceptisols and Entisols (Figures 2 and 3). Organic matter decomposition releases organic acids, mainly humic and fulvic acids, rich in carboxyl and phenolic functional groups. These groups bond metals to form complexes (Spark, 2003; Barančíková and Makovníková, 2003; Boguta and Sokolowska, 2013), reducing their solubility. Carboxyl is a major functional group from humic acid that interacts with heavy metals (Spark et al., 1997). A previous study by Klučáková and Pavlíková (2017) found that lignitic humic acid strongly bound Pb and Cu. Another possible mechanism suggested by Qu et al. (2019) is the formation of hydroxide-humic acid metal complexes. Their results also showed that Pb and Cd immobilized in co-precipitation complexes were similar to their adsorption. The result of this study corresponds to that suggested by Boechat et al. (2016), where humic and fulvic acids substantially declined in selected heavy metals, including Pb and Cd.

The soil sample used in this study exhibits different retention of Pb and Cd where Inceptisols retains Pb and Cd higher than Entisols, as indicated by the amount of soluble form of both metals (Figures 2 and 3). This result is associated with the initial characteristics of both soils. Inceptisols have higher clay content, soil

organic matter, and CEC than the other soil. Higher CEC will adsorb more metals due to higher negative charges in the soil. Humic substances at a pH of more than 3.0 also contribute to a negative charge and the formation of organo-metal complexes (Spark, 2003).

Our study also shows that soluble Pb in both soils was significantly lower than soluble Cd (Figure 4). The affinity of Pb to soil adsorption sites is higher than Cd; consequently, higher retention of the former element. The adsorption affinity (Kd) of Pb was greater than Cd, as reported by Usman (2008) and Covelo et al. (2007). Another study confirmed that the amount of Pb adsorbed by humic substances is higher, and the stability constant of the complex is greater than Cd. On the other hand, Cd bonded weaker to the substance than Pb (Klučáková and Pavlíková, 2017). Higher retention of Pb by the soil will lower its soluble form.

The correlation of pH and soluble Pb or Cd shows the dependency of the solubility of the metal on soil pH (Figure 5). As soil pH rises, soluble Pb and Cd are lower. Some studies show that the concentration of soluble Pb and Cd continuously declines as soil pH increases (Ok et al., 2010; Zhang et al., 2018; Soltan et al., 2018).

Conclusion

Addition of vermicompost significantly reduced the soluble Pb and Cd of Inceptisols and Entisols, being the lowest was achieved at 30 Mg ha^{-1}. The reduction of both heavy metals was more prominent in Inceptisols than Entisols. Soluble Pb in both soil samples was lower than Cd, indicating the higher retention affinity of the former. The decrease in the soluble heavy metals using vermicompost was followed by the increase in soil pH. This finding suggests that vermicompost at the rate of 30 Mg ha^{-1} is effective for the remediation of Pb and Cd contaminated soils.

Acknowledgments

Extent thank is delivered to the Institute of Research and Community Services, the University of Bengkulu, to provide the project's financial support through contract No. 1988/UN30.15/PG/2020, 23 June 2020. The assistance of technicians at the Soil Science Lab is highly appreciated.

References

AlKhader, A.M., 2015. The impact of phosphorus fertilizers on heavy metals content of soils and vegetables grown on selected farms in Jordan. *Agrotechnology* 5(1): 1000137.

Atafar, Z., Mesdaghinia, A., Naori, J., Homaee, M., Yunesian, M., Ahmadimoghaddam, M., Mahvi, A.H., 2010. Effect of fertilizer application on soil heavy metal concentration. *Environmental Monitoring and Assessment* 160:83–89.

Barančíková, G., Makovníková, J. 2003. The influence of humic acid quality on the sorption and mobility of heavy metals. *Plant, Soil and Environment* 49 (12): 565-571.

Barysz, M., Leszczyński, J., Bilewicz, A. 2004. Hydrolysis of the heavy metal cations: relativistic effects. *Physical Chemistry Chemical Physics* 6: 4553-4557.

Boechat, C.L., Pistóia, V.C., Ludtke, A. C., Gianello, C., Camargo, F. A.O., 2016. Solubility of heavy metals/metalloid on multi-metal contaminated soil samples from a gold ore processing area: Effects of humic substances. *Revista Brasileira de Ciência do Solo* 40:e0150383.

Boguta, P., Sokolowska. Z., 2013. Interaction of Humic Acids with Metals. Acta Agrophysica Monographiae. Instytut Agrofizyki im. Bohdana Dobrzanskiego PAN, 113 p.

Covelo, E.F., Vega, F.A., Andrade, M.L. 2007. Simultaneous sorption and desorption of Cd, Cr, Cu, Ni, Pb, and Zn in acid soils: I. Selectivity sequences. *Journal of Hazardous Materials* 147 (3): 852–861.

Cruywagen, J.J., van de Water, R.F., 1993. The hydrolysis of lead(II). A potentiometric and enthalpimetric study. *Talanta* 40(7): 1091-1095.

Ericson, B., Otieno, V.O., Nganga, C., St. Forth, J., Taylor, M.P., 2019. Assessment of the presence of soil lead contamination near a former lead smelter in Mombasa, Kenya. *Journal of Health and Pollution* 9(21): 190307.

FAO 2021. World Food and Agriculture - Statistical Yearbook 2021. Food and Agriculture Organization of the United Nations, Rome. 368p. Available at [04.06.2022]: Access date: http://www.fao.org/3/cb4477en/cb4477en.pdf

Gebeyehu, H.R., Bayissa, L.D., 2020. Levels of heavy metals in soil and vegetables and associated health risks in Mojo area, Ethiopia. *PlosOne* 15(1): e0227883.

Gimeno-García E., Andreu, V., Boluda, R., 1996. Heavy metals incidence in the application of inorganic fertilizers and pesticides to rice farming soils. *Environmental Pollution* 92: 19-25.

Kelepertzis, E., 2014. Accumulation of heavy metals in agricultural soils of Mediterranean: Insights from Argolida basin, Peloponnese, Greece. *Geoderma* 221-222: 82-90.

Khan, M.N., Mobin M., Abbas, Z. K., Alamri, S. A. 2018. Fertilizers and their contaminants in soils, surface and groundwater. In: Encyclopedia of the Anthropocene, Vol. 5. Dellasala, D.A., Goldstein, M.I. (Eds.). Elsevier. pp. 225-240.

Kinuthia, G., Ngure, K., Beti, V., Lugalia, D., Wangila, R., Kamau, L. 2020. Levels of heavy metals in wastewater and soil samples from open drainage channels in Nairobi, Kenya: community health implication. *Scientific Reports* 10: 8438.

Klučáková, M., Pavlíková, M., 2017. Lignitic Humic Acids as Environmentally-Friendly Adsorbent for Heavy Metals. *Journal of Chemistry* Article ID 7169019.

Lwin, C.S., Seo, B.H., Kim, H.U., Owen, G., Kim, K.R., 2018. Application of soil amendments to contaminated soils for heavy metal immobilization and improved soil quality—a critical review. *Soil Science and Plant Nutrition* 64(2): 156-167.

Mng'ong'o, M., Munishi, L.K., Ndakidemi, P.A., Blake, W., Comber, S., Hutchinson, T.H., 2021b. Accumulation and bioconcentration of heavy metals in two phases from agricultural soil to plants in Usangu agroecosystem-Tanzania. *Heliyon* 7(7): e07514.

Mng'ong'o, M., Munishi, L.K., Ndakidemi, P.A., Blake, W., Comber, S., Hutchinson, T.H., 2021a. Toxic metals in East African agro-ecosystems: Key risks for sustainable food production. *Journal of Environmental Management* 294: 112973.

Muktamar, Z., Hermawan, B., Wulandari, Prawito, P., Sudjatmiko, S., Setyowati, N., Fahrurrozi, F., Chozin, M., 2021. Vermicompost buffering capacity to reduce acidification of Pb and Cd contaminated inceptisols and entisols. *Journal of Tropical Soils* 26(1): 1-9.

Muktamar, Z., Sudjatmiko, S., Chozin, M., Setyowati, N., Fahrurrozi. 2017. Sweet corn performance and its major nutrient uptake following application of vermicompost supplemented with liquid organic fertilizer. *International Journal on Advanced Science, Engineering and Information Technology* 7(2): 602-608.

Ok, Y.S., Oh, S.E., Ahmad, M., Hyun, S., Kim, K.R., Moon, D.H., Lee, S.S., Lim, K.J., Jeon, W.T., Yang, J.E., 2010. Effects of natural and calcined oyster shells on Cd and Pb immobilization in contaminated soils. *Environmental Earth Science* 61: 1301–1308.

Qu, C., Chen, W., Hu, X., Cai, P., Chen, C., Yu, X.Y., Huang, Q., 2019. Heavy metal behaviour at mineral-organo interfaces: Mechanisms, modelling and influence factors. *Environmental International* 131: 104995.

Setyorini, D., Soeparto, Sulaiman, 2003. Kadar logam berat dalam pupuk. In: Prosiding Seminar Nasional Peningkatan Kualitas Lingkungan dan Produk Pertanian, Badan Litbang Pertanian. Jakarta, Indonesia. pp. 219-229. [in Indonesian].

Soltan, M.E., Al-ayed A.S., Ismail, M.A., 2018. Effect of pH values on the solubility of some elements in different soil samples. *Chemistry and Ecology* 35(3): 270-283.

Spark, D.L., 2003. Environmental Soil Chemistry. 2nd Edition. Academic Press. London. UK. 351p.

Spark, K.L., Wells, J.D., Johnson, B.B., 1997. The interaction of a humic acid with heavy metals. *Australian Journal Soil Research* 35(1): 89–101.

Sukarjo, Zulaehah, I., Purbalisa, W., 2019. The critical limit of cadmium in three types of soil texture with shallot as an indicator plant. AIP Conference Proceedings 2120: 040012.

Usman, A.R.H., 2008. The relative adsorption selectivities of Pb, Cu, Zn, Cd and Ni by soils developed on shale in New Valley, Egypt. *Geoderma* 144(1-2): 334-343.

Wang, F., Zhang, S., Ceng, P., Zhang, S., Sun, Y., 2020. Effects of soil amendments on heavy metal immobilization and accumulation by maize grown in a multiple-metal-contaminated soil and their potential for safe crop production. *Toxics* 8(4): 102.

Wei, B., Yu, J., Cao, Z., Meng, M., Yang, L., Chen, Q., 2020. The availability and accumulation of heavy metals in greenhouse soils associated with intensive fertilizer application. *International Journal of Environmental Research and Public Health* 17(15): 5359.

Zhang, Y., Zhang, H., Zhang, Z., Liu, C., Sun, C., Zhang, W., Marhaba, T. 2018. pH effect on heavy metal release from a polluted sediment. *Journal of Chemistry* Article ID 7597640.

Eurasian Journal of Soil Science 2023, 12(1), 92 - 97

Eurasian Journal of Soil Science

Journal homepage : http://ejss.fesss.org

Modelling of soil temperature by using Phase Change Material (PCM) to regulate the plant growing media temperature

Tuğba Gürmen *

Ege University, Faculty of Engineering, Department of Chemical Engineering, Bornova, İzmir, Türkiye

Article Info

Received : 09.02.2022
Accepted : 19.10.2022
Available online : 24.10.2022

Author(s)

T.Gürmen *

* Corresponding author

Abstract

The temperature control of the agricultural greenhouse is important issue and to sudden temperature, changes during the growing plants are one of the problems that need to be controlled. Temperature control can be achieved in greenhouses established with the novel technological systems, but these systems are expensive systems that requires technical knowledge and infrastructure. In this study, a seasonal thermal energy storage using Phase Change Material **(**PCM) composite material investigated to regulate day time soil temperature in the greenhouse. The overall purpose of the research was to identify the mechanisms of heat transfer in soil covered by phase change materials. The PCM was encapsulated in to expanded perlite and soil temperature with and without using the PCM were compared. By using the experimental data, a mathematical model that can simulate the temperature of the soil in the greenhouse was developed According to the results, the research included experimental works as well as theoretical analysis.

Keywords: Soil temperature, phase change material (PCM), greenhouse applications, modelling of soil temperature.

Introduction

In agricultural applications, especially in greenhouses the needed energy amount is high. The increasing costs of energy production and the limited resources make it necessary to develop new methods for the efficient use of energy. In an effective agricultural activity, energy uses must be in controlled and in the logical range. The food supplies in the world are directly depend on the energy (Ziapour and Hashtroudi, 2017). Already, developing in energy use in the agriculture is a response to population increasing, limited supply of useful lands and demand for better standards of living (Banaeian et al., 2011).

Temperature change during the crop production is the main problem for in terms of plant growth and yield. The advent of the greenhouse is intended to control the environment to improve the quality, stabilize the yield and prolong the production season. A well-designed greenhouse should maintain an optimum environment for healthy plant growth and maximum yield (Tuntiwaranuruk et al., 2006).

Because of the high-energy consumption and global warning in recent years, energy conservation and storage applications have become extremely important. Energy storage seems as a good opportunity to solve the energy problems as well as to improve new renewable and clean energy sources. To meet energy needs of the developed communities, the renewable energies can be used conjunction with energy storage systems. In addition, efficient and compact energy storage systems seem to be important parameters to improve the use of renewable sources (Kenisarin and Kenisarina, 2012; Gürmen, 2019).

Thermal energy storage can be stored as a change in internal energy of a material as sensible heat, latent heat and thermo-chemical or combination of these. The latent heat storage method, in which energy is stored in the form of latent heat in phase change materials (PCM), plays an important role in different application areas. This technique is particularly attractive with respect to other techniques due to two main advantages:

: https://doi.org/10.18393/ejss.1193903
: http://ejss.fesss.org/10.18393/ejss.1193903
Publisher : Federation of Eurasian Soil Science Societies
e-ISSN : 2147-4249

i) Phase change process is nearly an isothermal process.

ii) It has larger heat storage density with smaller temperature swing.

Phase change materials (PCM) are one of the most used materials in thermal energy storage and temperature control of many engineering applications (Zalba et al., 2003; Sharma et al., 2009; Zhou et al., 2009; Rathod and Banerjee, 2013). PCMs store energy by absorbing and releasing of heat in phase change processing in the form of the latent heat of fusion. Depending on their phase change states, PCM are classified in four categories liquid-gas, solid-liquid, solid-gas and solid-solid PCM (Prakash et al., 1985; Jamekhorshid et al., 2014; Gürmen, 2017).

The PCM could absorb sun energy inside greenhouses during the day, and release the heat in the night to provide a thermal comfortable environment for crops. This feature of PCM could noticeably reduce the temperature difference between day and night in greenhouses, which could effectively increase the crops yield (Mu et al., 2022). For this application, a PCM having suitable melting / freezing temperatures and heat of fusion should be selected.

In this study, PCM composite material was used in order to keep the soil temperature constant in the greenhouse. The PCM material used was prepared using the method of trapping PEG in expanded perlite pores. Owing to this encapsulation process, the solid-liquid phase change process takes place within the pores and leakage was prevented. The melting and freezing temperatures were determined for prepared composite, as 21°C and 6 °C, respectively and the phase change enthalpy was calculated as 130 J/g. Perlite has been preferred in the preparation of composite PCM due to its porous structure and being a natural rock widely used in agriculture. This study concerned to improve of mathematical and numerical models different modes of heat transfer interaction with the environment in the soil by the layer containing PCM. The experimental data obtained during measurements of the soil thermal properties conformed to the theoretical model.

Material and Methods

The main aim of this research was to identify the mechanisms of heat transfer in soil covered by PCM enclosed perlite to regulate the soil temperature. The research included experimental works as well as theoretical analysis.

The used PCM composite including PEG and EP was prepared using a vacuum impregnation method. Initially 25:75 mass ratio of PEG and EP were weighted with 0.001 g accuracy. Weighed EP was placed in the vacuum set and the prepared mixture was added it slowly under vacuum at 30°C. Then, the obtained mixture was placed into an oven at 60°C for 12 hours. The prepared form stable PCMs were included 25 % PEG wax by weight. The phase transition temperature and latent heat of prepared PCM composite material was determined by DSC analysis (Perkin Elmer Diamond TG/DTA) at a heating/cooling rate of 5◦C/min from −45◦C to 5◦C by using purified nitrogen at a flow rate of 10 ml/min.

In order to verifying the mathematical model, only a part of the soil is covered with the prepared PCM and other part was left uncoated in the same greenhouse, placed in Menderes, Izmir, Turkey. The soil was covered with of 10 mm-thick of PCM composite over the growing media. Temperatures at different levels of the soil were hourly measured by using thermometer. The experiments were performed from in March 2021.

The soil temperature was measured by using ST4-05 Soil Temperature Probe and the probes were placed into the soil at 10, 20 and 30 cm depth. Soil temperatures were measured every 60 minutes for 24 hours.

Mathematical Model

In the theoretical part of the research, a mathematical model of heat transfers in PCM covered soil developed. In the model, it was subjected to environmental impacts by radiation and convection. This includes the formulation of the set of equations that combine temperature profile in the soil with heat fluxes at its surface as well as the values of thermophysical properties of the soil that influences the process of heat transport.

The soil temperature with and without PCM composite inside an agricultural greenhouse having soil inside growing media is considered T_s (°C). When PCM composite covered soil in the greenhouse growing medium and the soil is heated by solar radiation, its energy is lost to the cover by convection, conduction and radiation.

To simplify the analysis, the following assumptions for the heat transfer processes in the soil were used for model development:

1. One dimensional heat transfer occurs; the temperature gradients exists along the height only
2. The heating system is quasi-state condition
3. The air and the soil temperatures in the greenhouse are homogeneous and isotopic.
4. Thermal properties are independent to temperature.

The layers in the growing media is shown in Figure 1.

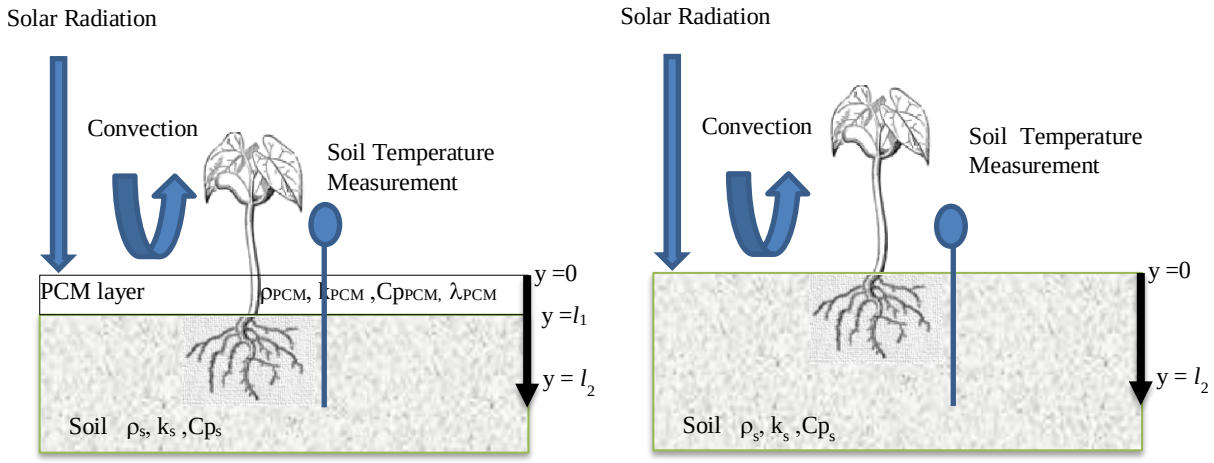

Figure 1. The layers in the growing media with and without PCM.

The one dimensional temperature distribution $T(y,t)$ in the soil is described by conductive heat transfer equation:

$$\rho C_p \left(\frac{\delta T(y,t)}{\delta t}\right) = \frac{\delta}{\delta y}\left(k_s \frac{\delta T(y,t)}{\delta y}\right)$$

where ρ density (kg/m^3), C_p specific heat (kJ/(kg K)), t time (s), k_s thermal conductivity of soil (W/(m K)).

Subjected to the boundary condition:

$$k_s \frac{\partial (T,y)}{\partial y} = h\big(T_i(t) - T(y,t)\big) + q_r(t)$$

At y=0 at surface

Convective heat transfer to the air is due to the natural convection. In the model simplified the calculation of the convective heat transfer coefficient McAdams correlation was chosen and h can be calculated by the following equation (Bergman et al., 2011).

$$h = 0.1\left(\frac{g\beta\Delta T}{\nu^2} Pr\right)^{1/3} \frac{1}{k_a}$$

where h convective heat transfer coefficient(W/(m^{2}K)), g gravity acceleration (9.8 m/s^2), ν kinematic viscosity (m^2/s) , β thermal expansion coefficient (1/K), Pr Prandtl Number, k_a thermal conductivity of air (W/(m K)).

When the air temperature is in the range between 0-45 °C, the above equation can be simplified to the form in which heat transfer coefficient is only a function of temperature difference (Jaworski, 2019):

$$h = 1.15\Delta T^{1/3}$$

$q_r(t)$ is solar radiation (W/m^2) transmitted through the greenhouse cover to the upper surface of soil.

$$q_r(t) = \varepsilon\sigma\left({T_s}^4 - {T_a}^4\right)$$

where ε emissivity, σ Stefan-Boltzmann constant (5.67 10^{-8}W/m^{2}K^4).

The transient heat transfer equation of PCM layer

$$\rho_{PCM} \frac{\delta H}{dt} = k_{PCM} \frac{\delta^2 T(y,t)}{\delta h^2}$$

where ρ_{PCM} density of PCM (kg/m^3), H enthalpy of PCM (kJ/kg), k_{PCM} thermal conductivity of PCM (W/(m K)).

Enthalpy of PCM

$$H = \int_{T_0}^{T_m} {C_p}_{PCM} dT + \lambda_{PCM} + \int_{T_m}^{T_2} {C_p}_{PCM} dT$$

where ${C_p}_{PCM}$ specific heat (kJ/(kg K)) and λ_{PCM} heat of fusion of PCM (kJ/kg).

Boundary condition:

$$\text{at y}=l_1 \qquad k_s \frac{\partial(T,y)}{\partial y} = 0$$

l is solid height from surface (m)

Initial condition: $T(y,t)_{t=0} = T_i$

Heat transfer equation for inside air of the greenhouse is formulated as:

$$C_{pa}\rho_a V_R \frac{\partial T_a(t)}{\partial t} = \sum Q_s - Q_{leak}$$

where Q heat transfer rate (W) and C_{pa} specific heat of air (kJ/(kg K)).

Table 1. Thermal physical properties of the soil and PCM

	ρ (kg/m^3)	Cp (kJ/kg K)	λ (kj/kg)	k (W/m K)	T_m (°C)
Soil	1110	1.13	-	0.097	-
PCM	1120	2.49	130	0.212	21

The proposed model of heat transfer in the soil describes their temperature changes described under thermal transfer processes by the boundary conditions. Selected problems, similar to those realized in an experimental study were solved numerically, using one dimensional control volume approach with Euler's method for integration in time.

Results and Discussion

Thermal properties of the used PCM is an important factor influencing the ability of energy storage of the PCM layer over the soil. The important point of applying PCM on the soil surface is to select PCM with suitable melting temperature. For selected climate condition and soil, when the melting temperature of PCM is high, the quantity of heat stored by PCM will be low. When the melting temperature is low, to obtain a comfortable soil temperature for plant will be hard, at night time. For this reason, the phase change temperature of the PCM to be used should be suitable for the selected climate region. For this reason, initially the thermal properties of the prepared PCM composite were determined by using DSC analysis and obtained data are given in Figure 2.The melting and freezing temperatures and latent heat values of the prepared composite PCM are 20.64 °C, 6.24 °C and 130.7 J/g, respectively.

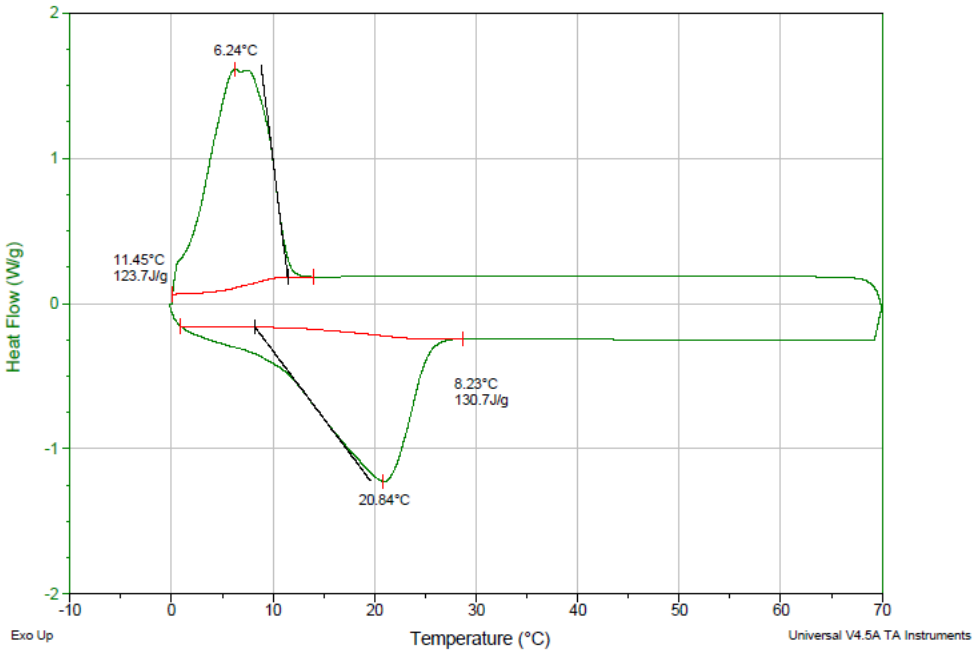

Figure 2. DSC curves for prepared composite PCM

The model's accuracy and applicability were tested and compared experimental results at surface, 10, 20 cm and 30 cm level from the surface which is suitable for plant growth. The experimental and model results were in agreement as shown in Figures 3, 4, 5 and 6.

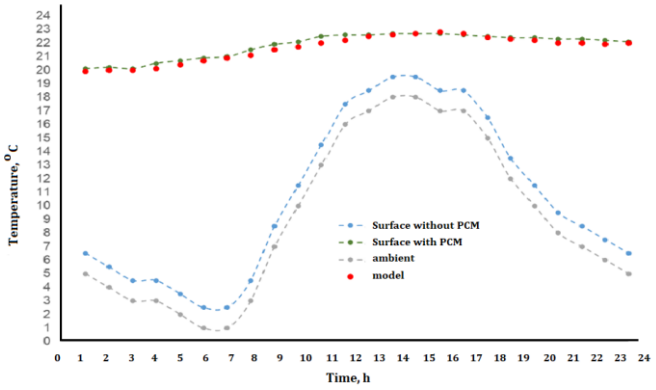

Figure 3. Comparison of temperatures between experimental and model results at soil surface

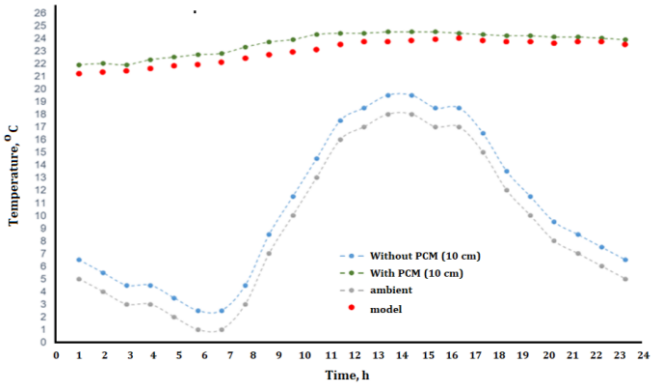

Figure 4. Comparison of temperatures between experimental and model results at 10 cm from the surface

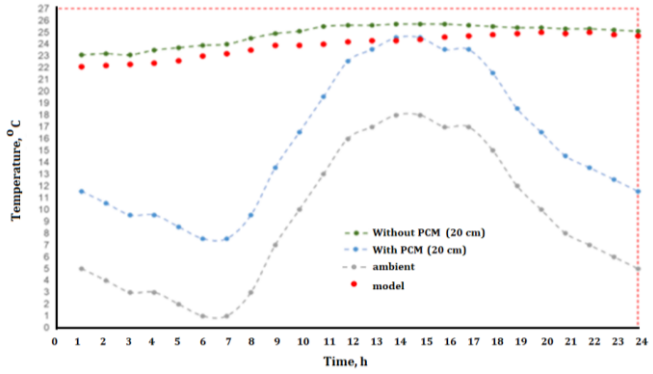

Figure 5. Comparison of temperatures between experimental and model results at 20 cm from the surface

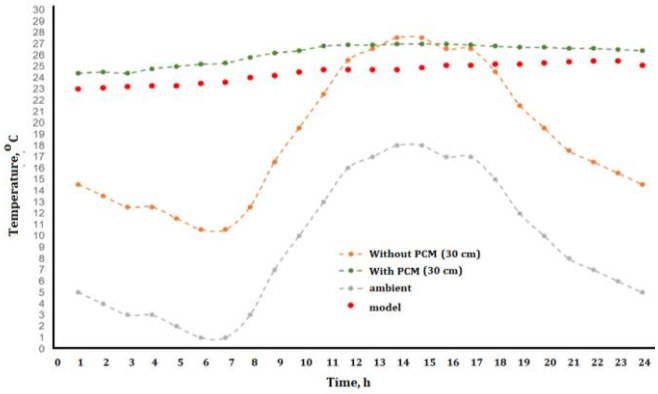

Figure 6. Comparison of temperatures between experimental and model results at 30 cm from the surface

The experimental results show that, soil temperature becomes nearly constant when the soil was covered with PCM layer as expected. Using the PCM layer, the obtained soil temperature ranges was from 21 to 27 °C and this range is appropriate for the plant growth. The maximum temperature value difference between the PCM covered and not covered soil at surface, 10, 20 and 30 cm from the surface was found as 18.5, 17.45, and 16.35 and 14.75 °C, respectively. Tuntiwaranuruk et al. (2006) studied with rice husks which was covered the soil to reduce soil temperature and they reported that the reduction due to rice husks covering soil in maximum values of soil temperature at 10 and 20 cm from the surface was found as 5.00 and 2.83 °C, respectively. This study rice husks used to decrease solar radiation effect. In order for plants to grow healthy, it is important that their roots be not affected by temperature changes throughout the day. It has been determined that soil temperatures can be stabilized thanks to the soil covered by PCM. The average value of the soil temperatures were measured as 21.82, 23.62, 23.82 and 26.11°C at surface, 10, 20 and 30 cm depth from surface, respectively. It is obvious that soil temperature without PCM is lower than that with PCM. According to the results, it can be seen that PCM also helps to improve the heat transfer between the soil surface and air in the greenhouse.

The soil temperatures calculated from the mathematical model were found to be in well agreement with the measured temperatures for each level of the soil. The average value of soil temperature differences between the measured temperatures and the temperatures calculated from the proposed model were 0.2, 0.67, 0.91 and 1.46 °C at surface, 10, 20 and 30 cm depth from surface, respectively. Wang et al. (2020) reported that, the simulation results are higher than the observed values at depths of 0.2m and 0.3m. In order to determine the suitability of the proposed model, standard deviations were calculated and standard deviations between mathematical model and measurement temperatures were found as 0.16, 0.21, 0.35 and 0.36 for surface, 10 cm, 20 cm and 30 cm depth, respectively. Mashonjowa et al. (2013) reported values of the mean standard errors between the calculated and measured air and crop temperatures of 1.8 °C and 1.9 °C, respectively. In the present study, the proposed model gave more approximate results for soil temperature.

Although the model compatibility is high in the studied soil depths, it is seen that the standard deviation increases slightly as the soil depth increases. This deviation is thought to be due to the increase in the difference between air temperature and soil temperature as the depth increases.

Conclusion

In the present paper, a mathematical model of analysing the thermal performance PCM over the soil is developed. It is concluded that the proposed mathematical model can be used to predict soil temperature with and without PCM over the soil in an agricultural greenhouse. According to the experimental results, it is seen that by covering the soil in the greenhouse with PCM, a suitable environment for plant growth will be provided by preventing sudden changes in soil temperature during the periods when day and night temperature differences are high. Thus, the costs of heating systems used in greenhouses can be reduced.

References

Banaeian, N., Omid, M., Ahmadi, H., 2011. Energy and economic analysis of greenhouse strawberry production in Tehran province of Iran. *Energy Conversion and Management* 52(2): 1020–1025.

Bergman, T.L., Lavine, A.S., Incropera, F.P., Dewitt, D.P., 2011. Fundamentals of Heat and Mass Transfer, 7th ed., John Wiley Sons. Inc. 1051p.

Gürmen Özçelik, T., 2017. Preparation, characterization and thermal properties of paraffin wax – expanded perlite form-stable composites for latent heat storage. *Materials Science* 23(1): 39-43.

Gürmen Özçelik, T., 2019. Investigation of glycerol-Ni(NO3)26H2O /perlite composites as form stable phase change materials. *Research on Engineering Structures and Materials* 6(2): 141-151.

Jamekhorshid, A., Sadrameli, S.M., Farid, M., 2014, A review of microencapsulation methods of phase change materials (PCMs) as a thermal energy storage (TES) medium. *Renewable and Sustainable Energy Reviews* 31: 531 – 542.

Jaworski, M., 2019. Mathematical model of heat transfer in PCM incorporated fabrics subjected to different thermal loads, *Applied Thermal Engineering* 150: 506–511.

Kenisarina, M.M., Kenisarina, K.M., 2012, Form-stable phase change materials for thermal energy storage. *Renewable and Sustainable Energy Reviews* 16: 1999 – 2040.

Mashonjowa, E., Ronsse, F., Milford, J.R., Pieters, J.G., 2013. Modelling the thermal performance of a naturally ventilated greenhouse in Zimbabwe using a dynamic greenhouse climate model. *Solar Energy* 91: 381–393.

Mu, M., Zhang, S., Yang, S., Wang, Y., 2022. Phase change materials applied in agricultural greenhouses. *Journal of Energy Storage* 49: 104100.

Prakash, J., Garg, H.P., Datta, G., 1985, A solar water heater with a built-in latent heat storage. *Energy Conversion and Management* 25(1): 51 – 56.

Rathod, M.K., Banerjee, J., 2013, Thermal stability of phase change materials used in latent heat energy storage systems: A review. *Renewable and Sustainable Energy Reviews* 18: 246 – 258.

Sharma, A., Tyagi, V.V., Chen, C.R., Buddhi, D. 2009, Review on thermal energy storage with phase change materials and applications. *Renewable and Sustainable Energy Reviews* 13(2): 318 – 345.

Tuntiwaranuruk, U., Thepa, S., Tia, S., Bhumiratana S., Krasaechai, A., 2006. Comparison between measured and predicted ventilation rates in a naturally ventilated greenhouse. *Acta Horticulturae* 699: 439-448.

Wang, J., Lee, F.W., Ling, P.P., 2020, Estimation of thermal diffusivity for greenhouse soil temperature simulation. *Applied Science* 10(2): 653.

Zalba, B., Marín, J.M., Cabeza, L.F., Mehling, H., 2003, Review on thermal energy storage with phase change: materials, heat transfer analysis and applications. *Applied Thermal Engineering* 23(3): 251 – 283.

Zhou, X., Xiao, H., Feng, J., Zhang, C., Jiang, Y., 2009. Preparation and thermal properties of paraffin/porous silica ceramic composite. *Composite Science and Technology* 69(7-8): 1246 – 1249.

Ziapour, B.M., Hashtroudi, A., 2017. Performance study of an enhanced solar greenhouse combined with the phase change material using genetic algorithm optimization method, *Applied Thermal Engineering*, 110: 253-264.

Eurasian Journal of Soil Science 2023, 12(1), 98 - 103

Eurasian Journal of Soil Science

Journal homepage : http://ejss.fesss.org

Effect of humic substances on yield and nutrient contents of Eggplant Santana (*Solanum melongena*) plants in gray-brown soil

Ulviyya Mammadova *

Institute of Soil Science and Agrochemistry, Baku, Azerbaijan

Article Info

Received : 03.03.2022
Accepted : 22.10.2022
Available online : 01.11.2022

Author(s)

U.Mammadova *

* Corresponding author

Abstract

Humic substances promote the conversion of nutrients into forms available to plants. It also stimulates seed germination and viability, and its main effect usually being more prominent in the roots. This study was conducted in a randomized complete block design with three replications in Gobustan, Azerbaijan, in 2021 growing season, to determine the effects of different doses (0, 250, 500 and 1000 ppm) of humic substances such as humic acid (HA), fulvic acid (FA) and humic fulvic acid (HFA) on fresh yield and nutrient contents (N, P and K) of Eggplant Santana (*Solanum melongena* var. *esculentum Santana*) plants in a field experiment. According to the results of this study, humic substance treatments increased the fresh yields and leaf nutrient contents of Eggplant Santana, and this increase was found to be significant. The highest value for highest fresh yields and leaf NPK contents of Eggplant Santana plants were obtained from 1000 ppm HFA dose. These results suggest that 1000 ppm HA and FA combination to the standard humic substances application will be sufficient to obtain adequate fresh yield and nutrient contents in Eggplant Santana leafs.

Keywords: Humic acid, fulvic avid, soil, yield, Eggplant Santana, nutrients.

Introduction

Humic substances, namely humus, which is an important component of the soil organic matter as well as in geological organic deposits such as lake sediments, peats, brown coals and shales and these are very important components of soil that affect physical and chemical properties and improve soil fertility (IHSS, 2022). Because of the different contribution ways on plant growth, humic substances are used in different areas of agriculture (Chen and Aviad, 1990). Owing to chelating properties of humic substances with metallic cations, availability of many nutrients increase and thus plant growth is affected positively (Cansu and Erdal, 2018). Additionally, humic substances increase root and root hair growth leading to expanded root surface area and thus nutrient uptake capacity increases (Pinton et al., 1999; Cesco et al., 2002). Humic substances might show antistress effects under abiotic stress conditions such as, unfavorable temperature, pH, salinity, etc. Humic materials could improve growth of plant under soil condition with enhancing nutrients uptake and reducing toxic elements uptake (Kulikova et al., 2005). Sharif et al. (2002) found that the humus material has indirect effects on plant growth because it improves soil properties, i.e., water holding capacity, permeability, aggregation, hormonal activity, aeration, organic matter mineralization, and solubilization and nutrients availability (Nardi et al. 2002).

In many studies, humic substance such as humic acid and fulvic acid preparations were reported to increase the uptake of mineral elements, to promote the root length, and to increase the fresh and dry weights of plants (Tan and Nopamornbodi, 1979; Duplessis and Mackenzie, 1983; Adani et al., 1998; Mackowiak et al., 2001; Nardi et al., 2002; Dursun et al., 2002; Arancon et al., 2003; Cimrin and Yilmaz, 2005; Ulukan, 2008,

: https://doi.org/10.18393/ejss.1197785
: http://ejss.fesss.org/10.18393/ejss.1197785
Publisher : Federation of Eurasian Soil Science Societies
e-ISSN : 2147-4249

Eyheraguibel et al., 2008; Saruhan et al., 2011; Merwad, 2017; Tursun et al., 2019). Although there are many studies showing the positive effect of humic substances on plant growth and plant nutrient uptake, negative or no effect of humic substances have been reported (Tahir et al., 2011; Leventoglu and Erdal, 2014). Due to the positive effect of humic substances on the visible growth of plants, these chemicals have been widely used by the growers instead of other substances such as pesticides etc. This, however, has led to growers using higher amounts of these substances (Khaled and Fawy, 2011). Furthermore, healthy and environmentally friendly food production is a priority for scientists and researchers. Organic agriculture presents itself as an efficient alternative, although there are concerns about yield (Awad et al., 2022).

The ultimate goal of the present study was to investigate the influence of different doses of humic substances on fresh yield and nutrient contents (N, P and K) of Eggplant Santana (*Solanum melongena* var. *esculentum Santana*) plants in a field experiment. In addition, the study compared humic substances (humic acid, fulvic acid and humic fulvic acid) applied as a soil application using drip irrigation to evaluate the optimal application doses and humic substances under gray-brown soils in Gobustan, Azerbaijan.

Material and Methods

Location of the field experiment, climate conditions, timing and plant materials

A field trial was conducted at "Ugur" Farm in Gobustan, (40°32'3.59" N and 48°55'9.59" E), Azerbaijan, in the spring season of 2021 on Eggplant Santana with different levels of humic substances (HA, FA and HFA). The geographical location of the field trial is situated on the west part of Azerbaijan (Figure 1). In spite of the location parameters agro-climate condition is profitable to the gardening, horticulture and vegetable growing. For many years several vegetables (tomato, cucumber, all kinds of cabbages, onion and eatable green grasses) are being cultivated in the territory. There was large olive gardens around the vegetable cultivated field which territory has been decreased. In Gobustan mostly gray-brown soils exist. These soils are characterized by a gray-brown color. Before conducting the experiment, the soil sample was analyzed from Institute of Soil Science and Agrochemistry, Baku, Azerbaijan. Soil textural class named as clay loam (30% clay, 35% silt and 35% sand). The soil was characteristically alkaline reaction (pH 8), total soluble salt was 0.3%, soil organic matter was 1.43%, total nitrogen was 0.089%, available phosphorus ($NaHCO_3$ extractable) was 12.4 mg P kg^{-1} and available potassium was 123 mg K kg^{-1}. The variety of Eggplant Santana was produced by Research Institute of Crop Husbandry of Ministry of Agriculture of Azerbaijan Republic. The variety of *Solanum melongena* tested was var. *esculentum Santana*, which was sown on 12 April 2021 This Eggplant Santana requires a moderate amount of water and it thrives best in direct sunlight or full sun meaning that it loves at least 6-8 hours of bright direct light. For these reasons, the selected Eggplant Santana variety is the most prevalent in the study region as a result they are more adaptable to the climatic conditions in Gobustan, Azerbaijan. Weather conditions were presented in Figure 2.

Figure 1. Research area

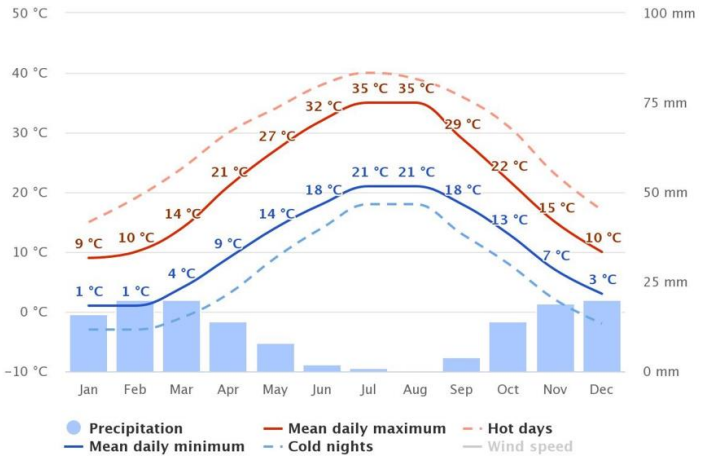

Figure 2. Monthly average temperature (A) and distribution of precipitation (B) of the experimental area

In study field, the summers are warm, dry, and mostly clear and the winters are freezing, snowy, and partly cloudy. The study area is classified as semi-arid climate with mild winters and long hot summers, with a daily average air temperature of 19-20°C and an annual precipitation of 200 mm at the experimental site. The average annual temperature is 16°C and the average relative air humidity is about 78.25 %. The average

temperature can reach 21°C in August, while the lowest average temperature can reach 7°C in December. The earliest frost in the region is usually at the end of October, while the last frost is around the end of March. Most rainfalls occur in winter, and there is almost no rainfall from July to September. The highest humidity (70%) occurs in winter, while the lowest (30%) occurs in summer.

Treatments, Experimental Design and Humic substances application

As basal fertilization, 70 kg ha^{-1} N, 35 kg ha^{-1} P, 60 kg ha^{-1} K were applied using ammonium nitrate, mono ammonium phosphate and potassium nitrate. Eggplant Santana (*Solanum melongena var. esculentum Santana)* are planted as 50x50 cm were used as plant materials. As liquid humic substances, Fulvagra® liquid 25 and Humicraft® liquid made by Humintech GmbH was used. These humic substances contain humic acid, fulvic acid, water soluble N and K_2O ratios as given Table 1.

Table 1. Humic substances component used

Components	Fulvagra® liquid 25 (FuL) Volume (%w/w)	Humicraft® liquid (HuL) Volume (%w/w)
Total organic substances	8	27
Dry matter	20	30
Fulvic acids	18	1
Humic acids	1	8
Free amino acids	-	10
Potassium humates	-	10
Total N	-	1
Water Soluble K_2O	-	2
pH	3-3.5	8.5-9.5
Bulk density, kg/L	1.10	1.12

The experiment was planned according to randomized blocks with 3 replications and each replicate consisted of ten (10 seeds in a parcel) plant and parcel dimensions were designed to have dimensions 1.6×2= 3.2 m^2. Once the Eggplant Santana seedlings that were to be grown commercially were obtained, they were planted into row spacing and row tops so that they were in parcels of dimensions 40×40 cm. The experiment was carried out between 10.04.2021 and 21.10.2021. In the experiment, for soil application 4 levels of humic substances (humic acids-HA, fulvic-acids-FA and humic-fulvic-acids-HFA) corresponding to 0, 250, 5000 and 1000 ppm were given to before planting seedlings and water irrigation using with drip irrigation system lasted to this term. The amounts of humic substances applied to the land with water are given in the Table 2.

Table 2. Humic substances application doses with water

Aplication doses, ppm	HA	FA	HFA
0	0	0	0
250	30 L ha^{-1} HA from HuL	35 L ha^{-1} FA from FuL	25 L ha^{-1} HFA from HuL (100 ppm) + FuL (150 ppm)
500	20 L ha^{-1} HA from HuL	25 L ha^{-1} FA from FuL	20 L ha^{-1} HFA from HuL (200 ppm) + FuL (300 ppm)
1000	15 L ha^{-1} HA from HuL	15 L ha^{-1} FA from FuL	10 L ha^{-1} HFA from HuL (400 ppm) + FuL (600 ppm)

Evaluation of Leaf Nutrients

At the end of the experiment, in order to determine leaf nutrient concentrations, samples were collected from the four sides of plants from the shoots. Then, samples were brought to laboratory and washed with water, dilute acid (0.2 N HCl) and distilled water. Later, samples were dried at 65±5 ^{0}C for 2 days. Afterwards, samples were dried, grounded and wet digested by using HNO_3+$HClO_4$ (4:1) mixture. Total N was determined according to Kjeldahl method. Leaf P concentration was measured vanadomolybdphosphoric method, K concentrations were determined using atomic absorption spectrophotometer (Jones, 2001).

Results and Discussion

Fresh Eggplant Santana yield, t ha^{-1}

The application of various humic substances such as HA, FA and HFA gave an increase in the Fresh Eggplant Santana yields compared with untreated (control) soil (Figure 3). This is explained by the fact that the addition of humic materials improves physical and chemical characteristics of gray-brown soil. This finding stands in agreement with those of Mackowiak et al. (2001), Nardi et al. (2002), Cimrin and Yilmaz (2005) and Merwad, (2017). It was determined that the main effect of humic substances is as follows: HFA>FA>HA>untreated soil. In the 2021 growing seasons, the highest Fresh Eggplant Santana yields were obtained from the treatment of 1000 ppm HFA (50.2 t ha^{-1}) and 1000 ppm FA (45.4 t ha^{-1}) while the lowest Fresh Eggplant Santana yields were obtained from the control (15 t ha^{-1}). When the average of doses of treatment was calculated, the

treatment of HFA gave a significantly higher Fresh Eggplant Santana yield (40.4 t ha^{-1}) than the other treatments. Improvement of soil conditions and establishing equilibrium among plant nutrients are also important for soil productivity and plant production. Humic substances and organical improvement of soil increased the yields of some field crops in several studies (Ulukan, 2008). Studies on the effects of humic substances on plant growth, showed improved effects on growth, independent of nutrition (Dursun et al., 2002; Saruhan et al., 2011). Duplessis and Mackenzie (1983) found that the grain yield of legumes, such as mung bean, soybean and pea increased by the use of these humic substances. Some researchers found that humic acid increased the yields in some plants. Studies indicate that humic substances causes increased weights of above-ground parts of plants such as common wheat (Malik and Azam, 1985), parsley (Tursun et al., 2019), strawberry, tomato, marigold, pepper (Adani et al., 1998; Arancon et al., 2003), corn (Tan and Nopamornbodi, 1979; Eyheraguibel et al., 2008).

Nutrient contents of Fresh Eggplant Santana leaf, %

The concentration of different nutrients, namely, nitrogen, phosphorus and potassium, were determined in Eggplant Santana leaf grown under application of various humic substances such as HA, FA and HFA. The results obtained at the harvesting stage of growth were evaluated as percentage in dry weight. The nutrient concentrations of Eggplant Santana leaf among the HA, FA and HFA treatments are shown in Figure 4, 5 and 6. In general, it was determined that soil applications of humic substances had a significant effect on the NPK concentration of Eggplant Santana leaf. When compared with the control treatment, NPK concentration of Eggplant Santana plant leaf were higher both application doses of humic substances. Chen and Aviad (1990), Fagbenro and Agboda (1993) and David et al. (1994) have reported promoted growth and nutrient uptake of plant due to the addition of humic substances. The plants take more mineral elements due to the better developed root systems. In addition, the stimulation of ion uptake in applications with humic substances led many researchers to propose that these materials affect membrane permeability (Zientra, 1983). It is related to the surface activity of humic substances resulting from the presence of both hydrophilic and hydrophobic sites (Chen and Schnitzer, 1978). Therefore, the humic substances may interact with phospholipids structure of cell membranes and react as carriers of nutrients through them (Aşık et al., 2009).

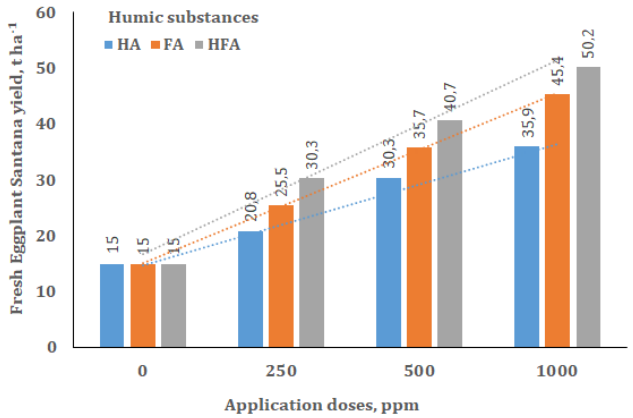

Figure 3. The effects of humic substances on Fresh Eggplant Santana yield, t ha^{-1}

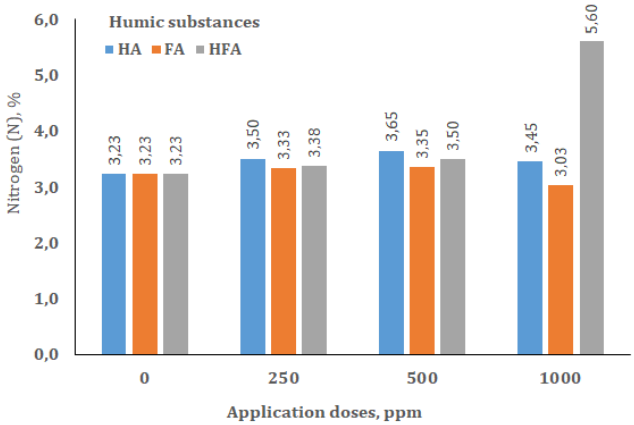

Figure 4. The effects of humic substances on Nitrogen contents of Fresh Eggplant Santana leaf, %

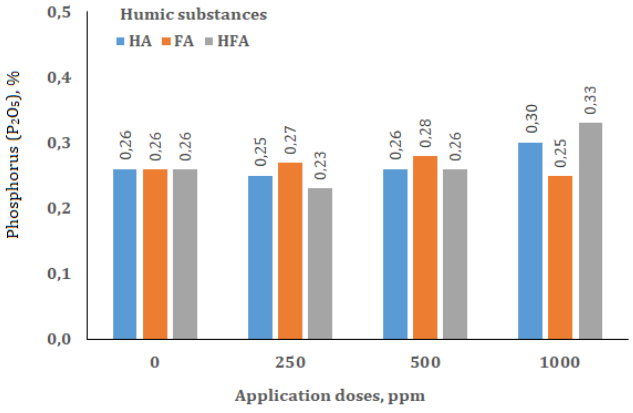

Figure 5. The effects of humic substances on Phosphorus contents of Fresh Eggplant Santana leaf, %

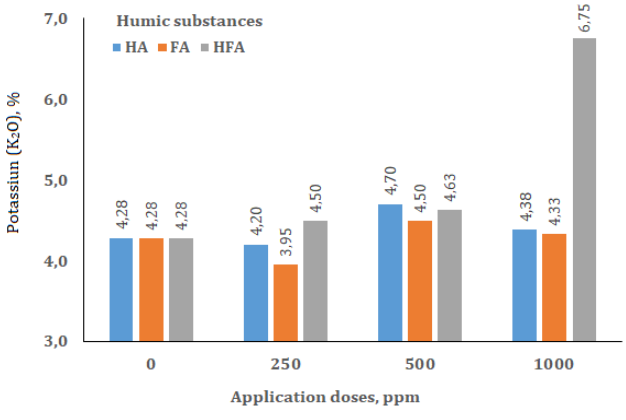

Figure 6. The effects of humic substances on Potassium contents of Fresh Eggplant Santana leaf, %

The highest NPK concentrations of Eggplant Santana leaf were obtained from 1000 ppm HFA dose. Nitrogen content of Eggplant Santana plant leaf was significantly affected with the applications of different humic substances sources and their doses when compared with the control. Nitrogen content of Eggplant Santana plant leaf varied from 3.23% in the control to 5.65 % in 1000 ppm HFA dose (Figure 4). Phosphorus content of plant leaf was not affected by the treatments and ranged from 0.23% in 250 ppm HFA dose to 0.33% in 1000 ppm HFA dose. The highest phosphorus content of plant leaf was determined in 1000 ppm HFA dose which was higher than the other treatments but it was not significantly different (Figure 5). Potassium content of plant leaf was affected by the treatments and followed a similar trend with nitrogen content of plant leaf. The lowest potassium content of plant leaf was found in the 250 ppm FA dose, and the highest potassium content of leaf was measured in 1000 ppm HFA dose (Figure 6). In general, it was determined that 1000 ppm humic substances increased the nitrogen (N), phosphorus (P_2O_5) and potassium (K_2O) contents of Eggplant Santana plant leaf over the control. It is in agreement with Fagbenro and Agboola (1993), Bohme and Thi Lua (1997), Atiyeh et al. (2002), Sanchez–Sanchez et al. (2002) and Nikbakht et al. (2008).

Conclusion

Technically, humic substances such as humic acid (HA), fulvic acid (FA) and humicfulvic acid (HFA) are not fertilizers, although most farmers do consider them so, and their applications are environmentally friendly; furthermore it is considered one of the most important production factors in sustainable agriculture practice. It can be concluded from this study that different doses of humic substance treatments increased the fresh yields and leaf nutrient contents of Eggplant Santana compared to the control groups, and this increase was found to be significant. The highest value for highest fresh yields and leaf NPK contents of Eggplant Santana plants grown in gray-brown soils were obtained from 1000 ppm HFA dose. These results suggest that 1000 ppm HA and FA combination to the standard humic substances application will be sufficient to obtain adequate fresh yield and nutrient contents in Eggplant Santana leafs. More research is needed to optimize the combined effect of different HFA application rates and mineral fertilizers on the crop performance and soil quality parameters under defined field conditions; more importantly, long-term studies involving different soil types, crops and climate patterns in warranted to truly exploit the benefits of humic substances.

Acknowledgment

The research results existing in this paper based on “The State Program for the Socio-Economical Development of Azerbaijan Republic regions within 2019-2023 years”. I would like to thank Editorial team of journal and anonymous reviewers for their constructive comments.

References

Adani, F., Genevini, P., Zaccheo, P., Zocchi, G., 1998. The effect of commercial humic acid on tomato plant growth and mineral nutrition. *Journal of Plant Nutrition* 21(3): 561-575.

Arancon, N.Q., Lee, S., Edwards, A., Atiyeh, R., 2003. Effects of humic acids derived from cattle, food and paper-waste vermicomposts on growth of greenhouse plants. *Pedobiologia* 47(5-6): 741-744.

Aşık, B.B., Turan, M.A., Çelik, H., Katkat, A.V., 2009. Effects of humic substances on plant growth and mineral nutrients uptake of wheat (Triticum durum cv. Salihli) under conditions of salinity. *Asian Journal of Crop Science* 1(2): 85-97.

Atiyeh, R.M., Lee, S., Edwards, C.A., 2002. The influence of humic acids derived from earthworm-processed organic wastes on plant growth. *Bioresearch Technology* 84(1): 7–14.

Awad, A.A.M., El-Taib, A.B.A., Sweed, A.A.A., Omran, A.A.M., 2022. Nutrient contents and productivity of triticum aestivum plants grown in clay loam soil depending on humic substances and varieties and their interactions. *Agronomy* 12: 705.

Bohme, M., Thi Lua, H., 1997. Influence of mineral and organic treatments in the rhizosphere on the growth of tomato plants. *Acta Horticulturae* 450: 161–168.

Cansu, M., Erdal, İ., 2018. Effect of humic substance applications on mineral nutrition and yield of Granny Smith and Jersey Mac apple varieties. *Tarım Bilimleri Dergisi* 24(2): 162-169.

Cesco, S., Nikolic, M., Romheld, V., Varanini, Z., Pinton, R., 2002. Uptake of ^{59}Fe from soluble ^{59}Fe-humate complexes by cucumber and barley plants. *Plant and Soil* 241: 121-128

Chen, Y., Aviad, T., 1990. Effect of humic substances on plant growth. In: Humic substances in soil and crop sciences: Selected reading, MacCarthy, P., Clapp, C.E., Malcolm, R.L., Bloom, P.R. (Eds). Soil Science Society America, Madison, WI, USA. pp: 161-187.

Chen, Y., Schnitzer, M., 1978. The surface tension of aqueous solutions of soil humic substances. *Soil Science* 125(1): 7-15.

Cimrin, K.M., Yilmaz, I., 2005. Humic acid applications to lettuce do not improve yield but do improve phosphorus availability. *Acta Agriculturae Scandinavica, Section B — Soil & Plant Science* 55(1): 58–63.

David, P.P., Nelson P.V., Sanders, D.C., 1994. A humic acid improves growth of tomato seedling in solution culture. *Journal of Plant Nutrition* 17(1): 173-184.

Duplessis, G.L., Mackenzie, A.F., 1983. Effect of leonardite applications on phosphorus availability and corn growth. *Canadian Journal of Soil Science* 63(4): 749-751.

Dursun, A., Güvenç, I., Turan, M., 2002. Effects of different levels of humic acid on seedling growth and macro and micronutrient contents of tomato and eggplant. *Acta Agrobotanica* 56(2): 81-88.

Eyheraguibel, B., Silvestre, J., Morard, P., 2008. Effects of humic substances derived from organic waste enhancement on the growth and mineral nutrition of maize. *Bioresource Technology* 99(10): 4206-4212.

Fagbenro, J.A., Agboola, A.A., 1993. Effect of different levels of humic acid on the growth and nutrient uptake of teak seedlings. *Journal of Plant Nutrition* 16(8): 1465–1483.

IHSS, 2022. What are humic substances. International Humic Substances Society. Available at [Access date: 03.03.2022]: https://humic-substances.org/what-are-humic-substances-2/

Jones, J.B., 2001. Laboratory guide for conducting soil tests and plant analyses. CRC Press, New York, USA. 363p.

Khaled, H., Fawy, H.A., 2011. Effect of different levels of humic acids on the nutrient content, plant growth, and soil properties under conditions of salinity. *Soil and Water Reserach* 6(1): 21-29.

Kulikova, N.A., Stepanova, E.V., Koroleva, O.V., 2005. Mitigating activity of humic substances direct influence on biota. In: Use of humic substances to remediate polluted environments: From theory to practice. Perminova, I.V., Hatfield, K., Hertkorn, N. (Eds.). NATO Science Series, vol 52. Springer, Dordrecht. pp. 285-310.

Leventoglu, H., Erdal, İ., 2014. Effect of high humic substance levels on growth and nutrient concentration of corn under calcareous conditions. *Journal of Plant Nutrition* 37(12): 2074-2084.

Mackowiak, C.L., Grossl, P.R., Bugbee, B.G., 2001. Beneficial effects of humic acid on micronutrient availability to wheat. *Soil Science Society of America Journal* 65(6): 1744–1750.

Malik, K.A., Azam, F., 1985. Effects of humic acids on wheat (Triticum aestivum L.) seedling growth. *Environmental and Experimental Botany* 25(3): 245-252.

Merwad, A.M.A., 2017. Effect of humic and fulvic substances and Moringa leaf extract on Sudan grass plants grown under saline conditions. *Canadian Journal of Soil Science* 97(4): 703–716.

Nardi, S., Pizzeghello, D., Muscolo, A., Vianello, A., 2002. Physiological effects of humic substances in plant growth. *Soil Biology and Biochemistry* 34(11): 1527-1536.

Nikbakht, A., Kafi, M., Babalar, M., Xia, Y.P., Luo, A., Etemadi, N., 2008. Effect of humic acid on plant growth, nutrient uptake, and postharvest life of Gerbera. *Journal of Plant Nutrition* 31(12): 2155-2167.

Pinton, R., Cesco, S., Santi, S., Agnolon, F., Varanini, Z., 1999. Water-extractable humic substances enhance iron deficiency responses by Fe-deficient cucumber plants. *Plant and Soil* 210: 145-157.

Sanchez–Sanchez, A., Sanchez-Andreu, J., Juarez, M., Jorda, J. and Bermudez, D. 2002. Humic substances and amino acids improve effectiveness of chelate FeEDDHA in lemon trees. *Journal of Plant Nutrition* 25(11): 2433–2442.

Saruhan, V., Kusvuran, A., Kokten, K., 2011. The effect of different replications of humic acid fertilization on yield performances of common vetch (Vicia sativa L.). *African Journal of Biotechnology* 10(29): 5587-5592.

Sharif, M., Khattak, R.A., Sarir, M.S., 2002. Effect of different levels of lignitic coal derived humic acid on growth of maize plants. *Communications in Soil Science and Plant Analysis* 33(19-20): 3567-3580.

Tahir, M., Khurshid, M., Khan, M.Z., Kazmi, M.H., 2011. Lignite-derived humic acid effect on growth of wheat plants in different soils. *Pedosphere* 21(1): 124-131.

Tan, K.H., Nopamornbodi, V., 1979. Effects of different levels of humic acids on nutrient content and growth of corn (Zea mays L.). *Plant and Soil* 51: 283-287.

Tursun, T., Akıncı, Ş., Bozkurt, E., 2019. Determination of the effect of humic acid on growth and development parameters of Parsley (Petroselinum sativum Hoffm.) grown in boron soil. *Notulae Botanicae Horti Agrobotanici Cluj-Napoca* 47(1): 183-193.